MICROFILTRATION

membrane development and module design

15

Erik Roesink

Betty

MICROFILTRATION

MEMBRANE DEVELOPMENT
and
MODULE DESIGN

PROEFSCHRIFT

ter verkrijging van
de graad van doctor aan de Universiteit Twente,
op gezag van de rector magnificus
prof. dr. ir. J. H. A. Smit
volgens het besluit van het College van Dekanen
in het openbaar te verdedigen
op vrijdag 12 mei 1989 te 14.00 uur

door

Hendrik Dirk Willem Roesink

geboren op 17 november 1952 te Colmschate (gem. Diepenveen)

Dit proefschrift is goedgekeurd door de promotor: Prof. Dr. C. A. Smolders
Assistent promotor: Dr. ir. I. G. Rácz
Referent: Dr. ing. M.H.V. Mulder

Acknowledgements:

The work described in this thesis was financially supported by the Dutch Ministry of Economic Affairs, in the framework of the Dutch research program on membranes (IOP- m) and X-FLOW BV.

The printing-expenses of this thesis were contributed by
X-FLOW BV, Enschede, The Netherlands.

ISBN 90 - 9002843 - 9

Printed by: ALFA, Enschede, The Netherlands

Go down sunshine, see what tomorrow brings.....

- A. Korner -

Ter herinnering aan mijn grootvader,
Hendrik Roesink, die de verdediging van
dit proefschrift nog zo graag had willen
meemaken.

To Ria, Derk en Margot

VOORWOORD

Zo ben je leraar en zo ben je een "membraanspecialist", maar daarbij heb je wel de hulp van veel mensen nodig. Dus dank aan:

- Kees Smolders voor het geven van tweede kans onderwijs aan een oud gediende en voor de prettige begeleiding en samenwerking
- Dick Koenhen en Paul van der Velden, die als "oud mentoren" net dat extra duwtje gaven nodig om aan deze klus te beginnen
- Marcel Mulder voor zijn niet te evenaren passeerbewegingen en voor zijn kritische begeleiding op de nodige afstand, maar altijd aanwezig wanneer nodig
- Imre Rácz voor zijn stimulerende begeleiding en samenwerking
- Jaap van 't Hof, waarvan ik de kunst van het spinnen heb mogen afkijken, en waarmee ik veel en vaak heb mogen bomen over membraanvorming, spinkoppen, voetballen en w.v.t.t. kwam
- Hans Hegeman, Ruurd Lammers, Sander Jansen, Maarten Almering, Peter van Berkel, Mike Smith, Erwin Voors, Peter Schwering, Harrie Bos, Kenji Matsubayashi en Stella Korre, die allen in de vorm van een opdracht, stage of i.d. een bijdrage hebben geleverd aan dit proefschrift
- Marcin Otto, Johan Ronner, Ingrid Wienk, Zandrie Borneman, Stephan Oude Vrielink, Monique Beerlage, W. Potman, Thonie van den Boomgaard, Yvo de Boer, die allen als mede-auteur van een hoofdstuk een bijdrage aan dit proefschrift hebben geleverd
- Zandrie Borneman, die in het laatste jaar ongeveer 50 % van de meetresultaten bij elkaar heeft weten te sprokkelen en zonder wiens hulp dit proefschrift er heel anders zou hebben uitgezien.
- Ingo Blume, voor zijn bijdragen aan hoofdstuk 1 en hoofdstuk 9 en voor het, op het laatste moment, nog eens doornemen van het proefschrift om de laatste schoonheidfoutjes op te sporen
- Gert van den Berg, Petrus Cuperus en Derk Bargeman voor de zinnige discussies tijdens de werkbesprekingen in klein verband
- John Heeks omdat hij altijd klaarstond wanneer hij nodig was en voor zijn functie als sfeermaker in de groep
- kamergenoot Remko Boom, voor de discussies over membraanvorming
- de mensen van het apparatencentrum, glasinstrumentenmakerij en de technische dienst van de afdeling chemische technologie
- Lute Broens, voor zijn enthousiasmerende ondersteuning en zijn vaderlijke raadgevingen
- Dick Koenhen, voor het blijven uitoefen van zijn mentorschap
- iedereen, die ik vergeten ben persoonlijk te noemen en toch genoemd had moeten worden !

Het was goed werken in de membranengroep van Kees Smolders zowel door de goede sfeer als door de pluriforme samenstelling, waardoor er voor elk probleem altijd wel een aanspreekpunt aanwezig was, houden zo.....en bedankt.

Erik Roesink

CONTENTS

CHAPTER 3 THE INFLUENCE OF SPINNING CONDITIONS ON THE MORPHOLOGY OF MICROPOROUS CAPILLARY MEMBRANES

CHAPTER 4 POLYETHERIMIDE - POLYVINYLPYRROLIDONE BLENDS AS MEMBRANE MATERIAL

CHAPTER 1

MICROFILTRATION - DEVELOPMENT FROM AN OLD LABORATORY FILTRATION METHOD INTO A HIGH-PERFORMANCE SEPARATION TECHNIQUE

H.D.W. Roesink

1.1 INTRODUCTION

Through history people have been transforming materials with respect to properties, composition and shape. The materials were used for clothing, as nutrients and for building houses. Processes like crushing, grinding, mixing, sieving are as old as mankind and filtration is already mentioned in ancient Chinese writings as well as in pre-Christian Hebrew scrolls. Egyptian tombs contain illustrations of filtration and it is known that the Carthaginians filtered their wine [1]. These processes were carried out by means of simple tools. Later, people used all kinds of more sophisticated metal equipment for processes like filtration, distillation or crystallization.

In the chemical industry the role of separation processes is prominent. These separation processes can be divided in techniques to separate phases and techniques to separate compounds. Phase separation techniques will be applied if the feed consists of two or more distinct phases; these processes make use of the difference in physical properties of the phases, such as differences in density or particle size (sieving, filtration, centrifugation, flotation). In component separation processes the feed is mixed on a molecular level and the separation occurs on the basis of differences in properties, such as vapour pressure, chemical nature, affinity, freezing point or charge (distillation, stripping, drying, extraction, crystallization, ion exchange) [2].

Membrane filtration is a separation technique that only recently has been adequately developed for the process industry, although already at the beginning of this century membrane filters were used for analytical purposes mainly (see below). Membrane filtration can be applied for phase separation techniques (microfiltration and ultrafiltration) and component separation techniques (reverse osmosis, gas separation, pervaporation, dialysis) [3,4].

Microfiltration is a membrane separation process for the treatment of suspensions and emulsions. It will retain particles down to a size of approximately 0.1 μm, which places it between the

ultrafiltration process (1-100 nm) and the convential coarse filtration (> 5 μm).
A survey of the most important membrane separation processes is given in table 1.

Table 1: *Membrane separation processes applied in the process industry. (L= liquid: G= gaseous: S= solid)*

Membrane process	Phases (feed/permeate)	Driving force	Separation mechanism	Applications
Microfiltration	L+S/L G+S/G	pressure (0.1 - 500 kPa)	difference in size	Purification, concentration of suspensions and emulsions; gas purification; sterile filtration
Ultrafiltration	L/L	pressure (0.1 - 1 MPa)	difference in size	separation of macromolecules from solutions; concentration of solutions.
Reverse Osmosis	L/L	pressure (1 - 10 MPa)	solution/ diffusion	desalination of salt and brackish water; separation of low molecular weight components from liquids.
Dialysis	L/L	concentration	solution/ diffusion	removal of low molecular components; hemodialysis (artificial kidney)
Electrodialysis	L/L	electric potential	difference in charge	desalination of water or process streams
Gas separation	G/G	pressure (0.1 - 10 MPa)	solution/ diffusion	oxygen enrichment of air; CO_2/CH_4 separation
Pervaporation	L/G	partial vapour difference	solution/ diffusion	dehydration of solvents concentration of ethanol

The commercial breakthrough of membrane separation technology started with Loeb and Sourirajan (late 1950s) [3], who discovered a way to make an asymmetric reverse osmosis membrane. Such a membrane consists of a dense toplayer, which is responsible for the separation characteristics, supported by a porous sublayer. Since the toplayer of asymmetric membranes can be extremely thin (0.5 μm), the fluxes of these membranes were high enough enabling reverse osmosis to compete with the traditional desalination processes, e.g., flash distillation. Very soon (mid 1960s) [3] the introduction of industrial ultrafiltration processes followed as a spin-off of the development of the asymmetric membranes and module development. Ultrafiltration is applied especially in the food, dairy and beverage industry and in the automobile industry where it is used on a very large scale for the recovery of paint. The introduction of microfiltration as a large scale separation technique was enabled by the development of highly resistant membranes (polypropylene, polyamide, polysulfone) and very much stimulated by the application of the cross-flow system,

which had already been used in reverse osmosis and ultrafiltration applications. Cross-flow microfiltration used for large scale applications is a relatively young technique. Currently one observes in microfiltration, the earliest of membrane separation technologies, a positive influence from the newer technologies (ultrafiltration and reverse osmosis) in improving fluid mechanics and module design.
In this chapter the development of the microfiltration process is described in terms of membrane, module and process development.

1.2 MICROFILTRATION MEMBRANES

1.2.1 Historical development

The development of the microfiltration membranes started with the systematic studies of membrane filtration at the beginning of this century by Bechold [1]. He was the first who noted that the pore size in what he called "ultra filters" could be altered by changing the composition of the casting solution. Bechold measured the pressure required to force a bubble of air through a wet filter against the surface tension of the water in its capillaries. This "bubble point measurement" is still used to determine the maximum pore size of membrane filters. Around 1918, in Göttingen (Germany), Zsigmondy and Bachmann developed the first methods for producing nitro-cellulose membranes that were applicable on a commercial scale. Zsigmondy and Bachmann were the first to use the name "membrane filter", a name that is still used for flat microfiltration membranes. The Membranfiltergesellschaft Sartorius-Werke in Göttingen was the first company that produced membrane filters on a commercial scale (1927) and still prepares similar membranes. Although in the period before World War II membrane filters were only used for the determination of particle size of proteins or filtering viruses, the period just after World War II brought membrane filters to prominence. In Germany, in cities that had suffered heavy bomb damage, Dr. G. Mueller and others applied membrane filter techniques to the bacteriological examination of water. Membrane filters of about one-half micron pore size were used for E. Coli determination in water-supply systems that were destroyed in air raids [1]. Soon after the war, researchers in the United States and England studied membrane filtration technology inspired by the work done in Germany, where most membrane research had been performed. In 1947 Dr. Goetz visited Germany and obtained data from the Membranfiltergesellschaft Sartorius-Werke. A few years later (1950) he developed a new production method capable of producing membranes with improved flow rates and uniformity of pores, which finally led to the foundation of the Millipore Corporation in 1954.
Until 1963, microfilters were predominantly made of nitro-cellulose or cellulose esters. As new applications began to emerge, membranes with improved chemical resistance and heat stability were needed and investigations of other materials and fabrication methods for membrane filters were

started [5].

1.2.2 Membrane materials

Polymers form the most important group of materials used for the fabrication of microfiltration membranes. Ceramics and also metals are other groups of (inorganic) membrane materials. Metallic microfiltration membranes can be made of nonwoven fibres or sintered stainless steel spheres, but these have been commercialized only on a very small scale [7].
Most used ceramic microfiltration membranes are prepared by means of a sol/gel process. The Anotec ® membranes are produced by electric anodic oxidation of aluminium metal and are charaterized by a unique parallel pore structure (figure 1a, a honeycomb surface structure and a relatively high surface porosity.
Mechanical stable ceramic membranes consist of either alumina [6], silicon nitride, silicium, zirconia, carbide or carbon. A survey of commercially available ceramic membranes is given in table 2 [7].

Table 2: *Commercially available ceramic membranes.*

Manufacturer	Trade name	Pore size	Membrane material	Support material
Carre	Ucarsep	4 nm - 100 nm	ZrO_2 (dynamically formed)	C
Norton	Ceraflo	0.2 µm - 1.0 µm	α - Al_2O_3	α - Al_2O_3
Alcoa/S.C.T.	Membralox	0.2 µm - 5 µm	α - Al_2O_3	α - Al_2O_3
		4 nm - 100 nm	γ - Al_2O_3	α - Al_2O_3
		4 nm - 100 nm	ZrO_2	α - Al_2O_3
TDK	Dynaceram	≅ 10 nm	α - Al_2O_3	α - Al_2O_3
Asahi Glass	MPG	4 nm - 50 nm	glass (90 % SiO_2)	glass
		0.2 µm - 3 µm	glass	glass
Schott Glass		10 nm - 100 nm (?)	glass	glass
NKG		0.2 µm	SiC	SiC
		2.5 µm - 13 µm	α - Al_2O_3	α - Al_2O_3
S.F.E.C.	Carbosep	10 nm - 100 nm	ZrO_2 (dynamically formed)	C
Alcan/Anotec	Anopore	2.5 nm - 200 nm	γ - Al_2O_3	γ - Al_2O_3
Ceram Filtre		0.15 µm - 8 µm	SiC	SiC

Ceramic membranes can be made in several layers (figure 1b) with different pore sizes (asymmetric structures). Especially ceramic membranes offer interesting possibilities in membrane technology, since they have the following advantages [7]:

- Thermal stability
- Mechanical stability
- Chemical resistance
- Controlled, defined, stable pore structure
- Backflush capacity
- Reduced fouling/flux loss
- High throughput/volume

Although especially the first four advantages are rather obvious for ceramic membranes, it has to be stressed that the advantages mentioned can also be named for polymeric membranes. Some ceramic membranes (e.g., S.F.E.C) have physically attached sublayers to obtain desirable separation properties and therefore are susceptible to abrasion and exhibit a minimal backflush ability.
The commercialization of ceramic membranes is limited by the module development [7]. Problems are both technical (wetted seals that are not ceramic) and economical (high module costs relative to polymeric membranes when compared on a surface area basis).

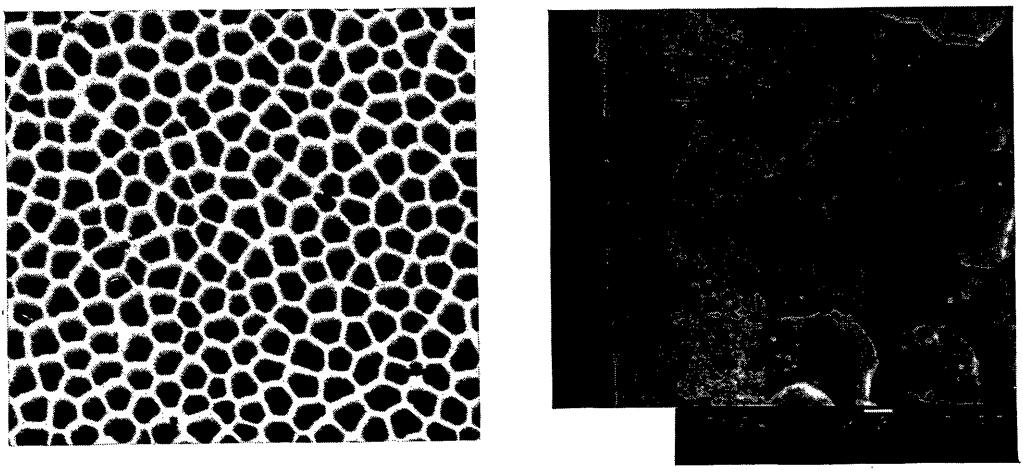

-a- -b-

Figure 1: *-a- Honeycomb structure in the toplayer (top view) of a ceramic Anotec® membrane.*
-b- Cross section of an multilayer alumina membrane.

Despite the benefits for ceramic membranes mentioned above, polymer membranes have in general advantages over ceramic membranes like:

- Ease of processing
- Availability of wide structure variations
- Possibility to realize any configuration
- High strength-to-weight ratio
- Ability to have properties tailored to a specific use by structural changes
- Flexibility
- Low costs.

The disadvantages of polymer membranes are, as already mentioned, the inferior stability at high temperatures, the reduced chemical resistance and also the time dependent relaxation phenomena, which change membrane properties in time (especially for high pressure separations).

Cellulose like materials are still used for the fabrication of membrane filters, but nowadays micofiltration membranes are also made of: acrylic copolymers, polyvinyl chloride, polystyrene, polyetherimide, polyimide, polycarbonate, polyamide, fluorocarbon polymers, polysulfone, polyethersulfone, polypropylene.

Desirable properties for the polymer membranes are [8]:

- Controllable pore size down to 0.1 μm or less
- Narrow pore size distribution and high surface porosity
- Mechanical strength to withstand pressure and resistance to abrasion
- Chemical resistance to allow for a wide range of feed components and cleaning agents
- Hydrophilic; good wettability and low fouling properties or resistance to adsorption of feed components
- Thermostable; retention of the basic properties over a wide temperature range
- Workability; should be easily shaped into sheets or tubes and incorporated into modules
- Low costs

The development of new highly resistant membranes seems to follow the development of the new engineering plastics. Examples of these new engineering plastics are polyetherimide (e.g., Ultem®), polyethersulfone (e.g., Victrex®), polyetheretherketone (e.g., Victrex®) and polyphenyleneoxide (e.g., Noryl®), which all are used for membrane development, since they exhibit a high chemical resistance coupled with a high thermal stability.

The membrane market is a relatively small market for polymer producers. Consequently the membrane producers are more or less dependent on the development of new resistant engineering polymers.

1.2.3 Fabrication of polymeric microfiltration membranes

Two types of polymeric microfiltration membranes can be distinguished: the depth filter and the "real" membrane filter (surface filtration). Depth-filters are characterized by a symmetric structure, which means that particles are trapped in the porous filter structure so that at elevated transmembrane pressures a certain break-through of particles can be expected. During the last two decades "real" membranes for microfiltration have been developed. The pore size at the membrane-feed interface is such that all particles will be retained or that eventually small particles can pass if that is desired. The most ideal pore size structure would be a structure where the smallest pores are found at the membrane-feed interface while the pore size increases across the membrane (asymmetric structure). These structures can be obtained by using the phase inversion technique, which is the most used fabrication method for microfiltration membranes.

Polymer membranes can be made in the following ways:

- *PHASE INVERSION*

The concept of phase inversion in membrane formation has been introduced by Kesting [9] and can be defined as follows:

A homogeneous polymer solution is transformed into a two-phase system in which a solidified polymer rich phase forms the continuous membrane matrix and a polymer poor phase fills the pores.

The phase inversion process starts using a homogeneous polymer solution and it is the most versatile and most used preparation method only restricted by the solubility of the polymer. The homogeneous polymer solution is shaped in a certain configuration (e.g., flat, capillary, hollow fibre) followed by a phase inversion of the dissolved polymer into a solid phase, which ultimately forms the membrane (figure 2a). The phase inversion is induced by a thermodynamical instability, either by a change in composition or a change in temperature of the polymer solution. The formation mechanism of membranes during the phase inversion is intensively studied by the group of Smolders. In the mid 1970's Koenhen, Broens et al. [10,11,12] presented various papers on this subject and Koenhen was one of the first who recognized that two processes determined the membrane formation: gelation and liquid-liquid demixing. From that time the investigations on the

subject of membrane formation continued, which resulted in publications of Van der Velden [13], Altena [14,15], Wijmans [16,17], Mulder [18] , Reuvers [19,20] and van 't Hof [21]. Other important contributions about the phase inversion process are given by Kesting [9], Frommer [22], Strathmann [23] and Sourirajan [24]. Besides the contribution of the academic world (see above), the industrial contribution is also very important for the development of the phase inversion process, although complete information from this source is rather scarce and often confidential.

The following phase inversion processes can be distinguished [17]:

1) *Immersion precipitation* - This technique was first used by Loeb and Sourirajan for the preparation of skinned reverse osmosis membranes. Characteristic for this technique is that a cast or extruded polymer solution is immersed in a nonsolvent coagulation bath, which causes the polymer to precipitate as a result of a nonsolvent inflow and a solvent outflow. Although Loeb and Sourirajan applied this technique to develop asymmetric membranes, consisting of a very dense toplayer supported by a sponge-like porous structure, Wijmans et al. [17] developed a method based on immersion precipitation for the preparation of skin-free microporous membranes.

2) *Precipitation from the vapour phase* - In this very early technique (Bechold, Zsigmondy, Bachmann) membrane formation is accomplished by inflow (penetration) of a nonsolvent into the polymer solution from the vapour phase. When volatile solvents are used the vapour can be saturated with solvent to avoid evaporation of the solvent from the polymer film and thus avoid formation of a dense skin (figure 2a).

3) *Precipitation by controlled evaporation* - The polymer is dissolved in a mixture of a good and a nonsolvent. When the volatile good solvent evaporates the composition of the polymer changes so that precipitation of the polymer occurs. This method is seldom used for the preparation of microfiltration membranes, since often a skinned membrane is the result.

4) *Thermal precipitation* - The polymer is dissolved at elevated temperatures in a mixture of solvent(s) and nonsolvent(s). Upon controlled cooling the solution becomes unstable and phase separation occurs, resulting in a porous membrane structure (figure 2b). In the mid 1970s Hydronautics developed a porous polypropylene tube based on this process. Later this process has been further developed by Enka Membrana, Wuppertal, West-Germany, resulting in the microporous Accurel® membrane [5,25,26].

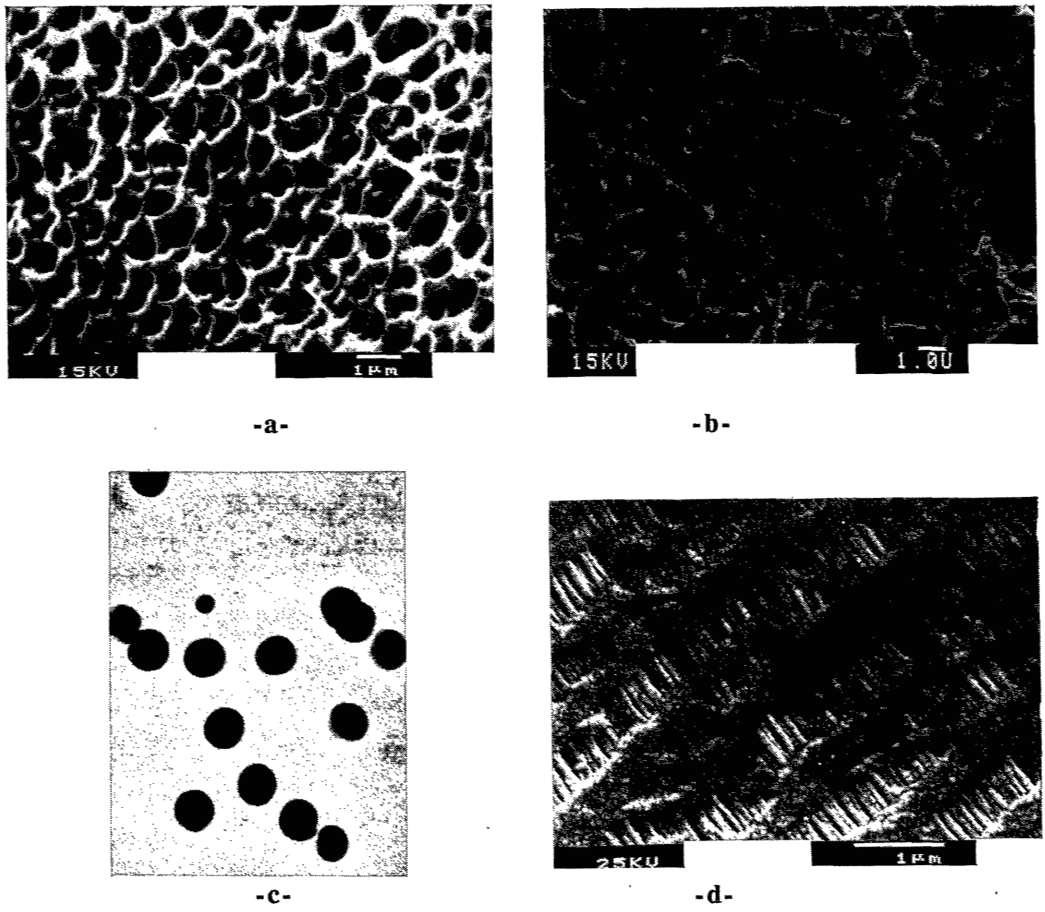

Figure 2: *Polymeric microfiltration membranes: -a- X-Flow® membrane prepared by immersion precipitation. -b- Accurel® membrane prepared by thermal precipitation. -c- Nuclepore® membrane prepared by track-etching. -d- Celgard® membrane prepared by stretching.*

- NUCLEATION TRACK-ETCHING

A homogeneous 5 to 15 µm thick polymer film (e.g., polycarbonate) is subjected to a high-energy particle radiation (metal ions) perpendicular to the material, in a nuclear reactor. Afterwards the film is immersed in an acid or basic bath in which the spots damaged by the radiation are etched into cylindrical pores. The porosity is determined by the residence time in the reactor, while the pore size is controlled by the residence time in the etching bath. Nuclepore® membranes are produced in this way. The advantage of this membrane type is the well defined pore size and the pore shape (figure 2c), i.e., an extremely narrow pore size distribution; disadvantages are the relatively low surface porosity and the thickness of the membranes, which is restricted to 15 µm. The pore size can be adjusted between 0.010 and 12 µm [3].

- *STRETCHING*

This technique is based on the stretching, perpendicular to the direction of extrusion, of homogeneous, partly crystalline polymer films. The crystalline parts are separated resulting in so-called microtears, which form the porous regions in the ultimate membrane. Stretched polytetrafluoroethylene membranes are sold under the trade name Gore-Tex® , while stretched polypropylene films and fibres are known under the name Celgard® (figure 2d) [3].

- *SINTERING*

Solid polymer powder (and eventually some additives) is pressed into various shapes, e.g., a film, followed by a sintering process at elevated temperature. This method is useful for insoluble and infusible polymers that cannot be processed in any other way. Porous polytetrafluoroethylene, polyethylene membranes are fabricated using a sintering process. An advantage of these membranes is the excellent thermal, mechanical and chemical resistance; the disadvantages are a wide pore size distribution and the difficulty to control the fabrication of these sintered membranes. The minimum pore size that can be achieved is about one micron.

- *NEW DEVELOPMENTS*

A recent development in the fabrication of microporous polymeric membranes is the Sunbeam process developed by Gelman Sciences Technology Ltd. This process starts with a mixture of oligomers, monomers, photo-initiators and surfactants that are photopolymerized to a stable crosslinked membrane matrix by an ultraviolet and/or electron beam treatment. The membranes can be made of hydrophilic or hydrophobic nature by using a great variety of oligomers and monomers like acrylic acid, acrylic esters, acryl amides and vinylpyrrolidone [27].

A survey of commercially available membranes is given in table 3 [28].

Table 3: *Commercial available polymeric microfiltration membranes.*

Material	**Manufacturer**	**Pore size** (μm)	**Geometry**	**Hydro-**	**Resistance** (Thermal/chemical)	**Applications**
Cellulosics	Amicon	0.2 - 0.8				bacterial analyses
	Domnick	0.2 - 3.0	flat, cartridges			
acetate, nitrate	Gelman	0.2 - 5.0				
or blends	MFS	0.2 - 5.0	flat,	-philic	poor	air filtration
	Millipore	0.025 - 8.0	cylindrical,		resistance	pharmaceuticals
	Nuclepore	0.1 - 5.0	cartridges.			
	SeS	0.025 - 8.0				
	Sartorius	0.1 - 8.0				
Hydrophobic cellulose nitrate	Sartorius	0.01 - 8.0		-phobic		steam filtration

Nylon	Domnick	0.2 - 0.65	cartridges	-philic	130 °C	
nylon 6	AKZO	0.2 - 0.65	flat	-phobic		
	Sartorius	0.6 - 0.8				
nylon 66	AMF Cuno	0.2 - 15	flat, cylindrical,	-philic	145 °C	
	Pall	0.04 - 5.0	cartridges	no wetting agents necessary		biotechnology pharmaceuticals
PVC or PVC/acrylic copolymers	Amicon	0.5 - 5.0	films or cast on non-woven PET or polyolefin	-phobic	poor	air filtration
	Millipore	0.6 - 2.0				
	Sartorius	0.2 - 8.0				
	Gelman	0.2 - 10.0			poor	clarification
PTFE	Berghoff	1 - 60			very good	laboratory use
	Domnick	0.2	cartridges			sterilization
	Gelman	0.2 - 5.0	flat			
	Millipore	0.2 - 10	cylindrical	-phobic		gas filtration
	SeS	0.2 - 10	cartridge			sterilization
	Nuclepore	0.2 - 1.0			130 °C	
	MFS	0.2 - 1.0			145 °C	
	Pall	0.2	cartridges			
	Sartorius	0.2 - 5	flat	-phobic		gas filtration
	Domnick	0.1 - 0.2	cartridges	-phobic	140 °C	
Polyethylene	Berghoff	2.0 - 5.0	tubes	-phobic	60 °C	
PVDF	Millipore	0.22 - 0.45	flat cylindrical cartridges	-phobic	good	
Polysulfone	DDS	0.1 - 5.0	flat cylindrical cartridges	-phobic	75 °C pH 1-13 (resistance)	
	AG Techn.	0.1 - 0.45	hollow fibres	-phobic		
	Gelman	0.1 - 0.65	flat, cartridges	-phobic		sterilization
Polysulfone ?	Stork-Wafilin	0.05 - 0.3	cylindrical		95 °C	process industry
Polyethersulfone	X-Flow	0.05 - 1	flat, cylindrical	-philic		biotechnology
Polypropylene	AKZO	0.47 - 0.6	cylindrical			
	Pall	1.5 - 40	flat, cartridges			pharmaceuticals food industry
	Domnick	0.6 - 100	cartridges	-phobic	60 °C continuous	
Polyvinyl-alcohol	Kuraray	0.01 - 0.5	hollow fibre			process industry
Unknown	Celanese	0.02 - 0.4	cylindrical	-philic or -phobic	180 °C	medical, electrochemistry
Polyetherimide, Polyimide	X-Flow	0.05 - 1	flat, cylindrical	-philic		process industry biotechnology

Membranes are fabricated in different configurations, which can be reduced to two essentially different geometries: flat and tubular (cylindrical). In the beginning only flat membranes were fabricated, while 30 years ago the fabrication of tubular membranes started. Tubular membranes can be prepared into different dimensions classified as follows:

- Tubular: outer diameter 5 - 25 mm
- Capillary membranes: outer diameter 0.5 - 5 mm
- Hollow fibre membranes: outer diameter 0.05 - 0.5 mm

In general tubular polymeric membranes are not self-supporting and mostly consist of a cylindrical support (nonwoven materials, ceramics, perforated stainless steel) on which at the inside a membrane is applied. Tubular membranes are applied in ultra- and microfiltration because cleaning of the tubular membranes is relatively easy. Capillary and hollow fibre membranes are self-supporting and an additional advantage of these membrane types is that a relatively high membrane surface to module volume ratio can be obtained. The latter two types of membranes are produced by a spinning process, i.e., a polymer solution is extruded through a tube-in-orifice spinneret and this extrudate is brought to phase separation to obtain a porous structure [29]. The spinning process is mostly used in combination with the phase inversion technique to produce microporous membranes. A porous polypropylene capillary membrane (Celgard®) is obtained by stretching a preformed capillary membrane [3].

1.2.4 The hydrophilicity of microfiltration membranes

As already mentioned in section 1.2.2 one of the desired properties for microfiltration membranes is a hydrophilic nature of the membranes. In most applications aqueous feed solutions are used, hence, the wettability of membranes is improved and no additional wetting agents or surfactants have to be used. Furthermore it is known that hydrophilic membrane materials show a much lower tendency to adsorb macromolecular components, e.g., proteins from the feed solution [28,30]. In fact no exact mechanism can be given for the adsorption of components from the feed on membrane surfaces. However it should be mentioned that in some cases increased hydrophilicity causes increased biofouling (due to adsorption), thereby contradicting common expectation [28].
The adsorption of components from the feed is commonly seen as the first step in the fouling mechanism of membranes, which finally may result in a strong decrease of the permeability of the microfiltration membranes during actual filtration. Unfortunately most polymers that are inherently hydrophilic are not thermally and/or chemically resistant. This means that in practice all kinds of methods are investigated to achieve an almost impossible combination of membrane properties: a thermal, mechanically and chemically resistant material with a hydrophilic nature. There are several

methods known to achieve a hydrophilic character of hydrophobic membranes. Very recently Stengaard [31] presented in his paper a survey of these methods. The methods given by Stengaard are based on the methods that were developed to obtain a composite membrane for reverse osmosis applications. He distinguishes the following possibilities:

- Chemical binding (grafting) of selected hydrophilic polymers and/or monomers onto the surface of a preformed support membrane [32,33].
- Coating of the surface of a support membrane by an organic solution of water insoluble hydrophilic polymers followed by a curing step.
- In situ polymerization of monomers on a support membrane, which results in thin polymeric structures containing hydrophilic groups.
- Ultraviolet light initiated in situ polymerization and grafting reactions on a support membrane to impart hydrophilic properties.

Stengaard et al. developed a method for the chemical grafting of hydroxyl- or amino- compounds onto ultrafiltration membranes (polyvinylidene fluoride). Using these membranes improved performance was obtained when fermentation broths were filtered. The method used by Stengaard and the other methods mentioned by him have one feature in common: it is always a post-treatment after the production of the support membrane, i.e., a two-step process that renders the membranes hydrophilic.

1.3 MICROFILTRATION MODULES

For the actual membrane separation process the microfiltration membranes have to be integrated in a module. The module development was strongly influenced by the introduction of the cross-flow system in membrane technology. In dead-end filtration (figure 3) the flow direction of the feed is perpendicular to the membrane surface, leading to the formation of a cake layer that causes a rapid flux decline. Consequently this mode is only used for solutions with a low particle concentration (e.g., the production of ultrapure water in the electronics industry).
In the cross-flow mode (figure 3) the feed flow is parallel to the membrane surface and the permeate is transported laterally. In this mode the feed flow will have a kind of scouring effect on the membrane surface resulting in much better performance characteristics. For large scale applications this mode is commonly accepted for all membrane separation techniques.

The following requirements for cross-flow microfiltration modules can be given:

- The flow conditions must ensure an adequate feed throughput, which reduces the formation of a cake layer
- Maximum of membrane area in a given module volume should be obtained
- Ease of disassembly for membrane replacement
- Ease of cleaning and sterilization, which is very important in the pharmaceutical, dairy and food industries
- Good chemical and pressure resistance
- Low cost

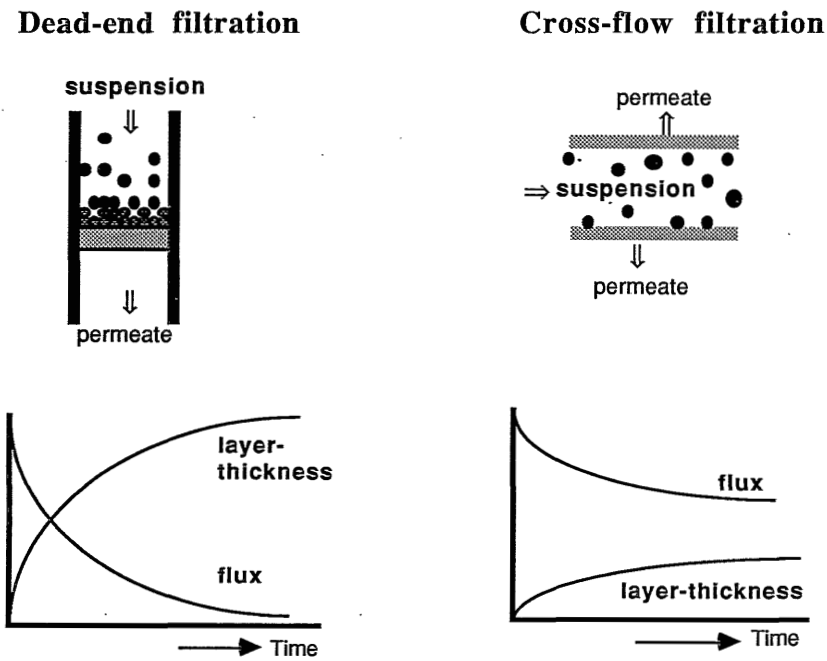

Figure 3: *Schematic representation of dead-end and cross-flow filtration.*

The design of modules is dependent on the membrane geometry that is applied and according to that a classification of module types can be given [34] (table 4):

Table 4: *Module types for cross-flow microfiltration.*

Module type	Advantages	Disadvantages	Remarks
FLAT			
Pleated cartridge	- High area per module	- Poor flow conditions	- Modified for cross-flow
Plate and frame systems	- Low membrane cost - Small replacement area - Reasonable compact - Reasonable flow conditions	- Difficult replacement of membranes - Prefiltration required	- Very widely used - No backflushing
Spiral wound	- Reasonable flow conditions - Compact - Capital cost per unit area - High area per module	- Prefiltration required - Difficult leak detection	- Seldom used for microfiltration - No backflushing
TUBULAR			
Tubular	- Least susceptible to plugging of the bore - Small replacement area - Easy cleaning (including mechanical; sponge ball) - Good flow conditions	- Capital cost - High pumping energy	- No backflushing
Capillary	- Capital cost per unit area - Easy replacement - High area per module - Good flow conditions	- Strength of the fibres	- Backflushing
Hollow fibre	- Capital cost per unit area - Easy replacement - Good flow conditions	- Strength of the fibres	- Backflushing - Prefiltration necessary

In the latter classification of modules it is assumed that in case of capillary membrane and hollow fibre modules the feed flow is through the bore of the capillaries. When shell-side fed modules (feed-outside design) are used, the flow conditions are dependent on the actual design.

As a rule of thumb it can be stated that the actual product flux during microfiltration is only one percent of the clean water flux of the applied membranes. This very strong flux decline is caused by the formation of a cake layer, adsorption of feed components, pore plugging, i.e., in general an

increased resistance. In order to avoid or to reduce flux decline various aspects have to be considered: feed composition, membrane, module, process-engineering. In practice this often reduces to the problem that the flux decline should be minimized for a feed solution and membrane module given. Therefore, the most widely used technique in membrane filtration to avoid the flux decline is the increase of feed flow velocity, to obtain a shearing effect so that the membrane is more or less scoured. But even when high flow velocities are used, it often is impossible to avoid the build-up of fouling layers in the module types mentioned in table 4. Consequently engineers developed other module types for micro - and ultrafiltration: mechanically agitated filters (shear filters). An example of such a filter is the Biodruck-filter developed by Sulzer AG, Winterthur, Switzerland. The filter unit consists of two coaxial cylinders of which the inner one is rotating while the outer one is fixed. Membranes can be fixed on both cylinder walls. In the narrow slit between inner and outer cylinder secondary flow phenomena, so-called Taylor vortices, will reduce the formation of a fouling layer. Although good results are obtained with this method, especially in biotechnical applications, the main disadvantages are the high energy consumption and the scale-up of the process. Due to the decoupling of shear generation and residence time of the feed in the module, the filter can act as a thickener [35]. Other examples of modules with moving parts (rotary microfiltration) are the Dyno-Filter and the Escher-Wyss Druckfilter [36].

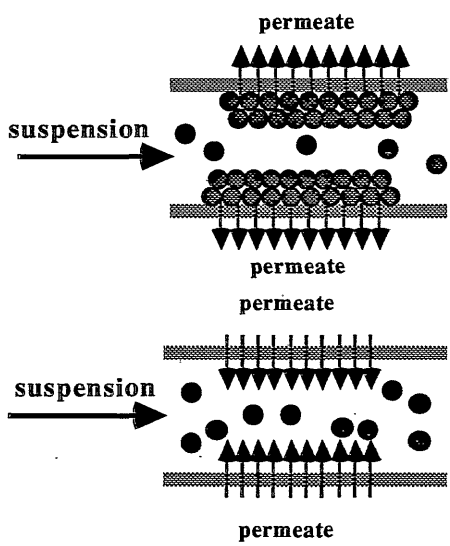

Filtration mode

Under pressure permeate will flow from the inside to the outside of the capillary membranes. After a while a layer will be formed that reduces the flux.

Backflush mode

Periodically the pressure at the permeate side is raised. The permeate flow through the membrane is reversed and removes the fouling layer. Meanwhile the suspension keeps on circulating to carry the removed layer away.

Figure 4: *Schematic representation of the difference between the filtration mode and the backflush mode.*

In the microfiltration process another possibility for cleaning the membrane surface during operation is the so-called backflush technique (figure 4). During filtration the direction of the permeate flow in the membrane is reversed from time to time, so that the backflushed permeate can remove an eventually formed cake layer. The result is that the net permeate flux is on a much higher level as without backflushing, although sometimes a chemical cleaning procedure is required anyway to maintain an optimal flux (figure 5). Essential for applying this technique is that the membranes are not damaged by the backflushing process. Another requirement is that there is a low level of adsorption of components from the feed onto the membrane, since it is impossible to remove adsorbed material with the backflushing technique.

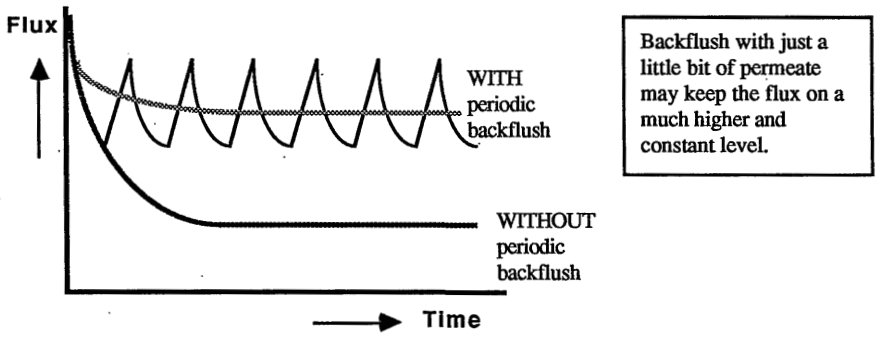

Figure 5: *The influence of backflushing on the permeate flux.*

1.4 APPLICATIONS

The commercial development of microfiltration started with the preparation of membrane filters that were used for bacterial analyses or more commonly in water microbiology and analytical applications. Today these membrane filters are used intensively [37,38] and form a large share in the market for microfiltration membranes, however, exact amounts for the sales of membrane filters cannot be given.

Although different estimations for the world market of membranes are presented in literature, there is a good agreement that microfiltration together with dialysis (hemodialysis) are the largest market sectors for membrane separation technologies. The annual growth rate for microfiltration equipment is estimated between 10 and 15 %.

Dead-end microfiltration is a large market sector representing 20 % of the total membrane market ($ 530M in 1987) in Europe [39]. The cross-flow processes of reverse osmosis , ultrafiltration and microfiltration account for 15 % of the total market with a combined value of $ 80M and an annual grow rate of 13 % [39] .

In general the cross-flow microfiltration process is used for purification, concentration and recycling [40]. Without trying to be complete a number of applications is listed below:

- Production of ultrapure water for the semi-conductor industry
- Cold sterilization of beverages and pharmaceuticals
- Pre-treatment for ultrafiltration or reverse osmosis processes
- Metal recovery: metals are precipitated as oxides or hydroxides and the colloidal particles are retained by microfiltration membranes
- Waste water clean-up
- Harvesting and washing of cells
- Plasmapheresis, the separation of blood cells and plasma
- Fermentation broth clarification
- Fruit-juice, wine or beer clarification
- Manure treatment
- Finely-divided catalyst recovery and recycle
- Pigment slurry concentration
- Latex dewatering
- Crude-oil concentration in product water
- Oil-water emulsion separation

Membrane distillation [41] is an application for hydrophobic microfiltration membranes. The characteristics of membrane distillation can be condensed to one important point, being that the permeant is transported as a vapour through the pores of a hydrophobic microfiltration membrane that is at least at one side in direct contact with the liquid. The hydrophobic nature is essential in this separation process to prevent wetting of the membrane, which acts as an interface between feed and permeate. The transport mechanism of membrane distillation involves three steps:

-1- Evaporation at the feed side of the membrane
-2- Transport of the vapour through the pores
-3- Condensation of the vapour at the permeate side of the membrane

Most applications of membrane distillation concern desalination of saline water and separating

organic aqueous solutions, e.g., the separation of ethanol and water [42]. A very interesting large-scale application of membrane distillation is the use of hydrophobic microporous materials in rain coats, ski jackets, jogging suits, footwear, protecting clothes etc. These hydrophobic microporous materials (e.g., the Gore-Tex ® stretched polytetrafluoroethylene) are breathable and waterproof since water vapour can permeate through the hydrophobic material while water droplets can not.

An example of a very new development for microfiltration membranes is the application in medical diagnostic systems. X-Flow, Enschede, The Netherlands, in combination with the University of Twente, Enschede, The Netherlands, developed a special type of microfiltration membrane that can be used for the separation of blood cells and plasma in small blood samples using a very simple filtration device. This membrane is incorporated in a system, developed by Prime-Care, which is used for the determination of the cholesterol content in human blood [43].

Another new application for microfiltration membranes is the use of microporous polyurethane membranes as an artificial skin [44]. Some advantages of the microporous artificial skin are that it adheres directly and firmly to the wound surface, allows adequate drainage through the membrane, prevents bacterial invasion, and reduces treatment time and pain. Furthermore the artificial skin is easy to handle, it can be sterilized by conventional techniques and is cost effective in reducing nurse and physician time due to direct visual wound inspection through the transparent material and the elimination of dressing changes during the healing process.

1.5 STRUCTURE OF THIS THESIS

An important conclusion from the development described above is that the impact of the microfiltration technique in the process industry would be of more importance if hydrophilic membranes with a high chemical and thermal resistance and better performances were available. In 1983 the Dutch government started an Innovation Oriented Program on Membranes (IOP-m), which funded membrane research at Dutch universities and research institutes, incorporating also industrial participations. One of the projects incorporated the development of a microporous hydrophilic capillary membrane and the design of a capillary membrane module. The investigations resulting in a patent [45] on the one-step preparation of hydrophilic microporous membranes from a polymer blend are described in this thesis.

In chapter 2 the membrane formation of the quaternary system polyetherimide (PEI)/ polyvinylpyrrolidone (PVP)/ N-methyl-2-pyrrolidone (NMP)/ water is described.

Polyetherimide

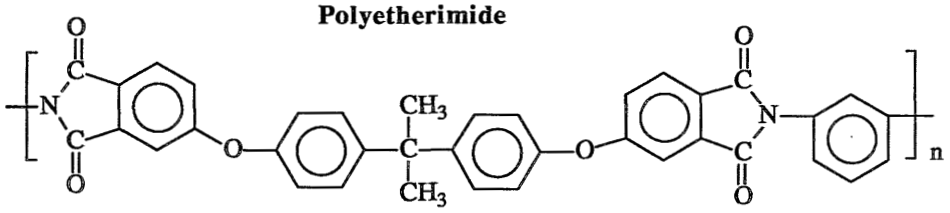

Polyvinylpyrrolidone

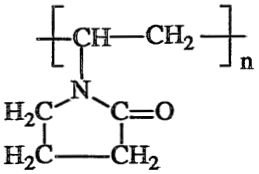

N-Methyl-2-pyrrolidone

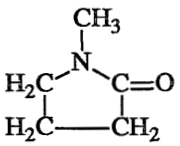

The four component system is characterized by thermodynamic and kinetic measurements. Especially the influence of PVP has been investigated. It is shown that the addition of PVP to the polymer solution will decrease the rate of the diffusion processes that occur during membrane formation. During the immersion precipitation of the four component membrane forming system some PVP will dissolve in the coagulation bath, but an appreciable amount of PVP will be present in the membrane matrix. The presence of PVP in the polymer membrane matrix plays an important role in the mechanism that leads to the formation of an interconnected pore structure. This mechanism also causes the formation of open microporous toplayers.

The results of the addition of PVP to the spinning solution and the influence of the spinning conditions on the formation of microporous capillary membranes is described in chapter 3. The pore size and porosity in the outer surface can be controlled by the temperature of the external coagulation bath and the residence time in the airgap. The control of the pore size at the inner surface is achieved by using mixtures of solvent and nonsolvent as the internal coagulation bath. In addition the influence of the composition of the internal coagulation bath on the shape of the bore of the capillary membrane is discussed.

The interaction between PEI and PVP is strong. This effect is demonstrated in chapter 4, in which homogeneous membranes are compared with porous membranes obtained by immersion precipitation, by measuring the outdiffusion rate of PVP and the glass transition temperatures. PEI and PVP form homogeneous blends as is demonstrated by glass transition measurements. The glass transition temperatures of PEI - PVP blends are higher than the weight average glass transition temperatures, which indicates that a strong interaction between the two polymers exists.

A porous phase inversion membrane, which is formed by immersion precipitation, contains a considerable amount of PVP. The concentration of PVP in the membranes is dependent on the concentration of PVP in the casting or spinning solution and also on the molecular weight of the PVP.

The PVP in the polymer membrane matrix will considerably swell, so that part of the pores will be blocked and when the membranes are used for filtration of aqueous solutions no permeability for water can be observed for untreated membranes. This means that a certain post-treatment is necessary to avoid swelling of the PVP in the polymeric membrane matrix and consequently to obtain permeabilities of the membranes that are in agreement with the pore size and porosity as can be observed with the scanning electron microscope (SEM). In chapter 5 different post-treatment methods for the porous membranes are described. It is shown that the PEI -PVP membranes are hydrophilic after the post-treatment, and that the PVP in the membranes is located at the surface of the pore walls.

To investigate the influence of the presence of PVP on the nonfouling properties of the PEI-PVP membranes, adsorption experiments are performed with bovine serum albumin (BSA). In chapter 6 flat PEI-PVP membranes were exposed to BSA solutions and the pure water flux was measured before and after BSA adsorption. The amount of adsorbed BSA was measured using radiolabeled ^{14}C BSA. The permeation experiments and the adsorption measurements are in very good correlation; it clearly demonstrates that the presence of PVP improves the nonfouling properties of the PEI-PVP membranes.

Some theoretical studies that may result in a new design of microfiltration modules with capillary membranes are presented in chapter 7 and 8. In chapter 7 it is shown that it may have an energetic advantage if the feed flow is at the outer surface of the capillary membrane (shell-side fed modules). Three different flow conditions of the feed in a module with capillary membranes are compared, i.e., flow of the feed through the bore of the capillary membranes, longitudinal flow of the feed in shell-side fed modules (i.e., flow direction parallel to the length axis of the capillary membranes) and transverse flow of the feed in shell-side fed modules (i.e., perpendicular to the length axis of the capillary membranes). The most favourable configuration is the transverse flow of the feed in shell-side fed modules.

In chapter 8 a model is presented to calculate the pressure drop in the bore of capillary membranes during filtration and during backflushing in shell-side fed modules. This model is experimentally verified by performing clean water experiments. The model can be used for the determination of the optimal length and diameters of the capillary membranes.

1.6 ACKNOWLEDGEMENT

The author likes to thank I. Blume for his contribution to this chapter.

1.7 REFERENCES

1 C. Gelman, Microporous membrane technology Part I. Historical development and applications, Analytical Chemistry, **37**(1965) 29.

2 J. W. F. Spitzen, Pervaporation - membranes and models for the dehydration of ethanol, PhD Thesis Chapter 1, University of Twente, Enschede, The Netherlands (1988).

3 H.K. Lonsdale, The growth of membrane technology, J. Membr. Sci., **10** (1982) 81.

4 H. Strathmann, Membrane separation processes, J. Membr. Sci., **9** (1981) 121.

5 M.C. Porter, Microfiltration, Synthetic membranes: Science, Engineering and Applications, P.M. Bungay et al. (Eds.), D. Reidel Publishing Company, (1986) 225.

6 R.A. Terpstra, B.C. Bonekamp and H.J. Veringa, Preparation, characterization and some properties of tubular alpha alumina ceramic membranes for microfiltration and as a support for ultrafiltration and gas separation membranes, Desalination, **70** (1988) 395.

7 H.L. Fleming, Latest developments in inorganic membranes, presented to 1987 BCC Membrane planning conference, Cambridge, Massachusetts, October 20 - 22 (1987).

8 R. Bertera, H. Steven, M. Metcalfe, Development of crossflow microfiltration, The Chemical Engineer, June (1984) 10.

9 R.E. Kesting, Synthetic polymer membranes, Mc Graw Hill, New York (1972).

10 D.M. Koenhen, M.H.V. Mulder and C.A. Smolders, Phase separation phenomena during the formation of asymmetric membranes, J. Appl. Polym. Sci., **21** (1977) 119.

11 L. Broens, D.M. Koenhen and C.A. Smolders, On the mechanism of formation of asymmetric ultra- and hyperfiltration membranes, Desalination, **22** (1977) 205.

12 L. Broens, F.W. Altena, C.A. Smolders and D.M. Koenhen, Asymmetric structures as a result of phase separation phenomena, Desalination, **32** (1980) 33.

13 P.M. van der Velden and C.A. Smolders, New cation-exchange membranes for hyperfiltration processes, J. Appl. Polym. Sci., **21** (1977) 1445.

14 F.W. Altena and C.A. Smolders, Phase separation phenomena in solutions of cellulose acetate. I- Differential scanning calorimetry of cellulose acetate in mixtures of dioxane and water, J. Polym. Sci. Polym. Symp., **69** (1981) 1.

15 F.W. Altena and C.A. Smolders, Calculation of liquid-liquid phase separation in a ternary system of a polymer in a mixture of a solvent and a nonsolvent, Macromolecules, **15** (1982) 1491.

16 J.G. Wijmans, F.W. Altena and C.A. Smolders, Diffusion during the immersion precipitation process, J. Polym. Sci. Polym. Phys., **22** (1984) 519.

17 J.G. Wijmans, J.P.B. Baaij and C.A. Smolders, The mechanism of microporous or skinned membranes produced by immersion precipitation, J. Membr. Sci., **14** (1983) 263.

18 M.H.V. Mulder, J. Oude Hendrikman, J.G. Wijmans and C.A. Smolders, A rationale for the preparation of asymmetric pervaporation membranes, J. Appl. Polym. Sci., **30** (1985) 2805.

19 A.J. Reuvers, J.W.A. van de Berg and C.A. Smolders, Formation of membranes by means of immersion precipitation. Part I. A model to describe mass transfer during immersion precipitation, J. Membr. Sci., **34** (1987) 45.

20 A.J. Reuvers and C.A. Smolders, Formation of membranes by means of immersion precipitation. Part II. The mechanism of formation of membranes prepared from the system celluloseacetate/acetone/water, J. Membr. Sci., **34** (1987) 67.

21 J.A. van 't Hof, Wet spinning of hollow fibre membranes for gas separation, PhD thesis, University of Twente, Enschede, The Netherlands (1988).

22 M.A. Frommer and D. Lancet, Reverse osmosis membrane research, H.K. Lonsdale and H.E. Podall (Eds.), Plenum Press, New York (1972) 85.

23 H. Strathmann and K.Koch, The formation mechanism of phase inversion membranes, Desalination, **21** (1977) 241.

24 S. Sourirajan and B. Kunst, Synthetic membranes, S. Sourirajan (Ed.), National Research Council Cananda, Ottawa (1979) 129.

25 T.J. van Gassel and S. Ripperger, Crossflow microfiltration in the process industry, Desalination, **53** (1985) 373.

26 W. Klein and W. Hoelz, Crossflow filtration in chemical processes, The Chemical Engineer, Oktober 1982.

27 Membrane and Separation Technology News, BBC, Inc., Norwalk, July (1985).

28 D. Defrise and V. Gekas, Microfiltration membranes and the problem of microbial adhesion, Process Biochemistry, August (1988) 105.

29 a. I. Cabasso, E. Klein, J. K. Smith, Polysulfone hollow fibers. I. Spinning and properties, J. Appl. Polym. Sci., **20** (1977) 2377.
b. ibid, **21** (1977) 165.

30 A.S. Michaels and S.L. Matson, Membranes in biotechnology: state of the art, Desalination, **53** (1985) 231.

31 F.F. Stengaard, Characteristics and performance of new types of ultrafiltration membranes with chemically modified surfaces, Desalination, **70** (1988) 207.

32 K.J. Kim, A.G. Fane and C.J.D. Fell, The performance of ultrafiltration membranes pretreated by polymers, Desalination, **70** (1988) 229.

33 F. Vigo, C. Uliana and G. Dondero, Ultrafiltration membranes obtained by polyacrylonitrile grafted onto polyvinyl chloride, Desalination, **70** (1988) 277.

34 P. Aptel and M. Clifton, Ultrafiltration, Synthetic membranes: Science, Engineering and Applications, P.M. Bungay et al. (Eds.), D. Reidel Publishing Company (1986) 249.

35 K. H. Kroner and V. Nissinen, Dynamic filtration of microbial suspensions using an axially rotating filter, J. Membr. Sci., **36** (1988) 85.

36 G. Schock, Mikrofiltration an überströmten Membranen, PhD Thesis, Rheinisch - Westfälische - Technische Hochschule, Aachen, West - Germany (1985).

37 T. D. Brock, Membrane filtration, Science Tech. Inc., Springer-Verlag Berlin Heidelberg New York (1983).

38 Membrane filtration: applications, techniques and problems, B. J. Dutka (Ed.), Marcel Deker Inc., New York and Basel (1981).

39 D. A. Laidler, The state of membrane science and technology in Europe, paper presented at the sixth annual membrane technology/planning conference, Boston, November 1-3 (1988).

40 S.L. Michaels, Crossflow microfilters, Chemical Engineer, **96** (1989) 84.

41 A.C.M. Franken, Membrane distillation - a new approach using composite membranes, PhD Thesis Chapter 1, University of Twente, Enschede, The Netherlands (1988).

42 A.C.M. Franken, J.A.M. Nolten, M.H.V. Mulder and C.A. Smolders, Ethanol/water separation by membrane distillation: effect of temperature polarization, pages 531 - 540. In: B. Sedlacek and J.Kahovec (Eds.), Synthetic polymeric membranes, De Gruyter, Berlin (1987).

43 Membraantechnologie 3, Programmacommissie Membraantechnology (PCM), Stam Tijdschriften B.V., November/December 1988

44 E. J. C. M. P. Lommen, Artificial skin, PhD Thesis, University of Groningen, Groningen, The Netherlands (1988)

45 US Patent 4.798.847 (17 January 1989), H.D.W. Roesink, D.M. Koenhen, M.H.V. Mulder and C.A. Smolders (assigned to X-Flow B.V., Enschede, The Netherlands).

CHAPTER 2

DEMIXING PHENOMENA AND MEMBRANE FORMATION IN THE FOUR COMPONENT SYSTEM POLYETHERIMIDE/ POLYVINYLPYRROLIDONE/ N-METHYLPYRROLIDONE/ WATER

H.D.W. Roesink, M.J. Otto[¥], J.A. Ronner, M.H.V. Mulder and C.A. Smolders

¥ - AKZO, Research laboratories, Arla CRT, Velperweg 76, PO Box 9300, 6800 SB Arnhem, The Netherlands.

2.1 SUMMARY

In this chapter thermodynamic and kinetic data on the demixing phenomena in the four component system PEI/PVP/NMP/H_2O are coupled with the membrane formation properties for that system. Phase separation experiments leading to a complete demixing into two liquid layers show that PVP is sometimes present in appreciable amounts in the polymer rich phase. Using kinetic data, light transmission experiments and leaching-out rates of PVP during precipitation, it can be deduced that during membrane formation a considerable amount of PVP must be entrapped in the polymer matrix.

From the study of the morphology of the membranes obtained it is shown that addition of PVP to the membrane forming system PEI/NMP/H_2O promotes the formation of an open interconnected pore structure in the sublayer of the microporous membrane as well as an open surface layer. A possible explanation for these effects is given in terms of a post-treatment effect, following the non equilibrium end-state of demixing. A cryogenic sample preparation technique (discussed in the appendix) in combination with the use of scanning electron microscopy made these effects visible. Finally the influence of PVP on the macrovoid formation has been investigated and discussed.

2.2 INTRODUCTION

Phase inversion processes are important for preparing synthetic polymeric membranes. Starting with a polymer solution, which is precipitated in a nonsolvent coagulation bath or is cooled down, all kinds of morphologies can be obtained by variation of relevant parameters.

The starting point for membrane preparation by phase inversion is a ternary system, consisting of a polymer, a solvent and a nonsolvent. To improve the performance, mechanical properties or wettability of the membranes it is often necessary to apply additives. Therefore, in practice mostly

multi component membrane forming systems are used. Polyvinylpyrrolidone (PVP) is one of the high molecular weight additives that is often used. When PVP is added to a polyetherimide (PEI) solution and films are cast with this solution, PVP will contribute to the polymeric membrane matrix despite the solubility of PVP in the coagulation bath (see also [1]).
As has been reported by others [2-8] and as will be shown in this chapter the addition of PVP can improve the membrane characteristics with respect to:

- micropores in the toplayer
- interconnectivity of the pores in the supporting sublayer
- prevention of macrovoid formation
- hydrophilicity (wettability)

In this chapter the influence of PVP on the membrane forming properties of the quaternary system PEI/PVP/NMP/H_2O will be investigated. Therefore the demixing phenomena of this system are compared with those of the ternary system PEI/NMP/H_2O.
The location of the binodal in the ternary system is determined using the titration method and light scattering measurements (turbidity method). The location of the binodal of the four component system has also been measured and compared with that of the ternary system. In addition composition analysis is done of the polymer (PEI) poor and the polymer (PEI) rich phase of a demixed four component solution PEI/PVP/NMP/H_2O to investigate whether PVP is present in the polymer rich phase.
Light transmission experiments according to Reuvers et al. [9,10] are performed to obtain more information about the type of demixing: instantaneous or delayed demixing. By measuring the concentration of PVP in the coagulation bath as a function of the immersion time it is shown that residual PVP must be present in the polymer matrix.
The morphology of the membranes is discussed in relation to the presence of PVP in the polymer solution and in the membrane matrix. PVP plays a very important role in the formation of an interconnected structure and in the microporous character of the toplayer as will be demonstrated in the section on the morphology of the membranes.
The role of PVP and some other process parameters in the formation of macrovoids will be discussed in accordance with the theory proposed by Reuvers [11].

2.3 BACKGROUND

2.3.1 The phase inversion process

In this work two phase inversion [12] processes will be discussed:

-1- *Immersion precipitation;* a cast or spun polymer solution is immersed in a nonsolvent coagulation bath and the polymer precipitates as a result of nonsolvent inflow and solvent outflow.

-2- *Phase inversion from the vapour phase;* a nonsolvent from the vapour phase penetrates the polymer solution and the polymer demixes and finally precipitates at high enough nonsolvent concentrations. In this work phase inversion in the vapour phase is applied to induce demixing processes in the polymer solution without solvent outflow; this facilitates formation of pores in the toplayer of the membranes. After the initiation of phase inversion in the vapour phase the ultimate membrane is obtained by immersion precipitation in water; during the latter process the polymer precipitates

In 1977 Koenhen et al. [13] were the first to show that two different types of phase separation determine the morphology of phase inversion membranes:

- gelation or aggregate formation at high polymer concentrations and low nonsolvent content

- liquid/liquid demixing followed by gelation at low polymer concentration and varying nonsolvent content

The results of these two different types of phase separation can be distinguished in an asymmetric membrane as is shown on an electron micrograph in figure 1.

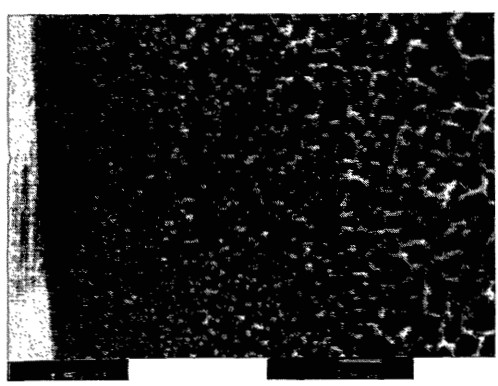

Figure 1: *Electron micrograph of an asymmetric PEI-membrane. Toplayer at the left hand side.*

This membrane was obtained by direct immersion of a polymer solution in a nonsolvent coagulation bath. At the interface of the coagulation bath and the polymer solution a rapid solvent outflow causes an increased polymer concentration, which results in a dense toplayer (by gelation or aggregate formation; see below). The separation characteristics of the membranes obtained are dependent on the structure of the toplayer: dense or porous. Reuvers [11] distinguished two types: type I membranes (formed by the mechanism of delayed onset of liquid-liquid demixing), which are mostly characterized by a gas separation, reverse osmosis or pervaporation type of performance and type II membranes (formed by the mechanism of instantaneous liquid-liquid demixing), which are characterized by a very thin toplayer and by an ultrafiltration type of performance.
The formation of the concentrated polymer layer hinders a further rapid outflow of solvent and the result is that in the future support layer of the membrane another type of phase separation occurs: liquid-liquid demixing, which results in a porous structure as can be seen in figure 1.
In general three modes of liquid-liquid demixing can be distinguished:

-1- nucleation and growth of the polymer rich phase
-2- nucleation and growth of the polymer poor phase
-3- spinodal decomposition

It is assumed that mode -3- does not occur during membrane formation since the spinodal region is only reached if the metastable region is passed. In the metastable region liquid-liquid demixing takes place and it is believed that this process is very fast [13]. A schematic representation of the demixing process in a ternary phase diagram is given in figure 2.

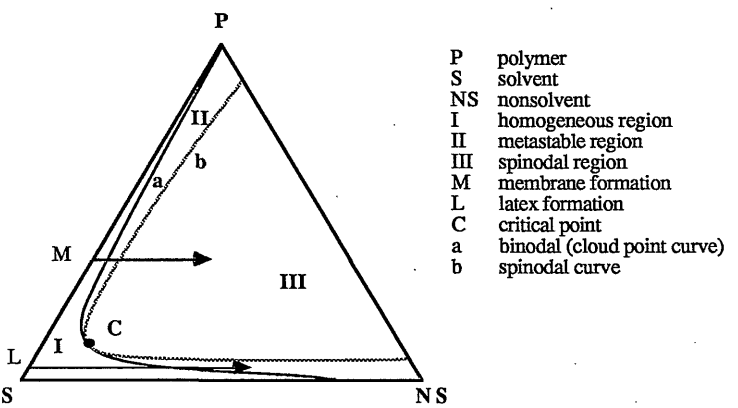

Figure 2: *Schematic representation of membrane and latex formation in a ternary phase diagram.*

Earlier workers from our institute, e.g., Koenhen [13], Broens [14] and Reuvers [15] already gave comprehensive descriptions of the membrane forming process in relation to the ternary phase diagram.

Whether mode -1- or mode -2- occurs depends on the location of the critical point in the ternary phase diagram. Only at rather low polymer concentrations mode -1- can be found. This leads to spheres of the polymer rich phase in a continuous dilute solution: a latex is formed. Mode -2- is more important for membrane formation since it leads to a continuous polymer matrix in which spherical pores, filled with the polymer poor phase are dispersed (see figure 2). For a maximal membrane performance it is important that the polymer poor phase also forms a continuous phase.

It has to be emphasized that in this thesis the polymer poor phase contains a considerable amount of PVP and that the polymer rich phase consists of two polymers as will be demonstrated later on. Polymer rich and polymer poor is defined here as rich and poor in polyetherimide.

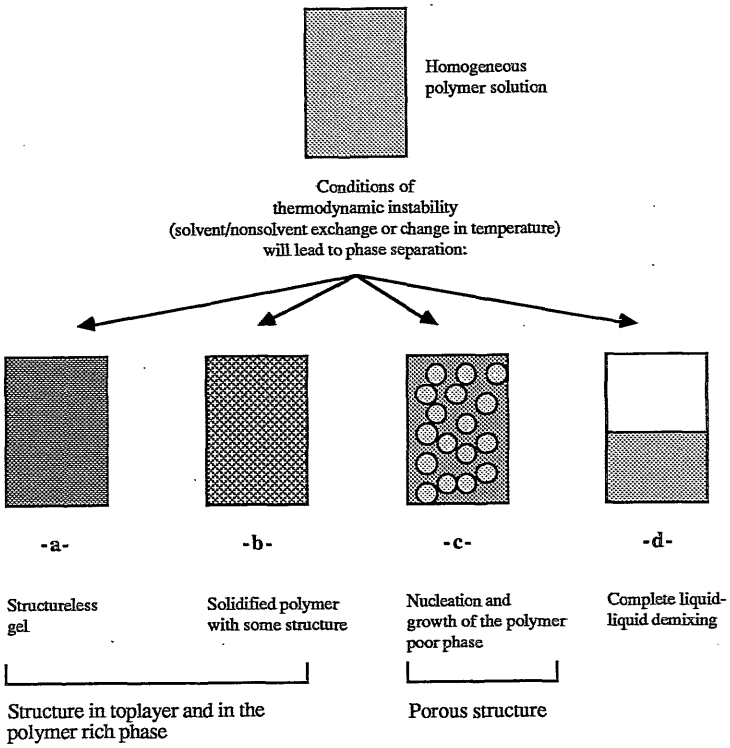

Figure 3: *Schematic representation of the different possibilities for phase separation in a homogeneous polymer solution.*

In figure 3 the following possibilities for phase separation in a homogeneous polymer solution are schematically represented:

-**a**- amorphous gelation
-**b**- gelation with some kind of structure: crystallization, aggregate formation, nodular structure formation.
-**c**- nucleation and growth of the polymer poor phase (kinetically frozen state)
-**d**- complete separation into two liquid layers upon liquid-liquid demixing (equilibrium state)

At high polymer concentrations phenomena -**a**- and -**b**- will occur readily. It can be found in the toplayers of membranes formed by immersion precipitation and in the continuous membrane matrix of the support layers. Whether -**a**- or -**b**- occurs depends on the nature of the polymer and on the process parameters.
Phenomenon -**c**- is basically the origin of the porous membrane structure and it will occur at moderate and low polymer concentrations. In fact this is not an equilibrium state. The equilibrium state of the liquid-liquid demixing is -**d**-: the polymer solution is separated into two separate liquid layers. The porous membrane structure is a non-equilibrium state of liquid-liquid demixing and it is a kinetically determined structure. When the liquid-liquid demixing process is proceeding, it will slow down and finally stop since the polymer rich phase solidifies or passes the glass transition and does not show any mobility at all.

2.3.2 Macrovoid formation

A very typical feature in membranes obtained by means of immersion precipitation, is the presence of large conical voids (macrovoids) with a length of several micrometers to sometimes the total thickness of the membrane. Reuvers [11] presented an extended survey of the different formation mechanisms of macrovoids. Based on empirical rules he formulated a model for the formation of macrovoids.
Reuvers formulated the conditions to avoid macrovoid formation in ternary membrane forming systems on the basis of the two types of demixing he defined [10]:

- In *type I* the demixing step is delayed over a certain period of time after immersion of the polymer solution in the coagulation bath. During the delay time all kinds of diffusion processes occur, however no liquid-liquid demixing occurs.

- In *type II* the demixing step is instantaneous; in this type of membranes macrovoids will be

formed, except when the polymer concentration and/or the nonsolvent concentration in the casting solution are high enough.

The following process parameters can be changed so that type I membranes (without macrovoids) are obtained instead of type II membranes:

- addition of solvent to the coagulation bath
- choosing a solvent-nonsolvent pair with lower mutual interaction
- increasing the polymer concentration

According to Reuvers [11], macrovoids are in fact growing nuclei of the polymer poor phase, which will not be inhibited during their growth. The composition in front of the freshly formed nucleus should remain stable for a relatively long period of time, so that the macrovoid can grow. This condition is reached, since in between the first layer of fresh nuclei and the coagulation bath an increased concentration of the polymer solution prevents rapid further penetration of water. Also freshly formed nuclei themselves can be seen as "a coagulation bath" with a high concentration of solvent.
This means that in and around the macrovoid a condition has been created so that locally delayed demixing (type I) can occur, while the end result is that a type II membrane is formed. Reuvers [15] made calculations to describe the diffusion processes for these situations. This model presented by Reuvers [11] was already formulated in a more qualitative way by Gröbe et al. [16] and Koenhen et al. [13].

2.4 EXPERIMENTAL

Materials

Polyetherimide (Ultem ® 1000) was kindly supplied by General Electric, Bergen op Zoom, The Netherlands. Polyvinylpyrrolidone (K 90) was purchased from Janssen Chimica, Belgium. N-methyl-2-pyrrolidone (Merck, synthesis grade) was used as a solvent. The molecular weights of the polymers were determined with size exclusion chromatography, the results are shown in table 1.

Table 1 *Physical constants of the components used.*

Component	density (g/cm^3)	molecular weight (M_w)
Polyetherimide (PEI)	1.27 (a)	32 800
Polyvinylpyrrolidone (PVP)	1.22 (b)	423 000
N-methyl-2-pyrrolidone (NMP)	1.03	99
Water (H_2O)	1.00	18

a - according to product information of General Electric
b - in literature values between 1.20 and 1.30 can be found

Determination of the cloud points

The cloud points for the system PEI/NMP/H_2O were measured using two different techniques: titration and light scattering upon cooling (turbidity method). Both methods are described by Wijmans et al. [17]. The titration method was used for low concentrations, while the light scattering method was used for high PEI concentrations (7.9 wt. % and 24.6 wt. %).
The cloud points for the four component system PEI/PVP/NMP/H_2O were also determined using the titration method (low concentrations) and light scattering measurements. These experimentally determined cloud points constitute the binodal.

The titrations were carried out in a vessel, provided with a nitrogen atmosphere and kept at a constant temperature of 20 °C. Since it took a long time before the polymer solution became homogeneous again after adding a solvent/nonsolvent mixture, the cloud point was supposed to be reached if the polymer solution stayed turbid for more than half an hour.
The cloud points determined with the light scattering method were measured at different temperatures and the cloud points at 20 °C were found by interpolation.

Analyses of the polymer rich and polymer poor phase in the four component system PEI/PVP/NMP/H_2O

Different amounts of water were added to polymer solutions with 5 wt. % total polymer; the weight ratio of PEI to PVP was 3:2. The conical flasks containing the polymer solutions were heated (70 -

90 °C) untill the solutions became clear (homogeneous solution). After this procedure the polymer solutions were cooled and kept at a constant temperature of 20 ± 0.2 °C. During the cooling process a two phase system was formed. It took some time before the two phases were separated completely and the phases were clear. The concentration determinations were done after two weeks. The two phases were separated and analysed. The NMP and water were evaporated at low pressure (0.02 mbar) and at a temperature of 100 °C. The vapours were condensed with liquid nitrogen. The water concentration in the condensed phase was determined using the Karl-Fischer method. The ratio of PEI to PVP in each phase was determined using NMR-analysis.

Membrane preparation

Membranes were prepared using three different methods:

-1- Hand casting: a polymer solution is cast on a glass plate and immersed in a nonsolvent coagulation bath.
-2- Machine casting: a polymer solution is cast on a nonwoven and, after a certain residence time in an airgap (phase inversion from the vapour phase), immersed in a nonsolvent coagulation bath.
-3- Spinning: a polymer solution is extruded through a spinneret and immersed in a nonsolvent coagulation bath. This process is described in chapter 3 in full detail [18].

One of the advantages of the machine casting and the spinning process is that a well defined phase inversion in the vapour phase can be obtained.

Sample preparation for scanning electron microscopy

The sample preparation techniques are discussed in the appendix (see 2.7).

Outdiffusion experiments

Hand cast flat polymer films were immersed in a water bath. The water bath was stirred and kept at a constant temperature of 25 °C. From time to time samples were taken to determine the PVP concentration in the coagulation bath. The concentration of PVP in the aqueous solutions were determined colorimetrically [1,19,20].

2.5 RESULTS AND DISCUSSION

2.5.1 Thermodynamics

2.5.1.1 *Ternary system PEI/NMP/H_2O*

Results of the cloud point measurements for the ternary system PEI/NMP/H_2O are shown in table 2.

Table 2 *Cloud point compositions measured by titration and by light scattering experiments.*

Temperature (°C)	PEI (wt. %)	NMP (wt. %)	H_2O (wt. %)	Molar ratio NMP/H_2O
		Titration		
20.2	0.4	94.1	5.5	3.1
20.6	1.9	93.1	5.0	3.4
20.5	3.7	91.3	5.0	3.3
20.9	5.7	89.4	4.9	3.3
20.8	7.6	87.6	4.8	3.3
20.0	9.4	86.0	4.6	3.4
20.1	11.7	83.9	4.4	3.5
		Light scattering		
20.0	7.9	87.2	4.9	3.2
20.0	24.6	71.7	3.7	3.5

In the ternary phase diagram in figure 4, which is constructed with the results given in table 2, it is demonstrated that the binodal is by approximation a line through the polymer point of the ternary phase diagram. In fact the binodal will intersect the polymer-nonsolvent axis at the point corresponding with a weight fraction of 0.0125 water (General Electric, product information about swelling experiments with water).This result also can be found for other ternary systems where nonsolvent has a very low interaction with the polymer, such as the membrane forming system polysulfone(PSf)/dimethylacetamide(DMAc)/H_2O [17,21]. In this system a shift of the binodal can be observed if other nonsolvents are used. The binodal for the system PSf/DMAc/Ethanol is shifted to the polymer-nonsolvent axis. Mulder et al. [21] explained this shift by changes in the thermodynamic interaction parameters between polymer (3) and nonsolvent (1) (χ_{13} decreases, meaning a better interaction) and between the nonsolvent (1) and solvent (2) (g_{12} increases).
In the situation that the binodal (cloud point curve) intersects the polymer-nonsolvent axis approximately at the polymer point, the ratio of solvent (S) to nonsolvent (NS) is constant for

compositions at the binodal (at least at the rising branche). This is shown by Kimmerle [22], who also proposed a kind of physical model, in which he suggested that due to the specific interactions of polymer, solvent and nonsolvent, every nonsolvent molecule has to be surrounded by a certain amount of solvent molecules to inhibit interaction between nonsolvent and polymer molecules and consequently prevent phase separation in the polymer solution.

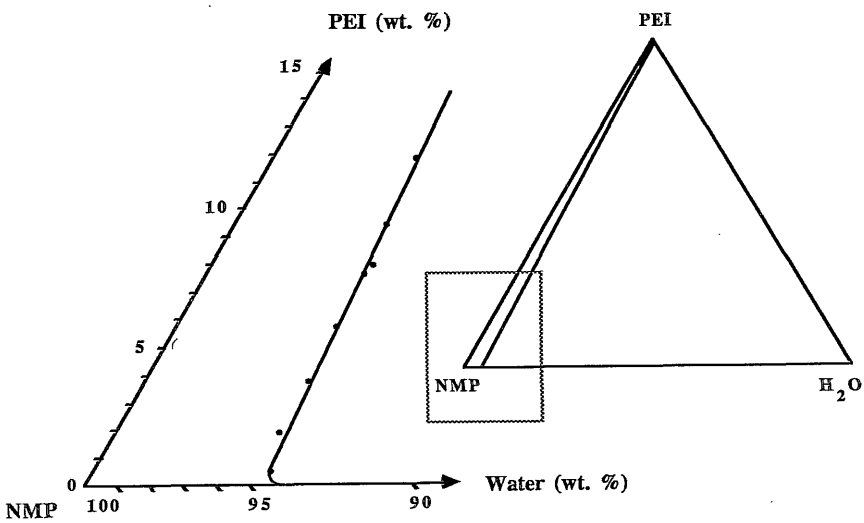

Figure 4: Cloud points in the ternary system PEI/NMP/H_2O measured by titration at 20 °C.

2.5.1.2 Quaternary system PEI/PVP/NMP/H_2O

The hydrophobic polymer polyetherimide and the hydrophilic, water soluble polymer polyvinylpyrrolidone are compatible polymers and form homogeneous blends [1]. The compatibility of PEI and PVP is a necessary condition for using PVP as an additive in the membrane forming system. Cloud point measurements were done with PEI/PVP/NMP/ H_2O solutions and a constant initial PEI /PVP ratio of 1.
The results are given in table 3.

Table 3 *Cloud point compositions of the quaternary system PEI/PVP/NMP/H_2O.*

Temperature (°C)	PEI (wt. %)	PVP (wt. %)	NMP (wt. %)	H_2O (wt. %)	Molar ratio NMP/H_2O	Molar ratio NMP/(H_2O+PVP)
			Titration			
21.0	0.6	0.6	93.3	5.5	3.1	3.0
20.4	0.9	0.9	92.9	5.3	3.2	3.1
20.4	1.1	1.1	92.6	5.2	3.2	3.1
20.9	1.3	1.3	92.2	5.2	3.2	3.1
20.7	1.9	1.9	91.4	4.8	3.5	3.3
21.0	2.2	2.2	91.0	4.6	3.6	3.3
21.2	2.9	2.9	90.3	3.9	4.2	3.8
20.9	3.5	3.5	89.5	3.5	4.6	4.0
21.4	3.8	3.8	89.1	3.3	4.9	4.1
20.6	4.4	4.4	88.3	2.9	5.5	4.4
20.6	4.8	4.8	87.6	2.8	5.7	4.5
20.1	5.6	5.6	86.3	2.5	6.3	4.6
20.7	7.1	7.1	83.7	2.1	7.2	4.7
			Light Scattering			
23	17.4	17.4	63.6	1.6	7.2	2.6

When the results for the ternary and the quaternary system are compared, the first conclusion is that in the quaternary system less water is necessary to start the demixing process. A comparison of some results has been made in table 4. In this table it can be seen that when the total polymer concentration is constant but half of the PEI is substituted by PVP the demixing starts with less water (compare 1 and 2 and also 3 and 4). When the concentration of PEI is constant but PVP is added, again less water is necessary to start demixing (compare 1 and 4).

Table 4 *Comparison of some cloud point results in table 1 and table 3.*

Nr:	PEI (wt. %)	PVP (wt. %)	Total polymer (wt. %)	NMP (wt. %)	H_2O (wt. %)
1	5.7	-	5.7	89.4	4.9
2	2.9	2.9	5.8	90.3	3.9
3	11.7	-	11.7	83.9	4.4
4	5.6	5.6	11.2	86.3	2.5

The conclusion from table 4 is that addition of PVP decreases the amount of water necessary for incipient demixing. It is remarkable that if PVP is considered as a nonsolvent in the quaternary system and the ratio of solvent and total nonsolvent is calculated, while for PVP the molecular weight of the monomer unit is used, a ratio of S/NS of 2.6-2.8 (see table 3 and table 5) is found for high concentrations of polymer. This is in reasonable agreement with the S/NS ratio of 3.5, which is found for the ternary system, although PVP cannot be considered as a nonsolvent since PEI and PVP are compatible over the whole composition range. Probably water changes the interaction between PEI and PVP.

Table 5 *Influence of the temperature on the cloud points for the quaternary system PEI/PVP/NMP/H_2O. The data at 20 °C are found by extrapolation.*

Temperature (°C)	PEI (wt.%)	PVP (wt.%)	NMP (wt. %)	H_2O (wt. %)	Molar ratio NMP/H_2O	NMP/(H_2O+PVP)
20	17.4	13.0	67.4	2.2	5.6	2.8
50	17.4	13.0	67.5	2.1	5.8	2.9
75	17.4	13.0	67.7	1.9	6.5	3.1
95	17.4	13.0	67.9	1.7	7.3	3.2
115	17.4	13.0	68.1	1.5	8.3	3.4

The influence of the temperature on the cloud points was also investigated. The experiments were done with the solution PEI/PVP/NMP=17.4/13.0/69.4. The results are shown in table 5 and most remarkable is the fact that at higher temperatures less water is necessary to start demixing. The solutions with 1.5 - 2.1 wt % water were clear at room temperature but became turbid after heating. These cloud points are given in table 5. This indicates that a lower critical solution temperature (LCST) could be present. On the other hand the instability gap in case of an upper critical solution temperature (UCST) could also have a different shape.

Solutions with 2.3 and 2.5 wt. % water stayed turbid even if they were cooled to - 15 °C. From these experiments it can be concluded that the water concentration at the cloud point at 20 °C is about 2.2 wt. %.

2.5.1.3 Complete demixing in the quaternary system

When a polymer solution containing PEI and PVP is immersed in a water bath, PVP may diffuse into the water. Whether all PVP will diffuse in the water bath is an important question with respect to the membrane formation and the membrane characteristics. The porous membrane matrix obtained after immersion precipitation is not a thermodynamic equilibrium state. In fact the liquid-liquid demixing process will be retarded since the concentrated phase may solidify and finally the demixing process will stop for kinetic reasons. The precipitation kinetics will determine the ultimate membrane structure to a great extent and also the concentration of PVP in the ultimate membrane matrix depends on the kinetics of the membrane formation. The concentration of PVP that can be found in the membrane matrix is also dependent on other parameters like molecular weight of the PVP, concentration of the PVP in the casting solution and the total polymer concentration, which will be shown in chapter 4 [1].

In the experimental section (2.4) the experiments for the analyses of the polymer rich and polymer poor phase of the quaternary system have been described. It is assumed that the two liquid phases obtained, have reached an equilibrium state. The results are shown in table 6.

Table 6 *Compositions of the polymer (PEI) rich and the polymer (PEI) poor phase for complete demixing in the quaternary system PEI/PVP/NMP/H_2O. Weight ratio PEI:PVP=3:2*

Polymer solution			**Polymer poor phase**				**Polymer rich phase**			
Polymer (wt.%)	**NMP** (wt.%)	**Water** (wt.%)	**Water** (wt.%)	**Total Polymer** (wt.%)	**PEI** (wt.%)	**PVP** (wt.%)	**Water** (wt.%)	**Total Polymer** (wt.%)	**PEI** (wt.%)	**PVP** (wt.%)
5.00	90.60	4.40	4.40	5.00	3.00	2.00	4.40	5.00	3.00	2.00
5.00	90.44	4.56	4.61	4.85	2.62	2.23	4.33	5.59	5.20	0.39
5.00	90.19	4.81	4.88	4.65	2.23	2.42	4.36	6.92	6.23	0.69
5.00	90.00	5.00	5.05	4.02	1.73	2.29	4.85	8.71	7.58	1.13
5.00	89.95	5.05	5.09	4.42	1.81	2.61	4.27	9.70	8.83	0.87
5.00	89.84	5.16	5.26	3.96	1.70	2.26	4.53	11.39	11.39	-
5.00	89.78	5.22	5.35	4.07	1.71	2.36	4.65	9.59	9.59	-

When 4.40 wt.% water was added to the polymer solution no phase separation occurred. Water concentrations ≥ 4.56 wt. % gave separation into two liquid phases, which were analysed.
From these results it becomes clear that even in the equilibrium state PVP can be found in the polymer rich phase, which could indicate the possibility of preparing membranes from a PEI/PVP/NMP solution for which PVP is present in the membrane matrix.

2.5.2 Kinetics: rate of precipitation

In the previous section it has been shown that in the polymer rich phase a considerable amount of PVP (about 10 wt. % PVP upon total polymer) could be detected after complete liquid-liquid demixing at low polymer concentration in PEI/PVP/NMP/H_2O solutions. The situation during membrane formation is completely different, although liquid-liquid demixing also occurs. During immersion precipitation there is a continuous nonsolvent inflow, so that the nonsolvent concentration increases in the polymer layer during membrane formation. Other important differences are that for membrane preparation high polymer concentrations are used and that during immersion precipitation the PVP can escape from the membrane forming phase by dissolving in the coagulation bath.

Reuvers et al. [10] developed a simple method to measure the light transmission of nascent flat membranes as a function of the immersion time; Vásárhelyi et al. [9] used the same method. Using this method the differences between instantaneous and delayed demixing can be observed very easily since the onset of liquid-liquid demixing is related to the light transmission of the polymer film.

The results of the experiments using the light transmission method are shown in figure 5. In figure 5a the influence of the addition of solvent (NMP) to the coagulation bath on the light transmission of a polymer solution *without PVP* is shown. It can be observed that at a solvent concentration smaller than 90 wt. % instantaneous demixing occurs while at concentrations higher than 90 wt. % NMP in the water bath delayed demixing occurs. Note that the change from type I to type II demixing occurs within 1 wt. % difference in solvent concentration of the coagulation bath.
In figure 5b again the influence of the addition of solvent to the coagulation bath is shown on the light transmission but now a casting solution *containing PVP* is used. The conclusion is that when PVP is added to the casting solution more solvent ($\geq$ 97 wt. %) in the coagulation bath is necessary to cause delayed demixing (Type I, see section 2.3 and [11]).

These results also show that liquid-liquid demixing can be a very fast process. In chapter 4 [1] it is shown that the content of PVP that can be analysed in the polymer membrane matrix is dependent on the kinetics of the demixing process. Furthermore it is clearly shown [1] that PVP is entrapped in the polymer rich phase during the precipitation. The interaction between PEI and PVP is good and it is hard to remove PVP from the membrane matrix completely. To avoid excessive swelling of the PVP during actual membrane use and to obtain permeabilities which correspond with pore size and porosity, an additional post-treatment of the membranes is always necessary [23].

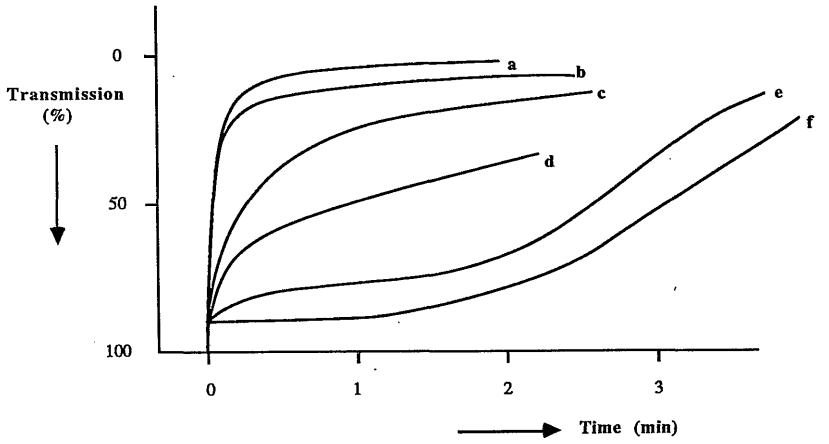

Figure 5a: *Light transmission as a function of the immersion time for different solvent concentrations in the coagulation bath (water). Casting solution PEI/NMP=15/85 (w/w). Composition of the coagulation bath (wt. % NMP): a: 0; b: 80; c: 88; d: 89; e: 90; f: 90.5;*

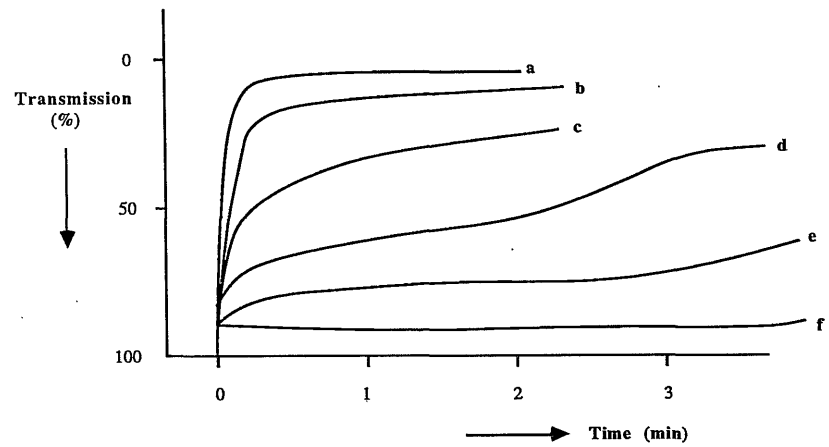

Figure 5b: *Light transmission as a function of the immersion time for different solvent concentrations in the coagulation bath (water). Casting solution PEI/PVP/NMP=15/15/70 (w/w/w). Composition of the coagulation bath (wt. % NMP): a: 0; b: 90; c: 94; d: 95; e: 96; f: 97;*

In this chapter it is shown that PVP is present in the membrane matrix by measuring the concentration of PVP in the coagulation bath as a function of the immersion time. The PVP content in the membranes is based on the PVP concentration measured in the coagulation bath. With NMR-analysis on the dry membrane itself, the same content can be found with an accuracy of 2 wt. %. More results about the outdiffusion of PVP will be presented in chapter 4 [1]. The results

obtained here are shown in figure 6. The amount of PVP that will be present in the ultimate membrane matrix is dependent on the concentration of PVP in the casting solution. The PVP content in the final membranes tends to reach a certain constant concentration for each casting solution used.

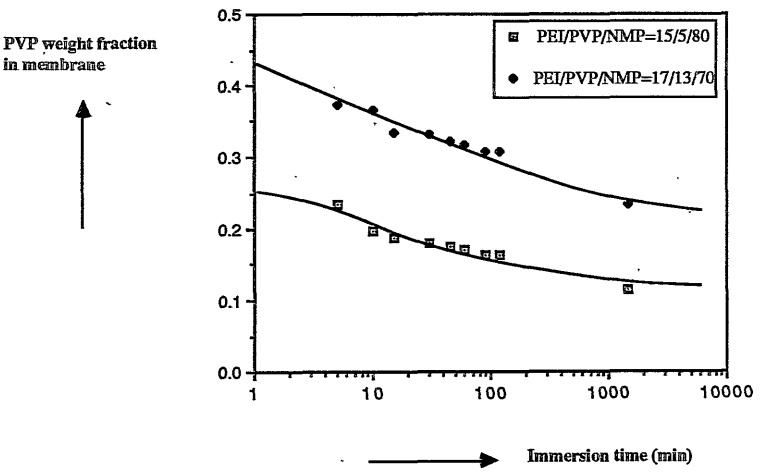

Figure 6: *Weight fraction of PVP 360 000 in the membranes for different casting solutions as a function of the immersion time in a water bath.*

One of the conclusions is that the outdiffusion of PVP is slow compared with the precipitation rate of the polymer solution, which does indicate that after the formation of a porous structure, which is a fast process, PVP is leaching out of the membrane matrix slowly.

According to the Stokes-Einstein equation the diffusion coefficients will increase if the viscosity of the polymer solution increases. Addition of PVP will increase the viscosity due to its high molecular weight and consequently the diffusion coefficients will increase. This effect is shown in figure 7. The light transmission of a cast polymer solution is measured as a function of the immersion time for different concentrations of PVP in the casting solution. In figure 7 it is shown that in all three situations a,b and c instantaneous demixing occurs, although a difference in the initial slope of the curve can be observed. This difference in the initial slope have to be ascribed to the difference in precipitation rate due to the decreasing diffusion coefficients upon adding PVP.

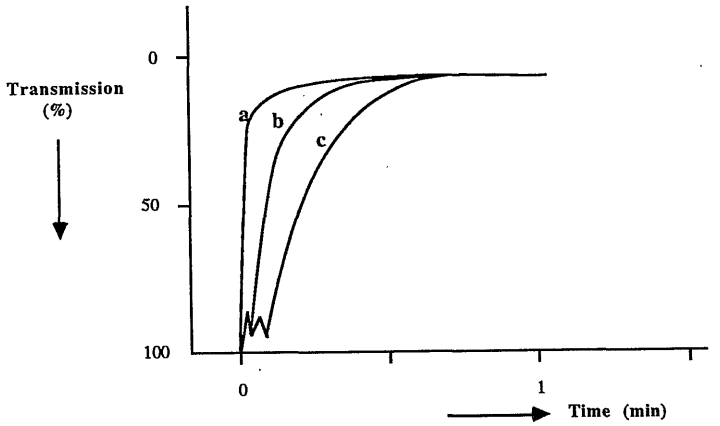

Figure 7: *Light transmission as a function of the immersion time in a water bath for different concentrations of PVP in the casting solution:*
a: PEI/PVP/NMP= 15/0/85
b: PEI/PVP/NMP= 15/15/70
c: PEI/PVP/NMP= 15/18/67

2.5.3 Morphology of the final membrane

In this section about the morphology the attention will be focussed on the interconnectivity of the pores and on the porosity of the toplayer. The quaternary systems studied can give microporous membranes. Much research work is being done to obtain microporous toplayers with pore sizes between 0.1 and 10 μm. In this chapter it will be stressed that a membrane with a microporous toplayer having a reasonable porosity and a narrow pore size distribution should have interconnected pores so that the permeability of the membranes is in agreement with pore size and overall porosity. It will be shown that the addition of PVP and a suitable post-treatment is necessary to obtain a satisfactory interconnectivity of the pores and open microporous toplayers.

Another important feature in phase inversion membranes is the presence of macrovoids. In this section the influence of the fourth component PVP and some other process parameters on the macrovoid formation will also be discussed in relation to the experimental data presented in the previous section.
Although there are typical differences between the membrane formation processes of capillary and flat membranes [18], in this section both membrane formation types will be used to show the effect of addition of PVP on the final membrane morphology.

2.5.3.1 Interconnectivity of the pores

The porous sublayer in phase inversion membranes is formed by liquid-liquid demixing. During growth of the nuclei coalescence takes place. This phenomenon of coalescence has been demonstrated by Koenhen et al. for the ternary system polyurethane/ dimethylformamide/ water [13] and it is assumed to occur more generally.
In order to obtain an open interconnected pore structure a certain extent of coalescence of the grown out nuclei should have occurred before the polymer rich phase completely solidifies. In this work it is emphasized that some coalescence during that stage of membrane formation is not sufficient to obtain a really interconnected open pore structure. As will be shown here, there must be an additional mechanism that creates the typical open pore structure.

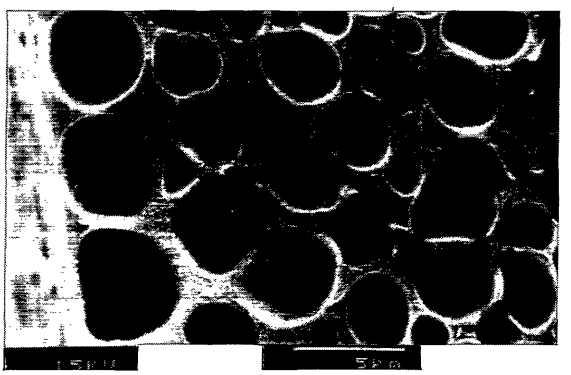

Figure 8: *Closed cell structure in a PEI membrane; casting solution without PVP.*

An example of a closed cell pore structure can be seen in figure 8. The electron micrograph here shows most cells to be closed, although on some places interconnectivity can be observed. This electron micrograph gives also a good illustration that the porous structure is the result of nucleation and growth of the polymer poor phase. This type of closed cell structure can be observed in many other membranes. Whether the structure does have sufficient interconnectivity should be investigated by means of permeation experiments since analysis with an scanning electron microscope is not sufficient.
The membrane shown in figure 8 is prepared starting with a ternary system PEI/NMP/H_2O=20/76/4. When PVP is added and membranes are prepared from the quaternary system a completely different structure is obtained. This can be observed in figure 9. An important question is whether this structure is the result of liquid-liquid demixing. The electron micrograph in figure 10 shows the structure of the same membrane as shown in figure 9, only the preparation

methods of the membrane samples were different.

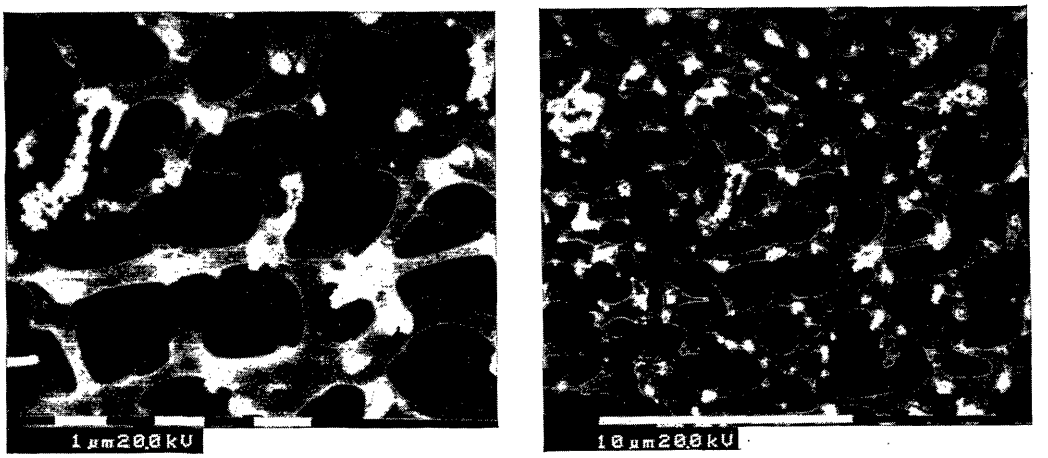

Figure 9: *Pore structure in a PEI-PVP membrane using the dry-preparation method.*

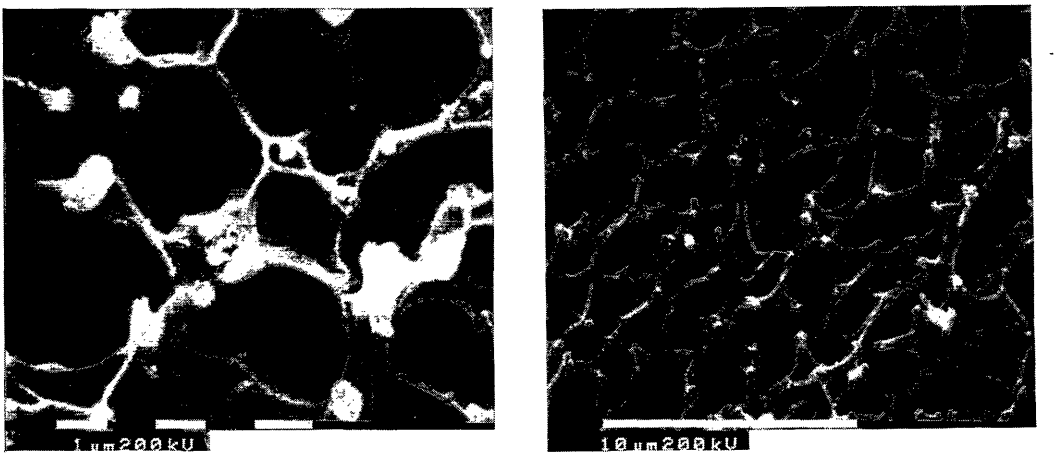

Figure 10: *Pore structure in the same membrane as shown in figure 9, but now using cryo-preparation. The scanning electron microscope is equipped with a cryo-unit.*

For the membrane in figure 9 a dry-preparation method was used, while for the membrane in figure 10 a cryo-preparation method was used (see appendix 2.7). Now the porous structure is

completely different from that in figure 9. The conclusion is that the interconnected porous structure shown in figure 9 is not the result solely of the phase inversion process but of an additional post-treatment of the membranes. The formation mechanism has started as a liquid-liquid demixing process, while a very open interconnected pore structure is the result. An explanation for the differences in figure 9 and figure 10 should be sought in the fact that PVP is present in the membrane matrix.

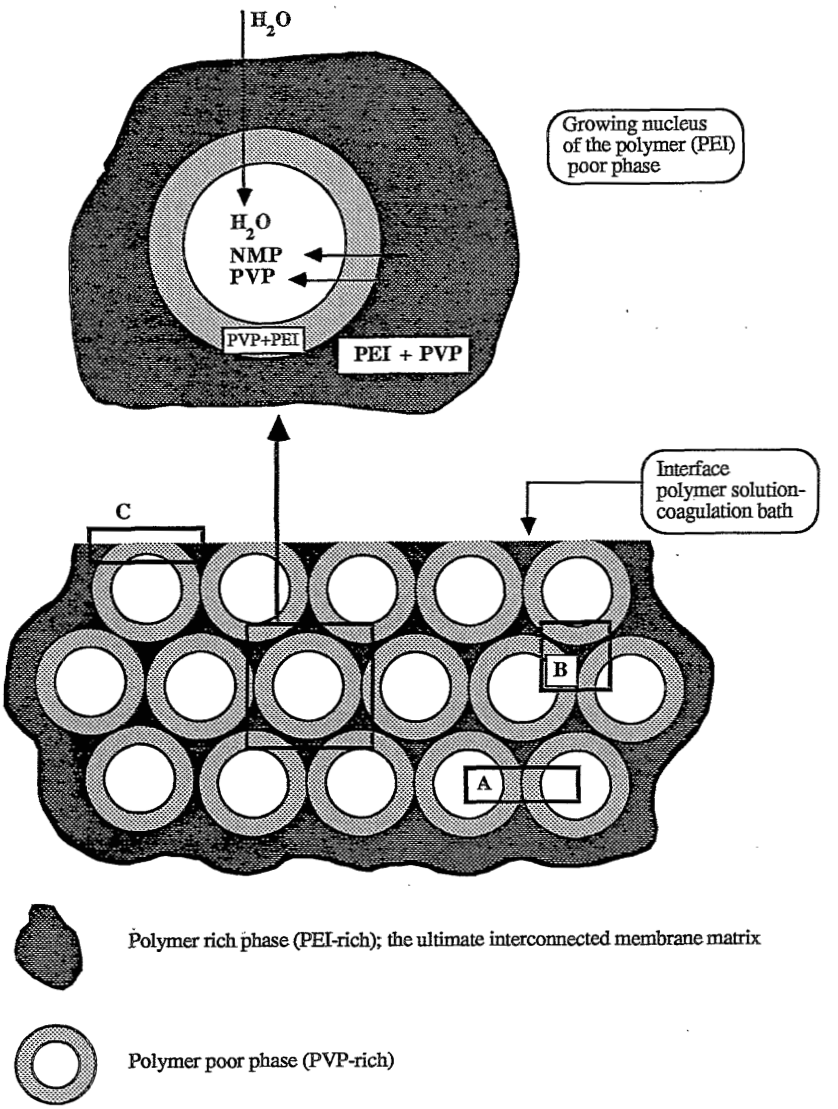

Figure 11: *Schematic representation of the liquid-liquid demixing process in the quaternary membrane forming system PEI/PVP/NMP/H_2O*

During the liquid-liquid demixing process a polymer rich phase is accumulating around the growing regions of the polymer poor phase. When the concentration of the polymer rich phase reaches a certain value it will solidify and the membrane matrix is fixed in its ultimate form. Since liquid-liquid demixing is a very fast process it is assumed that not all PVP has found its final distribution. During and also after the solidification of the polymer rich phase PVP will diffuse into the polymer poor phase since equilibrium for the distribution of PVP is reached very slowly (see 2.5.2). The result is a gradient in the composition of the polymer rich phase, the concentration of PVP will be the highest at the interface of polymer rich and polymer poor phase. In figure 11 a schematic representation is given of the final non-equilibrium state in the liquid-liquid demixing process. The outer surfaces of the pore walls consist of a PVP rich phase. Some PEI will be present since it is entrapped in the PVP network and since it has a relatively good interaction with PEI as will be shown in chapter 4 [1]. When a regular arrangement of spheres is assumed, a cross section of the situation is given in figure 11. In this schematic representation a more or less discrete distribution of PEI-enriched phases and PVP-enriched phases is assumed, although a more gradual distribution may be present due to diffusion processes. In the rectangle **A** the spheres are very close and as is shown the concentration of PVP in the pore walls is relatively high. In the square **B** the matrix material is a PEI-enriched phase with little PVP and this phase will form the continuous membrane matrix.

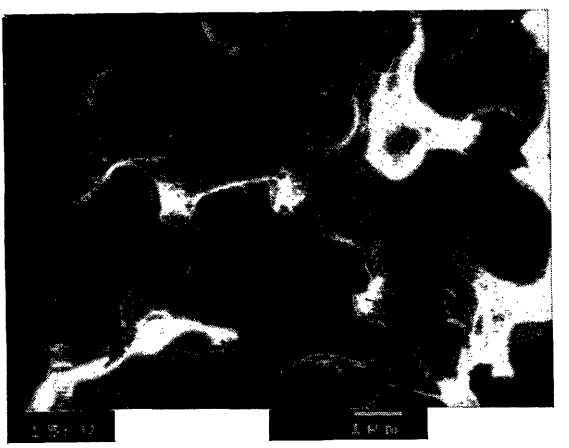

Figure 12: *Pore structure in the same membrane as shown in figure 9 and 10. The membrane is dried slowly at normal pressure. The freeze-fractured cross-section of the membrane is observed at normal temperature.*

After immersion in a water bath as done in all cases the pore walls are highly water swollen. When

these highly swollen pore walls are suddenly deswollen, they will shrink and finally collapse. The deswelling effect can be achieved by e.g., drying at high temperatures and/or low pressure, substitution of water by acetone (nonsolvent for PVP) or substitution of water by ethanol and hexane. The results of the deswelling effect can be observed in the completely open pore structure as in figure 9.
When the membranes were slowly air-dried at moderate temperatures, an intermediate state of the structures in figure 9 and figure 10 is obtained after freeze-fracturing (see figure 12).

The conclusion from these results is: using the cryogenic preparation technique and scanning electron microscopy it is possible to demonstrate that the pore walls are unbroken in a non-dried water swollen membrane. The porous interconnected structure that can be seen in figure 9 must be the result of collapse of pore walls during a certain post-treatment, e.g., a sudden deswelling. It demonstrates very clearly that the preparation method of the membrane sample is very important with respect to the observed structure and that the use of a cryo-unit is essential to study swollen membranes adequately.
More consequences of the post-treatment of the membranes will be given in chapter 5 [23].

2.5.3.2 Open microporous toplayers

When a cast or spun polymer solution is immersed directly in a nonsolvent bath the result is an asymmetric membrane: a dense skin supported by a porous sublayer. For reverse osmosis, gas separation or pervaporation this skin is necessary and essential for the separation process which is based on differences in solubilities and diffusion rates of the components in the dense skin. In ultrafiltration membranes a porous skin with small pores is present. For microfiltration applications an open microporous toplayer with pores in the range of 0.1 - 10 μm is desired. Furthermore the pore size distribution in the toplayer should be narrow and the microporous membranes should have permeation rates corresponding to pore size and porosity.
To obtain a microporous toplayer it is necessary that liquid-liquid demixing takes place in the toplayer [24]. In this work it will be shown that liquid-liquid demixing in the toplayer is not sufficient to obtain open microporous toplayers. Two different methods can be used to obtain liquid-liquid demixing in the toplayer :

- Phase inversion in the vapour phase: since nonsolvent penetrates from the vapour phase without a possibility for solvent outflow, the demixing starts at relatively low polymer concentrations so that liquid-liquid demixing in the toplayer can occur.

- Addition of solvent to the coagulation bath: if the solvent concentration of the coagulation

bath increases, the solvent outflow is retarded and the nonsolvent inflow is favoured so that the toplayer is formed by liquid-liquid demixing.

Wijmans et al. [24] developed this latter method and according to Wijmans it is possible that this method can be applied to every membrane forming ternary system. Although it has to be stressed that Wijmans also added PVP in one of the casting solutions used.
For the ternary system (PEI/NMP/H_2O) used in this chapter other results were found. On the electron micrographs in figure 13 the toplayers are not open although the membranes were immersed in a coagulation bath containing 90 wt. % solvent. The electron micrographs of the top surface shows that some "pores" can be observed, but from the analysis of the cross section it becomes clear that these pores are scarce openings in a rather dense toplayer. These results demonstrate that in contradistinction to the findings by Wijmans not always open microporous surfaces can be obtained by adding solvent to the coagulation bath.

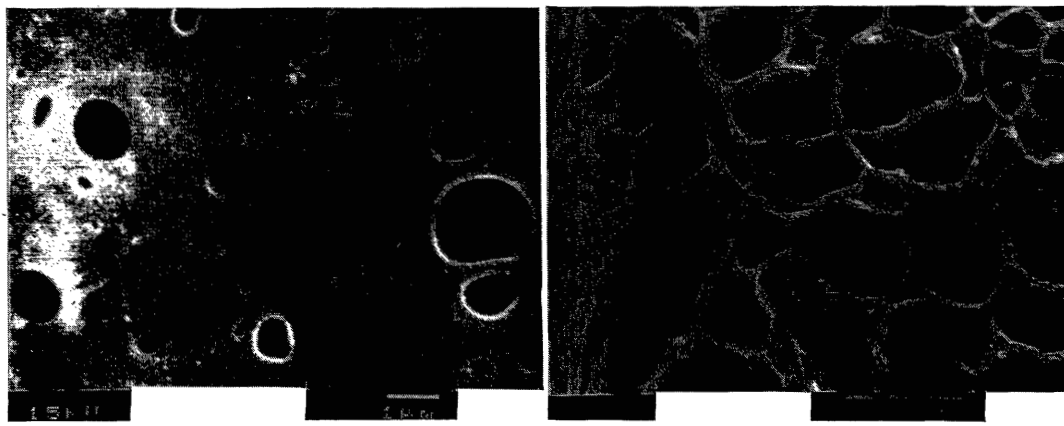

-a- -b-

Figure 13: *Electron micrograph of a flat PEI membrane (without PVP in the casting solution) immersed in a coagulation bath with 90 wt. % NMP.*
a - Top view of the toplayer b- Cross section (toplayer at the left hand side)

The same results were found for membranes prepared by phase inversion in the vapour phase followed by immersion precipitation in a water bath. A machine cast PEI-solution was first exposed for 12 s to water vapour in equilibrium with water of 60 °C and then immersed in the water bath of 60 °C. The result is shown in figure 14. On the electron micrographs it can be seen that no open microporous toplayer is formed. Although in the skin some scarce openings can be observed this toplayer also has a too low surface porosity and the membrane permeability is not in agreement with pore size and porosity over its cross section.

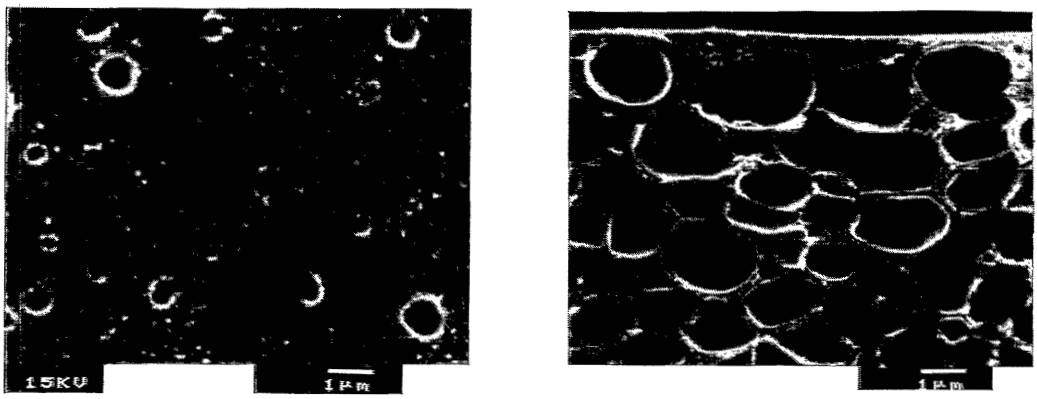

-a- -b-

Figure 14: *Electron micrograph of a flat PEI membrane (without PVP in the casting solution) prepared by phase inversion in the vapour phase (residence time 12 s) and afterwards immersion precipitation in a water bath at 60 °C. a - Top view of the toplayer b- Cross section (toplayer at the upper side)*

When PVP is added to the casting or spinning solution the toplayer has a perfectly open microporous structure as is shown in figure 15.

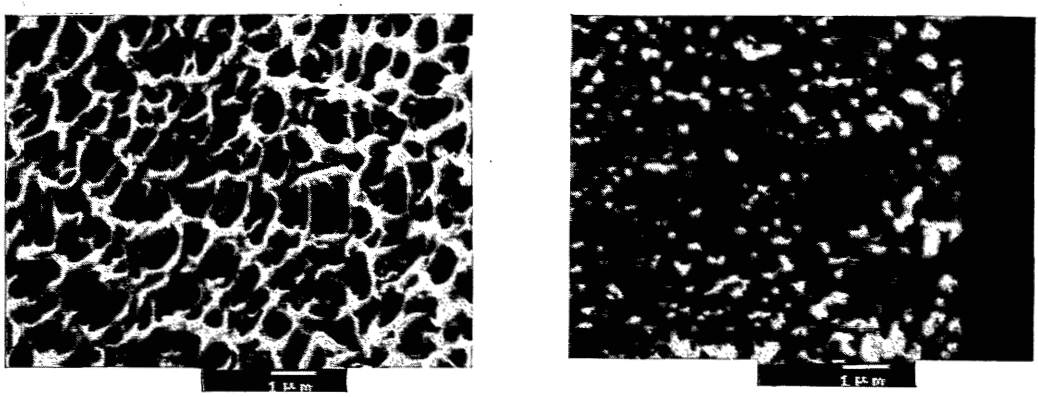

-a- -b-

Figure 15: *Electron micrograph of a PEI/PVP membrane.*
a - Top view of the toplayer b - Cross section (toplayer at the right hand side)

The reason for this is that the addition of PVP facilitates the formation of an open toplayer structure in the same way as has been described in the previous section on the interconnectivity of the pores. The situation at the polymer-coagulation bath interface is represented in figure 11. In the rectangle **C** a nascent pore in the toplayer is still a more or less closed cell. The wall at the coagulation bath interface exists of a PVP rich phase which can easily be collapsed, e.g., by drying, so that a porous toplayer is formed.

The conclusion from these results is that the mechanisms that lead to an open interconnected pore structure and an open microporous toplayer are essentially the same. The statement that liquid-liquid demixing and coalescence of the formed nuclei is sufficient to obtain a microporous toplayer as formulated by Wijmans et al. [24] should be extended. While liquid-liquid demixing should occur it also is essential that there must be a process to break or to remove the thinner parts of the walls between the pores. For that latter process a certain post-treatment of the membranes is necessary.

2.5.3.3 Macrovoid formation

From the model for macrovoid formation presented above (section 2.3.2) it appeared that macrovoid formation can be stimulated by creating conditions for delayed demixing directly in front the layer of formed nuclei. In this work it is found that addition of PVP to the casting or spinning solution can *prevent* the formation of macrovoids. This can be explained by using the mechanism proposed by Reuvers [11].

Three different methods to avoid macrovoid formation will be briefly discussed here:

-1- Phase inversion from the vapour phase followed by immersion precipitation in a water bath.
-2- Addition of solvent to the coagulation bath and immersion precipitation in this coagulation bath.
-3- Addition of PVP to the polymer solution and immersion precipitation in a water bath.

-1- Phase inversion from the vapour phase

In figure 16 two membranes are shown prepared from the same casting solution PEI/NMP/H_2O = 20/76/4. Membrane **-a-** is prepared by immersion precipitation in a water bath. Immediately after casting the nascent membrane is immersed in the water bath. Membrane **-b-** is prepared by phase inversion in the vapour phase (5 minutes in air with a relative humidity of 65 %). After the vapour phase exposure the membrane was immersed in a water bath. In membrane **-b-** no macrovoids are present since due to the nonsolvent vapour penetration the composition of the polymer solution is

very close to the binodal composition so that after immersion in the water bath everywhere in the membrane nuclei can be formed easily.

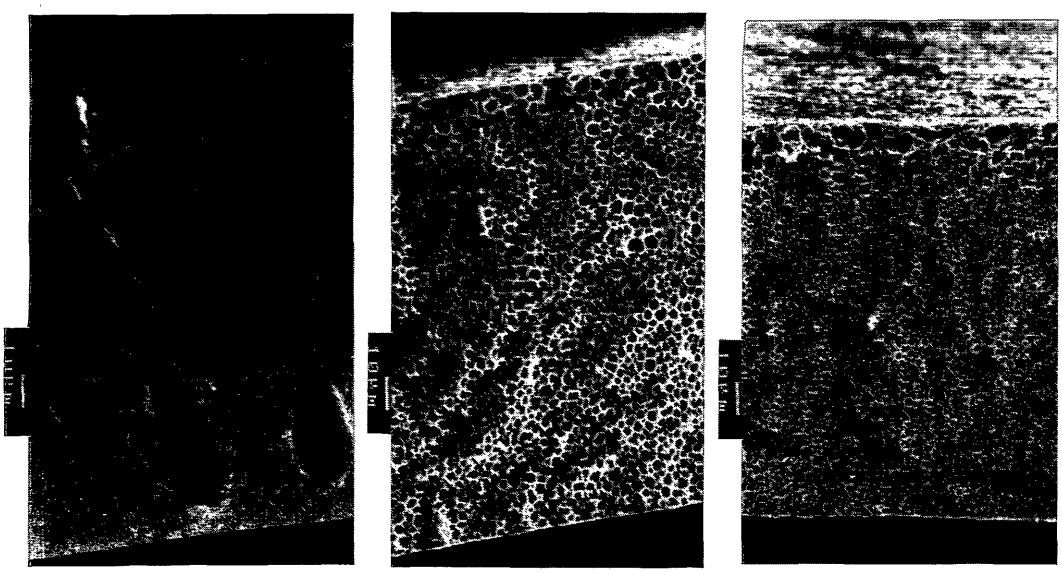

-a- -b- -c-

Figure 16: *Electron micrograph of a flat PEI membrane. Casting solution PEI/NMP/H_2O=20/76/4. Toplayers at the upper side.*
a - Immediately in coagulation bath (pure water) after casting.
b - After 5 min. in the vapour phase and final precipitation in a pure water bath.
c - Precipitation in a water bath containing 90 wt. % NMP.

-2- Addition of solvent to the coagulation bath

Addition of solvent to the coagulation bath changes the demixing type from instantaneous to delayed (see figure 5) at a certain critical value of the concentration of solvent. Macrovoids will not be formed under initial conditions of delayed demixing. The results are shown in figure 16. Membrane -c- is immersed in a coagulation bath containing 90 wt. % solvent (NMP) and 10 wt. % water. After 5 minutes in the solvent-nonsolvent mixture the membrane is placed in a pure water bath for final precipitation. During the time in the first solvent-nonsolvent bath the nonsolvent concentration in the polymer film will increase, but no phase separation occurs yet. When the polymer film is placed in the pure water bath the liquid-liquid demixing will start immediately but since the polymer solution is more or less saturated with nonsolvent nuclei are formed everywhere. Therefore, no macrovoids will be formed.

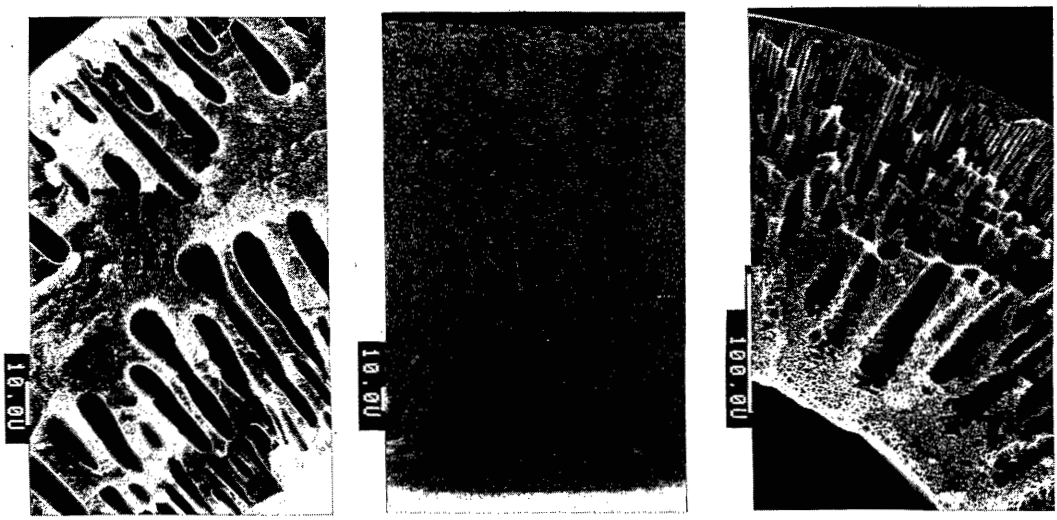

-a- -b- -c-

Figure 17: *Electron micrograph of a cross section of capillary membranes. Casting solutions: a - PEI/NMP=27.5/72.5 (w/w): b - PEI/PVP/NMP=17/13/70: c - PEI/PVP/NMP=19/5/76*

-3- Addition of PVP to the polymer solution.

In figure 17 three cross sections of capillary membranes are shown. Membrane **-a-** is spun from a PEI/NMP=27.5/72.5 solution. After a residence time of 0.2 s in the airgap the nascent membrane is immersed in a water bath (25 °C). Membrane **-b-** is spun from a solution with PVP (PEI/PVP/NMP=17/13/70), while membrane **-c-** is spun from a PEI/PVP/NMP=19/5/76 polymer solution. The electron micrograph **-c-** illustrates that a certain minimal value of the concentration of PVP is necessary to avoid macrovoid formation completely. It was found that at PVP concentrations ≥ 7.5 wt. % no macrovoids could be observed in the capillary membranes.

It is assumed that instantaneous demixing occurs in all three cases, which are presented in figure 17. But as can be understood from figure 5 the addition of PVP to the polymer solution decreases the tendency to form macrovoids since the conditions for delayed demixing in and around the nuclei turn out to be less favourable. The condition for undisturbed growth of nuclei are not fulfilled. Moreover as is shown in table 4 the addition of PVP diminishes the concentration of water necessary for nucleation so that more nuclei can be formed.

2.6 CONCLUSIONS

In this work the effect of polyvinylpyrrolidone on the morphology of polyetherimide microporous membranes is studied, making use of thermodynamic and kinetic data. The fact that polyvinylpyrrolidone is present in the polymer membrane matrix after phase inversion is very important for the morphology of the membranes. Polyvinylpyrrolidone is entrapped in the matrix due the good interaction with polyetherimide and the fact that solidification of the membrane matrix is a very fast process compared with the outdiffusion of polyvinylpyrrolidone.

Former descriptions of preparing open microporous toplayers using immersion precipitation in a solvent/nonsolvent coagulation bath are insufficient. The presence of polyvinylpyrrolidone facilitates the formation of open interconnected pore structures and open microporous toplayers. This is shown to be caused by a post-treatment effect of the membranes after the phase inversion process. Cryogenic sample preparation for electron microscopy made this clear.

The addition of polyvinylpyrrolidone to the polymer solution hinders the formation of macrovoids since the conditions for undisturbed growth of the freshly formed nuclei just below the toplayer are not fulfilled.

2.7 APPENDIX- Sample preparation for scanning electron microscopy

2.7.1 Introduction

Before a membrane specimen is examined at ambient temperature in an electron microscope water and solvents have to be removed. This is necessary because the high-vacuum environment ($< 10^{-4}$ kPa) within the microscope causes water and solvents to rapidly evaporate from a fresh sample, resulting in alterations in specimen morphology but also in contamination of the microscope. Although solvents and other low molecular weight components will be present at low concentrations it can be assumed that only the water has to be removed for the membranes used in this work. The removal of water from the specimen by dehydration and drying, even under controlled conditions is a potentially damaging process and can significantly affect the structure and the dimensions of a sample, especially of biological samples.
Low temperature scanning electron microscopy (LTSEM) appears to be a good candidate as an ideal method for the observation and analysis of hydrated specimens. In this work two different sample preparation methods have been used and will be discussed:

-1- *Dry-preparation technique:* quenching, breaking, drying, sputtering and observation of the sample at ambient temperatures. The well flushed membranes were quenched in liquid nitrogen (l-N_2) and freeze-fractured to obtain a fresh cross sectional surface. The wet membrane samples (at room temperature) were placed in an ethanol bath to replace the water in the membranes and then in a hexane bath to replace the ethanol. Since hexane is a very volatile solvent the membrane samples were air-dried to remove the hexane.
After this procedure the membranes were transferred to a Balzers Union SCD 040 sputter unit where a charge conducting gold layer was applied.

-2- *Cryo-preparation technique:* samples were quenched in nitrogen slush (melting nitrogen; 63 °K), transferred under low pressure to the cold stage of the preparation chamber, freeze-fractured, coated with a gold layer in the preparation chamber and moved into the cooled microscope stage. This cryo-preparation technique will be discussed extensively below.

2.7.2 The cryo-preparation technique

2.7.2.1 *Experimental set-up*

For LTSEM observations a CryoTrans system of Biorad attached to a Philips 505 scanning electron microscope was used. It consists of a cold stage inside the microscope, a cryo-preparation chamber attached to the SEM with a stainless steel transfer tube, a simple quenching unit and a transfer device. The cold stage is fastened at the original stage of the microscope therefore allowing for retaining the tilting possibilities and x,y and z shifts. It is cooled with dried nitrogen gas which on its turn is cooled with l-N_2. The temperature of the stage is controlled electronically (although obviously also dependent on the cooling gas flow rate) with high accuracy, so the microscope resolution is retained. The cold stage can be removed in short time so that the normal use of the SEM at ambient temperatures is not obstructed.
Prior to observations the specimens were quenched in nitrogen slush prepared in the quenching unit. With a transfer device the specimen was transported to the cryo-preparation chamber. During this transport the specimen is cooled and under low pressure. The cryo-preparation chamber is equipped with an airlock chamber allowing for keeping the chamber under vacuum during introduction of the samples. In the cryo-preparation chamber the frozen samples were freeze-fractured or cut with a cooled knife, sublimed (freeze etched), coated with gold (sputtering) and under vacuum transported to the cold stage of the microscope.

2.7.2.2 *Experimental method*

After the preparation of the capillary membranes [18] the membranes were kept wet (demineralized water) and a piece of about 8 mm length was cut off and placed in the aluminium sample holder. The excess water was blotted with a tissue and the sample holder was plunged into the nitrogen slush. In there it was attached to the transfer unit rod and so transported to the preparation chamber. Immediately after quenching specimens brook spontaneously, so that already a fresh cross section was obtained. In order to reveal the actual structure of the membrane the specimens were warmed up a little to - 70 °C (203 °K) to sublime the frozen water from the fractured surface. Sublimation was carried out for 5 to 10 minutes. After sublimation, the specimens were cooled down to approximately -160 °C (110 °K) and sputtered with a gold layer. Then the specimens were transported to the cold stage of the microscope. All cryo observations were carried out at a temperature below - 130 °C (143 °K) to ensure that no further sublimation occurred. In order to investigate whether the spontaneously obtained fractured surfaces were representive for the whole specimen one specimen was also cut with the cooled knife in the preparation chamber at -160 °C (110 °K) and further treated as described before. No differences in the morphology of both specimens could be observed.
For investigations of the membrane outer surface the samples were attached to the sample holder horizontally and then treated as described above. The sublimation time had to be longer here (25 minutes at -70 °C), probably due to the larger distance between the membrane surface and the metal sample holder which is temperature controlled.

2.8 ACKNOWLEDGEMENTS

The authors thank D.M Koenhen and R. Boom for the enlightening discussions on the subject. P.C.M. van Berkel, Z. Borneman and A.C.L. Jansen are acknowledged for performing part of the experiments.

2.9 REFERENCES

1 H.D.W. Roesink, Z. Borneman, M.H.V. Mulder and C.A. Smolders, Polyetherimide-polyvinylpyrrolidone blends as membrane material, PhD Thesis Chapter 4, University of Twente, Enschede, The Netherlands (1989).
2 I. Cabasso, E. Klein, J.K. Smith, Polysulfone hollow fibers. I Spinning and properties, J. Appl. Polym. Sci., 20 (1976) 2377.
3 I. Cabasso, E. Klein, J.K. Smith, Polysulfone hollow fibers. II Morphology, J. Appl. Polym. Sci., 21 (1977) 165.
4 I. Cabasso, K.Q. Robert, E. Klein, J.K. Smith, Porosity and pore size determination in polysulfone hollow fibers, J. Appl. Polym. Sci., 21(1977) 1883.

5 P. Aptel, N. Abidine, F.Ivaldi, J.P.Lafaille, Polysulfone hollow fibers - Effect of spinning conditions on ultrafiltration properties, J. Membr. Sci., **22** (1985) 199.

6 T.A. Tweddle, O. Kutowy, W.L. Thayer, S. Sourirajan, Polysulfone ultrafiltration membranes, Ind.Eng.Chem.Prod.Res.Dev., **22** (1983) 320.

7 L.Y. Lafrenière, F.D.F. Talbot, T.Matsuura, S.Sourirajan, Effect of polyvinylpyrrolidone additive on the performance of polyethersulphone ultrafiltration membranes, Ind. Eng. Chem. Res., **26** (1987) 2385.

8 Q.T. Nguyen, L.L. Blanc, J. Neel, Preparation of membranes from polyacrylonitrile-polyvinylpyrrolidone blends and the study of their behaviour in the pervaporation of water-organic liquid mixtures, J. Membr. Sci., **22** (1985) 245.

9 K. Vásárhelyi, J. A. Ronner, M.H.V. Mulder and C.A. Smolders, Development of wet-dry reverse osmosis membranes with high performance from cellulose acetate and cellulose triacetate blends, Desalination, **61** (1987) 211.

10 A.J. Reuvers and C.A. Smolders, Formation of membranes by means of immersion precipitation. Part II. The mechanism of formation of membranes prepared from the system cellulose-acetate/ acetone/ water, J. Membr. Sci., **34** (1987) 67.

11 A. J. Reuvers, Membrane formation, PhD Thesis Chapter 7, University of Twente, Enschede, The Netherlands (1987).

12 R.E. Kesting, Synthetic polymer membranes, Mc Graw Hill, New York, 1972

13 D.M. Koenhen, M.H.V. Mulder and C.A. Smolders, Phase separation phenomena during the formation of asymmetric membranes, J. Appl. Polym. Sci., **21** (1977) 199.

14 L. Broens, F.W. Altena, C.A Smolders and D.M. Koenhen, Asymmetric membrane structures as a result of phase separation phenomena, Desalination, **32** (1980) 33.

15 A.J. Reuvers, J.W.A. van den Berg and C.A. Smolders, Formation of membranes by means of immersion precipitation. Part I. A model to describe mass transfer during immersion precipitation, J. Membr. Sci., **34** (1987) 45.

16 V. Gröbe, G. Mann and G. Duwe, Ausbildung von Structuren bei der Koagulation vom Polyacrylonitrillösungen, Fasenforsch. Textiltechn., **17** (1966) 142.

17 J.G. Wijmans, J. Kant, M.H.V. Mulder and C.A. Smolders, Phase separation phenomena in solutions of polysulfone in mixtures of a solvent and a nonsolvent: relationship with membrane formation, Polymer, **26** (1985) 1539.

18 H.D.W. Roesink, I.M. Wienk, M.H.V. Mulder and C.A. Smolders, The influence of spinning conditions on the morphology of microporous capillary membranes, PhD Thesis Chapter 3, University of Twente, Enschede, The Netherlands (1989).

19 E. Schchori and J.Jagur-Grodzinski, Polymeric alloys of polyvinylpyrrolidone with a macrocyclic polyether-polyamide, J. Appl. Polym. Sci., **20** (1976) 1665.

20 R.L. Larkin and R.E. Kupel, Quantitative analysis of polyvinylpyrrolidone in atmosphere samples and biological tissues, Amer. Ind. Hyg. Assoc. J., **26** (1965) 558.

21 M.H.V. Mulder, J. Oude Hendrikman, J.G. Wijmans and C.A. Smolders, A rationale for the preparation of asymmetric pervaporation membranes, J. Appl. Polym. Sci., **30** (1985) 2805.

22 K. Kimmerle, Quantitative Betrachtung des Phaseninversionsprozesses bei der Herstellung von Membranen, PhD Thesis, University of Stuttgart, Stuttgart, West-Germany (1988).

23 H.D.W. Roesink, S. Oude Vrielink, M.H.V. Mulder and C.A. Smolders, Post-treatment of hydrophilic membranes prepared from polyetherimide-polyvinylpyrrolidone blends, PhD Thesis Chapter 5, University of Twente, Enschede, The Netherlands (1989).

24 J.G. Wijmans, J.P.B. Baaij and C.A. Smolders, The mechanism of formation of microporous or skinned membranes produced by the immersion precipitation process, J. Membr. Sci., **14** (1983) 263.

CHAPTER 3

THE INFLUENCE OF SPINNING CONDITIONS ON THE MORPHOLOGY OF MICROPOROUS CAPILLARY MEMBRANES

H.D.W. Roesink, I.M. Wienk, M.H.V. Mulder and C.A. Smolders.

3.1 SUMMARY

In this chapter the development of a new type of hydrophilic microporous capillary membrane is described. The preparation method is based on the phase inversion technique. Two different ways to obtain phase separation are used: phase inversion from the vapour phase and immersion precipitation. Capillary membranes are spun from a solution of a thermostable, chemically resistant, hydrophobic polymer polyetherimide (PEI) and the completely miscible hydrophilic polymer polyvinylpyrrolidone (PVP). The influence of some important spinning parameters on the morphology of the membranes has been studied. The temperature of the external coagulation bath and the residence time in the air-gap are spinning parameters suitable to control the pore size at the outer surface and the pore size distribution across the membrane. The ratio of solvent to nonsolvent in the internal coagulation bath controls the pore size at the inner surface. It has been found that stretching of the capillary membrane after leaving the spinneret also is an important factor for the morphology at the inner surface and for the shape of the bore.
The pore size of the membranes can be varied between 0.05 μm and 1 μm, so that these capillary membranes can be used for microfiltration.

3.2 INTRODUCTION

During the last decade many new thermoplastic materials that show excellent thermostability and chemical resistance have been developed. Among these new generation engineering plastics are polyethersulfone, polysulfone, polyimide, polyetherimide, polyetheretherketone, polyphenyleneoxide, polyphenylenesulfide etc. In general these polymers have a hydrophobic nature.
Microfiltration membranes based on these hydrophobic polymers could have a wide range of applications if it were possible to give these membranes a hydrophilic nature.
In this chapter membranes are prepared consisting of polyetherimide and the hydrophilic character of the membranes is obtained by adding the hydrophilic polymer polyvinylpyrrolidone to the

spinning solution. In fact the membrane material is a blend of polyetherimide and polyvinylpyrrolidone. The nature of this blend has been investigated and the results have been presented in chapter 2 and 4 [1,2].
For the dry-wet spinning process, which is used in this chapter, a certain viscosity level of the spinning solution is a necessary requirement to enable the formation of a capillary membrane. A well-known method to increase the viscosity of the spinning solution is to add a high molecular weight component to the spinning solution. High molecular weight polyvinylpyrrolidone (PVP K90) is often used as an additive in spinning solutions [3,4,5,6,7]. It was commonly accepted in the articles cited that PVP did not contribute to the polymeric membrane matrix since PVP is soluble in generally employed coagulation baths. Furthermore, these articles showed that addition of PVP to the spinning solution facilitated the formation of microporous toplayers.
The latter effect has also clearly been demonstrated in chapter 2 [1]. Moreover it was found that an appreciable amount of PVP is present in the membrane matrix (see chapter 2 and 4) [1,2]. In these chapters also the influence of the addition of PVP on membrane formation and on membrane characteristics, like interconnectivity, is discussed.
In this chapter the influence of the spinning conditions on the morphology of microporous capillary membranes is described.The morphologies obtained will be discussed in accordance with existing theories about membrane formation.

3.3 BACKGROUND

3.3.1 Phase inversion

Using the phase inversion technique all kinds of morphologies can be obtained. In this chapter only the phase inversion from the vapour phase and immersion precipitation will be discussed. Typical for immersion precipitation of a polymer solution without additives in a pure nonsolvent is the asymmetric structure of the membranes obtained. The asymmetric membrane consists of a dense toplayer which is supported by a porous sublayer. The dense toplayer is the result of the initial high solvent outflow from the polymer film and a low nonsolvent inflow, so that the polymer concentration at the boundary increases, and the demixing process starts at a relatively high polymer concentration. In fact the toplayer is formed by gelation (or aggregate formation) [8,9]. The toplayer will diminish the solvent outflow so that the demixing processes in the sublayer occur at a relatively low polymer concentration. This demixing process in the sublayer is called liquid-liquid demixing and after solidification of the polymer rich phase the result is a sponge-like porous structure. The mechanism for this membrane formation process has been studied by workers like Frommer et al. [10], Strathmann et al. [11], Koenhen et al. [9], Broens and Altena

[12], Wijmans et al. [13] and Reuvers et al. [8].

Since in the membrane forming system, which is discussed in this chapter, two polymers are used, while one of the polymers (PVP) will partly dissolve in the coagulation medium, the polymer poor phase will contain a reasonable amount of polymer (PVP) [1,2]. The polymer rich phase consists of two polymers (PEI and PVP). Polymer poor in this thesis means poor in PEI.

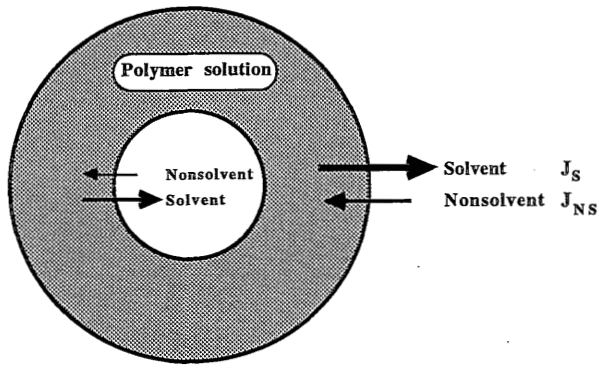

Figure 1: *Schematic representation of the solvent/nonsolvent exchange in a capillary membrane during immersion precipitation, in the case that an internal and external coagulation bath is used.*

When a polymer solution is immersed in a nonsolvent bath there is a solvent outflow (J_S) and a nonsolvent inflow (J_{NS}) (see figure 1) both controlled by diffusion. By changing the ratio of the solvent outflow and nonsolvent inflow the morphology of the toplayer of the membranes can be controlled. At high J_S/J_{NS} ratios the eventual demixing process in the toplayer will start at relatively high polymer concentrations, so that the toplayer will be formed by gelation (or aggregate formation). At lower ratios of J_S/J_{NS} the demixing process can start at relatively low polymer concentrations and the toplayer will be formed by liquid-liquid demixing, which results in a microporous toplayer.

Wijmans changed the ratio J_S/J_{NS} by adding solvent to the coagulation bath. More solvent in the coagulation bath means that the solvent outflow decreases, while the nonsolvent inflow decreases less rapidly [13].

When the toplayer is no longer formed by gelation (or aggregate formation) but by liquid-liquid demixing, it becomes microporous. It is characteristic for different membrane forming systems that the toplayer becomes microporous after the solvent concentration in the coagulation bath reaches a certain high threshold value. This value is dependent on the nonsolvent content at the liquid-liquid

boundary in the quasi ternary phase diagram [13]. The membrane forming system used in this chapter is very sensitive for water (2.3 wt.% of water at the liquid-liquid boundary) and it shows instantaneous demixing due to the strong interaction between water and the solvent N-methylpyrrolidone (NMP). Apparently a high solvent concentration in the coagulation bath is needed to decrease the solvent outflow to a sufficient degree in order to form a microporous toplayer.
For the system PEI/PVP/NMP/H_2O a minimum solvent content of 75 wt.% in the coagulation bath is required to obtain pores greater than 0.05 μm in the toplayer. This is in line with data found by Wijmans et al. [13] for the membrane forming system polysulfone/ dimethylacetamide/ water.

It has to be emphasized that a microporous toplayer in this thesis means a membrane surface with pores in the microfiltration range (0.05 -10 μm), with a reasonable porosity and a permeation rate of the membrane for pure water in agreement with that pore size and porosity (see also [1]).

A low ratio of J_S/J_{NS} can also be obtained when phase inversion from the vapour phase is applied. In this very old technique developed at the beginning of this century [14] membrane formation is accomplished by penetration of a nonsolvent from the vapour phase.
The ratio of solvent outflow and nonsolvent inflow can be controlled in this situation with parameters like: concentration of the nonsolvent vapour in the air, volatility of the solvent, temperature of the polymer solution and of the air-vapour mixture.

3.3.2 Spinning of capillary microporous membranes

A schematic representation of the different solvent/nonsolvent exchange regimes of the phase inversion techniques during the spinning of capillary membranes is given in figure 2.
The solvent/nonsolvent exchange regimes are:

I *Phase inversion from the vapour phase (controlling pore size and porosity at the outer surface).*
The polymer solution consisting of one or more polymer(s) and one or more solvent(s) is exposed to a nonsolvent vapour. If the solvent is not very volatile the outflow due to evaporation is only very small. When a volatile solvent is used the vapour phase can be saturated with solvent, so that solvent outflow is minimized. Essential for this regime is that there is a certain nonsolvent inflow from the vapour phase, and no or a low solvent outflow, so that demixing starts at a relatively low polymer concentration.

II *Immersion precipitation in a solvent/nonsolvent mixture (controlling pore size and porosity at the inner surface).*
Solvent/nonsolvent mixtures will decrease the solvent outflow to the bore liquid so that microporous surfaces can be formed if the solvent concentration has a certain threshold value.

III *Immersion precipitation in pure nonsolvent.*
The structure at the outer surface is initiated during regime I, while regime II determines the inner surface structure. The solvent content in the membrane after regime I and II is still high. Precipitation in a pure nonsolvent bath will kinetically influence the demixing phenomena already initiated and will finally take care of fixation of the porous membrane structure (by solidification of the polymer rich phase).

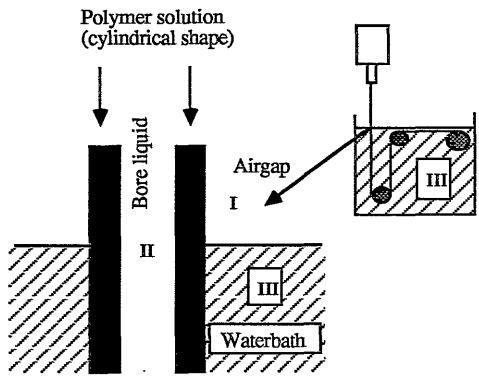

Figure 2: *Solvent/nonsolvent exchange regimes in the spinning process used in this work.*
I - Phase inversion from the vapour phase
II - Immersion precipitation in a solvent/nonsolvent mixture
III - Immersion precipitation in a nonsolvent bath

Most theories about membrane formation deal with the precipitation of flat polymer films. Membrane formation during the spinning process is essentialy the same, although there are some important differences.

- The diffusion processes will start at two sides
- Diffusion takes place in radial direction so that diffusion is accelerated going from the outside to the inside and retarded the other way
- The internal coagulation bath has a restricted volume so that the

composition of this bath changes significantly during the spinning process

- To enable the formation of a capillary membrane from the polymer solution, a certain viscosity level is required. Often this high viscosity is obtained by adding a second polymer to the polymer solution, which is soluble in the coagulation bath.
- The capillary membrane can be stretched due to the gravity force or to the fact that there is a certain take-up speed.

3.3.3 The bore shape

When polymeric melts with a high viscosity are extruded through an orifice, the dimensions of the orifice and eventual stretching forces are dictating the ultimate shape of the extrudate. The theories to explain or predict the shape of the extrudate in relation to the shape of the orifice are rather complex and much knowledge about the relation between dimensions of the orifice and the extrudate is based on empirical rules.
In the dry-wet spinning process the situation is even more complicated, because of the phase separation phenomena in the polymer solution after leaving the spinneret. Most problems are encountered with the circumferential shape of the capillary bore of the membranes.

A typical extrusion phenomenon is the so-called die-swell (see figure 3). The effect of the die-swell is due to elastic recovery of the viscous spinning solution. After leaving the spinneret, the polymer molecules regain the more random conformation and the larger coil diameter they had before extrusion. The result is that the outer diameter of the capillary membrane will be larger than the corresponding diameter of the orifice. After a certain length the outer diameter decreases. This effect is reinforced by lack of viscosity of the nascent membrane, so that gravitation forces and the take-up speed can elongate the capillary membranes.
So during the first stages of spinning there will be radial forces and axial forces and both may have an influence on the bore diameter and bore shape (see figure 3). Of crucial importance moreover is the rate at which the local demixed polymer solution at the circumference of the bore solidifies, or can be deformed to accomodate the changing bore volume. The solidification rate and the change in bore volume are dependent on the composition and the flow rate of the bore liquid. Depending on the ratio of local forces and the local visco-elastic properties for the interfacial material one could imagine that for decreasing bore volumes (as depicted in figure 3) irregular circumferential bore shapes might occur. For instance, if the circumference has already been formed and partly solidified, but the surface layer should be flexible enough, an irregular wavy circle could well result as the bore shape. If the surface layer would be non-flexible over a larger thickness, the capillary elongation might even lead to tearing apart such surfaces. It will be clear, that the composition of the internal coagulation bath, its temperature and of course the composition and temperature of the

spinning solution are important variables for the final bore shape.

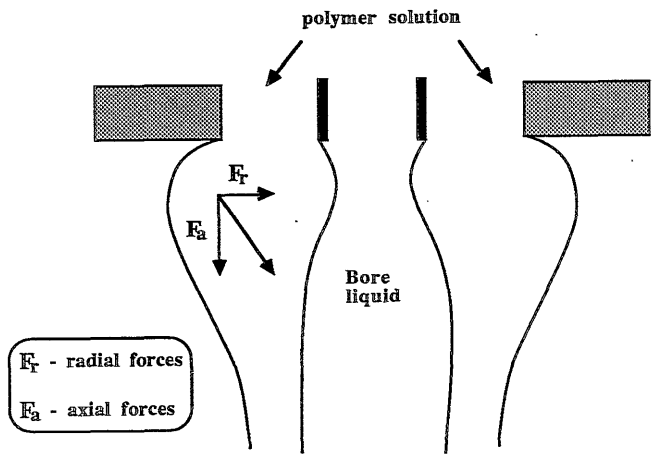

Figure 3: *Schematic representation of the die-swell at the inside and at the outside of a capillary membrane leaving the spinneret.*

3.4 EXPERIMENTAL

Materials

In the membrane forming system two polymers are used. The hydrophobic, thermostable and chemical resistant polyetherimide (PEI) and the hydrophilic, water soluble polyvinylpyrrolidone (PVP K90, MW =360 000), which was purchased from Janssen Chimica. Polyetherimide (Ultem® 1000) was friendly supplied by General Electric, Bergen op Zoom, The Netherlands. N-methyl-2-pyrrolidone (Merck, Synthetic grade) was used as a solvent, while water was used as a nonsolvent.

The spinning process

In the dry-wet spinning technique (figure 4) a degassed and filtered polymer solution is pumped through a spinneret. The degassed and filtered bore liquid (the internal coagulation bath) is delivered pulse-free with a HPLC- pump (Kratos, spectroflow 400). The spinneret is positioned above a water bath (external coagulation bath). Before entering the water bath the polymer solution is in contact with water vapour. Unless mentioned otherwise the vapour is in equilibrium with the water bath at a given temperature.

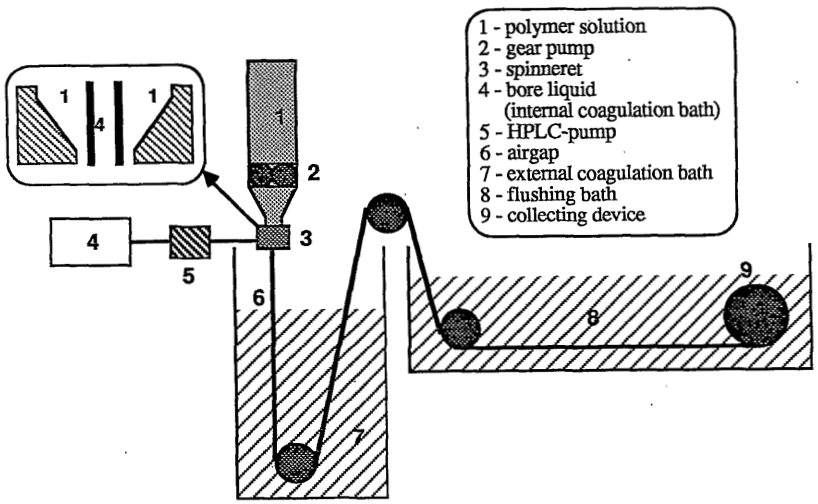

Figure 4: *Experimental set up for the dry-wet spinning process for the preparation of capillary membranes.*

The spinneret used for most experiments had an extrusion orifice of 2 mm; the radius of the inner injection tube was 0.8 mm (spinneret 2 in figure 5). The wall thickness of the inner tube was 0.15 mm.

Type	Outer diameter of the injection capillary d (mm)	Extrusion length of the injection capillary o (mm)	Diameter of the orifice D (mm)	Orifice length l (mm)
1	0.8	0	1.2	1.0
2	0.8	0	2.0	1.0
3	0.9	0	2.5	1.0
4	0.8	0	3.0	1.0
5	0.9	6	3.0	1.0
6	0.9	0	2.5	7.5
7	0.9	-5.6	2.5	7.5

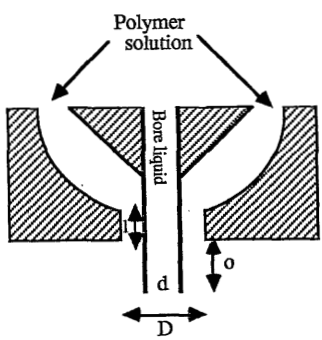

Figure 5: *Schematic representation and the dimensions of the spinnerets used in this work.*

Experiments are done with the standard spinning solution **A** (30 °C) PEI/PVP/NMP=17/13/70 and with a solution **B** (30 °C) PEI/PVP/H_2O/NMP=17/13/2/68 (all compositions in this chapter will be given in weight percentages).

The viscosity of the polymer solution (**A**) is measured with a rotary viscometer (Brabender).The viscosity is dependent on the shear rate (figure 6). The polymer solution shows a non-Newtonian behaviour (slightly shear thinning).

The extrusion rate of the polymer solution is 3.2 ml/min. Water vapour in the airgap is in equilibrium with the external coagulation bath. The take-up speed of the capillary membranes during these experiments is 3 m/s. The bore liquid is a solvent/nonsolvent mixture NMP/H_2O, unless specified otherwise. The flow rate of the bore liquid is 1 ml/min.

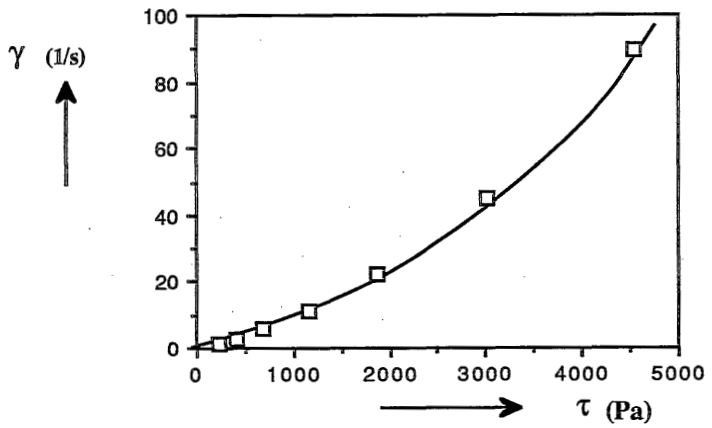

Figure 6: *Shear rate (γ) versus the shear stress (τ) for the standard spinning solution PEI/PVP/NMP=17/13/70, measured with a rotary viscometer at 30 °C.*

Characterization of the capillary membranes

The morphology of the membranes is studied using a Jeol JSM-35 or a Jeol JSM-T 220 A scanning electron microscope (SEM). The well flushed membranes were quenched in liquid nitrogen and freeze-fractured to obtain a fresh cross section. The wet membrane samples were placed in an ethanol bath to replace the water by ethanol and then in a hexane bath to replace the ethanol by hexane. After air drying the samples were coated with a charge conducting layer of gold by means of a Balzers Union SCD 040 sputter unit.

As pore size the mean local pore diameter is used and it is derived from the scanning electron micrographs.

It appears (see chapter 2 [1]) that the pore structure of the microporous membranes is strongly dependent on the preparation technique used. In this chapter a dry-preparation technique is used, since the structure obtained in this way is very representative for the structure of the membranes when they are used for actual filtration (see chapter 5 of this thesis) [15].

3.5 RESULTS AND DISCUSSION

The following spinning parameters have been studied in relation to the morphology of the membranes:

- composition of the polymer solution
- temperature of the external coagulation bath
- composition of the internal coagulation bath (bore liquid)
- length of the airgap
- conditions in the airgap
- take-up speed

The influence of the spinning parameters on the morphology of the membranes is studied with respect to the following structure parameters:

- microscopic structure of the capillary membranes; pore size, pore size distribution, porosity.
- macroscopic structure of the capillary membranes; shape of the bore, shape of the outer circumference of the capillary membranes.

3.5.1 Microstructure of the membranes

3.5.1.1 *Pore size at the outer surface*

As has been shown in figure 2 the solvent/nonsolvent exchange regime in the airgap is phase inversion from the vapour phase, so that incipient demixing occurs by the mechanism of nucleation and growth (liquid-liquid demixing). Nucleation is initiated by the diffusion of water vapour into the polymer solution. The number of nuclei and the growth conditions of the nuclei will determine the ultimate pore size and porosity. Water vapour concentration, temperature and residence time in the airgap are the most important parameters in controlling pore size and porosity at the outer surface of the capillary membranes.
The water vapour concentration in the airgap and the composition of the polymer solution will determine the onset of nucleation. The growth rate of the formed nuclei is influenced by the mass transfer of water vapour in the airgap and in the surface layer.
If the partly demixed nascent membrane, formed in the airgap, enters the external coagulation bath the solvent/nonsolvent exchange regime is immersion precipitation in a pure nonsolvent and the ultimate membrane structure will be formed and fixed.

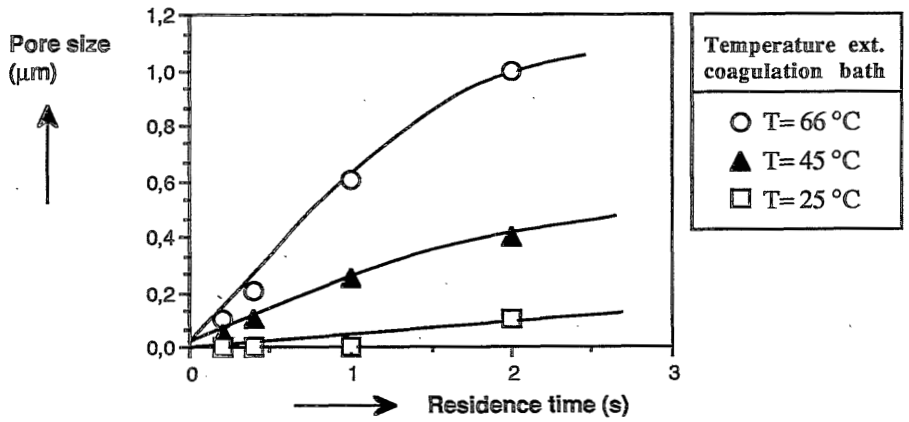

Figure 7: *Pore size at the outer surface versus the residence time in the airgap for three different temperatures of the external coagulation bath.*

In figure 7 the relationship between the residence time in the airgap and the pore size at the outer surface is shown for different temperatures of the external coagulation bath. At increasing temperature the water vapour concentration will increase; the driving force for the in-diffusion of water increases, mass transfer is enhanced and nuclei growth is facilitated resulting in larger pores. In addition the temperature in the airgap is another factor that enhances mass transfer. Hence two effects resulting in larger pores are: higher water vapour concentration and higher diffusion coefficients.
The surface porosity of the capillary membranes was also measured and always was between 20% and 30%. Obviously the growth of nuclei is stimulated more than the nucleation itself.

Although the time before complete solidification occurs is very short after immersion in the external coagulation bath, nuclei in the outer surface layer will have some time to grow futher, so that the temperature of the external coagulation bath might influence the last stages of the growth. To investigate these growth effects the following experiment was performed.
A nitrogen stream with a constant temperature and humidity is supplied to the sealed airgap, so that the atmosphere in the airgap is not in equilibrium with the external coagulation bath as it is in all other experiments. The temperature of the external coagulation bath is varied from 20 °C to 62 °C. In all cases a pore size of 0.03 µm (residence time in the airgap 2 s) at the outer membrane surface was found. Hence the only influence of the temperature of the external coagulation bath in normal situations on the pore size at the outer surface, results from the increased water vapour concentration and the increased temperature in the airgap.

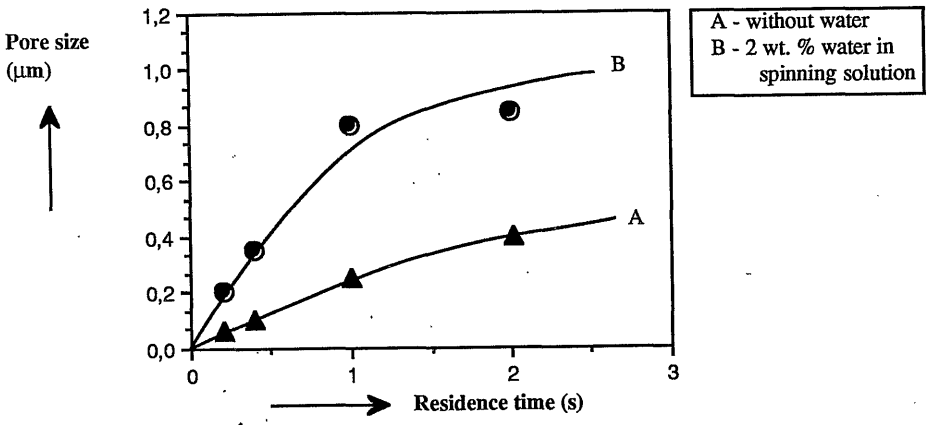

Figure 8: *Pore size at the outer surface versus the residence time in the airgap for two different spinning solutions. Temperature external coagulation bath is 45 °C. Spinning solutions: A- PEI/PVP/NMP=17/13/70 and B - PEI/PVP/NMP/H_2O= 17/13/68/2*

It will be clear that the addition of water to the spinning solution will facilitate nucleation. A second effect is that, because of the presence of water in the solution, nucleus growth may be accelerated. The effect of the residence time in the airgap on the pore size at the outer membrane surface for two different spinning solutions is shown in figure 8. Solution **A** is the standard solution without water, while solution **B** contains 2 wt.% water. The temperature of the external coagulation bath is 45 °C; the other process parameters are the same as mentioned in the experimental section. Under the same spinning conditions, in the solution with 2 wt.% water the onset of demixing is facilitated, so that the same residence time gives larger pores.

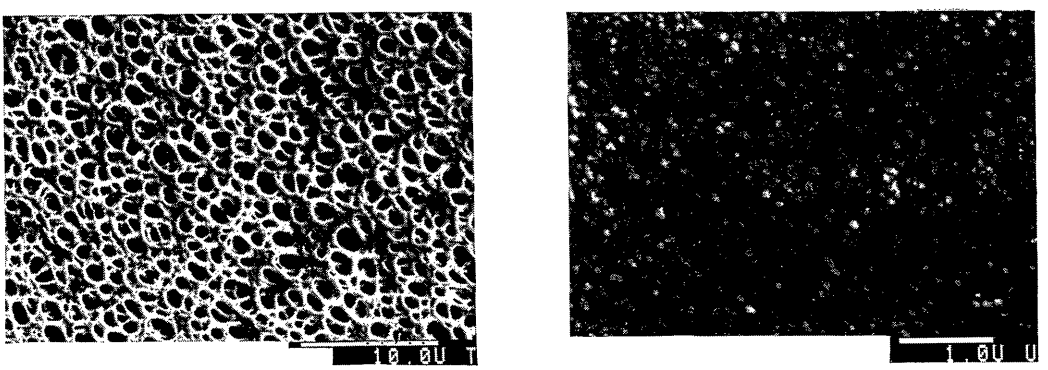

-a- **-b-**

Figure 9: *Electron micrographs of outer membrane surfaces (top views). Membranes are spun from the standard spinning solution PEI/PVP/NMP=17/13/70.*
a- External coagulation bath 66 °C, residence time in airgap 2 s, mean pore size 1 μm.
b- External coagulation bath 45 °C, residence time airgap 0.2 s, mean pore size 0.05 μm.

The results in this section show that the pore size at the outer surface can be controlled by the temperature of the external coagulation bath, the addition of nonsolvent (water) to the spinning solution and the residence time in the airgap. The porous outer surfaces are very smooth while the pore size distribution is quite narrow (figure 9).

3.5.1.2 *Pore size and pore size distribution across the membrane wall*

The most ideal structure for filtration purposes is one in which the pore size is increasing from the outer surface to the inner surface, presuming that the feed is in contact with the outer surface during filtration. In fact the main resistance for transport should be at the surface that is in contact with the feed solution. Such a pore size gradient is normally obtained when a polymer solution film after casting is brought immediately in contact with a nonsolvent. In the case of capillary membranes using phase inversion from the vapour phase the situation is different. Penetration of water vapour at the outer surface will cause liquid-liquid demixing. The penetration depth of the demixing front during the residence time in the airgap is dependent on the water vapour concentration, temperature in the airgap and composition and temperature of the polymer solution.
The residence time in the airgap is too short to cause complete precipitation, so that after phase inversion in the vapour phase the final precipitation takes place in a water bath. When the capillary membrane contacts the external coagulation bath, the outflow of solvent is possible, making the residual polymer solution more concentrated and hence growth phenomena more retarded. Furthermore the inflow of nonsolvent is increasing, so that nucleation rates might increase. After the capillary membrane contacts the external coagulation bath, the conditions are such that solidification of the polymer rich phase (starting from the outer surface) is fast so that formed nuclei will not grow any further.
The result is a minimum in the pore size over the cross-section of the membrane (figure 10 and the electron micrograph in figure 11).

At increasing temperatures of the external coagulation bath the water vapour concentration will increase, so that the demixing front can penetrate deeper into the nascent membrane. At a certain temperature the demixing front has penetrated so far that the effect of solvent outflow after entering the external coagulation bath is not resulting in a minimum in the pore size distribution anymore. In fact the solvent outflow is minimized and hardly any gradient in the pore size can be observed (see figure 10 and 11).

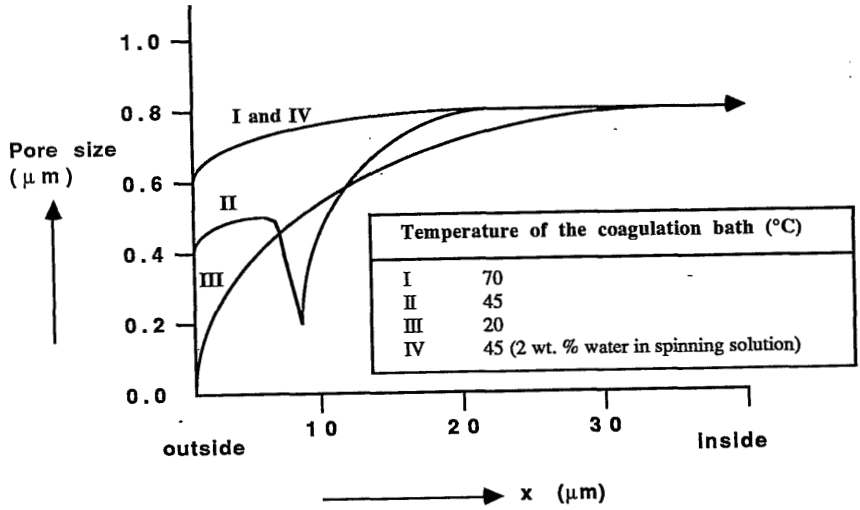

Figure 10: *Schematic representation of the pore size gradient over the cross section of a capillary membrane. The pore sizes are given for three temperatures of the external coagulation bath. Local pore sizes are taken from electron micrographs.*

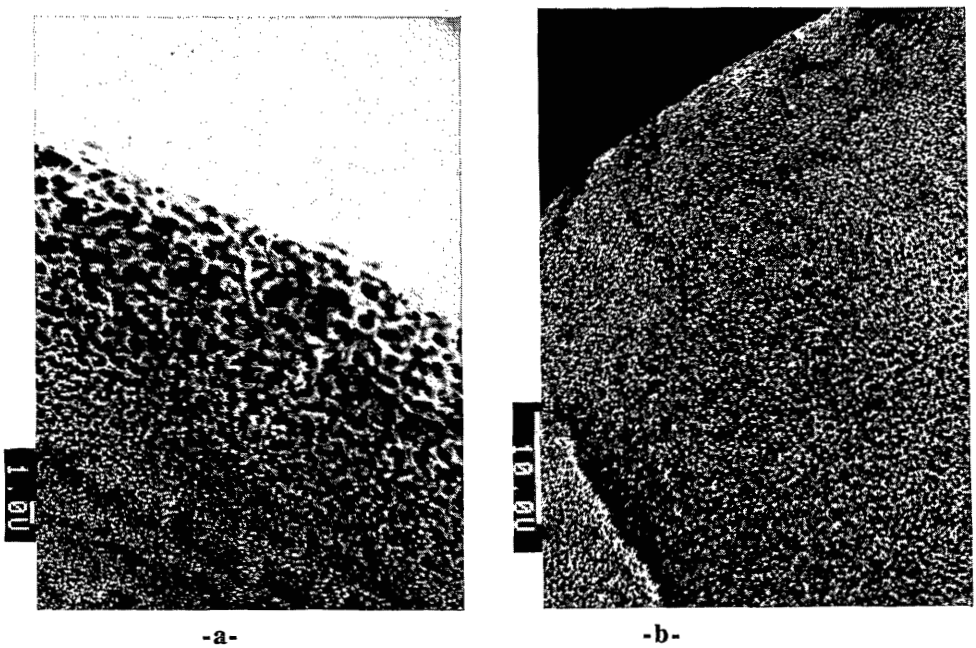

Figure 11: *Electron micrographs of the cross section of capillary membranes spun from the standard spinning solution PEI/PVP/NMP=17/13/70; outer surface at the upper side.*
a - With a minimum in the pore size; external coagulation bath 45 °C.
b- Without a minimum in the pore size; external coagulation bath 70 °C.

At relatively low temperatures of the external coagulation bath no minimum in the pore size can be observed, since the demixing front has not penetrated to any distance yet (see figure 10 and the results in the appendix 3.7).

When water is added to the spinning solution the demixing front can penetrate deeper into the polymer solution in a certain residence time compared with the situation without water present in the spinning solution. Figure 12 shows two electron micrographs of cross sections of capillary membranes spun without (a) and with (b) water in the spinning solution. The result is that the minimum in the pore size is hardly visible in the situation that 2 wt. % water has been added to the spinning solution.

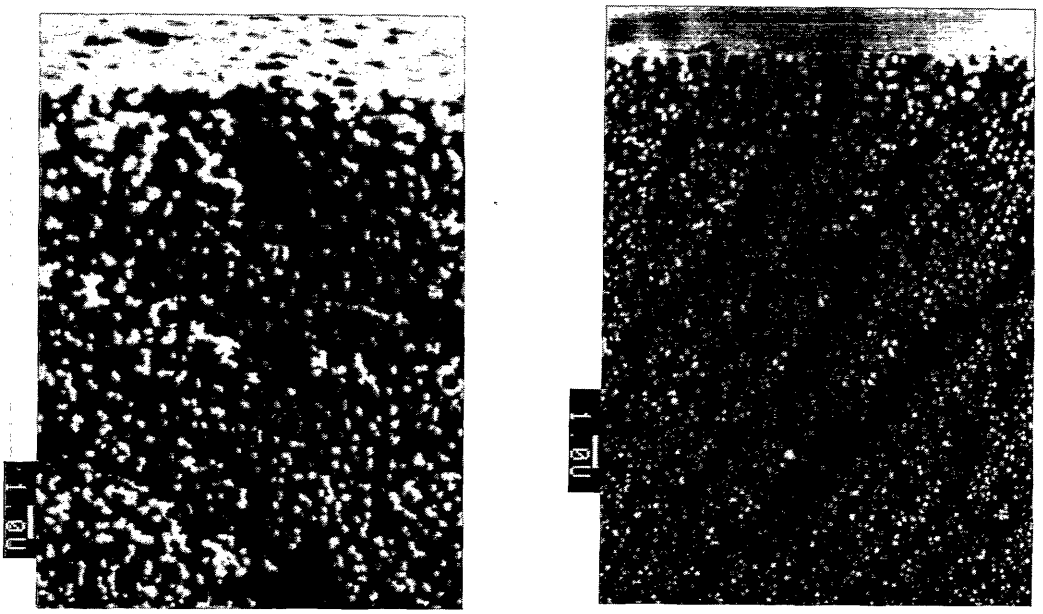

-a- -b-

Figure 12: *Electron micrograph of a cross section of a capillary membrane spun from (-a-) the standard spinning solution PEI/PVP/NMP=17/13/70 and from (-b-) the solution with 2 wt. % water (PEI/PVP/NMP/H2O=17/13/68/2); temperature external coagulation bath 45 °C; outer surface at the upper side.*

The penetration depth of the demixing front during the precipitation in the vapour phase is estimated by measuring the diffusion coefficient of water vapour in the polymer solution. At a temperature of the external coagulation bath of 70° C and a residence time of 1 s in the airgap the penetration depth is 14 μm, which is in good agreement with the results shown in figure 11. (See

appendix 3.7)

The results in this section show that due to the phase inversion from the vapour phase followed by immersion precipitation in a nonsolvent coagulation bath, sometimes a mimimum in the pore size across the membrane wall can be found. This undesirable minimum is not found at high water vapour pressures in the airgap or by addition of some nonsolvent to the polymer solution.

3.5.1.3 *Pore size and pore size distribution at the inner surface*

Although phase inversion from the vapour phase is a very suitable technique to control the pore size and porosity at the outer membrane surface, also the inner surface has to be considered.

Here a solvent/nonsolvent mixture is applied as the internal coagulation bath (bore liquid). As shown above the ratio of solvent outflow and nonsolvent inflow has to be in a certain range in order to obtain microporous toplayers. If the solvent concentration of the internal coagulation bath increases, the solvent outflow is retarded and the nonsolvent inflow is favoured so that the toplayer is typically formed by liquid-liquid demixing. Above a certain threshold concentration of solvent in the internal coagulation bath, pore sizes will increase with solvent concentration.

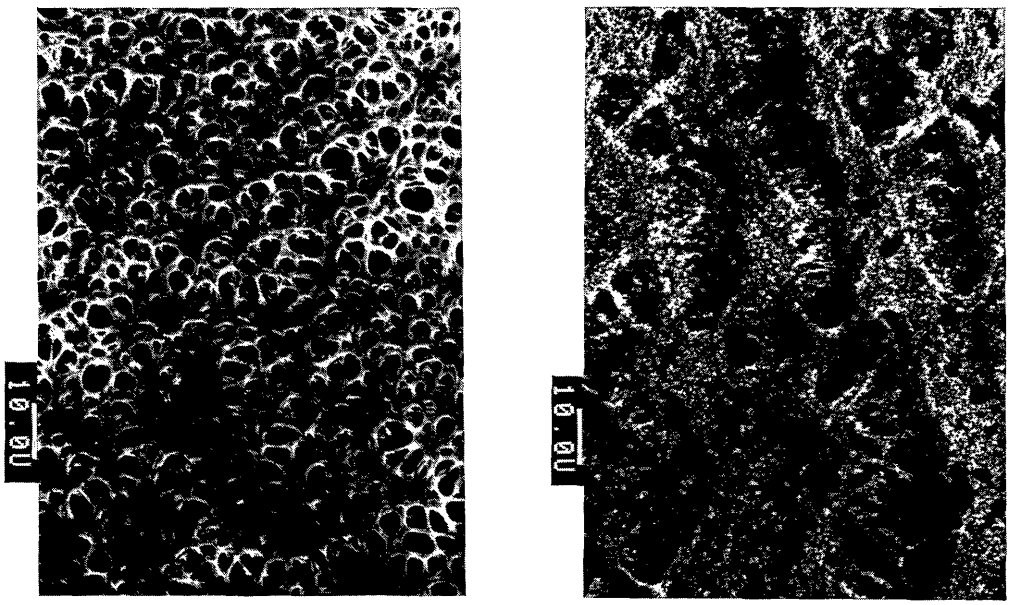

-a- -b-

Figure 13: *Electron micrograph of the inner surfaces of capillary membranes spun from the standard spinning solution PEI/PVP/NMP=17/13/70. a- Solvent concentration internal coagulation bath 90 wt. %. b- Solvent concentration internal coagulation bath 85 wt. %.*

The results for capillary membranes are shown on the electron micrographs in figure 13. The membranes are spun using the standard spinning solution PEI/PVP/NMP/=17/13/70 (30 °C). Using a solvent concentration of 75 wt. % in the internal coagulation bath the pore size at the inner surface is smaller than 0.05 μm (not shown). At a solvent concentration of 80 wt. % the pores are roughly 0.1 μm. Using a solvent concentration of 90 wt. % pores of 6-8 μm are formed (see figure 13a). When solvent concentrations between 80 and 90 wt. % are used the result is not only the correspondending pore size in the range of 0.05-8 μm, but a more or less ruptured porous structure at the inner surface (see figure 13b). This latter effect is caused by the elongation of the capillary membranes in combination with the time before solidification at the inner surface occurs.

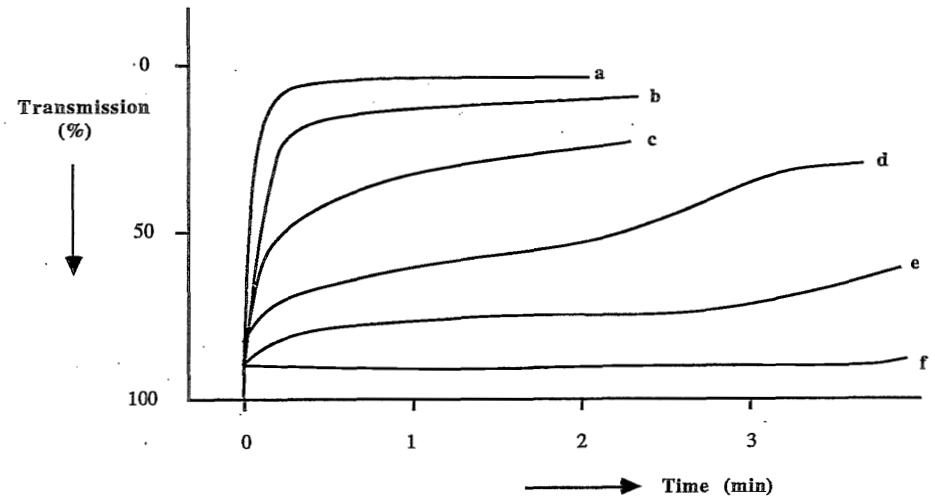

Figure 14: *Light transmission of flat membranes as a function of the immersion time for different solvent concentrations in the coagulation bath (water). Casting solution PEI/PVP/NMP=15/15/70. Concentration NMP in the coagulation bath (wt. %): a: 0 b: 90 c: 94 d: 95 e: 96 f: 97*

With a simple set up the light transmission of a cast flat membrane as a function of time can be measured [8,14]. This method was used by Reuvers et al. to investigate whether a membrane forming system exhibits instantaneous demixing or delayed demixing [8]. Some results of the membrane forming system PEI/PVP/NMP=15/15/70 are presented in figure 14 to demonstrate the difference between instantaneous demixing (a - e) and delayed demixing (f). It can be seen in figure 14 that although in the situations a - e instantaneous demixing occurs, a big difference between the curves does exist. In situation -e- it takes definitely more time before precipitation occurs than it does in situation -a-. Figure 14 also shows that it takes more time before a certain decrease in transmission is reached when more solvent is added to the coagulation bath.

Although it is impossible to compare the results of the light transmission experiments for flat membranes with the situation during spinning of capillary membranes and also it is not proven that the shape of the curves in figure 14 can be related to the precipitation rate in the toplayer, it does give a good indication about the time before a certain minimum transmission is reached as a function of the solvent concentration in the coagulation bath.

When the inner surface structures are formed and solidified quickly (solvent concentration in the internal coagulation bath smaller than 80 wt. %) the axial forces will not influence the structure at the surface. Also when it takes a relatively long time (solvent concentration > 90 wt. %) to solidify the inner surface structures the influence of these forces will be rather small.
When solvent concentrations between 80 wt. % and 90 wt. % are used the structure at the inner surface is more or less ruptured due to elongation of the capillary membranes (see figure 13b). The result is a porous ruptured structure and a rough surface compared with that of the outer surface.

3.5.2 Macroscopic morphology of the membranes

In this section the roundness of the capillary membranes and the irregularities in the circumferential shape of the bore are discussed. The electron micrographs in figure 15 show examples of the shape of the bore when different solvent concentrations in the internal coagulation bath are used.
When pure water is used as an internal coagulation bath the inner surface structure will be formed and solidified very rapidly, so that the radial and axial force do not have much influence on the shape of the bore. The shape of the bore is round or oval (see figure 15a). When solvent is added to the internal coagulation bath it takes more time to form and solidify the inner surface structure. And consequently the bore of the capillary membrane may deform. The result in this situation is a more or less irregular shape of the bore of the membranes (see figure 15b and 15c). When the solvent concentration reaches a certain large value, the definitive fixation will take so long, that the inner surface can accommodate surface to volume constraints and the shape of the bore is round (see figure 15d). This required value for the solvent concentration in the internal coagulation bath is dependent on the type of nonsolvent used. Water as nonsolvent requires 88 wt. % NMP (solvent), ethanol 50 wt. % NMP and polyethyleneoxide only 13 wt. % NMP to obtain a round shape of the bore of the membrane. In addition it can be mentioned that the solvent loss of the polymer solution to the bore liquid will be very low at high solvent concentrations in the internal coagulation fluid.
Experiments were done with spinneret 3 (see figure 5). The results are summarized in table 1 and can be seen in figure 15.

Table 1: *Dimensions of the bore of capillary membranes as a function of the composition of the internal coagulation bath. Spinning solution PEI/PVPN/MP=17/13/70, take-up speed 2.4 ml/min, flow rate of internal coagulation bath 1 ml/min, flow rate of polymer solution 3.2 ml/min. Temperature of the external coagulation bath was 70 °C and an airgap length of 4 cm was used. NMP-water mixtures were used as internal coagulation bath. Spinneret 3 (figure 5) was used, with an orifice of 2.5 mm and a capillary diameter of 0.9 mm (area 0.64 mm^2) For each NMP concentration at least three samples of capillary membranes were analysed with SEM.*

NMP concentration of the internal coagulation bath (wt. %)		Actual area of the bore (mm^2)	Circumference of the bore (mm)	Area based on computed diameter * (mm^2)	Outer diameter of the membrane (mm)
0	(see fig. 15a)	0.45	3.1	0.77	1.6
55	(see fig. 15b)	0.77	3.6	1.03	1.7
75	(see fig. 15c)	0.70	3.5	0.97	1.7
88	(see fig. 15d)	0.63	2.8	0.63	1.6

* the computed diameter (c/π) is calculated from the measured circumference (c).

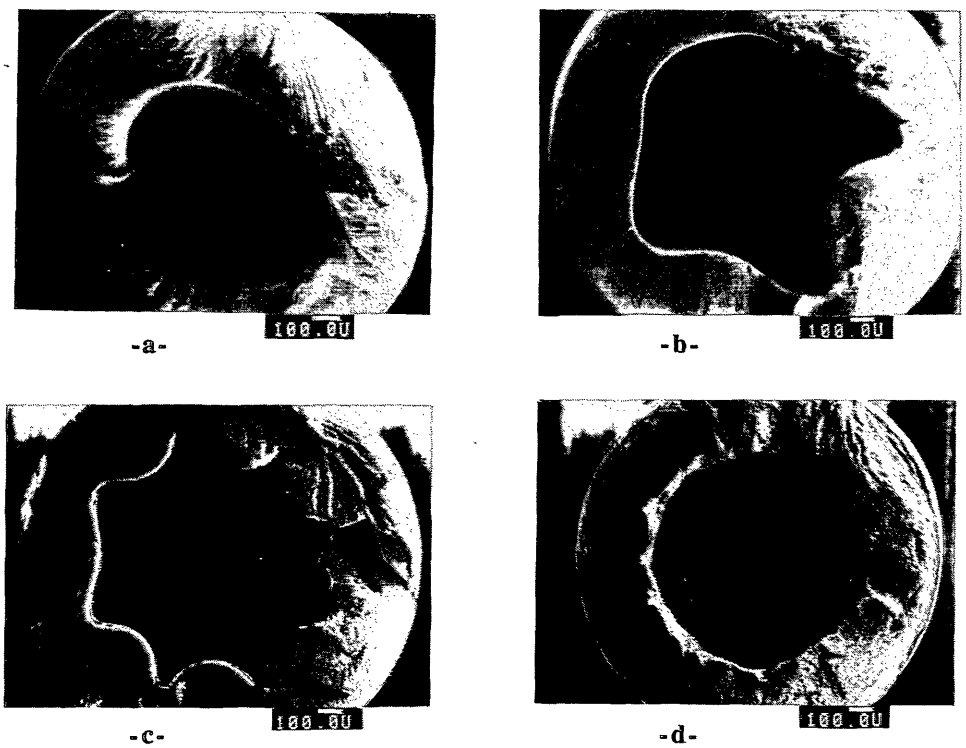

Figure 15: *Shape of the bore of capillary membranes for different solvent concentrations in the internal coagulation bath.*
a - 0 wt. % NMP in bore liquid *b - 55 wt. % NMP in bore liquid*
c - 75 wt. % NMP in bore liquid *d - 88 wt. % NMP in bore liquid*

The circumference of the bore is taken from the electron micrographs and simply measured with a piece of rope. When water is used as the bore liquid, the actual area of the bore is smaller than the area of the inner capillary. This is caused by the die-swell at the inside of the membranes.
A maximum can be found in the area and circumference of the bore. A basic reason for the expansion of the bore area is the fast solvent outflow from the polymer solution when low concentrations of solvent are applied in the internal coagulation bath. Since there is a competition between the solvent loss from the polymer solution, the solidification rate of the inner surface and the presence of radial forces it is reasonable that a maximum in the area of the bore can be observed in the series as given in table 1.

When the actual area of the bore of the capillary membrane is compared with the area of the capillary in the spinneret (0.64 mm^2), the results in table 1 indicate that the irregular shape is not only caused by insufficient bore liquid. This same result was also found by Van 't Hof for polyethersulfone hollow fibres [16].

3.5.2.1 *Effect of the flow rate of the bore liquid on the shape of the bore*

The effect of increasing the flow rate of the bore liquid having a solvent concentration of 40 wt. % is shown in figure 16a and 16b. In these experiments spinneret 2 (figure 5; diameter orifice 2.0 mm and outer diameter of the injection capillary 0.8 mm) was used; the other spinning conditions are the same as in the former experiment. Using a solvent concentration of 40 wt. % already at a flow rate of 1 ml/min a round shape of the bore was obtained (see figure 16). When pure water was employed as the internal coagulaton bath a flow rate of 1.5 ml/min was necessary to obtain a round shape of the bore. Considering these experiments the influence of the flow rate is very obvious.

At higher solvent concentration (between 75 and 88 wt. %) in the internal coagulation bath it is not possible to obtain a round shape by increasing the flow rate of the internal coagulation bath. In figure 14 the influence of the solvent concentration in the coagulation bath on the light transmission has been shown. It is assumed that at these high solvent concentrations the solidification of the inner surface has not proceeded far enough to withstand changes in surface to volume ratios, so that even at elevated flow rates of the internal coagulation bath still irregularities can still be found in the bore of the capillary membranes.

An important conclusion is that for relatively strong coagulants (low solvent concentrations) a round shape of the bore can be obtained by increasing the flow rate of the internal coagulation bath. At higher solvent concentrations in the internal coagulation bath the interface between coagulation bath and polymer solution is unstable and it is not possible to obtain a round shape of the bore by

increasing the flow rate of the internal coagulation bath. When a certain threshold value of solvent in the internal coagulation bath is reached a round shape of the bore can be found again.
An increase of the solvent concentration of the bore liquid, at a fixed flow rate of the bore liquid, can favour a round shape of the bore of the membranes, but at the same time it means also an increase of the pore size at the inner surface.

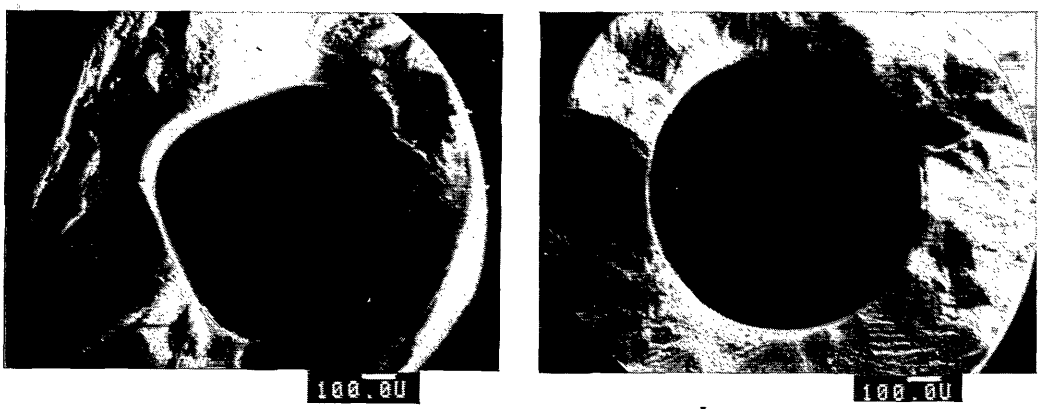

-a- -b-

Figure 16: *Shape of the bore of capillary membranes for different flow rates of the internal coagulation bath. The membranes were spun with spinneret 2 (figure 5) from the standard spinning solution PEI/PVP/NMP=17/13/70. Flow rate of the spinning solution 3.2 ml/min, take-up speed 2.4 m/min. Temperature of the external coagulatuion bath was 70 °C and an airgap length of 4 cm was used. Solvent concentration of the bore liquid 40 wt. %.*
a - Flow rate 0.8 ml/min b- Flow rate 1.0 ml/min

3.5.2.2 *Effect of the dimensions of the spinneret on the shape of the bore*

The influence of the dimensions of the spinneret on the shape of the bore of the capillary membranes was also investigated. Different types of spinnerets were used (see figure 5). The spinnerets were used under such conditions that it was impossible to obtain a round shape of the bore by simply increasing the flow rate of the internal coagulation bath. No influence of the dimension of the spinneret on the shape of the bore of the capillary membrane was found. In the situation that spinneret 5 was used (figure 5) a wavy shape at the *outer* surface was also found (see figure 17). For this experiment using the standard spinning solution PEI/PVP/NMP=17/13/70, the temperature of the external coagulation bath was 70° C and a mixture of NMP and PEG 400 (10 wt. % NMP) was used as the internal coagulation bath. The lenght of the airgap was 3 mm.
An explanation for this effect is based on the die-swell at the outside and the solvent loss of the polymer solution upon immersion. If the nascent membrane enters the external coagulation bath the outer membrane surface will start to solidify. Since the airgap length is only 3 mm the outer surface

will solidify when the outer diameter is on its maximum value. In the external coagulation bath the outer diameter of the membrane will tend to decrease, due to solvent loss. Therefore, as the outer surface is already formed and solidified, but still is flexible, irregularities in the shape of the capillary membrane can be the result. When the airgap length was increased a round outside shape of the capillary membrane was obtained again.

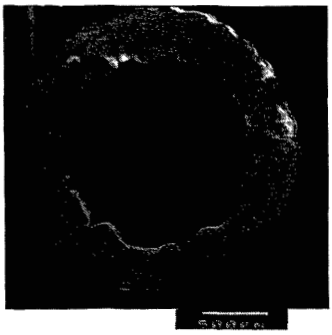

Figure 17: *Cross section of a microporous capillary membrane spun from the standard spinning solution PEI/PVP/NMP=17/13/70. Spinneret 5 (figure 5) was used. Airgap length 3 mm.*

3.6 CONCLUSIONS

This study has shown that using the phase inversion technique microporous capillary membranes can be made based on the new thermostable and chemically resistant polymer polyetherimide and the hydrophilic polymer polyvinylpyrrolidone. The preparation method is based on a combination of two phase inversion techniques: phase inversion from the vapour phase and immersion precipitation.
Pore sizes at the outer surface of the capillary membranes can be adjusted between 0.05 μm and 1 μm, by varying the temperature of the external coagulation bath, the composition of the spinning solution and/or the residence time in the airgap.

A minimum in the pore size across the membrane wall can be avoided by increasing the temperature of the external coagulation bath or by adding nonsolvent to the polymer solution.

Adjusting the pore size at the inner surface is achieved by changing the ratio solvent/nonsolvent in the internal coagulation bath but it is much more complicated than adjusting the pore size at the outer surface. At certain solvent concentrations in the bore liquid the inner surface can be ruptured as a result of stretching of the capillary membrane.

Under certain conditions the inner surface will not be able to accommodation of required surface to volume ratios and in combination with the solidification rate of the inner surface the result can be all kinds of irregular forms in the bore shape.

3.7 APPENDIX- Estimation of the penetration depth of the demixing front.

Measured amounts of polymer solution (PEI/PVP 360 000/NMP=17/13/70) in an shallow cylindrical vessel were placed in an atmosphere containing water vapour at a certain temperature. The water vapour was in equilibrium with water at that temperature. The weight increase of the polymer solution in time was measured and from these data a diffusion coefficient was determined. Calculations were done on the basis of the penetration model of a diffusing component in a semi infinite homogeneous medium. Using this model the following equation can be derived [17]:

$$J=(c_i-c_0)* \sqrt{(D/\pi*t)} = V/A * dc/dt \qquad (1)$$

The boundary conditions are:
- at t=0 the concentration of water in the polymer solution is c_0
- at t>0 the concentration of water at the interface x=0 is c_i.
- at large distance from the interface the concentration of water is c_0.

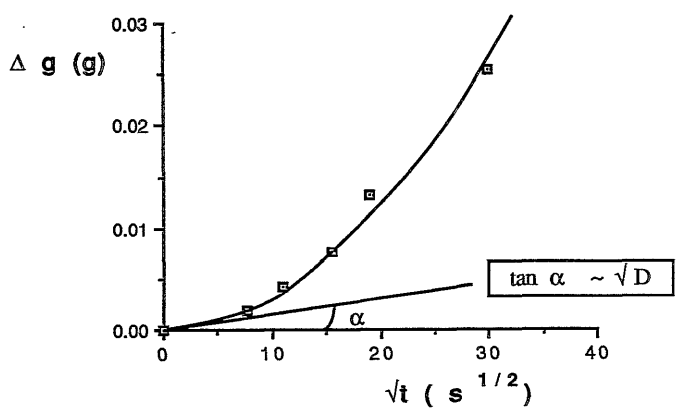

Figure 18: *Weight increase due to water vapour diffusion into a polymer solution (PEI/PVP/NMP=17/13/70) versus the square root of time measured at 42 °C.*

When the diffusion coefficient is independent of concentration and resistance of mass transfer in the gas phase is assumed to be absent, the following expression can be derived:

$dc/dt=A/V*(c_i-c_0)*\sqrt{(D/\pi*t)}$ or after integration: (2)

$\Delta g=2*A*(c_i-c_0)*\sqrt{(D/\pi)}*\sqrt{t}$ (3)

The results for the diffusion experiments at 42 °C are shown in figure 18. The plots for the diffusion experiments at other temperatures were similar. Because no straight lines were found the measured values were fitted with the best possible function, the slope at $\sqrt{t}=0$ was taken and the diffusion coefficient was calculated from that slope.
For these calculations penetration into a homogeneous medium instead of penetration into a demixed system was assumed. The fact that water vapour penetrates into a demixing system probably causes the non-linearity in the Δg versus $\sqrt{t}$ plots.
The distance x from the outer surface, where a minimum in the pore size over the cross section is found, is assumed to be at the place where a water concentration is reached just enough for incipient demixing and this distance x is calculated with the following equation [17] :

$$\frac{c_i-c}{c_i-c_o} = \mathrm{erf}\frac{x}{2*\sqrt{(D*t)}} \qquad (4)$$

For c the concentration at the liquid-liquid binodal is used [1]. For t the residence time in the airgap is taken. For the calculations of the minimum in the pore size with equation (4) penetration into a flat medium instead of into a cylinder was assumed. The results are shown in table 2 and in figure 19.

Tabel 2: *Results of water vapour penetration calculations in PEI/PVP/NMP=17/13/70 solutions for three temperatures. c_0 = 8.9 kg/m^3.*

Temperature water vapour (C°)	**c (kg/m^3) (from binodal)**	**c_i (kg/m^3)**	**D (m^2/s) *10^{11}**	**Location (x) of the minimum in pore size at a residence time in airgap of 1 s. (μm)**
28	18.4	95	0.036	1
42	18	69	0.76	6
70	16	32	10.0	14

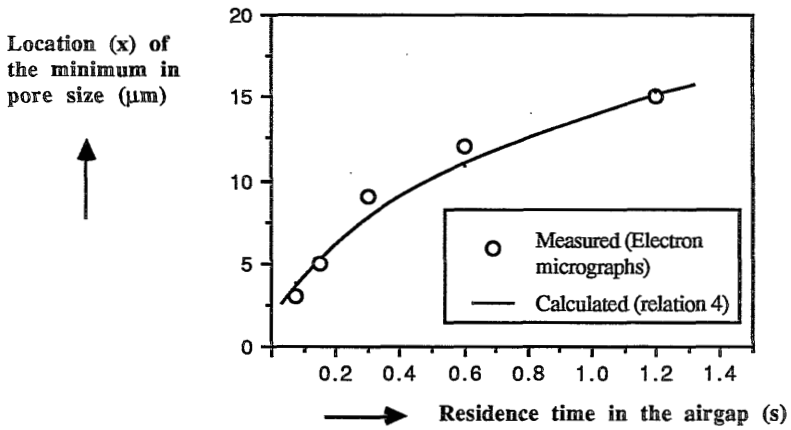

Figure 19: *Location of the minimum in pore size (calculated with relation 4; the measured values were taken from electron micrographs) versus the residence time of the capillary membrane in the airgap. Temperature external coagulation bath was 70 °C, spinning solution PEI/PVP/NMP=17/13/70.*

Although the calculation of the diffusion coefficients is rather inaccurate, it is clear that the results in the appendix are in good agreement with the experimental results about the minimum in pore size presented in previous sections.

3.8 NOTATION

J	-	flux	$kg/m^2\ s$
J_{NS}	-	flux of nonsolvent	$kg/m^2\ s$
J_S	-	flux of solvent	$kg/m^2\ s$
A	-	area	m^2
V	-	volume	m^3
D	-	diffusion coefficient	m^2/s
t	-	time	s
Δg	-	weight increase of the polymer solution	kg
c	-	concentration of water at the liquid-liquid boundary	kg/m^3
c_0	-	concentration of water at t=0 in the solution	kg/m^3
c_i	-	concentration of water at the interface at t>0	kg/m^3

3.9 ACKNOWLEDGEMENTS

M.J. Almering is acknowledged for performing part of the spinning experiments.

3.10 REFERENCES

1 H.D.W. Roesink, M.J. Otto, J.A. Ronner, M.H.V. Mulder and C.A. Smolders, Demixing phenomena and membrane formation in the four component system polyetherimide/ polyvinylpyrrolidone/ N-methylpyrrolidone/ water, PhD Thesis Chapter 2, University of Twente, Enschede, The Netherlands (1989).

2 H.D.W. Roesink, Z. Borneman, M.H.V. Mulder and C.A. Smolders, Polyether-imide-polyvinylpyrrolidone blends as membrane material, PhD Thesis Chapter 4, University of Twente, Enschede, The Netherlands (1989).

3 I. Cabasso, E. Klein, J.K. Smith, Polysulfone hollow fibers. I. Spinning and properties, J. Appl. Polym. Sci., **20** (1976) 2377.

4 I. Cabasso, E. Klein, J.K. Smith, Polysulfone hollow fibers. II. Morphology, J. Appl. Polym. Sci., **21** (1977) 165.

5 I. Cabasso, K.Q. Robert, E. Klein, J.K. Smith, Porosity and pore size determination in polysulfone hollow fibers, J. Appl. Polym. Sci., **21** (1977) 1883.

6 P. Aptel, N. Abidine, F. Ivaldi, J.P. Lafaille, Polysulfone hollow fibers - Effect of spinning conditions on ultrafiltration properties, J. Membr. Sci., **22** (1985) 199.

7 L.Y. Lafrenière, F.D.F. Talbot, T. Matsuura, S. Sourirajan, Effect of polyvinylpyrrolidone additive on the performance of polyethersulfone ultrafiltration membranes, Ind. Eng. Chem. Res., **26** (1987) 2385.

8 a- A.J. Reuvers, J.W.A. van den Berg and C.A. Smolders, Formation of membranes by means of immersion precipitation. Part I. A model to describe mass transfer during immersion precipitation, J. Membr. Sci., **34** (1987) 45.
b- A.J. Reuvers and C.A. Smolders, Formation of membranes by means of immersion precipitation. Part II. The mechanism of formation of membranes prepared from the system CA/ acetone/ water, J. Membr. Sci., **34** (1987) 67.
c- A.J. Reuvers, Membrane formation, PhD Thesis, University of Twente, Enschede, The Netherlands (1987).

9 D.M. Koenhen, M.H.V. Mulder and C.A. Smolders, Phase separation phenomena during the formation of asymmetric membranes, J.Appl. Polym. Sci., **21** (1977) 199.

10 M.A. Frommer and D. Lancet, in Reverse Osmosis Membrane Research, H.K. Lonsdale and H.E. Podall (Eds.), Plenum Press, New York (1972) 85.

11 H. Strathmann and K.Koch, The formation mechanism of phase inversion membranes, Desalination, **21** (1977) 241.

12 - L. Broens, F.W. Altena, C.A. Smolders and D.M. Koenhen, Asymmetric membrane structures as a result of phase separation phenomena, Desalination, **32** (1980) 33.
- F.W. Altena, Phase separation phenomena in cellulose acetate solutions in relation to asymmetric membrane formation, PhD Thesis, University of Twente, Enschede, The Netherlands (1982).

13 - J.G. Wijmans, J.P.B. Baaij and C.A. Smolders, The mechanism of formation of microporous or skinned membranes produced by immersion precipitation, J. Membr. Sci., **14** (1983) 263.
- J.G.Wijmans, Synthetic membranes, PhD Thesis, University of Twente, Enschede, The Netherlands (1984).

14 C. Gelman, Microporous membrane technology. Part I. Historical development and applications, Analytical Chemistry, **37** (1965) 29.

15 H.D.W. Roesink, S. Oude Vrielink, M.H.V. Mulder and C.A. Smolders, Post-treatment of hydrophilic membranes prepared from polyetherimide-polyvinylpyrrolidone blends, PhD Thesis Chapter 5, University of Twente, Enschede, The Netherlands (1989).

16 J.A. Van 't Hof, Wet spinning of asymmetric hollow fibre membranes for gas separation, PhD Thesis Chapter 2, University of Twente, Enschede, The Netherlands (1988).

17 J.Crank, The Mathematics of Diffusion, Clarendon, Oxford (1975).

CHAPTER 4

POLYETHERIMIDE-POLYVINYLPYRROLIDONE BLENDS AS MEMBRANE MATERIAL

H.D.W. Roesink, Z. Borneman, M.H.V. Mulder and C.A. Smolders.

4.1 SUMMARY

In this chapter the preparation of both homogeneous membranes obtained by solvent evaporation and phase inversion membranes from polyetherimide-polyvinylpyrrolidone blends is described. The membrane forming properties of these blends are compared with those of other polymer blends, i.e., polyethersulfone - polyvinylpyrrolidone and polyimide - polyvinylpyrrolidone blends.

Polyetherimide (PEI) is compatible with polyvinylpyrrolidone (PVP) at all weight ratios. For homogeneous membranes single glass transition temperatures are found, which indicates that the membrane material is a homogeneous blend. When homogeneous membranes are immersed in water no weight decrease can be observed, only at high temperatures and high PVP concentrations PVP will leach out.

When phase inversion membranes are prepared from blends of PVP and the polymers mentioned, the amount of PVP that remains in the membrane matrix after membrane formation depends on the molecular weight of the PVP, the interaction between PVP and the second polymer in the blend and the rate of solidification. When high molecular weight PVP is added to a PEI casting solution heterogeneous blends (two glass transition temperatures) are formed, while addition of low molecular weight PVP will give homogeneous blends (one single glass transition temperature).

4.2 INTRODUCTION

Most of the commercially available membranes are made by a phase inversion technique. Theories to explain the morphology of this type of membranes as a function of different process parameters are based on ternary membrane forming systems. Such a system consists of a polymer, a solvent for the polymer and a nonsolvent. When membranes are produced on a commercial scale often a multi component membrane forming system is used. Additives, which can be of low or high molecular weight, are used to obtain desirable membrane properties. The use of the additives is merely based on empirical rules. One of the high molecular weight additives that is often used is

polyvinylpyrrolidone (PVP).

For the dry-wet spinning process of hollow fibres or capillary membranes a certain viscosity level of the polymer solution is required. High molecular weight PVP can be used as an additive since it increases the viscosity and while it is soluble in many solvents, including water, it can dissolve in the coagulation bath and it therefore might not be present any more in the ultimate porous membrane structure.

Cabasso et al. [1,2,3] used polysulfone (PSf) solutions for the preparation of microporous hollow fibres and added PVP with a molecular weight of 10 000 and 40 000 to these solutions. Hollow fibre membranes were spun, using the phase inversion technique. The water permeability of the final membranes increased when the amount of PVP in the spinning solution was increased. Their idea about the influence of PVP on the membrane formation was that the initially homogeneous solution of PSf/PVP separated into microdomains and that the PVP eventually dissolved out of the matrix, when water was used as a nonsolvent. So, an important effect of adding PVP to the spinning or casting solution is an improvement of the permeability [1,2,3,4,5]. In fact adding PVP can substantially improve the membrane structure with respect to interconnectivity of the pores and porosity of the membrane toplayers as is shown in chapter 2 [6].
Lafrenière et al. [7] studied the influence of the ratio of PVP to polyethersulfone (PES) on the ultrafiltration properties of flat membranes. They found a relationship between permeability and PVP/PES ratio. They suggested that PVP might be entrapped in the PES network of a phase inversion membrane and then forms an integral part of the polymeric structure. The analysis of their membranes revealed that the PVP to PES weight ratio in the membranes was less than 0.04 while this ratio in the casting solution was from 0.4 to 1.0. They concluded that the primary effect of the presence of PVP in the casting solution is an effect on the structure of the casting solution and, as a consequence, on the pore size and the pore size distribution of the membranes. They also found an improvement of the hydrophilicity of the ultrafiltration membranes.

From literature it appears that, although PVP at first was used to increase the viscosity of the spinning solutions, it also has an important influence on the morphology and the properties of the membranes. The PVP in the polymer solution will almost completely dissolve in the coagulation medium if the phase inversion technique is used.

When a polymer solution is cast on a non-porous support and one allows the solvent to evaporate, the result will be a homogeneous membrane, which can be used for separation processes based on differences in solubility and/or diffusion rates in the membrane material of the components that have to be separated. Such membranes can be used for pervaporation, dialysis and gas separation.

Suitable separation properties (high selectivity and a high permeability) can be obtained by using additives or, more specifically, by blending two polymers. In this way it might be possible to control membrane performance.

Nguyen et al. [8] prepared homogeneous membranes by blending polyacrylonitrile (PAN) and PVP (MW=360 000). The membranes were used for pervaporation of water-organic liquid mixtures. Although they reported that the membranes were not modified during a pervaporation experiment of 50 hours, they did not report anything about leaching out of PVP during these experiments.
Schchori et al. [9] blended polyether-polyamide with PVP (MW=360 000) and prepared homogeneous membranes. The membranes were tested for reverse osmosis applications and they found that the blends were homogeneous and that the water soluble PVP did not leach out even after a prolonged storage in water. The PVP had a stabilizing effect on the polyether-polyamide, so that the blends were more thermally stable than the homopolymers. As far as we know, Schchori et al. are the first to report about retaining PVP in the precipitated polymer mixture. When a solution of the PVP-blend was poured into stirred water (which can be compared with the immersion precipitation process) almost 90 wt. % of the PVP was retained by the finely dispersed precipitate.

PVP (MW=20 000) forms with cellulose acetate phthalate a homogeneous blend, which is water insoluble and can be used for reverse osmosis applications. Kurokawa et al. [10] report that there was no leaching out of the PVP. PVP (MW=360 000) can form blends with polyisocyanates that are water insoluble and are used for reverse osmosis [11].
Ultrafiltration and dialysis membranes have been made from cellulose nitrate-PVP (MW=3500) blends [12].

In conclusion, PVP is often used as an additive in membrane forming systems for the preparation of homogeneous membranes. PVP is compatible with different polymers and the main function it has seems to be that it can maintain the selectivity while it increases the permeability.

In our laboratory a new type of hydrophilic microfiltration membranes based on polyetherimide (PEI) and PVP has been developed [6,13]. It was found that in the porous membrane matrix, prepared by phase inversion, a substantial amount of PVP is still present and that certainly not all of the PVP dissolves in the precipitation bath, as reported by other investigators.
In this chapter the membrane forming properties of three polymers blended with PVP are compared. These polymers are polyetherimide (PEI), polyethersulfone (PES) and polyimide (PI). Some results for polyacrylonitrile are presented too.
From these polymer blends both homogeneous membranes and phase inversion membranes have been prepared.

The homogeneous blend membranes were characterized by determination of the glass transition temperature and by studying the outdiffusion of PVP when immersed in water.
The phase inversion membranes were characterized by measuring the PVP outdiffusion rate during the immersion precipitation in water, the outdiffusion rates of PVP from the final membranes in water and by determination of the glass transition temperatures.

4.3 EXPERIMENTAL

Materials

Polyetherimide (Ultem ® 1000) was kindly supplied by General Electric, Bergen op Zoom , The Netherlands. Polyethersulfone (Victrex ® 4800P) was purchased from ICI Ltd. The polyimide (2080) was purchased from Upjohn. Polyvinylpyrrolidone (MW=360 000 and MW=10 000) was purchased from Janssen Chimica, Belgium. Polyacrylonitrile (PAN) was purchased from Du Pont. N-methyl-2-pyrrolidone (NMP; Merck, synthesis grade) was used as a solvent.
Molecular weights and molecular weight distributions were determined with size exclusion chromatography (table 1).

Table 1: *Molecular weights of the polymers used in this work.*

Polymer	Solvent	M_n	M_w
PEI (Ultem® 1000)	$CHCl_3$	20 000	33 000
PES (Victrex ®)	DMF	25 000	47 000
PI (Upjohn 2080)		18 000	53 000
PAN		—	516 000
PVP 10 000	$CHCl_3$	46 000	61 000
PVP 360 000	$CHCl_3$	330 000	423 000

Preparation of membranes

The homogeneous membranes were prepared by solution casting followed by an evaporation step in a nitrogen atmosphere. To obtain a solvent free membrane the membranes were placed in a vacuum oven at 50 °C for at least 24 hours and eventually rinsed in a water bath. After this

procedure the homogeneous membranes contained less than 1 wt. % solvent.

Flat phase inversion membranes were made by casting a polymer solution film (25 °C) on a glass plate followed by immersion precipitation in a water bath (25 °C).

Differential scanning calorimetry (DSC)

A Perkin Elmer DSC Differential Scanning Calorimeter in combination with a System 4 microprocessor Controller and a Model 3700 Thermal Analysis Data Station (TADS) was used for DSC measurements. Nitrogen gas was purged through the sample chambers at all times. The polymer samples were placed in aluminium sample pans which were sealed with perforated covers. A heating rate of 20 °C/min and a cooling rate of 320 °C /min were used. The T_g was determined in the second or third run and it was defined as the midpoint temperature of the second order transition. The system was calibrated using indium and lead.

Dynamic mechanical measurements

Samples of homogeneous or phase inversion membranes were placed into a Myrenne (ATM 3) torsion pendulum instrument. The torsion moduli G' and G" were measured in a nitrogen atmosphere at a constant frequency of 1 Hz and a heating rate of 1 °C /min. The maximum of G" is taken as the T_g.

Contact angle measurements

Thin polymer films were made by dipping glass surfaces in a solution of PEI/PVP in NMP (5 wt. %). The glass plates were placed in a vacuum oven at a temperature of 50 °C for three days to remove the solvent. Small water droplets were placed on the polymer surfaces and the contact angle was calculated from the dimensions of the droplet [14]. Each contact angle is the average of at least ten measurements. Contact angles could be measured with an accuracy of $\pm 3°$.

Intrinsic viscosity measurements

The intrinsic viscosities of the blends were measured in N-methylpyrrolidone at 25 ± 0.2 °C using an Ubbelohde viscometer.

Thermogravimetry (TGA)

A Perkin Elmer TGS-2 Thermogravimetrical Analyser in combination with a System 4 Microprocessor Controller and a model 3700 Thermal Analysis Data Station were used for these experiments. During all experiments a nitrogen atmosphere was provided by a continuous gas flow of 85 ml/min.

Outdiffusion experiments

Solvent free homogenous blend membranes or cast polymer films on a glass plate were placed in a water bath. The water bath was stirred and kept at a constant temperature. At certain time intervals samples of the leaching bath were taken to find the PVP concentration. The concentration of PVP in the aqueous solutions was determined colorimetrically [9,15]; 2 ml acetic acid and 5 ml iodine reagent ($2{,}5*10^{-3}$ M I_2 + $1{,}3*10^{-2}$ M KI in 2,5 % aqueous $ZnSO_4$) were added to 8 ml samples of solutions to be tested.

4.4 RESULTS AND DISCUSSION

4.4.1 Contact angle measurements

Polyetherimide (PEI) and PVP are miscible over the whole composition range. The homogeneous polymer films used in this chapter were all transparent and showed no sign of phase separation. PVP is a hydrophilic polymer, while PEI has much more a hydrophobic character. When homogeneous membranes are made from PEI/PVP (MW= 360 000) solutions, the contact angle of water on the polymer surface is a function of the PVP content. The results are shown in figure 1.

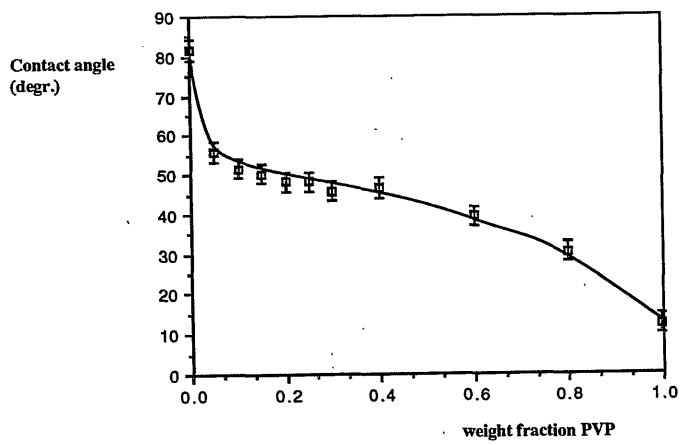

Figure 1: *Contact angle of water on PEI/PVP (MW 360 000) films as a function of the PVP content in the films.*

The contact angle decreases from 82° for pure PEI to about 50° when 10 wt. % PVP is present in the film. Upon increasing the PVP content to 80 wt. % the contact angle decreases to about 30°. The results show that an amount of 5-10 wt. % PVP in the polymer film is sufficient to obtain a

fairly wettable membrane surface.

4.4.2 Outdiffusion experiments

4.4.2.1 Homogeneous membranes

Using an amount of 25 wt. % PVP 360 000 in the homogeneous membranes (polymer films) outdiffusion experiments showed that PVP was insoluble in water when mixed with PEI, PES or PI (see table 2). Even after one month in a water bath at 80 °C no outdiffusion of PVP could be measured and also for low molecular weight PVP (MW =10 000) there is still no outdiffusion of PVP from PEI/PVP films.

When the PVP content in the PEI mixtures was increased or the molecular weight of the PVP was decreased and/or the temperature of the water bath was increased some outdiffusion of PVP could be measured.

It appears from these experiments that PVP forms very stable polymer mixtures (with respect to the PVP outdiffusion) with PEI and also with PES and PI, although the number of experiments for the latter group of polymers was only limited.

Table 2: *Outdiffusion of PVP from homogeneous membranes in a water bath for different PVP blends.*

Blend (film)	**PVP weight fraction (w/w)**	**MW of PVP**	**PVP weight fraction (w/w) present in the films after immersion in a water bath**		**percentage of PVP disappeared (based on PVP present in film)**
PES/PVP	0.25	360 000	after 31 days at 80° C	0.25	0 %
PI/PVP	0.25	360 000	after 31 days at 80° C	0.25	0 %
PEI/PVP	0.25	360 000	after 31 days at 80° C	0.25	0 %
PEI/PVP	0.43	360 000	after 41 days at 80° C	0.43	0 %
PEI/PVP	0.80	360 000	after 18 days at 25° C	0.79	6 %
			and 41 days at 80° C	0.73	32 %
PEI/PVP	0.25	10 000	after 41 days at 80° C	0.25	0 %
PEI/PVP	0.43	10 000	after 35 days at 25 °C	0.43	0 %
			and 45 days at 80 °C	0.36	26 %
PAN/PVP	0.25	360 000	after 21 days at 25° C	0.25	0 %
			and 18 days at 80° C	0.21	20 %
PAN/PVP	0.50	360 000	after 21 days at 25° C	0.46	15 %

The experiments with PAN/PVP blends demonstrated that not every polymer forms stable blends with PVP. The homogeneous membrane with a weight fraction of 0.25 showed no outdiffusion of PVP in water at room temperature. At higher temperatures of the water bath and at higher weight fractions of PVP the homogeneous PAN/PVP films showed indeed some outdiffusion of PVP, which is an indication that the PAN/PVP blends are less stable than PEI, PES or PI blends with PVP.

4.4.2.2 Phase inversion membranes

For phase inversion membranes the preparation method is completely different compared with that of homogeneous membranes obtained by solvent evaporation. Characteristic for the phase inversion process is a solvent/nonsolvent exchange combined with the fact that the PVP (polymer II) can dissolve in the coagulation bath, while PEI (polymer I) is confined to the membrane phase. A schematic representation of the phase inversion process is given in figure 2.

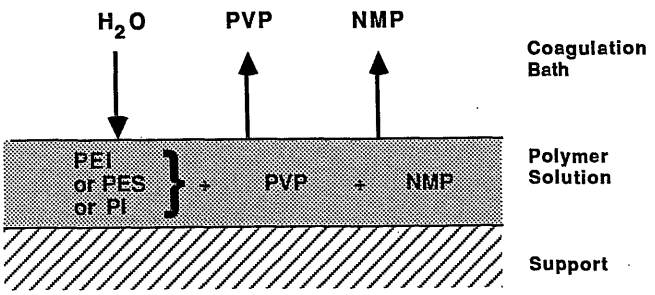

Figure 2: *Schematic representation of the exchange of solvent, nonsolvent and polymer during immersion precipitation.*

The porous structure of the membrane matrix is formed by a liquid-liquid demixing process [6,13]. As a result of this demixing process the membrane emerges as a two phase system consisting of a solidifying continuous polymer (I) rich phase and a liquid dispersed polymer (I) poor phase, but rich in polymer II. These phases represent the membrane matrix and the pores respectively. The time at which complete solidification or gelation occurs of the polymer (I) rich phase is an important parameter.
The solutions that were used for membrane casting are shown in table 3.

miscibility and/or the presence of micro-heterogeneities [19]. Single glass transition temperatures for the homogeneous films were also found performing dynamic mechanical measurements. In general dynamic relaxation techniques are the most sensitive ones for measuring glass transitions [16]. The glass transition temperatures measured with a torsion pendulum were in good agreement with those found with DSC experiments.

Table 4: *Glass transition temperatures of homopolymers and of homogeneous blend membranes measured with DSC.*

Material	Weight fraction of PVP	T_g (°C)	k (Gordon-Taylor)
PEI	-	217	
PES	-	225	
PI	-	321	
PVP 360 000	-	177	
PVP 10 000	-	125	
PEI/PVP 360 000	0.25	215	5
PEI/PVP 360 000	0.43	206	2
PEI/PVP 360 000	0.80	191	2
PEI/PVP 10 000	0.25	205	5
PEI/PVP 10 000	0.43	198	1.3
PES/PVP 360 00	0.25	201	0.3
PI/PVP 360 000	0.25	317	11

There are several semi-empirical classical equations that can be used to correlate and/or to predict the glass transition temperature for a miscible system when its composition is known. The Gordon-Taylor equation [20] is frequently employed:

$$T_g = \frac{w_1 * T_{g1} + k * w_2 * T_{g2}}{w_1 + k * w_2} \qquad (1)$$

where T_g, T_{g1} and T_{g2} are the glass transition temperatures of the blend, of homopolymer 1 and of homopolymer 2 respectively; w_1 and w_2 are the corresponding weight fractions and k is the ratio between the volume expansion coefficients of the homopolymers in the mixture. Usually the k value is semi-quantitatively related to the strength of the interaction between the two polymers [20,21,22]. In figure 3 the relation between the PVP 360 000 weight fraction and the glass transition temperature of the blend for different k values can be seen. When k=1, the weight-average glass transition temperatures are found. A positive deviation is found for k>1; this

indicates a strong interchain interaction which can decrease the mobility of the polymer chains.

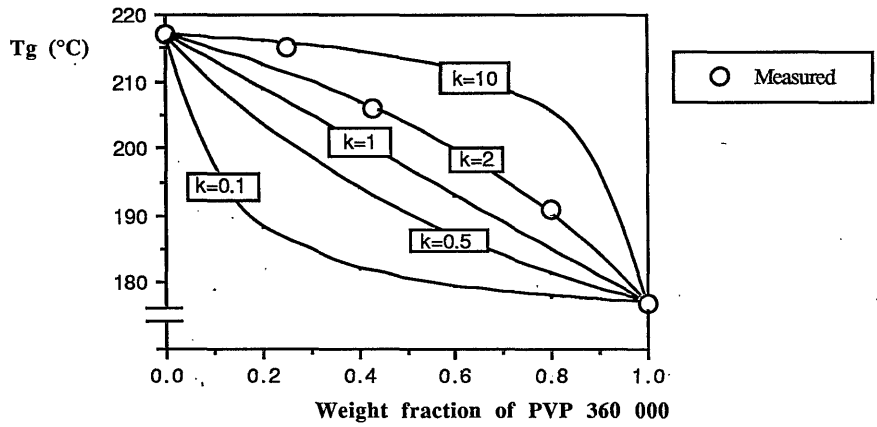

Figure 3: *Theoretical and measured glass transition temperatures as a function of the weight fraction PVP 360 000 in PEI/PVP blends. Theoretical glass transition temperatures are calculated using the Gordon-Taylor equation (1) with different values for k.*

Kwei [23] was one of the investigators who reported about a positive deviation of the glass transition temperature for various polymer blends. Kwei explained the positive deviations of the glass transition temperatures on the basis of (hydrogen bonding) interchain interactions.
Rodriguez-Parada et al. [20] found positive deviations of the glass transition temperature in so-called EDA (electron donor-acceptor) complexes. They suggested that thermally reversible crosslinked networks are formed. The positive deviation of the glass transition temperature indicates a very strong interaction between the polymer chains.
In the polymer system we studied no hydrogen bonding can be expected. The most obvious possibility is that the NCO-group of the pyrrolidone ring is involved in the interchain interaction. This amide group can interact with the imide group of the polyetherimide (dipole-dipole interaction) or the aromatic rings (donor/acceptor nature). Using infrared analysis (FTIR) a shift in the absorption spectra for the NCO-peak was found. For the PVP-spectrum a sharp minimum was found at 1653 cm^{-1}, while this minimum in the spectrum of the PEI/PVP blend was shifted to 1685 cm^{-1}. This shift indicates that the amide-group of the pyrrolidone ring is involved in the polymer-polymer interaction.

From the measured glass transition temperatures of the PEI/PVP blends it can be concluded that the strongest interaction between PEI and PVP occurs at a PVP content of 0 - 0.25, corresponding

with a ratio of the repeat units of PEI to PVP of 0 to 2, which means that the strongest interaction is that between one PEI unit and a maximum of two PVP units.
The plot of the intrinsic viscosity versus blend composition (figure 4) shows that intrinsic viscosities for PVP 360 000 weight fractions up to 0.3 are on the straight line while PVP weight fractions above 0.3 lie below this straight line. Kundu et al. [24] found for their polymeric system (Shellac and polyamideimide) that only compositions on the straight line in the intrinsic viscosity plot formed homogeneous blends.
The negative deviation in the intrinsic viscosity plot does not point to heterogeneities in PEI/PVP blends as is shown using the DSC and torsion pendulum experiments. It merely could indicate that the interaction between PEI and PVP decreases when the PVP concentration increases.

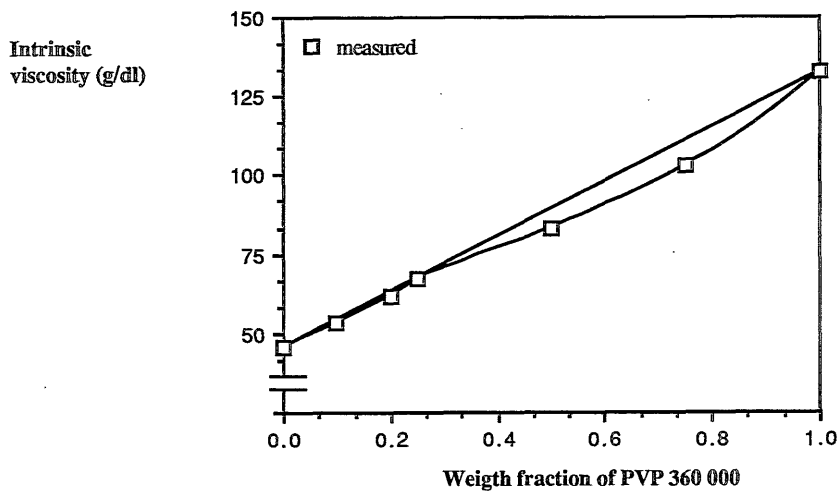

Figure 4: *Intrinsic viscosity versus blend (PEI/PVP 360 000) composition. The viscosities are measured at 25 °C and N-methyl-2-pyrrolidone was used as a solvent.*

4.4.3.2 Phase inversion membranes

As shown in a previous section an appreciable amount of residual PVP could be found in the phase inversion membranes. From DSC results and from the outdiffusion experiments with homogeneous films it could be concluded that PVP forms stable and homogeneous blends with PEI, PES and PI.
Another conclusion from the DSC experiments is that between PI and PVP there is a very strong interaction, while the interaction between PVP and PES is less strong. In fact the factor k, calculated with the Gordon-Taylor relationship (table 4) corresponds quite well with the

concentration of PVP found in the membrane matrix of the phase inversion membranes.

Using DSC experiments one single glass transition temperature for the phase inversion membranes had been found. The Tg for the PEI/PVP 360 000 membranes prepared from the casting solution PEI/PVP/NMP=17/13/70 is found to be 214 °C and it corresponds quite well with the PVP content of 25 wt. % (compare the data in table 3 and in figure 3).
However, dynamic mechanical measurements (torsion pendulum) showed that using the same phase inversion membranes (containing 25 wt. % PVP 360 000) two transition temperatures can be distinguished: one at 180 °C and one at 215 °C.

When phase inversion membranes were prepared from all PEI/PVP 10 000/NMP solutions mentioned in table 3 and the glass transition temperatures were measured using the torsion pendulum one single glass transition temperature (212 -214 °C) was found. These glass transition temperatures were slightly higher than would be expected based on the measurements using homogeneous PEI/PVP 10 000 films (table 4). This might be caused by the fact that in the phase inversion membranes the solvent content is negligible.

4.4.4 Evaluation

As was shown in section 4.4.2 the PVP content in the membranes can be considerable in PEI, PI and PES membranes. In this section it will be exposed how the kinetics of the demixing process can be responsible for the differences in residual PVP content in the phase inversion membranes.

Our hypothesis is that at high rates of the demixing process, the time at which solidification of the polymer (I) rich phase occurs is relatively short and that the PVP molecules will be entrapped during the solidification of the polymer (I) rich phase. At lower rates of the demixing process the PVP can diffuse into the polymer (I) poor phase and finally dissolves in the water bath.

The influence of the demixing rate will be illustrated by light transmission experiments. This type of light transmission experiments was performed by Reuvers et al. [25,26] to study demixing phenomena in relation to membrane forming properties.
From a homogeneous polymer solution a membrane (0.2 mm) was cast on a glass plate and brought immediately in a coagulation bath. The light transmission was measured as a function of time. The coagulation bath used contains a nonsolvent/solvent mixture (H_2O/NMP=0.25/0.75 (w/w)). When pure water is used the demixing rate is very fast (instantaneous demixing) and cannot be followed in any detail.
Assuming that the light transmission can be correlated with the time of solidification some

qualitative information is obtained about the time-span during which PVP can diffuse into the polymer poor phase. A long time-span before solidification occurs means that more PVP can diffuse into the polymer poor phase compared with a short time-span.
The time it takes to proceed from 70% to 40% transmission is taken as an indirect criterium for the demixing rate and therefore for the time of solidification. This is generally the steepest part of the curve and moreover it was difficult to obtain the starting point at 100% transmission with any accuracy and not always 0% transmission was reached (see also figure 5 in chapter 2 [6]).

Table 5: *Light transmission experiments for different casting solutions precipitated in a H_2O/NMP=25/75 (w/w) mixture.*

Casting solution	Time-span (s) from 70 % to 40% light transmission of the nascent membrane	PVP weight fraction in the membrane after 1 day at 25 °C.	Viscosity of the casting solution (Pa.s)	Gordon-Taylor Factor k*
PEI/PVP 360 000/NMP=15/5/80	2	0.15	6.3	5
PEI/PVP 10 000/NMP=15/5/80	13	0.10	1.5	5
PI/PVP 360 000/NMP=15/5/80	13	0.20	8.5	11
PES/PVP 360 000/NMP=15/5/80	68	0.04	4.9	0.3

* The factor k is calculated from the glass transition temperature determined using DSC (see table 4)

The results in table 5 show that the final PVP concentrations present in the membranes correspond rather well (inversely) with the light transmission experiments. It has to be stressed that during the actual membrane preparation instantaneous demixing occurs and no difference in demixing rate could be observed, between the PEI, PI and PES solutions. Still, from the results in table 5 can be conluded that the demixing rate for PES solutions is lower than the demixing rates for the PEI and PI solutions and one would expect the final PVP contents in PES membranes to be the lowest. The latter conclusion is also in good agreement with the interaction strengths based on the glass transition temperature measurements.

The influence of the molecular weight of PVP has been investigated using PEI/PVP blends. From experiments with homogeneous membranes (table 2) it appeared that low molecular weight PVP could be leached out relatively easily (compared with high molecular weight PVP) in the situation that higher temperatures of the leaching bath were used.
From the experiments with the phase inversion membranes some different results were found (table 3). The PVP 10 000 present in phase inversion membranes cannot be easily removed from the polymeric membrane matrix in contradistinction with the high molecular weight PVP that leaches out of the membranes. An explanation for these effects is based on the character of the blend of the

membrane material in the phase inversion membranes. For PEI/PVP 10 000 membranes single glass transition temperatures were found, which means that the material must be a homogeneous blend.

It was found that in the case of the phase inversion membranes containing PVP 360 000 not a completely homogeneous blend is formed, since two glass transition temperatures were found when using dynamic mechanical measurements. This conclusion is supported by electron micrographs of the cross section of the phase inversion membranes and by outdiffusion experiments with phase inversion membranes at elevated temperatures (table 3). The electron micrograph (figure 5) shows that there are inhomogeneities in the material of the phase inversion membranes, indicating a non-uniform distribution of PEI and PVP.

-a- -b-

Figure 5: *Morphology of the porous structure in the cross section of a PEI/PVP 360 000 phase inversion membrane. Electron micrograph -b- shows a detail of micrograph -a-.*

Our hypothesis is that the centre of the solid membrane material consists of a PEI-rich phase while near the surface a PVP-rich phase is present. The origin of this segregation is that during the immersion precipitation the PVP has a tendency to diffuse into the growing nuclei, which become the pores, so that at the interfacial region of the membrane pores a relatively high PVP concentration will be found [6].

Outdiffusion experiments with homogeneous polymer membranes showed that only polymer films with a very high PVP 360 000 content (80 wt. %) lost PVP in a water bath. Therefore, it can be concluded that the solid membrane material in the phase inversion membranes is not completely homogeneous and that due to the high PVP concentration at the interface of the pore walls PVP can leach out of the membrane material.

When PVP 10 000 is added to the casting solution the membrane material of the phase inversion membrane is a homogeneous blend and consequently (table 2), it is rather difficult to remove PVP from the membrane matrix. It is remarkable that using weight fractions PVP of 0.43 a higher content of PVP 10 000 compared with PVP 360 000 in the final porous membranes was found. This may be caused by the fact that casting solutions containing PVP 10 000 exhibit a higher demixing rate. Another effect might come from the difference in molecular weight. It is known that the compatibility of two polymers (e.g., polyethersulfone and polyethyleneoxide [27]) decreases if the molecular weight of one of the polymers increases. This is caused by the decrease in entropy change upon mixing high molecular weight components.
Though PEI and PVP are compatible in a ternary system (with a solvent) over the whole composition range it might be possible that the presence of water influences the interactions between PEI and PVP.

The fact that in the phase inversion membranes a considerable amount of PVP is present has a serious consequence for the use of this untreated membrane type as microfiltration membrane. The PVP that is in contact with water will swell considerably so that lower permeation rates are obtained then would be expected on the basis of the pore sizes, see chapter 5 [28].

4.5 CONCLUSIONS

PEI, PES and PI can form homogeneous and stable blends with PVP. For homogeneous membranes this situation can be obtained by using a simple solution casting process followed by evaporation of the solvent. Even after a prolonged storage in warm water there is no detectable outdiffusion of PVP if PVP contents lower than 43 wt. % are used, so these membranes can be used for all kinds of membrane separation processes.
For phase inversion membranes the situation is more complicated. During the immersion precipitation PVP will partly dissolve in the coagulation bath (water). PEI, PI and PES membranes still contain a certain amount of PVP which is different for each of the polymers. The explanation for these differences is based on the kinetics of the demixing process (especially the rate of solidification) and on the interaction between the polymers. The kinetics of the demixing process can be followed with light transmission experiments and it could be argued that the rate of demixing

and the time before solidification occurred correlated to some extent. The interaction strength between the polymers can semi quantitatively be related to the glass transition temperatures. Glass transition temperatures, which are higher than the weight average glass transition temperatures indicate that the interaction between the polymers is strong.
When PVP 10 000 is added to the casting solution PEI and PVP form a homogeneous blend in the resulting membrane material, while PVP 360 000 present in the solid PEI/PVP matrix is not distributed uniformely (more PVP is present close the pore interface) and PVP can leach out in a water bath.

4.6 ACKNOWLEDGEMENTS

The authors like to thank P.J.F Schwering and K. Matsubayashi for performing part of the experiments. D.M. Koenhen is acknowledged for the enlightening discussions on the subject.

4.7 REFERENCES

1 I.Cabasso, E. Klein, J.K. Smith, Polysulfone hollow fibers. I. Spinning and properties, J. Appl. Polym. Sci., **20** (1976) 2377.
2 I.Cabasso, E. Klein, J.K. Smith, Polysulfone hollow fibers. II. Morphology, J. Appl. Polym. Sci., **21** (1977) 165.
3 I.Cabasso, K.Q. Robert, E. Klein, J.K. Smith, Porosity and pore size determination in polysulfone hollow fibers, J. Appl. Polym. Sci., **21** (1977) 1883.
4 P.Aptel, N. Abidine, F.Ivaldi, J.P.Lafaille, Polysulfone hollow fibers - Effect of spinning conditions on ultrafiltration properties, J. Membr. Sci., **22** (1985) 199.
5 T.A. Tweddle, O. Kutowy, W.L. Thayer, S. Sourirajan, Polysulfone ultrafiltration membranes, Ind.Eng.Chem.Prod.Res.Dev., **22** (1983) 320.
6 H.D.W. Roesink, M.J. Otto, J.R. Ronner, M.H.V. Mulder and C.A. Smolders, Demixing phenomena and membrane formation in the four component system polyetherimide/ polyvinylpyrrolidone/ N-methylpyrrolidone/ water, PhD Thesis Chapter 2, University of Twente, Enschede, The Netherlands (1989).
7 L.Y.Lafrenière, F.D.F. Talbot, T.Matsuura, S.Sourirajan, Effect of polyvinylpyrrolidone additive on the performance of polyethersulfone membranes, Ind.Eng.Chem.Res., **26** (1987) 2385.
8 Q.T. Nguyen, L.L. Blanc, J. Neel, Preparation of membranes from polyacrylonitrile- polyvinylpyrrolidone blends and the study of their behaviour in the pervaporation of water-organic liquid mixtures, J. Membr. Sci., **22** (1985) 245.
9 E. Schchori, J. Jagur-Grodzinski, Polymeric alloys of poly(vinylpyrrolidone) with a macrocyclic polyether-polyamide, J. Appl. Polym. Sci., **20** (1976) 1665.
10 Y. Kurowaka, K. Ueno, N. Yui, Reverse osmosis rejection of organic solute from aqueous solution by using cellulose acetate phthalate - polyvinylpyrrolidone membrane, J. Coll. and Int. Sci., **74** (1980) 561.
11 R.L. Riley, C.R. Lyons, U. Merten, Transport properties of polyvinylpyrrolidone - polyisocyanate interpolymer membranes, Desalination, **8** (1970) 177.
12 M.Tamura, T. Uragami, M.Sugihara, Studies on syntheses and permeabilities of special membranes: 30. Ultrafiltration and dialysis characteristics of cellulose nitrate - poly (vinylpyrrolidone) polymer blend membranes, Polymer, **22** (1980) 829.
13 H.D.W. Roesink, I.M. Wienk, M.H.V. Mulder and C.A. Smolders, The influence of spinning conditions on the morphology of microporous capillary membranes, PhD Thesis Chapter 3, University of Twente, Enschede, The Netherlands (1989).
14 A. van der Scheer and C.A. Smolders, Dynamic aspects of contact angle measurements on adsorbed protein layers, J. Colloid Interface Sci., **63** (1978) 7.

15 R.L. Larkin, R.E. Kupel, Quantitative analysis of polyvinylpyrrolidone in atmosphere samples and biological tissues, Amer. Ind. Hyg. Assoc. J., **26** (1965) 558.
16 W.J. Macknight, F.E. Karasz and J.R. Fried in 'Polymer Blends', Vol. 1, D.R. Paul and S. Newman (Eds.), Academic Press, New York (1978) Chapter 5.
17 D.T. Turner, A. Schwartz, The glass transition temperature of poly (N-vinylpyrrolidone) by differential scanning calorimetry, Polymer, **26** (1985) 757.
18 Y.Y. Tan, G. Challa, The glass transition temperature of poly (N-vinylpyrrolidone) and the effect of water, Polymer, **17** (1976) 739.
19 M. Aubin, R.E. Prud'homme, Miscibility in blends of poly(vinyl chloride) and polylactones, Macromolecules, **13** (1980) 365.
20 J.M. Rodriguez-Parada, V. Percec, Interchain electron donor-acceptor complexes: a model to study polymer-polymer miscibility ?, Macromolecules, **19** (1986) 55.
21 G. Bélorgey, M.Aubin, R.E. Prud'homme, Studies of polyester/ chlorinated poly(vinyl chloride) blends, Polymer, **23** (1982) 1051.
22 G. Bélorgey, R.E. Prud'homme, Miscibility of polycaprolactone/ chlorinated polyethylene blends, J. Polym. Sci., **20** (1982) 191.
23 T. K.Kwei, The effect of hydrogen bonding on the glass transition temperatures of polymer mixtures, J. Polym. Sci, Polym. Lett. Ed., **22** (1984) 307.
24 A. K. Kundu, S. S. Ray, R. N. Mukherjea, Polymer blends 3. preparation and evaluation of the blends of shellac with polyamideimide from rosin, Angew. Makromol. Chem., **143** (1986) 197.
25 A.J. Reuvers and C.A. Smolders, Formation of membranes by means of immersion precipitation. Part II. The mechanism of formation of membranes prepared from the system cellulose-acetate/ acetone/ water, J. Membr. Sci., **34** (1987) 67.
26 K. Vásárhelyi, J.A. Ronner, M.H.V. Mulder and C.A. Smolders, Development of wet-dry reverse osmosis membranes with high performance from cellulose acetate and cellulose triacetate blends, Desalination, **61** (1987) 211.
27 D.J. Walsh and V.B. Bhanu Singh, The phase behaviour of a poly(ether sulfone) with poly(ethylene oxide), Makromol. Chem., **185** (1984) 1979.
28 H.D.W. Roesink, S. Oude Vrielink, M.H.V. Mulder and C.A. Smolders, Post-treatment of hydrophilic membranes prepared from polyetherimide - polyvinylpyrrolidone blends, PhD Thesis Chapter 5, University of Twente, Enschede, The Netherlands (1989).

CHAPTER 5

POST-TREATMENT OF HYDROPHILIC MEMBRANES PREPARED FROM POLYETHERIMIDE-POLYVINYLPYRROLIDONE BLENDS

H.D.W. Roesink, S. Oude Vrielink, M.H.V. Mulder and C.A. Smolders.

5.1 SUMMARY

When porous phase inversion membranes are made from a polymer solution consisting of polyetherimide (PEI) and polyvinylpyrrolidone (PVP), the polymeric membrane matrix contains an appreciable amount of PVP although this polymer is soluble in the nonsolvent coagulation bath. The PVP (MW = 360 000) in the membrane is located at the surface of the pore walls, while a PEI enriched phase forms a kind of membrane framework. The membrane matrix swells in contact with water so that much lower water fluxes are obtained than expected based on pore sizes and porosities as seen using the electron microscope.

In this chapter two different methods are presented to prevent the swelling of PVP in the membrane matrix. The first method is the crosslinking of PVP by a heat treatment. After the heat treatment the water fluxes of the membranes do correspond with pore size and porosity, while outdiffusion of PVP cannot be detected anymore.

The second method is the rapid removal of PVP using sodium hypochlorite (NaOCl). In this chapter it is demonstrated that it is possible to remove the major part of the PVP by a NaOCl treatment, so that water fluxes also are in agreement with pore size and porosity. After this NaOCl treatment the membranes still contain 2-7 wt. % of PVP and have a hydrophilic nature (wettable by water).

5.2 INTRODUCTION

In membrane separation processes like microfiltration and ultrafiltration hydrophilic membranes are preferred to hydrophobic ones because of the good wettability by aqueous solutions and of the reduced tendency to adsorb proteins, macromolecules etc. The low adsorption tendency will diminish the fouling of the membranes, so that higher filtration rates are obtained over a longer period, while also cleaning of the membranes will be more effective.

In previous chapters the development of hydrophilic microfiltration membranes based on polyetherimide-polyvinylpyrrolidone (PEI-PVP) blends has been described [1,2] and the character

of the blends in both homogeneous and porous phase inversion membranes has been discussed in chapter 4 [3]. Important conclusions in this latter work were:

- The membrane matrix of phase inversion membranes contains a considerable amount of PVP.
- The PVP (MW = 360 000) in the microporous phase inversion membrane is located at the surface of the pore walls.
- The PVP in the membrane matrix can only be leached out by water at extreme conditions (water temperature ≥ 80 °C)

When the microporous membranes are used for permeation measurements without any post-treatment, the water flux and the ethanol flux are negligible. The acetone flux for untreated membranes is high and in agreement with the pore size and porosity observed by scanning electron microscopy. The reason for this phenomenon is, that PVP swells in water and in ethanol whereas in acetone hardly any swelling can be observed. In fact water and ethanol are solvents for PVP while acetone is a nonsolvent.

In this chapter two different methods for the post-treatment of the membranes after they have been prepared (spun or cast) are described and discussed.
The first method is the crosslinking of the PVP in the membrane matrix, so that the swelling of PVP in water is reduced and consequently membranes are obtained with a high water permeability. An additional advantage of PVP crosslinking is that no PVP will leach out when the membranes are in contact with water.
In the second method it is shown that PVP can partly be removed so that swelling is reduced while the hydrophilic nature of the membranes is retained.

5.3 EXPERIMENTAL

Materials

Polyetherimide (Ultem ® 1000) was kindly supplied by General Electric, Bergen op Zoom , The Netherlands.Polyvinylpyrrolidone (MW = 360 000) was purchased from Janssen Chimica, Belgium. The structural formulas of both polymers are given in figure 1. N-methyl-2-pyrrolidone (Merck, synthesis grade) was used as a solvent.
Molecular weights and molecular weight distributions were determined with size exclusion chromatography (table 1).

Table 1: *Molecular weights of the polymers used in this chapter.*

Polymer	Solvent	M_n	M_w
PEI	$CHCl_3$	19 600	32 800
PVP 360 000	$CHCl_3$	330 000	423 000

Polyetherimide

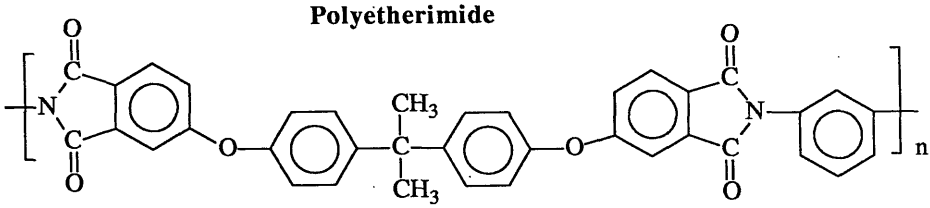

Polyvinylpyrrolidone

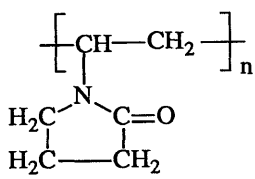

N-Methyl-2-pyrrolidone

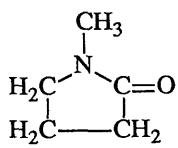

Figure 1: *Structural formula of N-methyl-2-pyrrolidone (solvent) and of the repeating unit of polyvinylpyrrolidone (PVP) and polyetherimide (PEI).*

Preparation of membranes

The homogeneous membranes were prepared by solution casting followed by an evaporation step in a nitrogen atmosphere. To obtain a solvent free membrane the membranes were placed in a vacuum oven at 50 °C for at least 24 hours and eventually flushed with water. After this procedure the homogeneous membranes contained less than 0.5 wt.% solvent, as was controlled using thermogravimetry.

Porous capillary membranes were spun using the dry-wet spinning technique. The membranes used in this work were two different types of capillary membranes (XF 015 and ER 88010607) spun from a PEI/PVP/NMP=17/13/70 (w/w/w) solution. The dry-wet spinning technique used

here has been described in chapter 3 in full detail [2].

Characterization of capillary membranes:

	XF 015	ER 88010607
outer diameter	2.0 mm	1.4 mm
inner diameter	1.2 mm	0.8 mm
average pore size outer surface	0.5 μm	0.8 μm
average pore size inner surface	0.2 μm	1 μm
PVP/PEI weight ratio in the membranes	0.25	0.29

Differential scanning calorimetry (DSC)

A Perkin Elmer DSC Differential Scanning Calorimeter in combination with a System 4 microprocessor Controller and a Model 3700 Thermal Analysis Data Station (TADS) was used for DSC measurements. Nitrogen gas was purged through the sample chambers at all times. The polymer samples (about 10 mg) were placed in aluminium sample pans which were sealed with perforated covers. A heating rate of 20 °C /min and a cooling rate of 320 °C /min were used. The T_g was determined in the second or third run and was defined as the midpoint temperature of the second order transition.

The system was calibrated using indium and lead.

Thermogravimetry (TGA)

A Perkin Elmer TGS-2 Thermogravimetrical Analyser in combination with a System 4 Microprocessor Controller and a model 3700 Thermal Analysis Data Station were used for these experiments. During all experiments a nitrogen atmosphere was provided by a continuous gas flow of 85 ml/min.

Permeation measurements

The fluxes were measured under cross-flow conditions using a capillary membrane of 20 cm length. The average transmembrane pressure was 1 bar. The temperature of the feed liquid was kept at 25±1 °C. The water flux was measured using tap water purified by reverse osmosis.

Swelling measurements

The swelling measurements were done with homogeneous membranes (polymer films). The dry

solvent free films were placed for 24 hours in a water bath, blotted dry with a tissue, weighed, dried and weighed again. For each film the water sorption was measured at least three times. The swelling value is expressed as a relative weight increase: g water/ g dry polymer film

Scanning electron microscopy

Two different preparation methods were used [1]:

- Wet membranes were quenched in liquid nitrogen and freeze-fractured to obtain a fresh cross section. The samples were dehydrated by means of an ethanol/hexane liquid exchange treatment and air-dried. After this procedure they were placed in a Balzers Union SCD 040 sputter unit to apply a charge conducting gold layer. The samples were examined in a Jeol JSM - T 220A electron microscope at room temperature.

- After quenching in liquid nitrogen and eventually freeze-fracturing, the membrane samples (cross section and surfaces) were kept at a temperature lower than - 130 °C . The samples were studied using a scanning electron microscope (Phillips 505) equipped with a cryo-unit (see chapter 2 [1]).

5.4 RESULTS AND DISCUSSION

5.4.1 Introduction

In chapter 4 [3] it had been demonstrated that the hydrophobic polymer PEI and the hydrophilic, water soluble polymer PVP are compatible polymers. PEI and PVP are completely miscible (in NMP) and the solution cast membranes prepared from these blends are homogeneously mixed blends. In phase inversion membranes the situation is more complicated. When high molecular weight PVP was used it was found that the polymeric material in the membrane is not a homogeneous material and it was shown [1,3] that there is a PVP enriched phase at the surface of the pore walls, while a PEI enriched phase forms the membrane framework.
The PVP enriched phase swells in contact with solvents for PVP, so that the actual water flux will be lower than the theoretical flux based on calculations (see below) using the pore size and porosity as can be found in electron micrographs (figure 2 and 3).
In order to reduce the effects of swelling, two methods have been investigated:

- Crosslinking of the PVP in the membrane matrix using a heat treatment or with the help of potassium persulphate
- Removal of the PVP from the membrane matrix using sodium hypochlorite

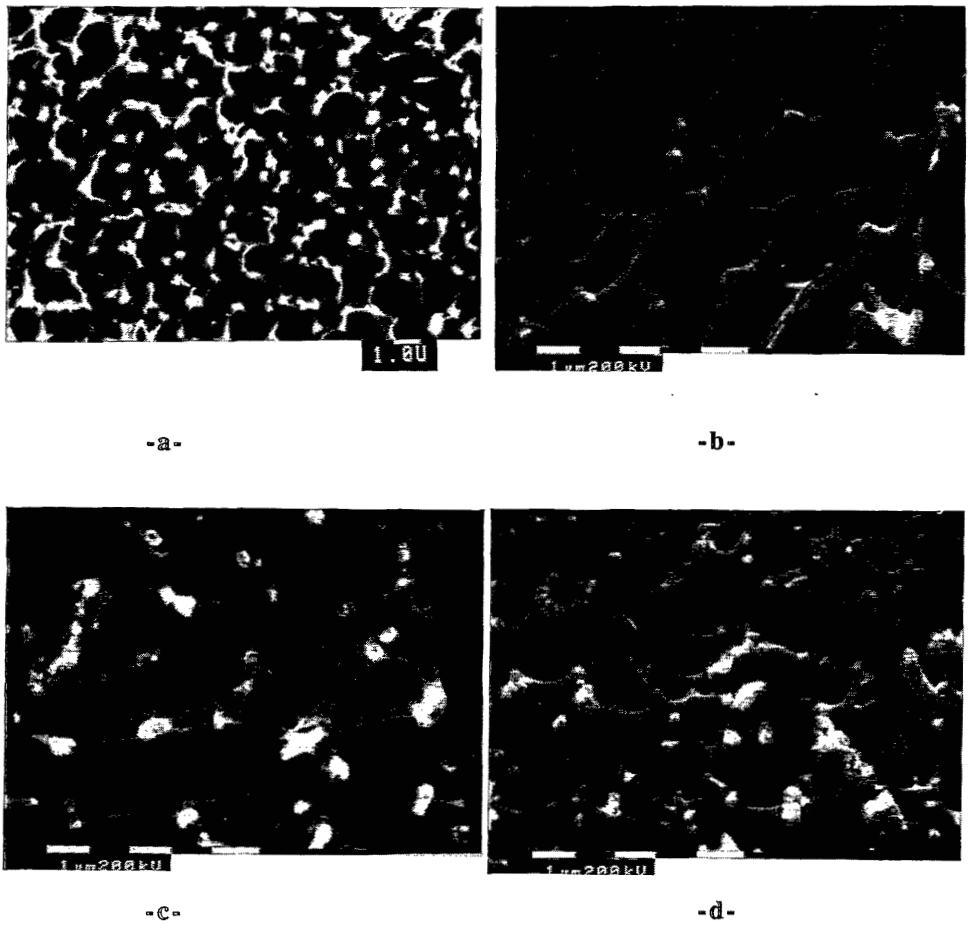

Figure 2: *Electron micrographs of cross sections of capillary phase inversion membranes:*
-a- porous structure (no cryo-unit, dry preparation technique)
-b- water swollen state of the porous structure (with cryo-unit)
-c- porous structure after heat treatment (with cryo-unit)
-d- porous structure after NaOCl treatment (with cryo-unit)

The porous structure that can be see in the electron micrograph in figure 2a was obtained using the dry-preparation technique. After freeze-fracturing, the membrane samples were dehydrated by

means of an ethanol/hexane liquid exchange treatment and air-drying. The influence of the preparation method has been discussed in chapter 2 [2] and an important conclusion in that work was that the structure of the membranes in a water swollen state is different from the structure in the dry state. The "swollen structure" in figure 2b that was obtained with the cryogenic preparation method shows a more or less closed cell structure. When using the same preparation method for the heat- and NaOCl-treated membranes (figure 2c and 2d) the final structure for both post-treatment methods was roughly the same while the result is markedly different from the swollen structure in figure 2b: more interconnectivity in the post-treated membranes can be observed. The structures in figure 2c and 2d are the same as can be observed using the electron microscope using the dry-preparation technique (figure 2a) [1].

The acetone flux for the untreated membranes is high so that at least in this situation no closed cell structure can be assumed. Since acetone is a typical nonsolvent for PVP, while its miscibility with water is good, the PVP bound water will disappear. Simultaneously the PVP will shrink and as a result the pore walls will collapse so that an open pore structure is the result and for acetone high permeabilities can be measured. When after an acetone permeation experiment the water flux is measured with the same membrane a very low water flux is found again ($< 10^{-6}$ m/s). This means that the observed closed cell structure that can be observed with the cryogenic preparation method cannot be the only reason for the very low water and ethanol fluxes. The reason for the low water flux of the membranes without post-treatment must be the swelling of the PVP and the blocking of the porous structure by the swollen PVP.

Table 2: *Fluxes of capillary membranes (XF 015) for different liquids. The membranes (20 cm length) were untreated, heat treated or treated with sodium hypochlorite. Fluxes (J_v) are in m^3/m^2 s ($x\ 10^4$), normalized fluxes (1/R, see text) are in 1/m ($x\ 10^{12}$).*

Medium	Untreated		Heat treatment 15 hr at 150 °C		NaOCl treatment 48 hr in 4000 ppm	
	J_v	1/R	J_v	1/R	J_v	1/R
water (η=0.89 mPas)	< 0.01	-	7.44	6.62	11.76	10.47
ethanol (η=1.1 mPas)	< 0.01	-	6.21	6.83	9.41	10.35
acetone (η=0.32 mPas)	16.03	5.13	24.87	7.96	19.90	6.37
NaOH (1mol/l) pH=14; η=0.89 mPas	< 0.01	-	6.98	6.21	7.97	7.09
HCl (1mol/l) pH=0.1; η=0.89 mPas	< 0.01	-	8.44	7.51	10.96	9.76

The acetone flux for untreated membranes is high and in good agreement with the theoretical flux based on calculations using the relation of Hagen-Poiseuille (1). It is assumed that this relation holds, although the membranes do not contain real cylindrical pores.

$$J_v = \frac{\varepsilon * r^2 * \Delta P}{8 * \eta * \tau * \Delta x} \qquad (1)$$

In the capillary membranes used for the permeation experiments, a minimum in the pore size over the cross section can be observed. The reason for this phenomenon has been discussed in a previous chapter [2]. The pore size in the minimum is around 0,1 µm, while this minimum pore size can be found over a thickness of 20 µm. When the porosity (ε) in this area is estimated at 0.15 (see figure 3) with a tortuosity (τ) of 1.5, the water flux should be 6.9×10^{-4} m/s and the acetone flux should be 19.2×10^{-4} m/s. This value is in good agreement with the acetone flux (table 2) measured for untreated membranes and with the other fluxes of the membranes after a certain post-treatment.

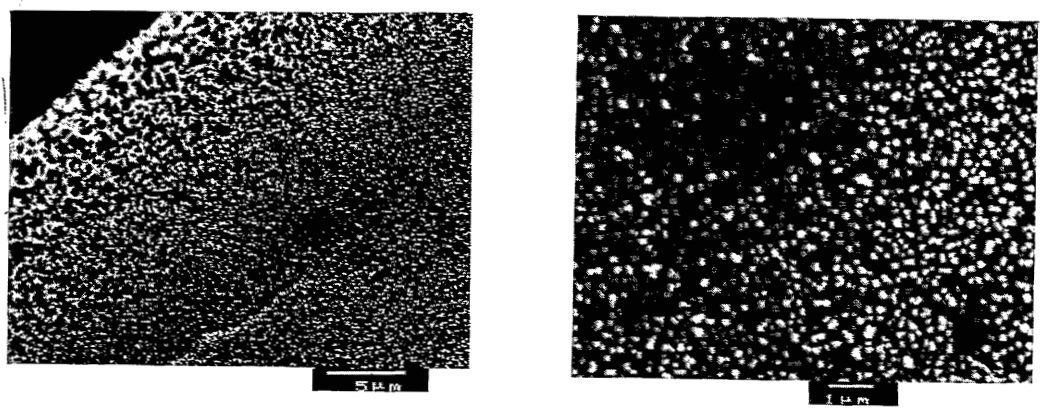

-a- -b-

Figure 3: *Electron micrographs of capillary phase inversion membranes (XF 015):*
-a- Part of the cross section with the minimum in pore size.
-b- Magnification of the pore structure in the area of the minimum pore size.

The flux can also be represented as:

$$J_v = \frac{\Delta P}{\eta * R} \quad \text{or} \qquad (2)$$

$$\frac{J_v * \eta}{\Delta P} = 1/R \qquad (3)$$

In this way a normalized flux (1/R) is obtained and the results for these normalized fluxes are shown in table 2. In fact the normalized flux is a correction for the viscosity of the liquids used and the transmembrane pressures applied.
Untreated membranes have a certain permeability for acetone, since acetone is a nonsolvent for PVP. A high permeability can also be found for hexane (a nonsolvent for PVP), although the exact hexane permeability for XF 015 capillary membranes was not measured.
On the other hand water and ethanol are solvents for PVP, therefore the PVP will swell, the membrane pores are blocked and no permeability can be measured anymore.

5.4.2 Crosslinking of PVP

PVP can be crosslinked in different ways. The following methods were investigated:

- Crosslinking using a potassium persulphate solution [4,5].
- Heat treatment at 150 °C in air [6].

The crosslinking with potassium persulphate was done in a 28 wt. % aqueous solution of $K_2S_2O_8$ at a temperature of 100 °C. After 7 hours the maximum water flux was obtained. This flux (2.2 x 10^{-4} m/s) is ca. 30 % of the flux obtained with a heat treatment (table 2). The reason for this low flux is the fact that the crosslinking occurs in the swollen state of the PVP, so that only a small reduction of the swelling value could be obtained.
Anderson et al. [4] suggest that the crosslinking with persulphate involves an abstraction of a hydrogen atom (attached to the ternary carbon atom) from the polymer chain by a SO^-_4 radical. When this macroradical meets another macroradical (inter- or intramolecular) a stable covalent crosslink can be formed. The crosslinking mechanism is shown schematically in figure 4.
The preparation of PVP gels by crosslinking with persulfates is described by Schildknecht in an US patent [5]. In this patent it is also mentioned that PVP may be rendered insoluble, apparently by

crosslinking, by heating the PVP powder in air at about 150 °C. The mechanism for this crosslinking mechanism has not been described in literature as far as we know.

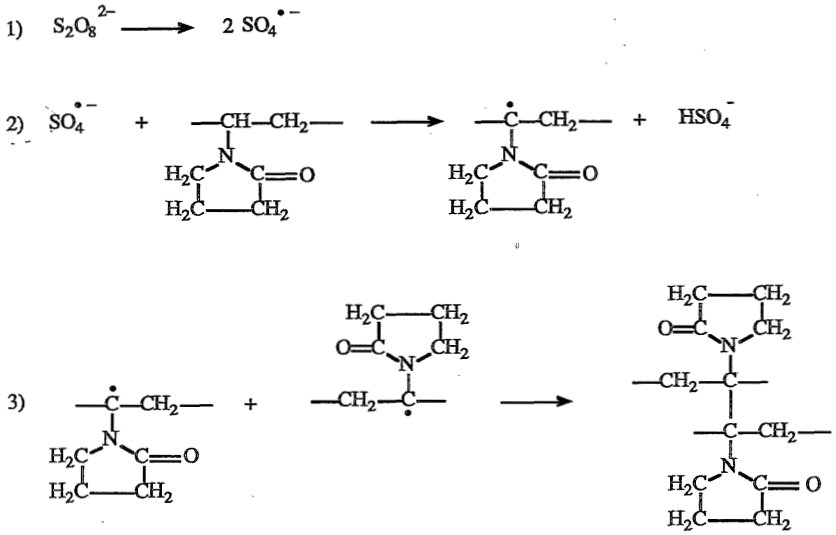

Figure 4: *Mechanism for the crosslinking reaction of PVP by persulfate.*

It was found that after a heat treatment (15 hours at 150 °C) PVP becomes insoluble in water, methanol, chloroform, dioxane, N-methyl-2-pyrrolidone and moreover that PEI/PVP membranes after a heat treatment do not dissolve anymore in these solvents, although there is a considerable swelling in N-methyl-2-pyrrolidone and other strong solvents for PEI. These results are in agreement with the observations of Schildknecht [5] that PVP becomes insoluble after a heat treatment.

The heat treatment procedure is as follows. Before any heat treatment is started, the PVP in the membranes is always brought into an unswollen state. The membranes are thoroughly flushed with water and after the flushing procedure the water is replaced by ethanol and then the ethanol is replaced by hexane. The hexane is allowed to evaporate after which the membranes are placed in an oven at 150 °C for a certain period of time.

The effect on the water flux of the residence time in the oven is shown in figure 5.

From these results it can be seen that the water flux increases with the residence time at high temperature and that at least 15 hours are necessary to reach a constant value.

Furthermore it was found that the swelling value of PEI/PVP films in water decreased as a result of

a heat treatment (table 3 and figure 6). Swelling experiments with porous membranes cannot be performed since it is practically impossible to remove the "free water" out of the pores.

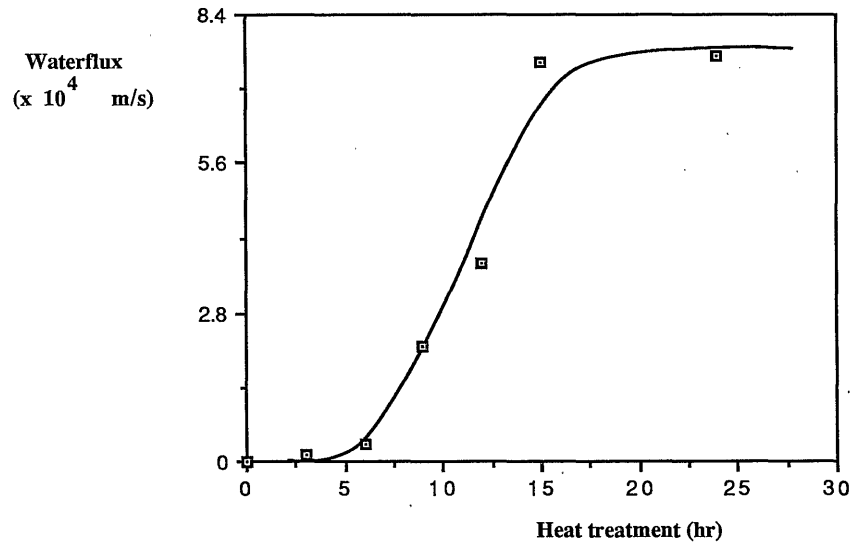

Figure 5: *Water flux for XF 015 capillary membranes as a function of the heat treatment at 150 °C.*

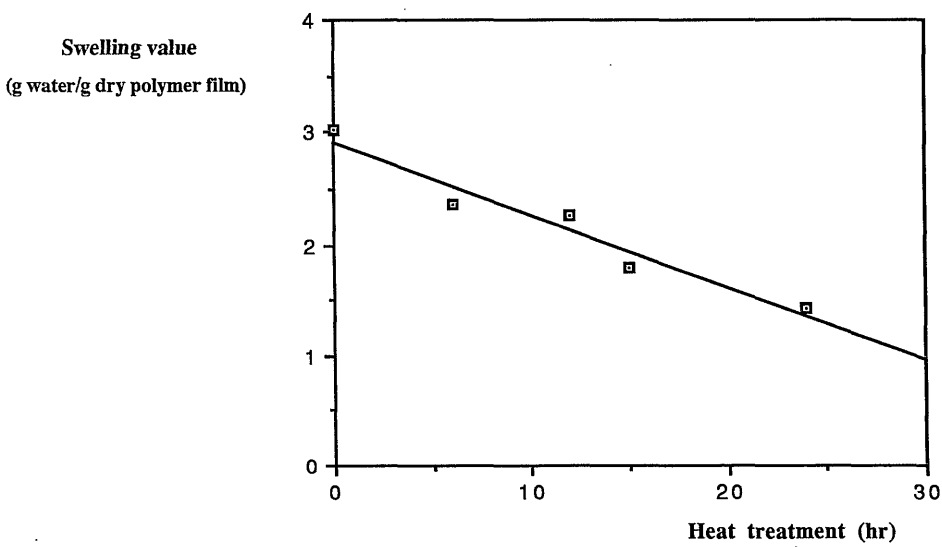

Figure 6: *Swelling value (g water/g dry polymer film) for PEI/PVP homogeneous films containing 80 wt. % PVP versus the heat treatment time at 150 °C.*

If the results of table 3 and figure 6 are compared with those in figure 5 it can be seen that a heat treatment of 15 hours corresponds with an optimum flux of the membranes. The swelling value is not yet minimal, but increasing the heat treatment time will not increase the water flux any further, while it will increase the brittleness of the membranes. So for permeation experiments the membranes are heat treated during 15 hours at 150 °C.

Table 3: *Swelling values of homogeneous PEI/PVP films in water at 25 °C. The swelling value is expressed as a relative weight increase (g water/ g dry polymer film).*

	SWELLING VALUE			
Heat treatment 150 °C	**weight % PVP in PEI/PVP films**			
Time (hr)	**0**	**25**	**43**	**80**
0	0.0125	0.13	0.26	3.02
6	„	-a)	-a)	2.37
12	„	-a)	-a)	2.26
15	„	0.06	0.13	1.80
24	„	-a)	-a)	1.42

-a) means not measured

After a heat treatment a considerable increase in the glass transition temperature (T_g) of pure PVP could be observed (table 4). When the homopolymer PVP is heated in a nitrogen atmosphere the increase in glass transition temperature (ΔT_g) is 13 °C, while in air an increase of 27 °C was observed. It is presumed that the T_g of PVP measured with a heating rate of 40 °C /min has the same value as that measured with 20 °C/min, although the T_g at 40 °C/min will be 2 or 3 °C higher according to Turner et al. [7]. As is known from literature [8,9,10,11] crosslinking of a polymer will increase T_g. Different relations are known that give a correlation between crosslinking density and ΔT_g [8,9,10,11]. A very simple expression is derived by Ueberreiter and Kanig [11]:

$$\Delta T_g = Z * D \qquad (4)$$

ΔT_g is the increase in T_g due to the crosslinking of the polymer, D is the crosslink density while Z is a constant. Glans and Turner [10] used crosslinked polystyrene to verify relation (4) and obtained plots of straight lines for ΔT_g versus crosslinking density, D.
Furthermore it was shown by Glans et al. [10] that an endothermic peak could be observed in the same temperature traject as the glass transition temperature in the first DSC run after the crosslinking reaction. This peak disappeared in the following run(s) after quenching while the height of the peak was dependent on the crosslinking density.

The fact that a heat treatment in a nitrogen atmosphere results in a ΔT_g of 13°C while for a heat treatment in air a ΔT_g of 27 °C was found, could indicate that oxygen is involved in the crosslinking mechanism.
An endothermic peak could be observed when DSC experiments were performed with heat treated PVP. This peak disappeared in the following runs. Although it is possible to determine a glass transition temperature from the position of the peak in the first run, the glass transition temperatures presented were determined in the second or third run.
When PVP was heat treated in a nitrogen atmosphere the peak height was twice that of the endothermic peak obtained after a heat treatment in air. These results for PVP are in good agreement with the results for polystyrene presented by Glans et al. [10].
Although the crosslinking density after a heat treatment in nitrogen is lower than after a heat treatment in air a heat treatment in nitrogen also makes PVP insoluble in solvents like water, chloroform, N-methylpyrrolidone and dioxane.

It is remarkable that the glass transition temperature of the heat treated PEI/PVP blend films did not increase at all (table 4) in contrast with the homopolymer PVP. This demonstrates that the degree of crosslinking in the PEI/PVP films is very low, but high enough to decrease the swelling value in water (table 3) and to avoid outdiffusion of PVP (table 5).

Table 4: *Glass transition temperatures of solvent free PEI/PVP films and of the homopolymer PVP in powder form. The glass transition temperatures are measured with differential scanning calorimetry (DSC). Heat treatment during 15 hr at 150 °C in air; PVP powder in air and in a nitrogen atmosphere.*

Weight % PVP in PEI/PVP film	**T_g (Before heat treatment)**	**T_g (After heat treatment)**	**Heating rate (°C/min)**
0	217	217	20
25	215	215	20
43	206	208	20
80	191	191	20
100	177	204 (Air)	40
		190 (Nitrogen)	40

Although no direct evidence has been found, the following arguments for crosslinking after a heat treatment can be given:

- PVP as a pure homopolymer and PEI/PVP blend films became insoluble after a heat treatment
- The glass transition temperature of pure PVP increased after a heat treatment (the glass transition

temperature of PEI/PVP blends did not increase however)
- The swelling value for PEI/PVP homogeneous films decreased after a heat treatment

In practice this means that a heat treatment of the membranes will decrease the swelling value, so that high permeabilities are possible (table 2).
Another advantage is that after a heat treatment no PVP leaches out of the membrane matrix, even at elevated temperatures. Experiments were done with XF 015 capillary membranes before and after a heat treatment at 150 °C during 15 hours (table 5).

Table 5: *Outdiffusion experiments with capillary membranes (XF 015), before and after a heat-treatment (15 hr at 150 °C). The membranes are placed in a water bath and the PVP concentration in this water bath is measured colorimetrically [3]. The amount of PVP in the membranes is calculated from the difference. After 18 days the temperature of the water bath is increased to 80 °C.*

	weight fraction of PVP in the membranes									
Time (days)	0	1	4	18 25 ° ⇒	24 80 °C	27	32	39	52	59
untreated	0.25	0.24	0.23	0.23	0.12	0.11	0.10	0.10	0.10	0.10
heat treated	0.25	0.25	0.25	0.25	0.25	0.25	0.25	0.25	0.25	0.25

5.4.3 Sodium hypochlorite treatment

Another post-treatment method to increase the water flux for microporous PEI/PVP membranes is the removal of the PVP out of the membrane matrix. In the porous membranes not all of the PVP is entirely mixed with PEI on a molecular level and it had been demonstrated already [1,3] that much of the PVP is located at the surface of the pore walls.
At moderate temperatures (25 °C) the PVP will leach out very slowly in a water bath. At elevated temperatures (80 °C) the PVP will leach out faster but always a substantial amount of PVP will be present in the porous matrix [3].
Although PVP is a chemically stable polymer, it was found that the removal of PVP out of the polymeric membrane matrix could be facilitated with sodium hypochlorite (NaOCl).
Experiments were carried out using capillary membranes (ER 88010607). The membranes were cut into pieces of 25 cm length, flushed with water (45 °C) during an hour and then placed in a vessel with demineralized water. The water was refreshed every 24 hours. From time to time samples of membranes were taken and analysed. The results are given in table 6.

Table 6: *PVP and NMP concentrations in PEI/PVP capillary membranes (ER 88010607) after flushing with water (45 °C) and a certain residence time in a water bath eventually followed by ethanol/hexane liquid exchange treatment or by a NaOCl-treatment (4000 ppm at 25 °C). The PVP concentration is measured by NMR, the NMP concentration is measured by using NMR and by TGA.*

Time in water of 25 °C (hours)	weight % PVP in membranes NMR	weight % NMP in membranes measured by: NMR	TGA
24	29	3.4	3.6
426 (18 days)	26	2.8	2.4
426+EtOH/Hexane	26	0	0
426+NaOCl (48 hr)	8	2.2	1.4
426+NaOCl (20 days)	2	-	-

The first two results demonstrate, that after a period of 18 days in a water bath the amount of PVP leached out of the membrane matrix is only small (3 wt. %). This is in good agreement with the results shown in table 5 (18 days at 25 °C), although two differences between the methods have to be emphasized. The results in table 5 were obtained without refreshing the water while the concentration of PVP in the water bath was measured. The results in table 6 were obtained by refreshing the water bath every day and measuring the amount of PVP in the membranes directly.
It is remarkable that the solvent (NMP) is so hard to remove from the membranes when flushed with water. When the water in the membrane matrix is replaced by ethanol and the ethanol by hexane, the solvent concentration in the membranes is negligible. This might be caused by the deswelling effect of the hexane or a higher affinity between ethanol and NMP compared with that between water and NMP.

After a NaOCl -treatment during 48 hours the PVP content had decreased to 8 wt. %. When the contact time with NaOCl was further increased the PVP content dropped to 2 wt. % (table 6).
Other experiments were done with XF 015 capillary membranes. The water flux of the membranes and the PVP content in the membranes was measured as a function of time using a 4000 ppm NaOCl-solution. The results are shown in figure 7 and 8. These results indicate that a treatment of 48 hours (2 days) in a 4000 ppm NaOCl-solution is enough to obtain a constant water flux for the membranes and also that after two days a constant residual PVP content in the membranes is reached. The content of PVP in the membranes after a NaOCl treatment can also be measured by weighing the dry membranes before and after the treatment, these values were in agreement with the values found with NMR.

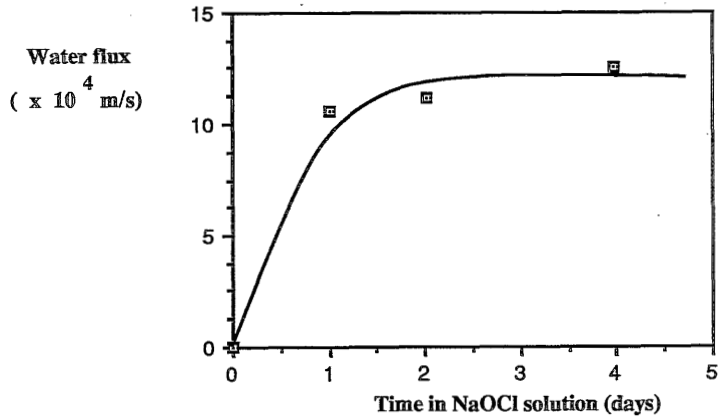

Figure 7: *Water flux of capillary membranes (XF 015) versus the treatment time in a 4000 ppm NaOCl solution. The water flux was measured with reverse osmosis water at 25 °C with a transmembrane pressure of 1 bar. The length of the membranes was 20 cm.*

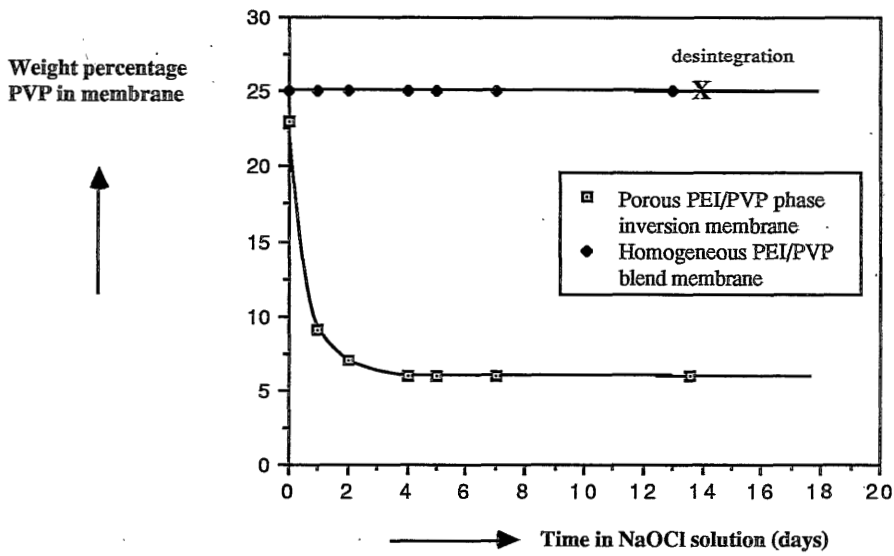

Figure 8: *Amount of PVP in porous phase inversion capillary membranes (XF 015 with a PVP content of 25 wt.% in the membrane matrix) and in homogeneous blend membranes (PVP content 25 wt.%) as a function of the residence time in a NaOCl solution (4000 ppm).*

Comparing the behaviour of homogeneous membranes of PEI/PVP blends with porous phase

inversion (capillary) membranes having both a PVP content of 25 wt. %, an enormous difference was found, when these membranes were placed in a 4000 ppm NaOCl solution. For this experiment the NaOCl solution was refreshed every day. The PVP content in the homogeneous membranes was constant over a period of 14 days, while the content of PVP in porous membranes decreased within one day to 9 wt. % and in the rest of time (14 days) decreased to 5 wt. %. These results correspond quite well with the results in figure 7, where it is shown that the optimum water flux is reached after 2 days.

When homogeneous membranes were immersed in a NaOCl solution (4000 ppm) a complete desintegration of the membranes after 14 days can be observed and a kind of suspension is formed. These effects depend strongly on the PVP content in the polymer film. Films with 80 wt. % of PVP desintegrated and formed a kind of suspension in 1 day while films with 25 wt. % of PVP desintegrated after 2 weeks.

When porous phase inversion membranes were placed in a NaOCl solution of 4000 ppm the PVP will leach out, but even after three months in this solution the membranes did not desintegrate as the homogeneous membranes with 25 wt. % of PVP did. The reason for this might be that in homogeneous membranes PVP and PEI are mixed on a molecular scale (homogeneous blend) but not so in the porous membrane (heterogeneous blend). If in porous membranes most of the PVP is washed out, a kind of PEI matrix with some residual PVP will remain, so that the membranes still are mechanically stable.

The former results are a very strong support for the fact that the high molecular weight PVP (MW=360 000), present in porous phase inversion membranes, is located at the surface of the pore walls, and that there is a framework of a PEI/PVP blend with low PVP concentration (2 - 7 wt. %). The remaining PVP in the polymeric membrane matrix is sufficient to render the membranes hydrophilic (in fact wettable for water). Experiments showed, that the water flux of NaOCl treated membranes was constant if the membranes were placed in a water bath for a period of three months.

In figure 9 the results of thermogravimetric analyses of PEI, PVP and membrane samples are shown. It can be observed that the thermal behaviour of the porous phase inversion PEI/PVP membranes (I) can be compared with the thermal behaviour of PVP in the first part and with PEI in the second part. This thermogravimetrical analysis is also a support for the fact that the matrix contains PEI and about 25 wt. %PVP since the thermogravimetrical analysis of a homogeneous membrane with 25 wt. % PVP has the same characteristics. The location of the point of inflection in curve I is dependent on the concentration of PVP.

After the NaOCl-treatment the behaviour is more like that of PEI, since the PVP concentration has decreased to about 2 wt. %. The extra weight loss is probably caused by degradation effects of PEI.

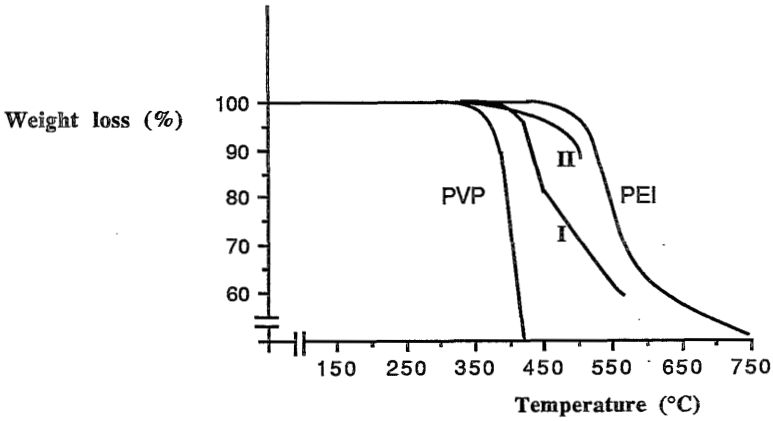

Figure 9: *Thermogravimetrical analysis of PEI, PVP, a porous phase inversion PEI/PVP membrane with 26 wt.% PVP (I) and the same porous membrane (II) after a NaOCl treatment (48 hr with 4000 ppm). Heating rate 20 °C/min.*

Summarizing it had been found that after a treatment with a NaOCl solution:

- the water flux was high and in agreement with pore size and porosity
- the PVP concentration in the membranes decreased to a constant low value
- the membranes were still wettable (hydrophilic)

As mentioned before it is hard to remove the PVP by simply leaching out in a water bath [3]. The results in this chapter show that a NaOCl treatment facilitates the rapid removal of PVP out of the porous membrane. The following possibilities for the reaction between PVP and NaOCl can be mentioned:

-1- *Decrease of the molecular weight of the PVP (chain scission), so that the PVP can be washed out more easily.*

The intrinsic viscosity of PVP/NaOCl solutions was measured at 30 °C using different concentrations of NaOCl. The viscosities were measured one day after the components were mixed. The molecular weight was calculated using the Mark-Houwink relation: $[\eta] = K * (M_v)^a$, with $k = 39.3 * 10^{-5}$ and $a = 0.59$ [18]. The measurements were done in duplo. The results in figure 10 show that indeed a decrease in molecular weight can be observed although the decrease is only a factor of two and it is not reasonable to assume that this decrease in molecular weight is enough to achieve the rapid removal of PVP upon a NaOCl treatment.

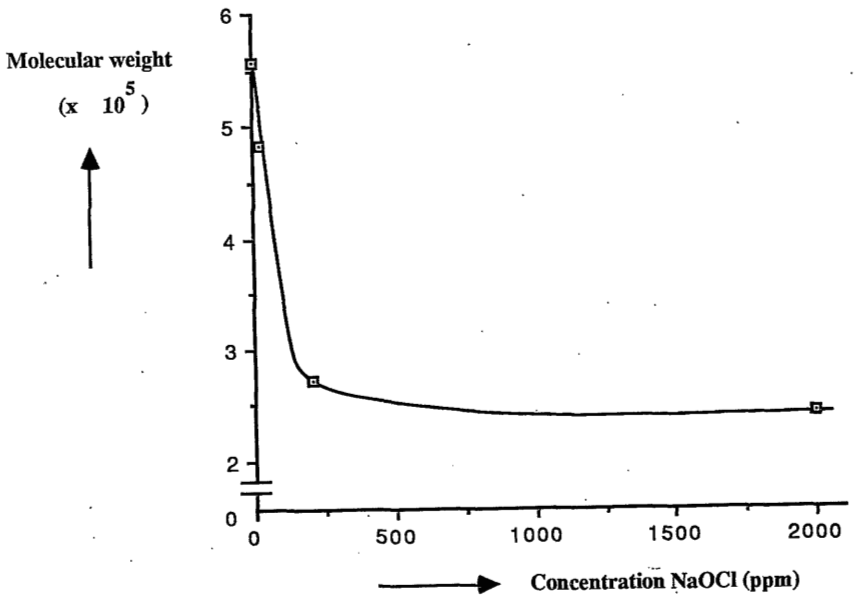

Figure 19: *Viscosimetric average molecular weight of PVP as a function of the concentration of the NaOCl solution. Viscosity measured always measured after 48 hours at 30 °C.*

-2- *Change in the chemical nature of the PVP so that the interaction with PEI will be changed and the removal of PVP is facilitated.*

As has been shown in chapter 2 [1], the surface of the pore walls consists of a PVP rich phase. But it also has been shown [3] that the interaction between PEI and PVP is very good and that due to the presence of some PEI in this PVP rich phase it is very hard to remove the PVP by simply washing it out in a water bath. Furthermore it had been shown that the NCO-group of the pyrrolidone ring is involved in the interaction between PVP and PEI [3]. Therefore it is assumed that by changing the chemical nature of the NCO-group the removal of PVP from the polymer matrix is facilitated.

As can be found in an appendix (5.6) it seems very likely that the second possibility plays a significant role in the rapid removal of PVP from the membrane matrix.

5.5 CONCLUSIONS

Phase inversion membranes made from PEI/PVP blends contain an appreciable amount of PVP in the membrane matrix. This PVP will swell when the membranes are in contact with solvents or swelling agents for PVP. As a consequence water fluxes for this type of membranes are very low.

In this chapter two different methods to prevent the swelling of PVP have been investigated.
The first method shows that it is possible to crosslink the PVP in the membrane matrix, so that the swelling value is decreased and water fluxes correspond with pore sizes and porosities. The membranes remain hydrophilic after the crosslinking, while no leachables (PVP) could be detected when the membranes were immersed in a water bath during months.
A second method is the rapid removal of PVP out of the membrane matrix with a NaOCl solution. In this work a possible reaction mechanism for a chemical modification of PVP through a reaction with and NaOCl is given. The change in chemical nature of PVP facilitates the removal of PVP out of the membrane matrix. The residual PVP present in the membrane matrix after a treatment with NaOCl solutions is 2-7 wt. % and this amount is enough to maintain a hydrophilic nature of the membranes.

5.6 APPENDIX - Reaction between PVP and NaOCl.

It is known from literature [14] that in the presence of acid or alkali in aqueous solutions at temperatures higher than 100 °C, some of the pyrrolidone rings are opened to give N-vinyl-γ-aminobutyric acid units. In alkaline solution mainly the anionic form will be found [14].

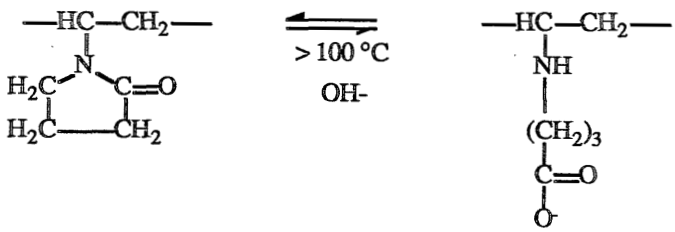

In the situation which was investigated in this chapter PVP and NaOCl react in aqueous solution at room temperature (25 °C), so that only alkaline hydrolysis cannot be expected with NaOCl. When porous PEI/PVP membranes were treated with NaOH solutions at elevated temperatures improved permeabilities of the membranes could not be obtained. Since PEI also reacts with NaOH at elevated temperatures, no further experiments were done.
A treatment of the porous PEI/PVP membranes (XF 015) with an acidified $KMnO_4$ solution gave a satisfactory water flux of $7 * 10^{-4}$ m/s (2500 l/m^2 hr bar); however the membranes became very brittle.
From these latter results could be concluded that in fact the oxidation of PVP plays an important role in the reaction between PVP and NaOCl.
In the literature a possible mechanism for the reaction between an N-substituted amide and NaOCl

could not be found but it is assumed that oxidation or chlorination of the nitrogen in the pyrrolidone ring will facilitate the ring opening of the pyrrolidone ring leading to alkaline hydrolysis.

According to what is known about the reaction between the pyrrolidone ring and oxidizing agents the following mechanism for the reaction between PVP and NaOCl (figure 11) is proposed. In fact the reaction of PVP and NaOCl can be considered as an oxidation of PVP in alkaline solution.

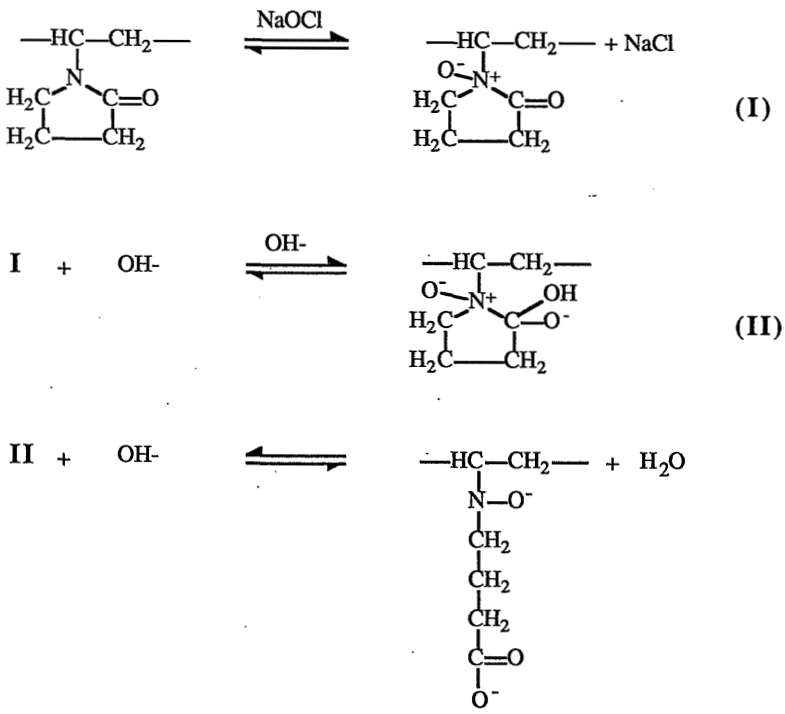

Figure 11: *Possible reaction mechanism for the reaction between NaOCl and PVP.*

The nitrogen in PVP can be considered as an electrophile since the pyrrolidone ring has the following resonance structure [14]:

The reaction between NaOCl and PVP in aqueous solution is strongly exothermic and one of the reaction products is NaCl as is found by analysis of the reaction products.
Furthermore infrared analysis of the reaction products of PVP and NaOCl showed absorptions that could be ascribed to COO^- and NO^- groups.
A support for our hypothesis about the reaction mechanism between PVP and NaOCl is the oxidation of tertiary amines to amine oxides [15], which is possible with peroxides and peracids.

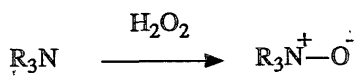

It is also known that tertiary amines can be chlorinated using NaOCl [16].

Although no direct evidence for the reaction mechanism presented between PVP and NaOCl, based on analysis of the reaction products or study of reaction kinetics had been found, it seems reasonable that this mechanism holds. Since viscosity measurements demonstrated that the molecular weight of the PVP only slightly decreased it is obvious that a NaOCl-treatment removes the high molecular weight PVP very fast. Reasons for this are that the ionogenic reaction polymeric product will swell enormously and moreover the interaction with PEI is changed, so that the outdiffusion of PVP is facilitated.

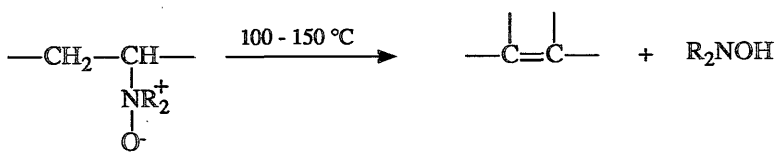

When membranes treated with a NaOCl-solution (4000 ppm) were heat treated for 15 hours at 150 °C, the membranes became hydrophobic (non-wettable by water). The water flux of these dry

membranes at normal transmembrane pressure differences was negligible, because water does not wet the porous membranes. If the membranes were pre-wetted with ethanol, the water flux was as before (10-12 x 10^{-4} m/s). From literature it is known, that amine oxides can be converted into alkenes [17]. The resulting alkene backbone of the PVP is hydrophobic (see above).

This possibility for the curing reaction is one more reason to accept the mechanism presented for the reaction between PVP and NaOCl.

5.7 ACKNOWLEDGEMENTS

The authors like to thank W.P. Trompenaars for the extended literature research on reactions between cyclic amides and oxidizing agents and for enlightening discussions on the subject.

5.8 REFERENCES

1 H.D.W. Roesink, M.J. Otto, J.A. Ronner, M.H.V. Mulder and C.A. Smolders, Demixing phenomena and membrane formation in the four component system polyetherimide/ polyvinylpyrrolidone/ N-methylpyrrolidone/ water, PhD Thesis Chapter 2, University of Twente, Enschede, The Netherlands (1989).

2 H.D.W. Roesink, I.M. Wienk, M.H.V. Mulder and C.A. Smolders, The influence of spinning conditions on the morphology of microporous membranes, PhD Thesis Chapter 3, University of Twente, Enschede, The Netherlands (1989).

3 H.D.W. Roesink, Z. Borneman, M.H.V. Mulder and C.A. Smolders, Polyetherimide-polyvinylpyrrolidone blends as membrane material, PhD Thesis Chapter 4, University of Twente, Enschede, The Netherlands (1989).

4 C. C. Anderson, F. Rodriguez, D. A. Thurston, Crosslinking aqueous polyvinylpyrrolidone solutions by persulfate, J. Appl. Polym. Sci., **23** (1979) 2453.

5 US Patent 2. 658. 045 (1953), C.E. Schildkecht (to GAF Corp.).

6 L. Blecher, D.H. Lorenz, H.L. Lowd, A.S. Wood and D.P. Wyman, in "Handbook of water-soluble gums and resins", Robert L. Davidson (Ed.), McGraw-Hill Inc. (1980) Chapter 21.

7 D.T. Turner and A Schwartz, The glass transition temperature of poly (N-vinyl pyrrolidone) by differential scanning calorimetry, Polymer, **26** (1985) 757.

8 L.E. Nielsen, crosslinking effect on physical properties of polymers, J. Macromol. Sci. Rev. Macromol. Chem., **C3** (1969) 69.

9 T.G. Fox and S. Loshaek, Influence of molecular weight and degree of crosslinking on the specific volume and glass temperature of polymers, J. Polym. Sci., **15** (1955) 371.

10 J.H. Glans and D.T. Turner, Glass transition elevation of polystyrene by crosslinks, Polymer, **22** (1981) 1540.

11 K. Ueberreiter and G. Kanig, Second-order transitions and mesh distribution functions of cross-linked polystyrenes, J. Chem Phys., **18** (1950) 399.

14 P. Molyneux, Water-soluble synthetic polymers: properties and behaviour, Volume I, CRC Press Inc., Boca Rabon, Florida (1982) 146.

15 Jerry March, Advanced Organic Chemistry, second edition, Mc Graw-Hill International Book Company (1977) chapter 19 page 1111.

16 W.P. Trompenaars, private communication.

17 Chapter 17, page 930 in reference [15].

18 L.C. Cerny, T.E. Helminiak and J.F. Meier, Osmotic pressures of aqueous polyvinylpyrrolidone solutions, J. Polym. Sci., **44** (1960) 539.

CHAPTER 6

CHARACTERIZATION OF NEW MEMBRANE MATERIALS BY MEANS OF FOULING EXPERIMENTS: ADSORPTION OF BOVINE SERUM ALBUMIN ON POLYETHERIMIDE - POLYVINYLPYRROLIDONE MEMBRANES

H.D.W. Roesink, M.A.M. Beerlage, W. Potman, Th. van den Boomgaard, M.H.V. Mulder and C.A Smolders.

6.1 SUMMARY

The hydrophilicity of polyetherimide-polyvinylpyrrolidone (PEI-PVP) microfiltration membranes can be adjusted by means of a suitable post-treatment. The influence of the nature of the membrane surface on fouling properties was studied using permeation experiments before and after exposure to a protein (BSA) solution and adsorption experiments with ^{14}C labelled BSA. A correlation between the permeation experiments and the radiolabelled BSA adsorption experiments was found. The PVP in the membrane matrix prevents BSA adsorption to take place to a large extent and it appeared that heat treated PEI-PVP membranes showed the same nonfouling behaviour as , e.g., cellulose acetate membranes.

6.2 INTRODUCTION

Flux decline is caused by phenomena like concentration polarization, gel layer formation, pore-blocking, adsorption and it is one of the most limiting factors in the acceptance of membrane separation processes like ultrafiltration and microfiltration. An extended survey of flux decline in membrane processes has been given by van den Berg et al. [1]. It especially occurs for complex fluids, that are used in the biotechnology and food industry. It is generally recognized that the adsorption of components of the fluids (e.g., proteins, surfactants, lipids) on membrane surfaces is a critical element in membrane fouling. Proteins adsorb on membrane surfaces particularly due to electrostatic forces and/or hydrophobic interactions between certain domains in a protein molecule and the hydrophobic membrane material. A key to improved fouling resistance is the development of hydrophilic, low surface charge membranes [2], since it is generally accepted that hydrophilic materials are less sensitive to adsorption than hydrophobic ones [2,3,4,5,6,7,8]. Unfortunately most inherently hydrophilic membrane

materials are not resistant against high temperatures, extreme pHs, cleaning agents etc. Therefore many investigations have been done to develop hydrophilic and resistant membranes. Most efforts have been performed to render intrinsic highly resistant polymer materials hydrophilic by suitable post-treatments [5]. In our research group a program has been started to develop such highly resistant, hydrophilic microfiltration and ultrafiltration membranes. The development of a microfiltration membrane already has been successful and is described in this thesis [9,10,11,12]. Membranes are prepared from a solution containing the highly resistant polymer polyetherimide (PEI) and the hydrophilic polymer polyvinylpyrrolidone (PVP) using the so-called phase inversion technique. One of the most important features of this development is the presence of an appreciable amount of PVP in the polymeric membrane matrix, despite the PVP being soluble in the aqueous coagulation bath. The membrane matrix material appears to be a heterogeneous blend. The PVP in the membrane matrix (up to 30 wt. % based on total polymer) is mostly located at the outer surface of the pore walls [9,11] and such membranes are hydrophilic. Since PVP swells considerably in contact with water, the water fluxes are very small. After a suitable post-treatment [13], which reduces swelling of PVP, the fluxes of the membranes are in agreement with the pore size and porosity as can be observed with the scanning electron microscope.

Two essentially different types of post-treatment have been developed [11,13]:

-1- *Crosslinking of the PVP in the polymeric membrane matrix by means of a heat treatment*
The PVP in the membrane pore walls is partly entrapped in a mixture of PEI and PVP. Due to the strong interaction between PEI and PVP, it is very hard to remove the PVP. Even in a water bath at elevated temperatures hardly any PVP will leach out of the untreated membranes. It appeared that by means of a simple heat treatment (see [13] and below) the PVP became insoluble in water and other solvents, probably by crosslinking. After a heat treatment the membranes were still hydrophilic, while no PVP leached out anymore, even at elevated temperatures (80 °C) of the water bath.

-2- *Removal of the PVP with a sodium hypochlorite solution*
It appeared that using a NaOCl treatment (see [13] and below) the PVP could be selectively removed from the polymeric membrane matrix. The membranes still were wettable by water, even when the membranes were used for aqueous filtration experiments during a period of three months. This is due to the fact that after the NaOCl treatment a certain amount of the PVP (2 - 7 wt. %) still is present in the membranes. As a result of this chemical treatment the nature of the membrane surface will change.
A special effect was obtained when the NaOCl treated membranes were heat treated. It

appeared that the membranes became hydrophobic, i.e., they were not wettable by water any longer. The reason for this effect probably is a chemical modification, due to the heat treatment, of the reaction product of PVP and NaOCl (see chapter 5 [13]).

As a result of the preparation method of the membranes from a polymeric blend and the post-treatment methods developed, it is possible to obtain both hydrophobic and hydrophilic membrane surfaces. The character of the hydrophilic membrane surface can be adjusted using different types and different concentrations of hydrophilic polymers or by applying different post-treatment methods.
A method to investigate the character of the membrane materials is to perform adsorption experiments. Smolders et al. [14] suggested four different types of model foulants that are typical in adsorption phenomena during membrane filtration. Two important variables are: size of the molecule and type of the intermolecular interaction (table 1).

Table 1: *Model foulants for systematic adsorption studies using membranes [14].*

	Amphipolar interactions (hydrophobic/hydrophilic)	**Unipolar interactions (hydrophilic)**
Low molecular weight	surfactants	sugar derivatives oligomeric polyethers
High molecular weight	proteins	carbohydrate polymers polyethers

In this chapter some preliminary results will be presented on the adsorption of bovine serum albumin (BSA) onto the new developed polyetherimide-polyvinylpyrrolidone membranes [12]. This model foulant compound has often been used in adsorption studies, especially with respect to ultrafiltration membranes [3,4,6,8,15,16,17,18]. By far the majority of experiments, described in literature, have been performed by exposing the toplayer of commercially available ultrafiltration membranes to the protein solution directly in the filtration set-up. In this work the microfiltration membranes are exposed to the protein solution in a separate device, since due the hydrophilic nature and the relatively large pore size of the microfiltration membranes (0.05 μm), the entire porous structure would be wetted by the protein solution anyway.
The fouling behaviour of different types of PEI-PVP membranes has been investigated using permeation experiments before and after exposure to a BSA solution. In a separate experiment the amount of adsorbed BSA on the membranes has been measured using radiolabelled ^{14}C BSA.

6.3 EXPERIMENTAL

Membranes

The flat membranes were machine cast from a PEI-PVP-NMP solution. The total polymer concentration was 25 wt.%, while the weight ratio PEI to PVP was 16 to 9. According to the manufacturer the M_w of the PVP was 360 000, while from size exclusion chromatography a M_w of 423 00 was found [9,11]. The temperature of the coagulation bath was 38 °C and the residence time in the humid air gap was 3 seconds. The pore size in the toplayer of the membranes is maximally 0.05 μm (figure 1). The weight fraction of PVP in the membranes is 20 wt. % (based on total polymer), since a part of the PVP will diffuse into the aqueous coagulation bath. It has to be emphasized that the PVP is located mostly at the surface of the pore walls [9,11].

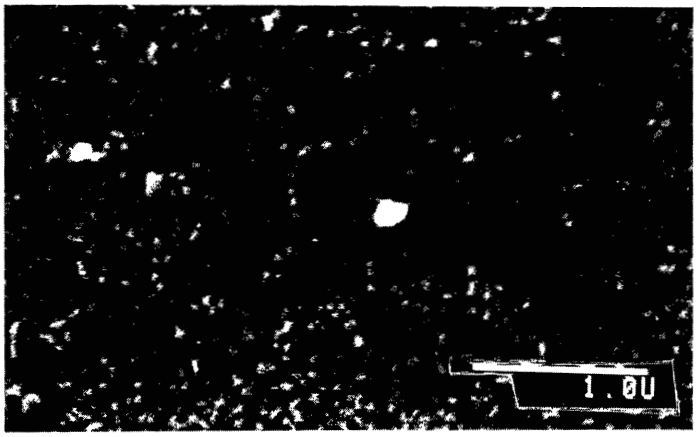

Figure 1: *Electron micrograph of a PEI/PVP microfiltration membrane (top view of the membrane surface). The membrane was heat treated. Maximal pore size 0.05 μm.*

The microfiltration membranes were used untreated or they were post-treated as follows [13]:

- Heat treatment: after preparation the membranes were thoroughly flushed with water. The water was removed by means of a solvent replacement technique using an ethanol/hexane liquid exchange treatment and the membranes were placed in an oven at 150 °C during 15 hours.

- NaOCl treatment: the membranes were thoroughly flushed after preparation and placed in a NaOCl solution (4000 ppm) during 48 hours. The membranes were thoroughly flushed with

demineralized water before adsorption and filtration experiments.

- Heat treatment after a NaOCl treatment: using an ethanol/hexane liquid exchange technique the membranes were dehydrated after the NaOCl treatment and placed in an oven at 150 °C during 15 hours. Since the obtained membranes were hydrophobic after this treatment, ethanol was used as a wetting agent before measuring the water flux.

Water pre-treatment

The demineralized and ultrafiltered water was purified using reverse osmosis. To prevent bacterial growth, sodium azide (0.02 wt. %) was added to the water.

BSA solutions

The BSA (No. A-2153, fraction V, 96 - 99 % albumin) was purchased from Sigma Chemical Company. The solutions of BSA were prepared in a phosphate buffer at pH=7.4 ± 0.05 with 0.1 M NaCl added, to give a solution with ionic strength I=0.125 N. The pH was adjusted in the range of 2.2 - 8 using a citric acid/ phosphate buffer. Sodium azide (0.02 wt. %) was added to all BSA solutions.

Permeation experiments

The pure water flux of the membranes was measured at 22°C in a dead-end filtration set-up. The transmembrane pressure was 1.5 - 2 bar. Water fluxes were measured volumetrically. The diameter of the circular membranes was 7.2 cm. The average water flux of heat treated membranes was 650 $l/m^2.hr.bar$, of NaOCl treated membranes 1600 $l/m^2.hr.bar$ and of heat-NaOCl treated membranes 1000 $l/m^2.hr.bar$. The deviation in the water fluxes of the used membranes is 20%. NaOCl treated membranes exhibit higher water fluxes since the PVP is removed from the polymeric membrane matrix [1]. Probably due to thermal effects the water flux decreases after an additional heat treatment.

The expressions used for the relative permeate flux, relative flux reduction and the relative resistance were the same as those used by Matthiasson [3] and Nilsson [4]. $RF=J_1/J_0$, with RF as the relative permeate flux, J_0 is the permeate flux before the BSA adsorption and J_1 the permeate flux after BSA adsorption. The relative flux reduction is expressed as 1-RF. The relative resistance of the adsorbed layer is expressed as $RR=1/RF-1$.

Membranes were characterized by measuring the pure water flux (J_0). They were removed then from the filtration set-up and placed in a BSA solution at 22 °C. After the BSA adsorption the membranes were rinsed with demineralized and ultrafiltered water during 5 minutes, placed in

the filtration set-up and the pure water flux (J_1) was measured again. The pure water flux of the membranes before the adsorption experiments (J_0) was constant for at least 2 hours. The water flux after the adsorption experiments was measured after a constant value (J_1) was reached.

Measurements with radiolabelled BSA

The ^{14}C labelled BSA proteins, with a specific activity of 1.85 MBq/mg, were purchased from Amersham International. The protein was labelled by reductive alkylation with ^{14}C -formaldehyde. The BSA solutions were prepared in the phosphate buffer (pH=7.4). Membrane samples of about 10 mg (2.2 cm^2 and a thickness of 0.2 mm.) were brought into contact with 10 ml of a protein solution containing a fixed ratio of unlabelled BSA and negligible amount of radiolabelled BSA. After a certain time the membrane samples were thoroughly flushed with the phosphate buffer and brought into 20 ml of scintillation fluid (Aqualuma). The amount of BSA adsorbed on the membrane samples was determined by measuring the adsorbed radiolabelled BSA in a scintillation detector (LKB 1219 Rackbeta).

6.4 RESULTS AND DISCUSSION

6.4.1 Permeation experiments

The effect of BSA adsorption on heat treated membranes is given as a relative flux reduction versus the equilibrium BSA concentration (figure 2). After an initial sharp increase a kind of plateau value of the flux reduction is reached. Aimar et al. [6] found similar results for adsorption studies using BSA and IRIS 3038 (polyacrylonitrile) membranes. The hydraulic resistance of the membranes reached a plateau value when the concentration of the BSA solution increased up to 50 g/l. Matthiasson [3,15] performed BSA adsorption experiments with commercially available polyamide, polysulfone and cellulose acetate membranes. He found an initial increase of the relative flux reduction for BSA concentrations in the range of 0 - 4 g/l followed by a plateau value of the BSA adsorption for BSA concentrations between 4 and 100 g/l. Matthiasson also performed flux reduction and adsorption experiments [15] with extremely high BSA concentrations (up to 400 g/l) and he found for the polyamide and the polysulfone membranes a second strong increase of the relative flux reduction at BSA concentrations above 200 g/l. Matthiasson explained these effects by presuming that not only monolayers are adsorbed but that multilayers are formed by some kind of surface attachment process [15]. The results for polyamide and polysulfone membranes contrasted with the effects of adsorption on cellulose acetate membranes. After formation of a monolayer the membrane

surface is of such a nature that no further adsorption of BSA occurs, even at elevated BSA equilibrium concentrations [15].
It can be assumed that in our experiments (see also below) a monolayer of BSA is formed in the situation that the membranes are heat treated. using the presented results. Following Aimar [6] it can be reasoned that the BSA adsorption isotherms followed Freundlich laws, since by using Langmuir fits no straight lines were obtained. When Freundlich laws can be applied, adsorption will continue after formation of a monolayer and no real plateau value is reached. More experiments have to be performed to investigate whether indeed a real plateau value is reached and a second strong increase of the amount of adsorbed BSA occurs at extremely high equilibrium concentrations.

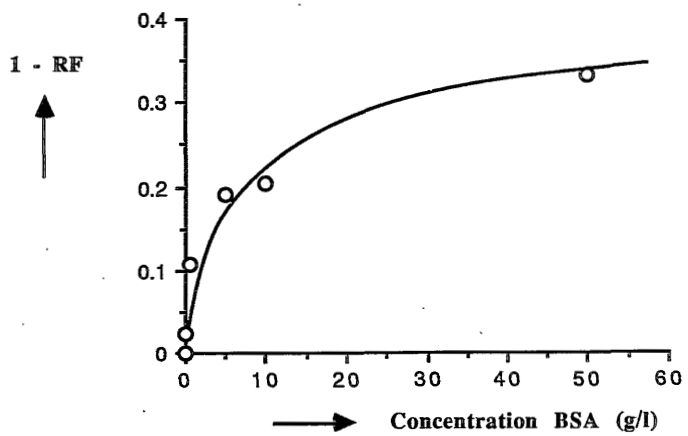

Figure 2: *Relative flux reduction (1-RF) of heat treated membranes during filtration of pure water following adsorption from a BSA solution as a function of the BSA concentration. Contact time: 16 hours.*

The time required for the adsorption (or flux reduction) to reach an equilibrium state was determined with a BSA concentration of 5 g/l. In figure 3 it can be observed that after 10 - 16 hours a plateau value of the flux reduction is reached. This relatively high value of the equilibrium time is in disagreement with other published results concerning adsorption kinetics. Matthiasson [3] performed BSA adsorption experiments (BSA concentration 2 g/l) using polyamide, polysulfone and cellulose acetate membranes and he found that after 5 - 60 minutes already a plateau value for the relative flux reduction was reached. Bornzin et al. [19] studied the kinetics of protein adsorption and found equilibrium times between 20 and 40 minutes for BSA adsorption (40 mg/l) onto Cuprophane (regenerated cellulose) surfaces. Equilibrium times

in the range of 5 - 60 minutes were reported by Nilsson [4], who performed adsorption experiments with different types of proteins on polysulfone (DDS GR61 PP) ultrafiltration membranes. Aimar et al. [6] measured the flux reduction as a function of the contact time between membrane (IRIS 3038) and BSA solutions (0.1 - 50 g/l). In contrast with Matthiasson and Nilsson, he found that depending on the BSA concentration, 5- 14 hours were required to reach a plateau value for the amount of adsorbed BSA. Aimar ascribes these differences to the followed experimental procedure. Matthiasson [3] rinsed the membranes after adsorption experiments with saline water (0.15 M NaCl), while Aimar [6] rinsed with pure distilled water, in which the solubility of BSA is very low. According to Aimar it could be possible that Matthiasson dissolved some weakly bound protein in the saline water, since the amount of adsorbed BSA analysed by Aimar is much larger.

Two different rinsing procedures were used in this work, i.e., in the situation of permeation experiments the membranes were rinsed with pure water, while in the situation of radiolabelled measurements phosphate buffer was used. In both situations, however, the same equilibrium time was found. In addition it can be mentioned that it was very difficult to remove adsorbed BSA proteins anyhow, even when cleaning agents were used. Hence the argument given by Aimar [6] is not valid for the present work.

An important difference between the experiments of Aimar [6] and Matthiasson [3] is the membrane material and it could quite well be possible that this is important for the kinetics of adsorption. Hence, more investigations concerning the kinetics of adsorption have to be performed.

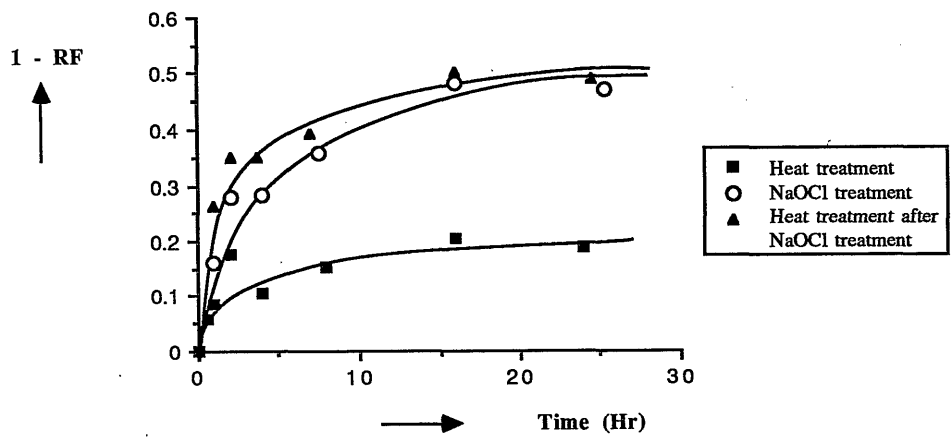

Figure 3: *Relative flux reduction (1-RF) during filtration of pure water as a function of the contact time of the membranes with a BSA solution (5 g/l).*

The conclusion from the permeation experiments is that the fouling behaviour (i.e., adsorption behaviour as will be shown below) is strongly dependent on the kind of post-treatment of the PEI-PVP membranes. As is mentioned in the introduction the membrane pore walls consists merely of PVP also in the situation that the membranes have been heat treated only, while a NaOCl treatment will partly remove the PVP. From figure 3 then it becomes clear that the presence of PVP in the polymeric membrane reduces the adsorption of BSA to a large extent and consequently the flux reduction. Although the NaOCl treated membranes are still fairly wettable by water and consequently hydrophilic, the flux reduction is of the same magnitude as the hydrophobic membranes. The latter type of membranes was obtained by applying a heat treatment after a NaOCl treatment. The obtained results indicate that the character of the hydrophilic membrane surface is very important. This effect was already reported by Defrise et al. [7] for microbial adhesion on microfiltration membranes.

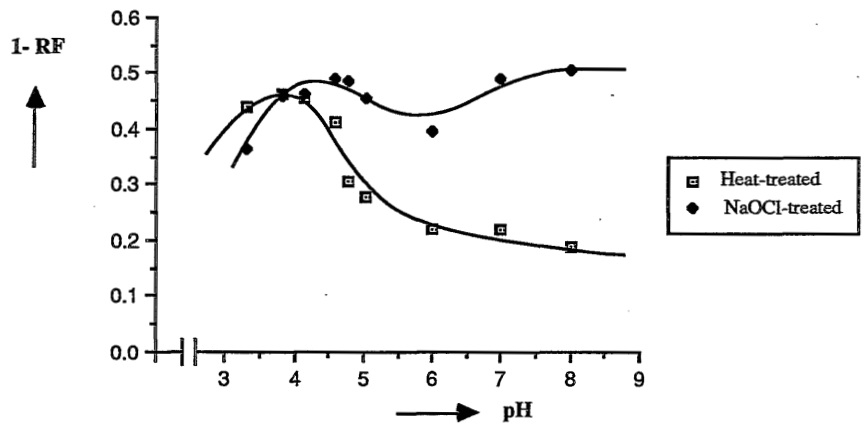

Figure 4: *Relative flux reduction (1-RF) as a function of the pH of the BSA solution to which the membranes were exposed. The membranes were heat treated or NaOCl treated. BSA concentration 15 g/l. Contact time: 16 hours*

The influence of the pH on the flux reduction has also been investigated. The results are shown in figure 4. The pH dependence found for heat treated membranes is in good agreement with results obtained by Matthiasson [3], who performed BSA adsorption experiments with different ultrafiltration membranes and with Hanemaaijer et al [8,18], who found a maximum

in the amount of BSA adsorbed onto polysulfone membranes at pH=4. Matthiasson found that the adsorption of BSA still increased at pH=4.7 (the isoelectric point: IEP) and a maximal value was reached at pH=3. Hanemaaijer et al. [8,18] explained the sharp increase around the IEP by the tendency of the proteins to associate. It has to be stressed that the dependency of pH and relative flux reduction is more or less identical for hydrophobic membranes (polysulfone) and for hydrophilic membranes (cellulose acetate) [3,8,18].
The relative flux reduction for NaOCl treated membranes as a function of the pH is more or less constant. The questional minimum at pH=6 cannot be explained. Since the NaOCl treated membranes probably contain COO^- - groups [13], the surface characteristics should depend on the pH.

6.4.2 Adsorption experiments with radiolabelled BSA

To compare the relative flux reduction with the amount of adsorbed BSA, adsorption experiments were performed with radiolabelled BSA. The adsorption isotherm of NaOCl treated membranes, presented as the amount of adsorbed BSA versus the equilibrium BSA concentration (figure 5), is in good agreement with the results using flux reduction experiments. The NaOCl treatment was used in the situation of the radiometric measurements to ensure that the amount of adsorbed BSA was high enough to be determined. The agreement is reasonable with respect to the shape of the curves and also a plateau value for the amount of adsorbed BSA is reached.

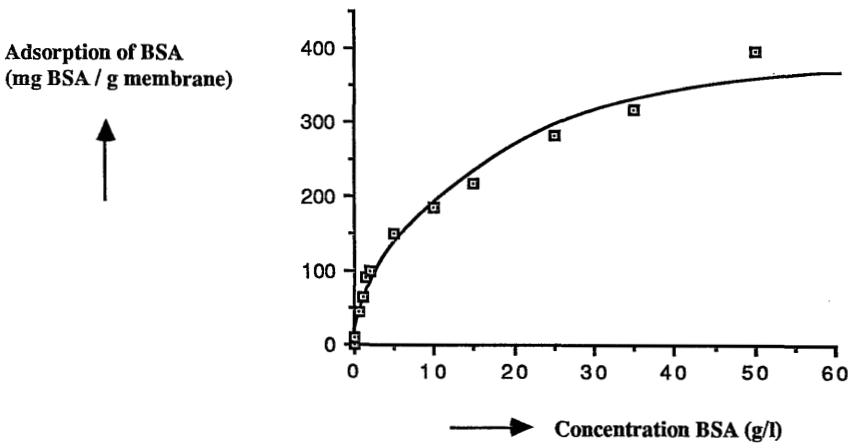

Figure 5: *Adsorption of BSA (radiometric measurement) on microfiltration membranes as a function of the BSA concentration. Contact time 16 hours. The membranes were NaOCl treated.*

The amount of adsorbed BSA correlates quite well with the relative flux reduction for the membranes after a certain post-treatment. Whether the measured amounts of radiolabelled BSA can be compared with the amount of unlabelled BSA has to be investigated. Van der Scheer et al. [20] performed experiments with mixtures of labelled and unlabelled proteins (human serum albumin: HSA) to investigate whether preferential adsorption of one of the proteins on polystyrene surfaces occurred. They found that indeed preferential adsorption of labelled HSA occurred. Van der Scheer et al. used a ^{125}Iodine label and it can be reasoned that this label may influence the protein structure to a greater extent than the ^{14}C label does, hence in the present work no preferential adsorption of radiolabelled BSA is assumed.
In figure 6 the same contact time (16 hours) as in section 6.4.1 is found before an equilibrium value has been reached. An additional conclusion from this result could be that in the present work indeed a different mechanism of adsorption must be assumed and that the differences in adsorption kinetics between Matthiasson [3] and the present results cannot be ascribed to the experimental procedure.

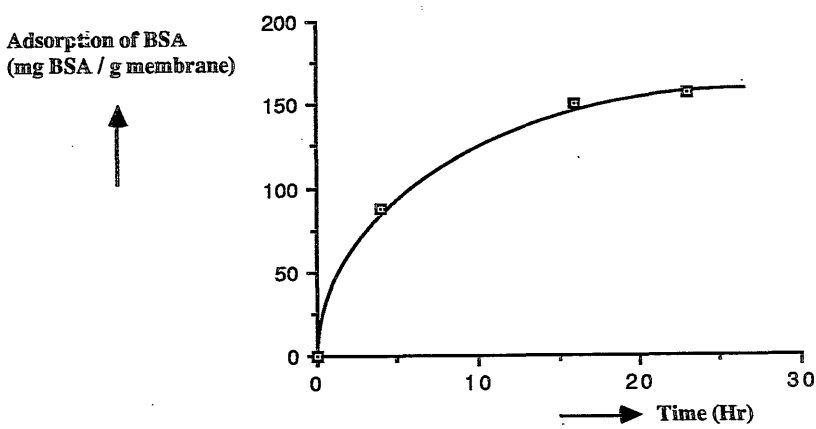

Figure 6: *Adsorption of BSA (radiometric measurement) on microfiltration membranes as a function of the contact time. The membranes were NaOCL treated. BSA concentration 5 g/l.*

The adsorption isotherms for differently treated membranes presented in figure 7 demonstrate again very clearly that the PVP present in the heat treated and untreated membranes reduces the adsorption of BSA. The differences between the NaOCl treated membranes (hydrophilic) and the hydrophobic heat-NaOCl treated membranes is again very small. The untreated membranes exhibit the lowest BSA adsorption, but as has already been shown [13], these membranes

cannot be used for permeation experiments since the PVP swells considerably. Using a cryogenic preparation technique in combination with a scanning electron microscope it could be demonstrated [9], that the swollen membrane structure is still porous. It may be concluded from the adsorption isotherms (figure 3 and 7) that the influence of the heat treatment on the chemical nature of the PVP is very small and moreover that the PVP is indeed located at the outer surface of the pore walls of the membranes.

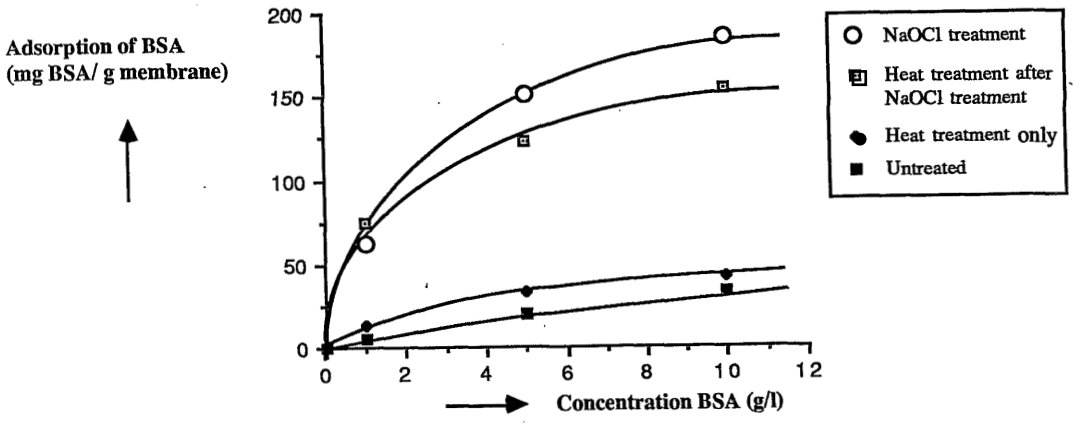

Figure 7: *Adsorption of BSA (radiometric measurement) on microfiltration membranes as a function of the concentration of BSA. The contact time was 16 hours.*

6.4.3 Evaluation

As is shown in the two previous sections, the permeation experiments and the radiometric measurements show a very clear correlation. The comparison of the amount of adsorbed BSA with experiments reported in the literature is troublesome, since the exact membrane surface area is unknown in the present work. In experiments with ultrafiltration membranes the exposed membrane surface can be used but in this work the entire porous membrane structure has been exposed to the BSA solution. A rough estimation of the specific membrane surface has been made by means of BET gas adsorption measurements. It appeared that the specific membrane surface was between 15 and 25 m^2/g membrane. When an average membrane surface area of 20 m^2/g membrane is taken, the amount of adsorbed BSA per m^2 membrane surface can be calculated. Using the results of figure 7 the amount of adsorbed BSA for NaOCl treated membranes and heat-NaOCl treated membranes is about 8 mg/m^2, while that for the

heat treated and untreated membranes is around 2 mg/m^2. The latter value is in good agreement with the amount of adsorbed BSA on cellulose acetate membranes (2 mg/m^2 according to Matthiasson [15] and Bornzin [19]), while the former values are not as high as those reported for polysulfone (20 mg/m^2) and polyamide membranes (30 mg/ m^2) [3]. Aimar [6] also reported much higher values of adsorbed amounts of BSA on IRIS 3038 membranes.
It can be concluded that the nonfouling properties of the hydrophobic PEI-PVP membranes with respect to BSA adsorption are better than those of commercially available polysulfone membranes and that the heat treated hydrophilic membranes exhibit the same nonfouling properties as cellulose acetate membranes. It must be stressed that the PEI-PVP membranes exhibit a much higher thermal stability and a much better chemical resistance than the cellulose acetate membranes.

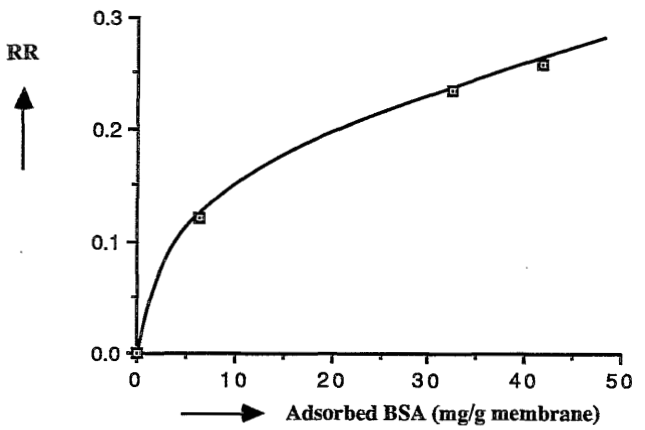

Figure 8: *Relative resistance (RR=1/[RF-1]) of the adsorbed BSA as a function of the amount of adsorbed BSA. The contact time was 16 hours and the membranes were heat treated.*

In figure 8 the relative resistance (RR) of the adsorbed BSA layer is plotted against the amount of adsorbed BSA. The data are obtained by combining data from figure 3 and figure 7. The result is comparable with results presented by Nilsson [4] and Matthiasson [3]. After an initial strong increase of the relative resistance up to an amount of adsorbed BSA of 10 mg/g, the relative resistance increases more gradually with the amount of adsorbed BSA. According to Matthiasson [3] this may indicate that at least two distinct adsorption steps can be

distinguished.

6.5 CONCLUSIONS

The presence of PVP in the polymeric membrane matrix has a positive effect on the nonfouling characteristics of the PEI-PVP membranes. Using permeation experiments it could be demonstrated that the relative flux reduction increased when the PVP from the membrane matrix was (partly) removed by means of a NaOCl treatment. The nonfouling characteristics of hydrophilic heat treated membranes are in good agreement with those of cellulose acetate membranes, while the hydrophilic NaOCl treated membranes and the hydrophobic heat-NaOCl treated membranes exhibit better nonfouling properties than commercially available polysulfone, polyamide and polyacrylonitrile membranes.
The amount of adsorbed BSA on the membranes was measured using radiolabelled BSA. The results showed a good correlation with the permeation experiments and also made clear that permeation experiments before and after adsorption, can be a very useful and a simple technique to characterize new membrane materials.

6.6 ACKNOWLEDGEMENT

The authors like to thank G.B van den Berg for the enlightening discussions on the subject.

6.7 REFERENCES

1 G.B. van den Berg and C.A. Smolders, Flux decline in membrane processes, Filtration and separation, March/April (1988) 115.
2 A.S. Michaels and S.L. Matson, Membranes in biotechnology: state of the art, Desalination, **53** (1985) 231.
3 E. Matthiasson, The role of macromolecular adsorption in fouling of ultrafiltration membranes, J. Membr. Sci., **16** (1983) 23.
4 J.L. Nilsson, Fouling of an ultrafiltration membrane by a dissolved whey protein concentrate and some whey proteins, J. Membr. Sci., **36** (1988) 147.
5 F.F. Stengaard, Preparation of asymmetric microfiltration membranes and modification of their properties by chemical treatment, J. Membr. Sci., **36** (1988) 257.
6 P. Aimar, S. Baklouti and V. Sanchez, Membrane-solute interactions: influence on pure solvent transfer during ultrafiltration, J. Membr. Sci., **29** (1986) 207.
7 D. Defrise and V. Gekas, Microfiltration membranes and the problem of microbial adhesion, Process biochemistry, August (1988) 105.
8 J.H. Hanemaaijer, T. Robbertsen, Th. van den Boomgaard and J.W. Gunnink, Fouling of ultrafiltration membranes. The role of protein adsorption and salt precipitation, J. Membr. Sci., **40** (1989) 199.
9 H.D.W. Roesink, M.J. Otto, J.R. Ronner, M.H.V. Mulder and C.A. Smolders, Demixing phenomena and membrane formation in the four component system polyetherimide/ polyvinylpyrrolidone/ N-methylpyrrolidone/ water, PhD Thesis Chapter 2, University of Twente, Enschede, The Netherlands (1989)

10 H.D.W. Roesink, I.M. Wienk, M.H.V. Mulder and C.A. Smolders, The influence of spinning conditions on the morphology of microporous capillary membranes, PhD Thesis Chapter 3 , University of Twente, Enschede, The Netherlands (1989).
11 H.D.W. Roesink, Z. Borneman, M.H.V. Mulder and C.A. Smolders, Polyetherimide - polyvinylpyrrolidone blends as membrane material, Chapter 4 PhD Thesis, University of Twente, Enschede, The Netherlands (1989).
12 US Patent 4.798.847 (17 January 1989), H.D.W. Roesink, D.M. Koenhen, M.H.V. Mulder and C.A. Smolders (assigned to X-FLOW BV, Enschede, The Netherlands).
13 H.D.W. Roesink, S. Oude Vrielink, M.H.V. Mulder and C.A. Smolders, Post-treatment of hydrophilic membranes prepared from polyetherimide - polyvinylpyrrolidone blends, PhD Thesis Chapter 5, University of Twente, Enschede, The Netherlands (1989)
14 C.A. Smolders and Th. van den Boomgaard, J. Membr. Sci., **40** (1989) 121.
15 E. Matthiasson and B. Hallström, Adsorption phenomena in fouling of ultrafiltration membranes. Published in: Proceedings from the third international congress on engineering and food, Dublin, Ireland, September (1983) 26.
16 F.F. Stengaard, Characteristics and performance of new types of ultrafiltration membranes with chemically modified surfaces, Desalination, **70** (1988) 207.
17 K.J. Kim, A.G. Fane and C.J.D. Fell, The performance of ultrafiltration membranes pretreated by polymers, Desalination, **70** (1988) 229.
18 J.H. Hanemaaijer, T. Robbertsen, Th. van den Boomgaard, C. Olieman, P. Both and D.G. Schmidt, Characterization of clean and fouled ultrafiltration membranes, Desalination, **68** (1988) 93.
19 G.A. Bornzin and I.F. Miller, The kinetics of protein adsorption on synthetics and modified surfaces, J. Colloid and Interf. Sci., **86** (1982) 539.
20 A. van der Scheer, J. Feijen, J. Klein Elhorst, P.G.L.C. Krugers Dagneaux and C.A. Smolders, The feasibility of radiolabeling for human serum albumin adsorption studies, J. Colloid Interface Sci., **66** (1978) 136 .

CHAPTER 7

MODULES WITH CAPILLARY MICROFILTRATION MEMBRANES. 1 - COMPARISON OF THE SHELL-SIDE FED MODULE WITH THE CAPILLARY BORE FED MODULE.

H.D.W. Roesink and I.G. Rácz.

7.1 SUMMARY

In membrane separation processes many efforts are given to predict permeate fluxes. Although good results have been obtained, the predictions always are dependent on the type of feed solution and the modules. In microfiltration applications the permeate flux is dependent on the shear stress at the membrane wall. It can be shown that the same permeate fluxes are found in different modules if the shear stress at the membrane wall is equal. In this chapter modules with capillary membranes are used and the shell-side fed module is compared with the capillary bore fed module. Two types of shell-side fed modules are considered: longitudinal flow and transverse flow of the feed solution. For these three module types the shear stress and the energy consumption in the module as a function of the volume flow of the feed solution is calculated for a module with 400 capillary membranes. The calculations based on theoretical models show that shell-side fed modules with tranverse flow have theoretical advantages: at the same permeate rate, the energy consumption in a shell-side fed module with transverse flow is one third of the energy consumption in a capillary bore fed module.

7.2 INTRODUCTION

Microfiltration is a pressure-driven solid/liquid separation technique involving colloids and fine particles in the approximate size range of 0.1 to 10 μm. The separation of the particles from the solvent, the macromolecules and smaller molecules is based on a sieving mechanism and particles are separated exclusively according to their dimensions. The transmembrane pressure difference normally is in the range of 50 to 500 kPa.

Two different modes of filtration are used:

I *Dead-end*

In this generally batch-wise operation mode the feed solution flows perpendicular to the membrane surface (figure 1).

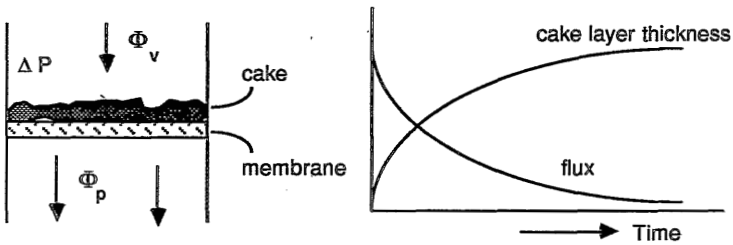

Figure 1: *Schematic representation of dead-end microfiltration.*

II *Cross-flow*

In this continuous operation mode the feed solution flows across the membrane surface (figure 2).

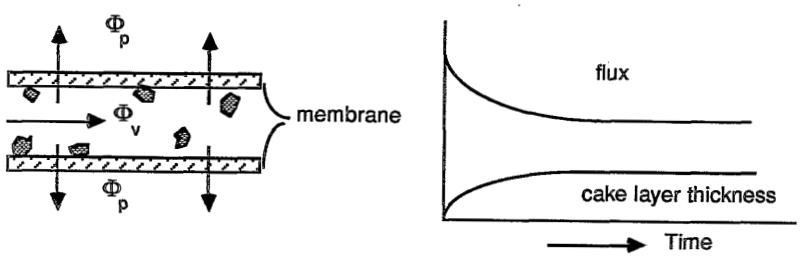

Figure 2: *Schematic representation of cross-flow microfiltration.*

A disadvantage of the dead-end filtration is the rapid flux decline. The reasons for the flux decline are different in each case of filtration, but in general the flux declines by an increased resistance, caused by the formation of a cake on the membrane surface. An extended survey of flux decline in membrane processes is given by Van den Berg et al. [1].

Using the cross-flow system the flux decline can be diminished since the build-up of foulants on the membrane surface is reduced. Cross-flow filtration is the most important mode for

pressure-driven membrane processes (reverse osmosis, ultrafiltration, microfiltration, gas separation).
But even using the cross-flow system flux decline is the dominant reason that microfiltration cannot be used in all potential applications. The flux decline, related to the clean water flux, can be as high as 99 % in microfiltration, when no backflushing technique is applied.
In order to avoid or to diminish flux decline during microfiltration the following aspects have to be considered:

-a- the feed composition

In microfiltration often multi component feed solutions are used containing particles, cell material, salts, proteins, macromolecules, lipids, surfactants, antifoam agents and others. A good knowledge of the physical and chemical properties of the feed solution is important for an optimal design of process and module. Important are the particle size, particle size distribution, adsorption phenomena of the different components, behaviour at different pH and temperatures, etc.

-b- the membrane

All important processes occur at the membrane/feed solution interface, so that the membrane plays a determining role in the fouling mechanism.
Important aspects are:

- The hydrophilic character of the membrane material.

Hydrophilic materials show less tendency to adsorb proteins or macromolecules than hydrophobic ones. Since adsorption of proteins often is the first step in the fouling mechanism of membranes, hydrophilic membranes are preferred.
Unfortunately many hydrophilic materials are not thermally resistant, although as described in this thesis a steam sterilizable and chemical resistant hydrophilic membrane is developed [2] and commercialized by X-Flow, Enschede, The Netherlands.

- The structure of the membrane.

Porosity, pore sizes and pore size distribution are important parameters. Important is also the fact whether the structure over the cross section of the membranes is symmetric or asymmetric. In an asymmetric structure the smallest pores should be in contact with the feed and the plugging of the membranes will therefore be minimized, while in symmetric membranes pores can more easily be plugged by particles.

-c- the module

Module design is strongly dependent on the geometry of the microfiltration membranes.

Microfiltration membranes can be obtained with the following geometry:

1 Flat: flat membranes are used in plate and frame systems.

2 Tubular: membranes are cast inside a porous tubular support, since the membranes are not self supporting. The feed stream flows through the tube. The outer diameter of the membranes is between 2 and 10 mm.

3 Capillaries: this membrane type is self supporting and the feed flows through the bore of the capillary or on the outside of the capillary. The outer diameter of capillary membranes is between 0.5 and 2 mm.

4 Hollow fibres: the smallest geometry of tubular membranes are the hollow fiber membranes (outer diameter of 30 - 500 μm). They are not often used in microfiltration applications, since plugging of the bore occurs easily.

With respect to flux decline the general considerations for module design are the fluid mechanics and mass transfer. The build-up of fouling layers should be minimized in order to optimize the membrane performance. In addition economic considerations (high membrane-surface to module-volume ratio, ease of replacement of the membranes, low energy costs) should be taken into account.
Comprehensive descriptions of membrane modules can be found in [3] and [4].

-d- the process handling

Given a certain feed solution and membrane module, the flux decline should be minimized. In literature many experiments can be found in which one tries to optimize the performance of a certain membrane system for a given feed suspension. For microfiltration applications the following process parameters are often used:

- Optimalization of the velocity of the feed suspension:

As will be illustrated later in this work the permeate flux is a function of the velocity of the feed suspension. Since a high velocity causes a high energy consumption, the optimum velocity has to be determined.
When polydisperse suspensions have to be filtered sometimes classification of the cake layer occurs [5], so that the specific resistance of the cake increases and the permeate flux decreases when the velocity of the feed suspension is increased.

- *Backflushing:*
In microfiltration applications backflushing can be applied if the membranes are not damaged when reversing transmembrane pressure. Using the backflushing technique it is possible to clean the membrane surface during the filtration process so that higher net permeate fluxes can be achieved. As during the backflush process no filtration occurs and some permeate is required, the backflushing process has to be optimized.

- *Changing the direction of the feed solution flow:*
To diminish the build up of a fouling layer or to destroy a build up layer in some microfiltration systems the direction of the feed suspension is changed from time to time.

To achieve the smallest flux decline possible it is important to consider all the aspects mentioned both separately as in their coherence. In this work attention is focussed on the capillary microfiltration module and especially on the difference of the shell-side fed module and the capillary bore fed module. The comparison of three capillary module types is based on theoretical considerations and models for microfiltration as presented in recent literature.

7.3 DIFFERENT FLOW CONDITIONS IN MODULES WITH CAPILLARY MEMBRANES

Membranes have been packaged in modules of various designs but in the majority of cases the feed solution moves across the membrane in tangential flow, while the permeate is removed laterally through the membrane. It is commonly accepted that the performance of pressure driven membrane processes is related to the (tangential) fluid mechanics across the membrane surface and that the build-up of foulants at the membrane surface can be predicted and controlled through an understanding of the fluid mechanics and mass transfer. But since mass transfer is dependent on the flow characteristics above the membrane surface it can be stated that good understanding of fluid mechanics is necessary to study mass transfer problems such as concentration polarization and fouling and that in fact fluid mechanics determine the performance of membrane modules (if the fouling layer causes the highest resistance). Very recently Belfort [3] presented a paper in which different modules were compared using fluid mechanics. In that work especially the cross-flow filtration was compared with dead-end filtration and a comparison is made between a porous tube and a porous two-walled slit. In addition a comparison was made for different commercially available membrane modules for reverse osmosis, ultrafiltration and microfiltration. One of the conclusion was that in general the permeability increases as the axial velocity of the feed solution increases. No special attention was given to the different configurations of capillaries or hollow

fibres in membrane modules.

For microfiltration applications capillary membranes are often used since they are self supporting, they can be easily produced in different dimensions and morphologies and furthermore a high membrane-surface to module-volume ratio can be obtained. Three possibilities for the feed flow can be distinguished (figure 3):

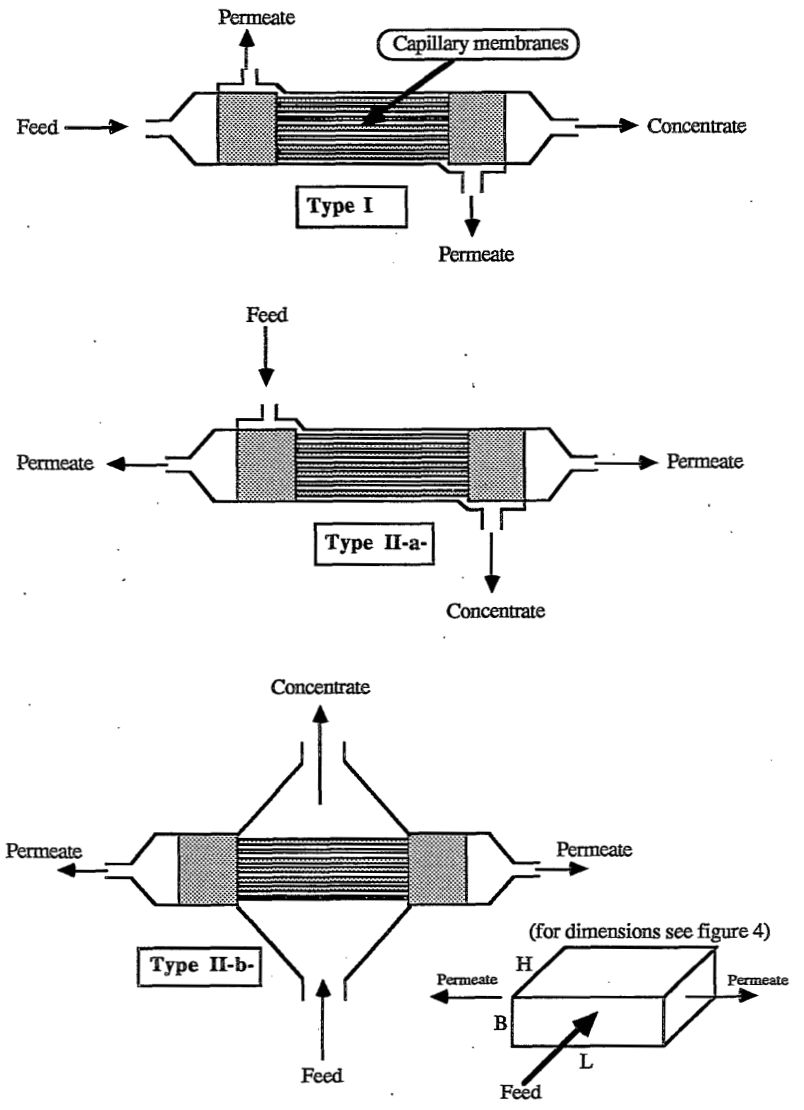

Figure 3: *Different flow conditions of the feed in capillary membrane modules.*

- I - The feed flow is through the bore of the capillaries; a capillary bore fed module design. Advantages of this shell-and-tube heat exchanger design are the well-controlled hydrodynamics of the feed and the good possibilities of cleaning.

- II -The feed flows outside the capillary membranes; a shell-side fed module design.
The shell-side fed module can be designed and constructed in many different ways as is illustrated in the patent literature [6]. Two essentially different types can be distinguished:

- a - *Longitudinal flow*: the flow of the feed is parallel to the capillary membranes and in fact the same design as for the capillary bore fed module can be used.

-b - *Transverse flow*: the flow of the feed is perpendicular to the capillary membrane axis and many sub-types of design are possible here.

As a disadvantage of the type II modules it can be mentioned that the flow conditions are not always well-controlled since e.g., channelling easily occurs and another disadvantage can be the fact that this module type easily plugs or is difficult to clean. These disadvantages are dependent on the actual design of this module type and since many different designs can be distinguished it is not appropriate to ascribe these disadvantages to all kinds of shell-side fed modules. In this work the type II modules will be treated as if the arrangement of the capillary membranes is ideal and e.g., no channelling occurs.

7.4 MODELS FOR MICROFILTRATION

To compare different module types a model is necessary to describe the permeate flux as a function of relevant process and equipment parameters. In this section a survey will be given of a number of important microfiltration models.

Yang and Cussler [7] used the same configurations (type I, II-a- and II-b-) to design hollow-fibre contactors. Although in their case the modules (contactors) were used for e.g.,. aqueous deaeration and carbon dioxide absorption, the mass transfer relations they used and derived can also be used for other filtration applications. They investigated the mass transfer correlations for the different configurations and found a good agreement for type -I- and type -II b-, while for type -II a- a higher mass transfer was found than predicted on the basis of the theoretical Sherwood relation (table 1). The explanation of Yang et al. [7] is based on some type of secondary flow that should occur. The theoretical mass transfer correlations are based on a single-tube correlation and

experiments are performed with Reynolds numbers between 4 and 40.

Table 1. *Mass transfer correlations for hollow-fibre modules according to Yang [6].*

Flow	Observed correlation	Literature
Type I (water inside fibres)	$Sh=1.64\ Pe^{0.33}$	$Sh=1.62\ Pe^{0.33}$
Type -II a- (water outside fibres)	$Sh=1.25\ (Re*d_H/L)^{0.93}\ Sc^{0.33}$ d_h= 4*cross-sectional area/wetted perimeter	$Sh=0.022\ Re^{0.60}Sc^{0.33}$
Type -II b- (water outside fibres)	$Sh=0.90\ Re^{0.40}\ Sc^{0.33}$	$Sh=0.91\ Re^{0.39}\ Sc^{0.33}$

Mass transfer correlations are very convenient in ultrafiltration to predict the permeate fluxes, since for the permeate flux the following relation has been derived:

$$J_v = k*\ln(c_w/c_o) \qquad (1)$$

An extended survey of mass transfer correlations for membrane operation (ultrafiltration and reverse osmosis) is given by Gekas et al. [8]. In the situation that in the concentration polarization layer a steady state between the convective transport of dissolved components to the membrane surface and the back diffusion of these components is reached, the prediction of permeate fluxes will be rather good.
In microfiltration this equilibrium will not be reached since the situation is different due to the particle size of the dissolved components. In ultrafiltration dissolved macromolecules will have to be retained, while in microfiltration applications suspensions are treated and particles of 0.1 - 10 μm size have to be retained. These differences were already investigated and discussed by Porter 1972 [9]. Porter found that the observed permeate fluxes for colloidal particles were as much as two orders of magnitude higher than predicted with theoretical mass transfer correlations. This effect is known as the "flux paradox for colloidal suspensions". The explanation for this effect is that the back-transport of the particles is not caused by Brownian diffusion as in the situation of macromolecules but by another mechanism: a shear-induced radial migration of colloidal particles from the membrane surface (the tubular pinch effect or inertial lift effect) [4,5,9].

Although the tubular pinch effect gives an acceptable explanation for the higher permeate fluxes in microfiltration applications some complications can be observed when polydisperse suspensions are filtered. Baker et al. [5] performed microfiltration experiments with a mineral slurry ($TiO_2.2H_2O$) and found that the permeate flux passed through a maximum when the cross-flow

velocity increased. This was explained by the shear-dependent classification mechanism which means that large particles are excluded from the cake as the cross-flow velocity increases, so that the specific resistance of the cake increases.

Schock [4] performed experiments with inorganic suspensions (kaolin and quartz meal) and was able to describe his experiments, performed in tubular membranes (inner diameter d_i) or in porous channels (height d_i) with the following expression:

$$J_v = 4.7*10^{-5} * Re^{1.26} * (\nu/d_i) * (d_p/d_i)^{0.44} \qquad (2)$$

The Reynolds number is related to the dimensions of the channel or the tube. Scholar concluded that the backdiffusion of particles is a function of the hydrodynamic situation in the direct neighbourhood of the membrane and of the particle size. This result was shown by Scholar by performing experiments with different module types and the same feed suspension. The permeate fluxes only depend on the shear stress at the membrane wall.

The same dependence of permeate flux and shear stress was found by Gernedel [10], who performed ultrafiltrations experiments with protein solutions and tubular membrane systems with different geometries.

Romero et al. [11] recently presented a model for cross-flow microfiltration based on hydrodynamic particle diffusion. A significant finding of the theory presented is the prediction of the formation of a stagnant particle layer beginning at a critical distance from the channel (tube) entrance. The model is able to predict the thickness of the stagnant layer and the reduced permeate flux as a function of the distance from the channel (tube) entrance. The practical result of the model is the prediction of permeate flux which in dimensionless form depends on three dimensionless quantities: x/x_{cr} (the axial position in the filter unit), ϕ_0 (volume fraction of particles in the bulk) and β_{st} (stagnant cake layer resistance). Although the predicted flux only can be determined numerically since the different expressions are rather complicated, a simple expression for the flux can be obtained in the limit of a large cake resistance and a relatively long filter unit.

$$J_v = 6*10^{-4} \, (d_p^4/L)^{1/3} \, \gamma_w \, [\eta^3 (\phi_0) \, Q_{cr}(\phi_0) / \phi_0 \, Q_{cr}(0)]^{1/3} \qquad (3)$$

where γ_w is the wall shear rate in the absence of a cake layer, η is the relative viscosity (viscosity of the suspension divided by viscosity of the particle-free fluid), $Q_{cr}(0)$ is the value for the dimensionless particle flux in the limit as $\phi_0 \rightarrow 0$ and at a maximum concentration of particles at the membrane surface.

Romero et al. performed experiments with monodisperse suspensions whereas in pratical situations polydisperse suspensions have to be filtered and according to Romero a need exists for the determination of an average or effective shear-induced diffusion coefficient in polydisperse suspensions. For details see the paper of Romero [11].

It is very interesting that the expression obtained by Romero et al. [11] is similar to an earlier result derived by Zydney and Colton [12].

$$J_v = 7.8*10^{-4} (d_p^4/L)^{1/3} \gamma_w \ln (c_w / c_o) \qquad (4)$$

in which c_w / c_o is the ratio of concentration of particles at the membrane surface and in the bulk. Zydney et al. based their model on shear-enhanced diffusivity of the large particles which arises from mutually induced velocity fields in the shear flow of concentrated suspensions. The expression they found is derived from the well-known film theory:

$$J(x) = k(x) \ln (c_w / c_o) \qquad (5)$$

in which k(x) is the local mass transfer coefficient. The local mass transfer coefficient for a linear velocity profile within the boundary layer and constant wall concentration can be evaluated from the analogous heat transfer problem (Lévêque, 1928):

$$k(x) = 5.38*10^{-3} (\gamma_w D^2/x)^{1/3} \qquad (6)$$

The effective particle diffusity is given by Eckstein et al. [13]:

$$D = 3*10^{-6} (d_p)^2 \gamma_w \qquad (7)$$

7.5 COMPARISON OF THE DIFFERENT CONFIGURATIONS

Although the prediction of permeate fluxes for monodisperse suspensions is rather good when using the models presented in the former section and especially an adequate determination of the effective shear-induced diffusivity coefficient (according to Romero [11]) should give a better prediction of the permeate flux in the case of polydisperse suspensions, there still remain complicated situations where suspensions have to be filtered that are not simply polydisperse but also contain other components like lipids, surfactants, salts, biological material etc. This means that for example also adsorption at the membrane surface and in the membrane pores becomes more and

more important, or that the particles could be deformable (cells).

The results of Schock [4], Gernedel [10] and Zydney [12] demonstrate that the permeate flux increases with the wall shear rate (or the shear stress, since there are well known relations between shear stress and shear rate).
Schock and Gernedel compared different configurations of microfiltration modules and concluded that with the same feed suspension for different modules the same permeate flux can be found if the shear stress at the membrane wall is identical.
Zydney and Colton showed that the permeate flux during the filtration of blood increased linearly with the wall shear rate and they discussed also some other plasmapheresis models in their paper [12], these models can be summarized with the following expression:

$$J_v = A\,(\gamma_w/L)^a \qquad (8)$$

Since the permeate flux is a function of the shear rate, a handsome tool is created to compare the three different capillary configurations since the shear stress can be expressed as a function of relevant design parameters.
For flow in a module the following relation can be used:

$$\tau_w = \frac{\Delta P_{mod} * A_c}{A_w} \qquad (9)$$

in which τ_w the shear stress at the membrane surface, ΔP_{mod} the pressure drop over the module, A_w the "wetted" surface area and A_c the cross sectional area of the module, available for feed flow.
The pressure drop in the module depends on the flow regime and can be expressed with the following relation:

$$\Delta P_{mod} = \xi * 1/2\ \rho v^2 * L/d_h \qquad (10)$$

ξ is the friction factor and depends on the flow regime in the module (table 2), ρ is the density of the feed solution, v is the average velocity of the feed solution, L is the length of the module and d_h the hydraulic diameter.

Table 2. *Friction factors for module types I and II-a-*

Module Type	Friction factor (ξ)	
	Laminar (Re ≤ 2320)	Turbulent
Type I $d_h = d_i$	64/Re	$0.2*Re^{-0.2}$
Type II-a-	64/Re	$0.2*Re^{-0.2}$

d_h= 4*cross sectional area/wetted perimeter

The pressure drop in module type II-b- can be calculated using relations which are used in the heat exchanger theory [14]. The calculation for the friction factor is given in the appendix.

When ΔP_{mod} is known the energy consumption in the module at the feed side can be calculated with the following relation:

$$\Delta E_{mod} = \Delta P_{mod} * v * A_c = \Delta P_{mod} * \Phi_v \qquad (11)$$

The three module types shown in figure 3 can now be compared using the relations for the pressure drop in the modules and using the expression for the shear stress. For the comparison of the three module types in fact the same module design has been used, only the flow conditions have been changed.
The dimensions of the module and the membrane surface are in accord to what can be seen as a standard module in microfiltration applications. The membrane surface area for type I module is 0.75 m^2, while for type II-a and II-b- the membrane surface area is 1.00 m^2. In fact this is already the first advantage for a shell-side fed module; the larger membrane surface area available at the same capillary length. For the comparison a square design of the housing is chosen, so that for all three types the same design can be used.

The following assumptions have been made for the comparison of the capillary membrane modules:

- the feed volume flows used are: 50, 25, 10, 5, 2.5 and 1 m^3/hr.
- 400 capillary membranes with d_o =2 mm and d_i =1.5 mm are used in the modules
- the effective length (L) of the capillary membranes is 0.4 m.
- the dimensions of the cross section of the modules and the arrangement of the capillary membranes are given in figure 3 and 4; the arrangement of the capillaries is ideal.
- all membrane surface area is used

- the pressure drop in the potted parts of the membranes of module type I is neglected
- the shear stress is constant over the module
- the pressure drop due to inflow and outflow phenomena is neglected
- for the dynamic viscosity 10^{-3} Pas is taken
- for the density 10^3 kg/m^3 is taken

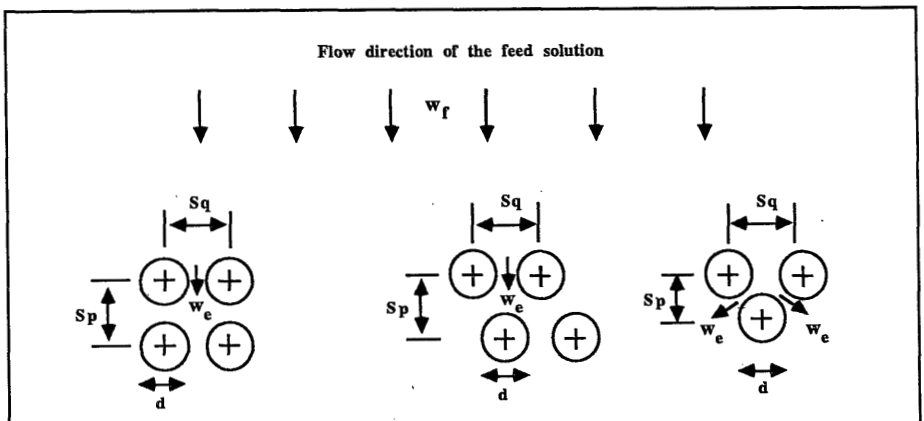

Square array of capillary membranes Sq=Sp=2.5 mm d=2mm	Triangular array of capillary membranes Sp=Sq=2.5 mm d=2mm	Triangular array of capillary membranes Sp=1.7 Sq=2.5 d=2 mm
a=Sq/d b=Sp/d	$w_e = a/(a-1) * w_f$	$w_e = a / 2(c-1) * w_f$ $c=\sqrt{\{(a/2)^2 + b^2\}}$
Dimensions of module housing: LxBxH = 400x50.5x50.5 mm	Dimensions of module housing: LxBxH = 400x51.75x51.75 mm	Dimensions of module housing: LxBxH = 400x51.75x35.3 mm

Figure 4: Three arrangements for capillary membranes in a type II-b (see figure 3) module.

Table 3. *Characterization of the capillary modules*

Module Type (see fig. 3,4)	Φ_v (m^3/hr)	v (m/s)	Re -	ΔP_{mod} (x 10^{-5} N/m^2)	τ_w (N/m^2)	ΔE_{mod} (J/s)	E_f -
Type I (capillary bore fed)							
	1	0.39	585	0.022	2.1	0.6	9.6
	2.5	0.98	1470	0.056	5.2	3.9	25.3
	5	1.96	2940	0.207	19.4	28.8	50.0
	10	**3.93**	**5895**	**0.726**	**68.0**	**201.7**	**100.0**
	25	9.82	14730	3.77	353.6	2618.1	249.6
	50	19.65	29475	13.1	1232.5	18194.4	497.7
Type II-a- (shell-side fed; longitudinal flow)							
	1	0.21	400	0.007	0.9	0.2	5.6
	2.5	0.54	1029	0.019	2.3	1.3	14.3
	5	1.07	2039	0.038	4.5	5.3	29.8
	10	2.14	4078	0.182	21.7	50.6	59.0
	25	5.37	10234	0.955	113.7	663.2	147.5
	50	10.74	20467	3.325	396.0	4618.1	294.9
Type II-b- (shell-side fed; transverse flow, square array; a=1.25 b=1.25)							
	1	0.07	138	0.001	0.4	0.03	1.9
	2.5	0.17	344	0.003	1.2	0.2	4.2
	5	0.34	688	0.007	2.8	1.0	9.0
	10	0.69	1375	0.025	10.0	7.0	17.7
	25	1.72	3438	0.148	76.8	102.7	33.8
	50	3.44	6876	0.580	298.0	805.6	68.4
Type II-b- (shell-side fed; transverse flow, triangular array; a=1.25 b=1.25)							
	1	0.07	138	0.001	0.4	0.03	1.9
	2.5	0.17	344	0.003	1.2	0.2	4.2
	5	0.34	688	0.011	4.4	1.5	8.8
	10	0.67	1375	0.040	16.0	11.1	17.5
	25	1.68	3438	0.223	89.2	154.9	43.9
	50	3.35	6876	0.741	296.3	1029.2	87.8
Type II-b- (shell-side fed; transverse flow, triangular array; a=1.25 b=0.85 c=1.055)							
	1	0.15	304	0.006	1.5	0.17	2.9
	2.5	0.38	762	0.020	5.0	1.4	7.1
	5	0.76	1524	0.064	15.9	8.9	14.2
	10	1.52	3048	0.206	51.1	57.2	28.3
	25	3.81	7622	0.952	236.1	661.1	70.8
	50	7.62	15244	3.034	752.4	4213.9	141.6

The calculations demonstrate (table 3) that the shell-side fed modules may have an advantage when

the energy consumption per unit permeate is considered.
To illustrate this effect more clearly an energy consumption-factor E_f is introduced. As stated before the permeate flux is proportional to the shear stress:

$$J_v = C * \tau_w \qquad (12)$$

in which C (m^3/Ns) is a proportionallity factor, J_v the permeate flux in m^3/m^2 s. C is dependent on the feed solution used and is assumed to be the same in all module types.
When ΔE_{mod} is divided by (τ_w *C*A_m), the energy consumption for 1 m^3 permeate produced is found (A_m is the membrane surface area in m^2). Since the exact value of this energy consumption factor cannot be calculated, since C is unknown, all energy factors E_f are obtained by dividing the calculated E_f values by the energy factor in the capillary bore fed module with a feed flow of 10 m^3/hr and multiplied by hundred.

From these analyses it becomes clear that the shell-side fed module has great advantages compared with the capillary bore fed module with respect to the energy consumption per permeate volume unit. When the shell-side fed modules are compared it can be seen that the transverse flow has much better characteristics than the longitudinal flow modules and on the other hand when the transverse modules are compared the differences are small, so that from this analysis the main conclusion can be that for shell-side fed modules the transverse flow is the best.

If the permeate rate is constant (approximately the same shear stress) and the capillary bore fed module is compared with the shell-side fed module the energy consumption of the shell-side fed module is only one third of that in the capillary bore fed module. At the same energy consumption the capillary bore fed module requires about four times the membrane surface that is present in the shell-side fed modules.
An additional advantage of the shell-side fed module with respect to the capillary bore fed module is that the same permeate output (the same shear stress) can be obtained with a much lower pressure drop in the module, so that when the same transmembrane pressure difference is required, a lower pressure in the filtration system can be used, which may be an additional advantage with respect to, e.g., compaction of the cake layer or deformation of the filtered particles.

It has to be emphasized that the comparison of the capillary membrane modules is based on theoretical considerations. Experiments with different feed suspensions have to be performed to investigate whether these conclusions can be confirmed.
A problem will be the construction of type II-b- modules, since for this module type the

arrangement of the capillaries is very important, but probably hard to realize. Since theoretical considerations demonstrate that the shell-side fed module with transverse flow has energetic advantages, this analysis should be a challenge for module designers and constructors. In our group the first results with the construction of a module with transverse flow have been very promising.

7.6 DISCUSSION

The results in the former section show that a shell-side fed module may have great advantages with respect to a capillary bore fed module. The reason for this is that in the shell-side fed module type II-b- very high shear stresses can be achieved while the energy consumption in this module type is moderate.

As is stated by many workers [10,15,16] it is necessary to minimize the length of the capillary membranes in capillary bore fed modules in order to obtain higher net fluxes. This is due to the build up of a fouling layer. The thickness of the fouling layer is a function of the length of the capillary or tubular membrane. It is unknown which relation exists between the thickness of the fouling layer and the dimensions of membrane types II-a- and II-b-.

A module type that is used for high performance applications in e.g.,. biotechnology is the Dyno-Filter or Escher-Wyss Druckfilter [4]. In this module type the feed suspension flows through a narrow slit between two rotating cylinders, which are supplied with flat membranes. In the slit secondary flow phenomena (Taylor-Görtler vortices) can be observed which improve the mass transfer in these module types.
Secondary flow phenomena play also an important role in so called corrugated membranes. Van der Waal and Ràcz [17,18,19] investigated different types of corrugations in flat membranes for reverse osmosis, ultrafiltration and also for microfiltration and ascribed the improved mass transfer results to local turbulences near the membrane surface.

As already mentioned by Yang et al. [7] in the case of module type II-a- secundary flow phenomena may occur. The secondary flow causes local turbulence and an increase of the local mass transfer so that higher permeation rates are obtained as those expected when based on the average flow velocity. The secondary flow phenomena may also be very important in module type II-b-.
As is know from the flow conditions in cross-flow heat exchangers (often a module II-b- design), many secondary flow phenomena can be observed [20]. These secondary flow phenomena, which can be observed in the wake opposite to the stagnation point of the capillary membrane, may

improve the mass transfer and so the permeation characteristics of the shell-side fed modules. The same type of Taylor-Görtler vortices as observed on concave surfaces [4], can be observed on convex surfaces [21] for high Reynolds numbers, although no range of Reynolds number is given in the literature cited. This means that in module type II-b- with transverse flow, secondary flow phenomena may be present in the vicinity of the stagnation point of the capillary membrane. Although the latter effects are rather hypothetical it may be an additional advantage of the transverse flow module design.

7.7 NOTATION

A_c	cross sectional area	m^2
A_m	membrane surface area	m^2
A_w	wetted surface	m^2
a	ratio of capillary cross section to mutual distance	-
b	ratio of capillary cross section to mutual distance	-
C	proportionallity factor	Nm/s
c_o	concentration in the bulk	kg/m^3
c_w	concentration at the membrane surface	kg/m^3
d_h	hydraulic diameter	m
d_p	particle diameter	m
d_i	inner diameter of capillary membrane	m
d_o	outer diameter of capillary membrane	m
D	diffusion coefficient	m^2/s
Ef	energy consumption factor	J/m^3
ΔE_{mod}	energy consumption in the membrane module	J/s
J_v	permeate flux	m/s
J(x)	local permeate flux	m/s
k(x)	local mass transfer coefficient	m/s
x	axial coordinate	m
L	length	m
N_r	number of resistances in flow direction	-
N_m	number of capillary membrane rows	-
ΔP_{mod}	pressure drop in the module	Pa
Pe	Peclet number: $d^2 v/DL$	
Re	Reynolds number: $(\rho v d)/\eta$	-
Sc	Schmidt number: $\eta/\rho D = \nu/D$	-
Sh	Sherwood number: kd/D	-

v	average velocity of the feed	m/s
w_f	velocity of the feed in an empty module	m/s
w_e	velocity of the feed in the most narrow slit	m/s
τ_w	shear stress	N/m^2
ν	kinematic viscosity	m^2/s
η	viscosity	Ns/m^2
γ_w	membrane wall shear rate	1/s
ξ	friction factor	-
ξ_l	friction factor for laminar conditions	-
ξ_t	friction factor for turbulent conditions	-
ϕ_v	volume flow of the feed	m^3/s
ϕ_p	volume flow of the permeate	m^3/s
ρ	density	kg/m^3

7.8 APPENDIX - Pressure drop in shell-side fed modules with transverse flow

The calculation method for the pressure drop in the module type II-b- is taken from [14], a standard text concerning heat transfer. The following basic relation is used for the pressure drop calculations:

$$\Delta P_{mod} = \xi * N_r * 1/2 * \rho * (w_e)^2 \qquad (13)$$

where ΔP_{mod} - the pressure drop in the module
ξ - the friction factor
N_r - the number of resistances in the flow direction
ρ - density of the solution
w_e - velocity of the solution in the narrowest slit

When arrangements of capillary membranes are used , so that $b \geq 1/2\ \sqrt{(2a+1)}$, the number of resistances is equal to the number of rows of capillary membranes (N_m). When $b < 1/2\sqrt{(2a+1)}$ the number of resistances equals N_m-1. The definition of a, b and c is given in figure 4.

The velocity in the narrowest slit can be calculated in relation to the velocity in the empty module w_f:

$$w_e = a/(a-1) * w_f \quad \text{for} \quad b \geq 1/2\ \sqrt{(2a+1)} \qquad (14)$$

$$w_e = a/2*(c-1)* w_f \quad \text{for} \quad b<1/2\sqrt{(2a+1)} \tag{15}$$

$$Re= (w_e * d_o * \rho)/ \eta \tag{16}$$

in which d_o the diameter of the capillary membrane and η the viscosity of the solution.

The friction factor for the pressure drop in a module with a square array of capillary membranes (figure 4) can be calculated using the following relations:

$$\xi = \xi_l + \xi_t [\ 1- \exp \{-(Re+1000)/2000\}] \tag{17}$$

in which:

$$\xi_l = f_l/Re \text{ and } \xi_t = f_t/ Re^{0.1(b/a)} \tag{18}$$

$$f_l = 280\pi[(b^{0.5}-0.6)^2 + 0.75]/(4ab-\pi)*a^{1.6} \tag{19}$$

$$f_t = [0.22 + 1.2\{(1-0.94/b)\}^{0.6}/(a-0.85)^{1.3}]* 10^{0.47(b/a - 1.5)} + \{0.03(a-1)(b-1)\} \tag{20}$$

The friction factor for the pressure drop in a module with a triangular array of capillary membranes (figure 4) can be calculated using the following relations:

$$\xi = \xi_l + \xi_t [\ 1- \exp \{-(Re+200)/1000\}] \tag{21}$$

in which:

$$\xi_l = f_l/Re \text{ and } \xi_t = f_t/ Re^{0.25} \tag{22}$$

$$f_l = 280\pi[(b^{0.5}-0.6)^2 + 0.75]/(4ab-\pi)*a^{1.6} \quad (b\geq 1/2\sqrt{(2a+1)} \tag{23}$$

$$f_l = 280\pi[(b^{0.5}-0.6)^2 + 0.75]/(4ab-\pi)*c^{1.6} \quad (b<1/2\sqrt{(2a+1)} \tag{24}$$

$$c=\sqrt{\{(a/2)^2+b^2\}} \tag{25}$$

$$f_t = 2.5 +\{1.2/(a-0.85)^{1.08}\}+0.4(b/a -1)^3 - 0.01(a/b -1)^3 \tag{26}$$

7.9 ACKNOWLEDGEMENTS

The authors like to thank M.I. Smith for his contribution to this chapter.

7.10 REFERENCES

1 G.B. van den Berg and C.A. Smolders, Flux decline in membrane processes, Filtration and separation, March/April (1988) 115.

2 H.D.W. Roesink et al., PhD Thesis Chapter 2,3,4,5 and 6, University of Twente, Enschede, The Netherlands (1989).

3 G. Belfort, Membrane modules: comparison of different configurations using fluid mechanics, J. Membr. Sci., **35** (1988) 245.

4 G. Schock, Mikrofiltration an Überströmten Membranen, PhD Thesis, Technische Hochschule Aachen, Aachen, West-Germany (1985).

5 R.J. Baker, A.G. Fane, C.J.D. Fell and B.H. Yoo, Factors affecting flux in crossflow filtration, Desalination, **53** (1985) 81.

6 US Patent 3 342 729 (1967), US Patent 3 557 962 (1971), US Patent 4 125 468 (1973). US Patent 3 976 576 (1976), US Patent 3 993 816 (1976), US Patent 4 082 670 (1978).

7 M.C. Yang, E. L. Cussler, Designing hollow-fiber contactors, AIChE Journal, **32** (1986) 1910.

8 V. Gekas and B. Hallström, Mass transfer in the membrane concentration polarization layer under turbulent cross flow. I- Critrical literature review and adaptation of existing Sherwood correlations to membrane operations, J. Membr. Sci., **30** (1987) 153.

9 M.C. Porter, Concentration polarization with membrane ultrafiltration, Ind. Eng. Chem. Prod. Res. Develop., **11** (1972) 234.

10 C. Gernedel and H.G. Kessler, Ultrafiltration kolloidaler Systeme und die den Widerstand der Ablagerungsschicht beeinflussenden Faktoren, vt-verfahrenstechnik, **15** (1981) 646.
For an extended survey of the work of C. Gernedel see:
C. Gernedel, Über die Ultrafiltration von Milch und die Widerstand der Ablagerungsschicht beeinflussenden Faktoren, PhD Thesis, Technische Universität München, München, West-Gemany (1980).

11 C.A. Romero, R.H. Davis, Global model of crossflow microfiltration based on hydrodynamic particle diffusion, J. Membr. Sci., **39** (1988) 157.

12 A.L. Zydney and C.K. Colton, A concentration polarization model for the filtrate flux in cross-flow microfiltration of particulate suspensions, Chem. Eng. Commun., **47** (1986) 1.

13 E.C. Eckstein, D.G. Bailey and A.H. Shapiro, Self-diffusion of particles in shear flow of a suspension, J. Fluid Mech., **79** (1974) 191.

14 VDI-Wärme atlas, Druckverlust bei der Strömung quer zu Rohrbündeln, 4. Auflage (1984).

15 R.H.Davis and S.A. Birdsell, Hydrodynamic model and experiments for crossflow microfiltration, Chem. Eng. Comm., **49** (1987) 217.

16 G. Schulz and S. Ripperger, Concentration polarization in crossflow microfiltration, J. Membr. Sci., **40** (1989) 173.

17 M.J. van der Waal and I.G. Rácz, Mass transfer in corrugated plate and frame modules. I- Hyperfiltration experiments, J. Membr. Sci., **40** (1989) 243.

18 M.J. van der Waal, S. Stevanovic and I.G. Rácz, Mass transfer in corrugated plate and frame modules. II- Ultrafiltration experiments, J. Membr. Sci., **40** (1989) 261.

19 I.G. Rácz, J. Groot Wassink and R. Klaassen, Mass transfer, fluid flow and membrane properties in flat and corrugated plate hyperfiltration modules, Desalination, **60** (1986) 213.

20 H. Brauer, Grundlagen der Einphasen- und Mehrphasenströmungen, Sauerländer, Aarau und Frankfurt am Main, West-Germany (1971).

21 A. Zukauskas and J. Ziugzda, Heat transfer of a cilinder in crossflow, Hemisphere publishing corporation, Washington New York London, Springer-Verlag Berlin, West-Germany (1985).

CHAPTER 8

MODULES WITH CAPILLARY MICROFILTRATION MEMBRANES. 2 - PRESSURE DROP IN CAPILLARY MEMBRANES DURING MICROFILTRATION AND BACKFLUSHING IN SHELL-SIDE FED MODULES.

H.D.W. Roesink, Y.R de Boer and I.G. Rácz.

8.1 SUMMARY

A large pressure drop at the bore side of membrane capillaries in combination with high membrane permeabilities, as can be found in microfiltration, may restrict membrane permeation efficiency. Therefore it is necessary to know the pressure drop in the bore of the capillary membranes as a function of relevant process parameters. In this chapter a model is presented for calculating this pressure drop in the bore of microfiltration capillary membranes during filtration and during backflushing in shell-side fed modules (feed outside design). The model is verified with clean water experiments. The results demonstrate that it is possible with this model to calculate the optimal dimensions (inner diameter and length) of the capillary membranes as a function of different process parameters.

8.2 INTRODUCTION

In chapter 7 [1] different techniques to diminish or to avoid flux decline during microfiltration were discussed. In that work it was also shown that shell-side fed modules (feed-outside design) may have advantages compared with capillary bore fed modules. Therefore in our group a program is started to investigate the development of a shell-side fed module with transverse flow conditions. When this shell-side fed module has to be used for microfiltration applications, the module type has to be suitable for backflushing, since using this technique higher net permeate fluxes can be obtained. Since the permeabilities of microfiltration membranes can be very high in the backflush mode and in the filtration mode especially just after backflushing, the dimensions of the capillary membrane (length and inner diameter) can restrict the transport of permeate through the bore of the capillary membranes.
In this chapter a model is presented for calculating the pressure drop in the bore of capillary membranes as a function of relevant parameters both in the filtration mode and in the backflush

mode. The presented model has been verified by performing experiments with tap water purified by reverse osmosis.

8.3 MODEL DEVELOPMENT

When the feed contacts the outer surface of capillary membranes (shell-side fed modules) and the permeate flows through the bore of the membranes (see the situation in figure 1), the effective transmembrane pressure difference will be reduced by the pressure drop in the bore of the capillary. Capillary membranes can be made so long that the internal pressure at the closed end of the membrane equals the external pressure, so that a part of the membrane surface is not effectively used for filtration.

The pressure drop in the bore also brings about that the permeate flux during the backflush mode is not constant over the length of the capillary membrane. Especially at the end of the membrane the permeate flux will be lower, so that the backflush efficiency is reduced.

To calculate the optimal dimensions of the capillary membrane at given circumstances one needs to know the pressure drop in the bore as a function of relevant parameters.

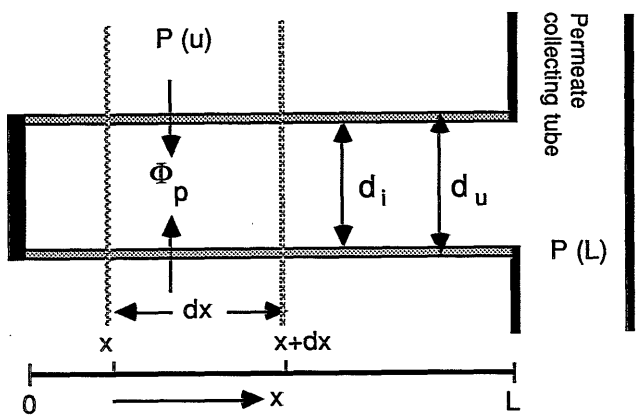

Figure 1: *Schematic representation of filtration with a capillary membrane.*

When there is a laminar flow in the bore of the membrane the pressure drop can be expressed by:

$$\frac{dP(x)}{dx} = -\frac{32*\eta*v(x)}{(d_i)^2} \qquad (1)$$

The permeate flow through the membrane can be given by:

$$d\Phi_p = C*\pi*d_u*\{P(u) - P(x)\}*dx \qquad (2)$$

P(u) is assumed to be constant. The mass balance for the given volume element in figure 1 is:

$$d\Phi_p = \Phi_{x+dx} - \Phi_x \qquad (3)$$

or divided by the cross sectional area:

$$\frac{d\Phi_p}{0.25*\pi*(d_i)^2} = v_{x+dx} - v_x \qquad (4)$$

Combination of (2) and (4) gives the following equation:

$$\frac{dv}{dx} = \frac{C*4*d_u*\{P(u)-P(x)\}}{(d_i)^2} \qquad (5)$$

When equation (1) is differentiated and the result is combined with (5), the result is the following differential equation:

$$\frac{d^2\{P(x)-P(u)\}}{dx^2} = a*\{P(x)-P(u)\} \qquad (6)$$

in which $a = \frac{128*\eta*C*d_u}{(d_i)^2}$

The boundary conditions for this differential equation are:

$x = L \quad \Rightarrow \quad P(x) - P(u) = P(L) - P(u)$

$x = 0 \quad \Rightarrow \quad \frac{d\{P(x) - P(u)\}}{dx} = 0$

The second boundary condition presumes that the end of the capillary membrane is not permeable. In the practical situation this boundary condition is fulfilled, e.g., by potting the end of the

membrane.

Using the boundary conditions the differential equation (6) has been solved and the following expression for the transmembrane pressure difference is obtained:

$$\frac{P(u) - P(x)}{P(u) - P(L)} = \frac{e^{x\sqrt{a}} + e^{-x\sqrt{a}}}{e^{L\sqrt{a}} + e^{-L\sqrt{a}}} \qquad (7)$$

With this solution an expression for the flow through the porous membrane wall can be derived:

$$\Phi_p = k^* \int_0^L (e^{x\sqrt{a}} + e^{-x\sqrt{a}})\, dx \qquad (8)$$

which results in $\Phi_p = (k/\sqrt{a}) * (e^{L\sqrt{a}} + e^{-L\sqrt{a}})$ (9)

in which $k = C^*\pi^*d_u^* \dfrac{P(u) - P(L)}{e^{L\sqrt{a}} + e^{-L\sqrt{a}}}$ (10)

In the backflush mode similar expressions are obtained:

$$\frac{P(x) - P(u)}{P(0) - P(u)} = \frac{e^{x\sqrt{b}} + e^{-x\sqrt{b}}}{e^{L\sqrt{b}} + e^{-L\sqrt{b}}} \qquad (11)$$

$$\Phi_p = (m/\sqrt{b}) * (e^{L\sqrt{b}} + e^{-L\sqrt{b}}) \qquad (12)$$

with $b = \dfrac{128^*\eta^*C}{(d_i)^3}$ and $m = C^*\pi^*d_i^* \dfrac{P(0) - P(u)}{e^{L\sqrt{b}} + e^{-L\sqrt{b}}}$

With these expressions it is possible to calculate the transmembrane pressure difference and the flux as a function of relevant parameters. This can be done for the filtration mode and for the backflush mode. The process parameters are:

P(u)	external pressure; in filtration mode the working pressure
P(L)	internal pressure
P(0)	backflush pressure
L	length of the capillary membranes
d_i	inner diameter of the capillary membrane
d_u	outer diameter of the capillary membrane
C	hydraulic permeability
η	viscosity of the feed solution

Since no pressure drop in the annular space of the membrane module is presumed, the external pressure P(u) is considered to be constant, although in chapter 7 [1] the pressure drop in the annular space of different types of shell-side fed modules has been calculated as a function of the volume flow of the feed solution. In this chapter only the influence of the pressure drop due to high permeabilties of the membranes is shown. It may be clear that a pressure drop in the module on the feed side can reinforce the effects that will be demonstrated in this chapter.

8.4 RESULTS AND DISCUSSION

Experiments with purified tap water using reverse osmosis were done to test the model. Measurements were performed using a one capillary membrane module, while a longitudinal flow was applied. Although in chapter 7 [1] the conclusion was that transverse flow might have advantages compared with longitudinal flow, it can be assumed that for clean water experiments the flow conditions will not be important. The experimental set up is shown in figure 2. Both in the filtration mode and in the backflush mode fluxes were measured gravimetrically. With a P(rogrammable) L(ogic) C(ontroller) different backflush conditions could be used. Capillary membranes, which were spun from a solution containing polyetherimide and polyvinylpyrrolidone were used, although also other high flux microfiltration membranes can be used. The development of these membrane type has been described in this thesis [2]. With one type of membrane the water flux for different lengths of the capillary membranes was measured in the filtration mode and in the backflush mode. From this results a mean hydraulic permeability was calculated, which was used in the model for further calculations. The hydraulic permeability was considered to be dependent only on the membrane type used. Hydraulic permeabilities in the filtration mode and in the backflush mode were the same. From the results shown in figure 3 it becomes clear that the water fluxes can be predicted very well with the proposed model, if the mean hydraulic permeability is used. Differences between calculated and measured values can be explained with the fact that the permeability is not constant over the length of the capillary membrane and that the pressure drop in the annular space of the module has been neglected.

Other results, not presented here, also showed that the presented model can predict the water fluxes for different dimensions and permeabilities of the capillary membranes.

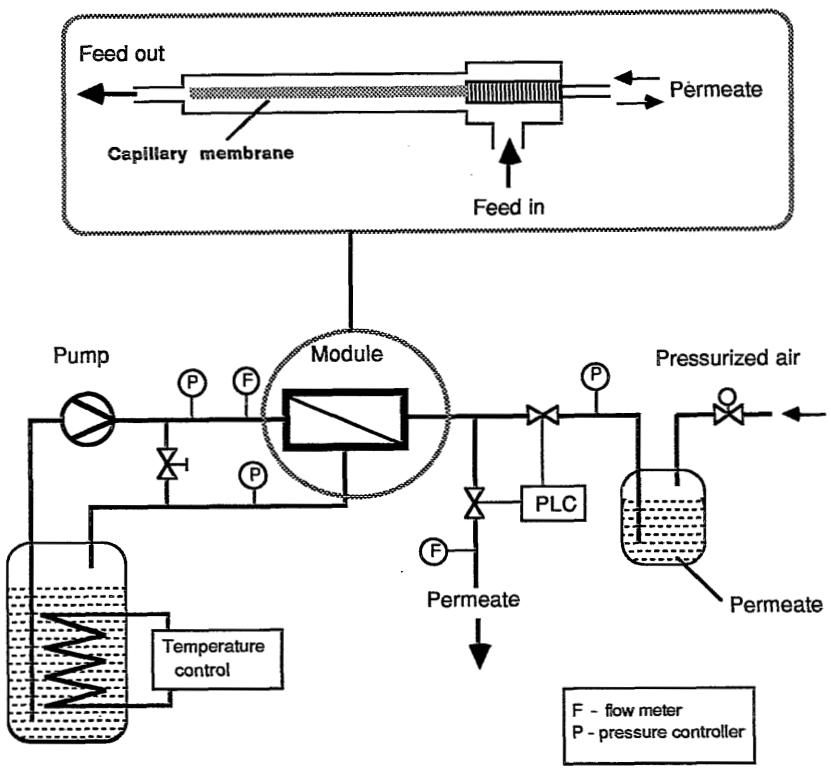

Figure 2: *Experimental set-up.*

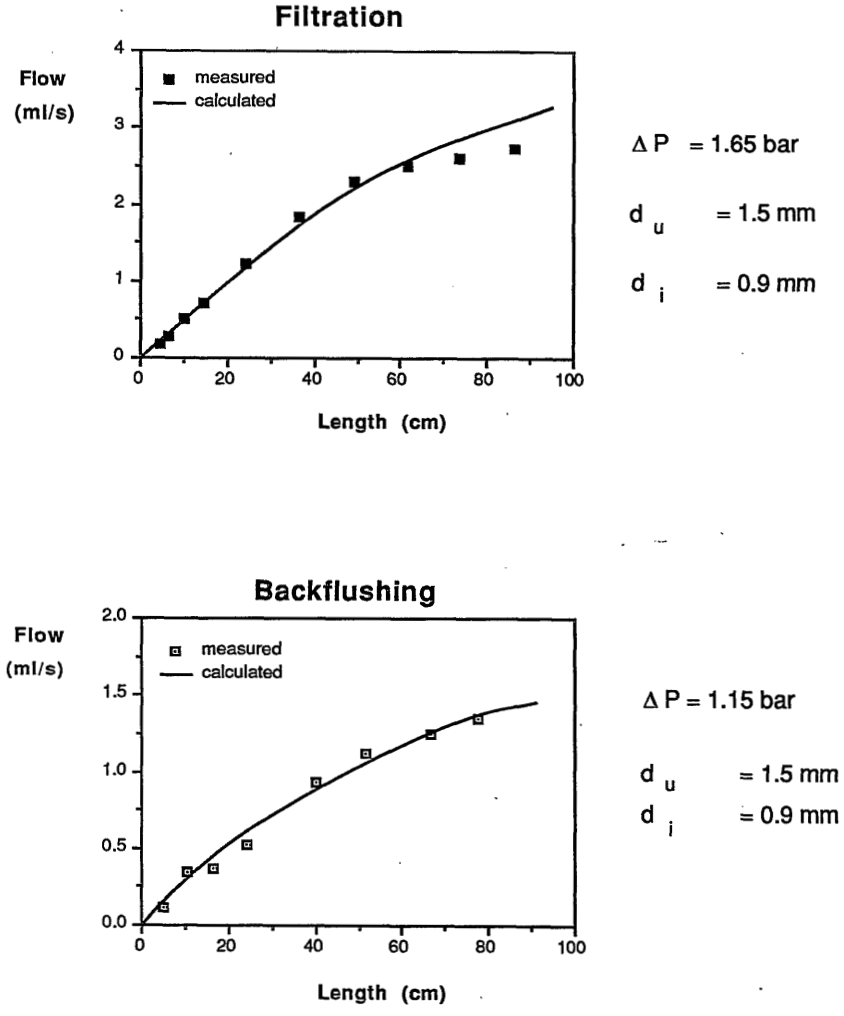

Figure 3: *Measured and calculated clean water flow as a function of the length of the capillary membranes.*

The conclusion from these experimental results is that using the presented model it is possible to predict the fluxes in the capillary membranes taking care of the pressure drop in the bore of the capillary membranes.

The permeabilities of the membranes are given as a hydraulic permeability (C). A hydraulic permeability of $5*10^{-9}$ m/Pa.s equals a flux (J_v) of about 1800 l/m^2 hr bar, which is a normal practical clean water flux for microfiltration membranes.

For the flux one can write:

$J_v = C * \Delta P$

The hydraulic permeability C can, in analogy with Ohm's law, be considered as a reciprocal resistance:

$C = 1/R.$

The resistance R is the membrane resistance when clean water is used. When suspensions are filtered the resistance R will increase as a result of the fouling of the membranes. During filtration of a suspension the total resistance R_{tot} is the result of different resistances [3].

$R_{tot.} = R_m + R_{cake} + R_{ads.} + R_{pluggging} + R_{cp}$

$R_{tot.}$	= total resistance
R_m	= membrane
R_{cake}	= cake or gel layer
$R_{ads.}$	= adsorption
$R_{pluggging}$	= pore blocking
R_{cp}	= concentration polarization

A low permeability during actual microfiltration means that there is a large resistance against solvent flow, caused by fouling of the membranes. As a rule of thumb it can be taken that the flux during filtration is 1 % of the clean water flux of the membranes if no backflushing technique is applied. If a backflushing technique is applied the flux decline is less; in this chapter a flux decline of 90 % is assumed to be reasonable.

In figure 4 and 5 some results are shown of calculations with the model. The length of the capillary membrane is 1 m, and in the figures 4 and 5 the transmembrane pressure difference as a function of the place (x) in the membranes is given. It is obvious that with a long capillary membrane, a small inner diameter and a high permeability, a part of the capillary membrane will not contribute to the flux of the membrane. When lower permeabilities are obtained the effect of the pressure drop is reduced. This pressure drop effect can be observed both in the filtration mode and in the backflush mode (compare figure 4 and figure 5).

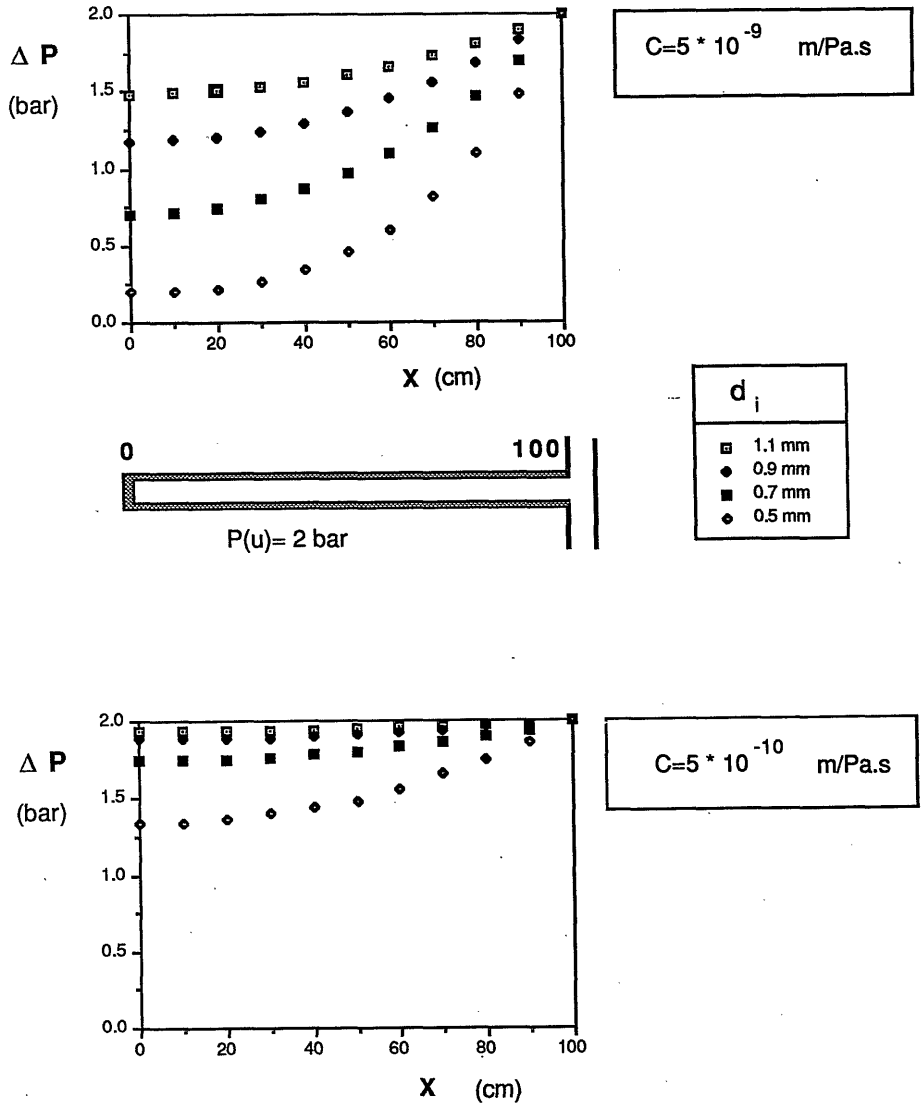

Figure 4: *Transmembrane pressure difference (ΔP) in the filtration mode calculated for a capillary membrane of 1 meter as a function of the place (x) in the capillary membrane for different permeabilities (C) and inner diameters (d_i).*

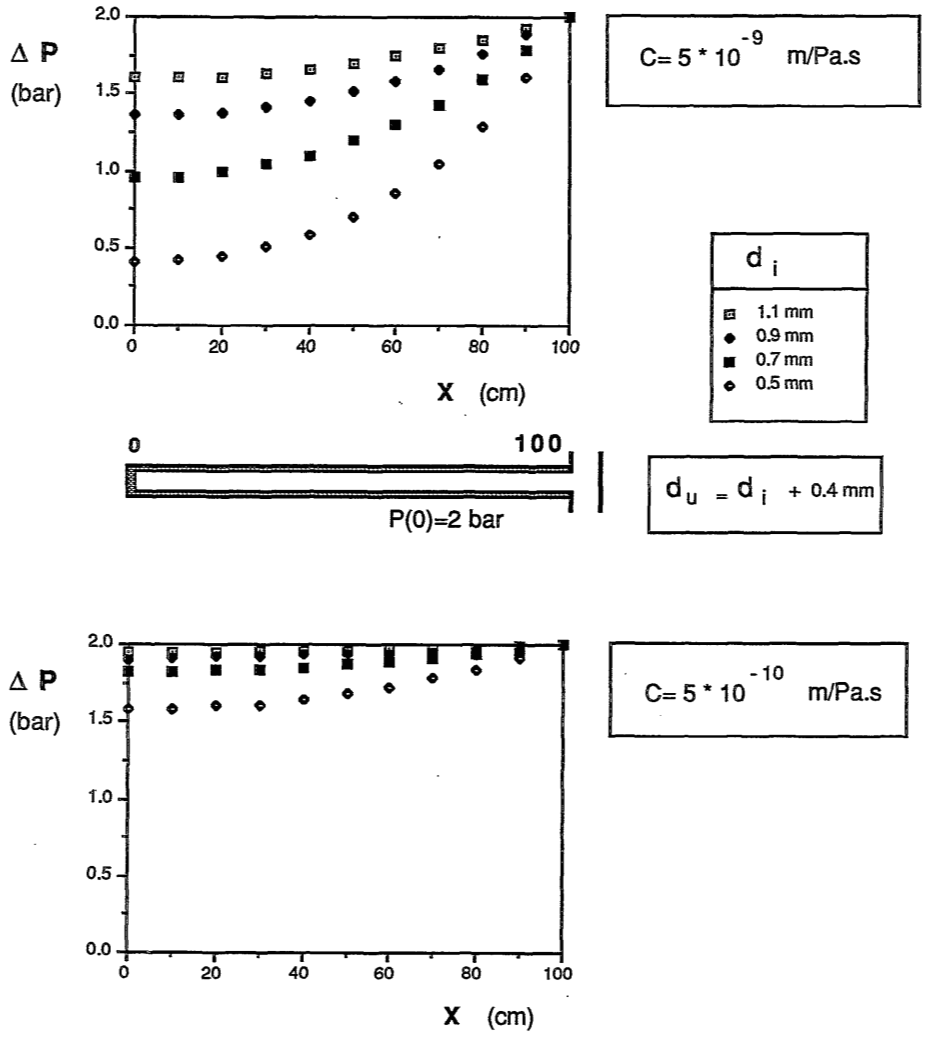

Figure 5: *Transmembrane pressure difference (ΔP) in the backflush mode calculated for a capillary membrane of 1 meter as a function of the place (x) in the capillary membrane for different permeabilities (C) and inner diameters (di).*

Because the flux during a microfiltration process is low (as a rule of thumb 10 % of the clean water flux can be obtained or in this situation 180 l/m^2 hr bar or 5 * 10^{-10} m/Pa s.) the conclusion could be that a membrane with a length of 1 meter is a proper choice.

But in practice the situation in the backflush mode will be more complex. In the backflush mode the

total resistance will decrease, since the formed cake layer will disappear. The question is how fast and how well the cake layer can be removed from the membrane surface. When at the beginning (x=L) of the capillary membrane the cake layer has already been removed, while at the end (x=0) the cake layer is still present, the situation becomes unpredictable. Research with all kinds of suspensions has to be done to gain more insight in these phenomena.

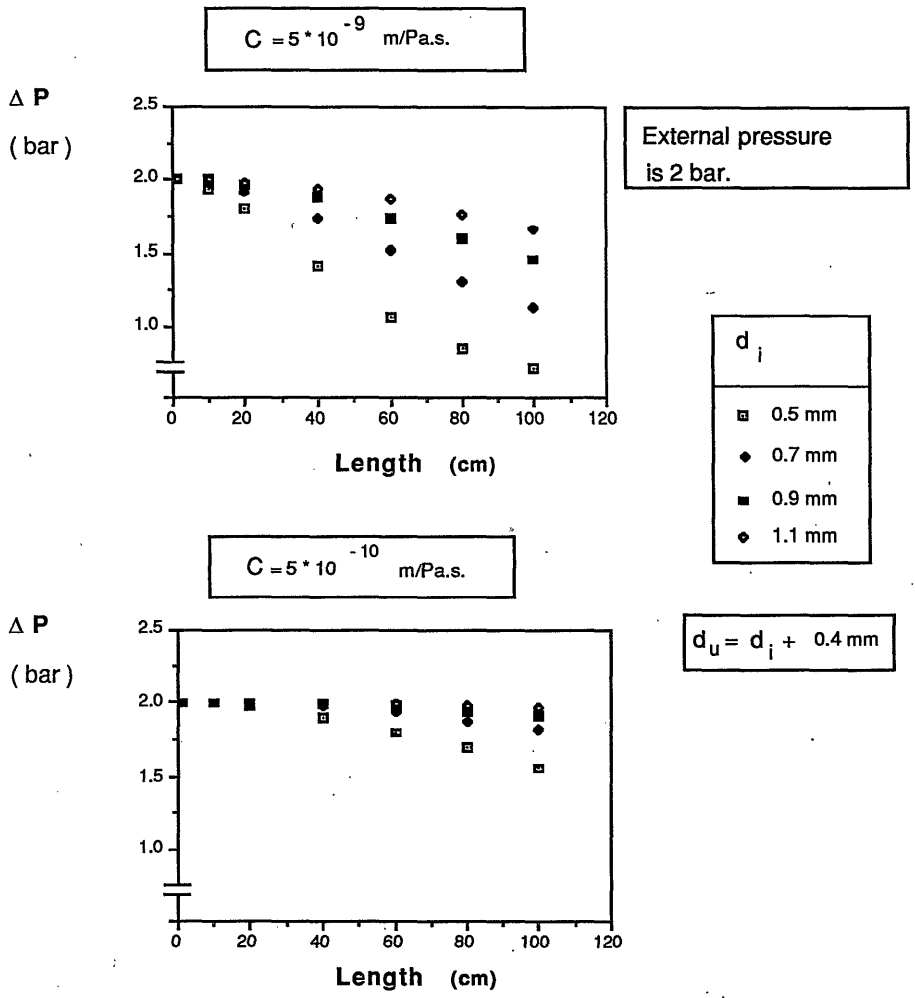

Figure 6: *Calculated transmembrane pressure difference (ΔP) in the filtration mode as a function of the membrane length for different inner diameters (d_i) and permeabilities (C).*

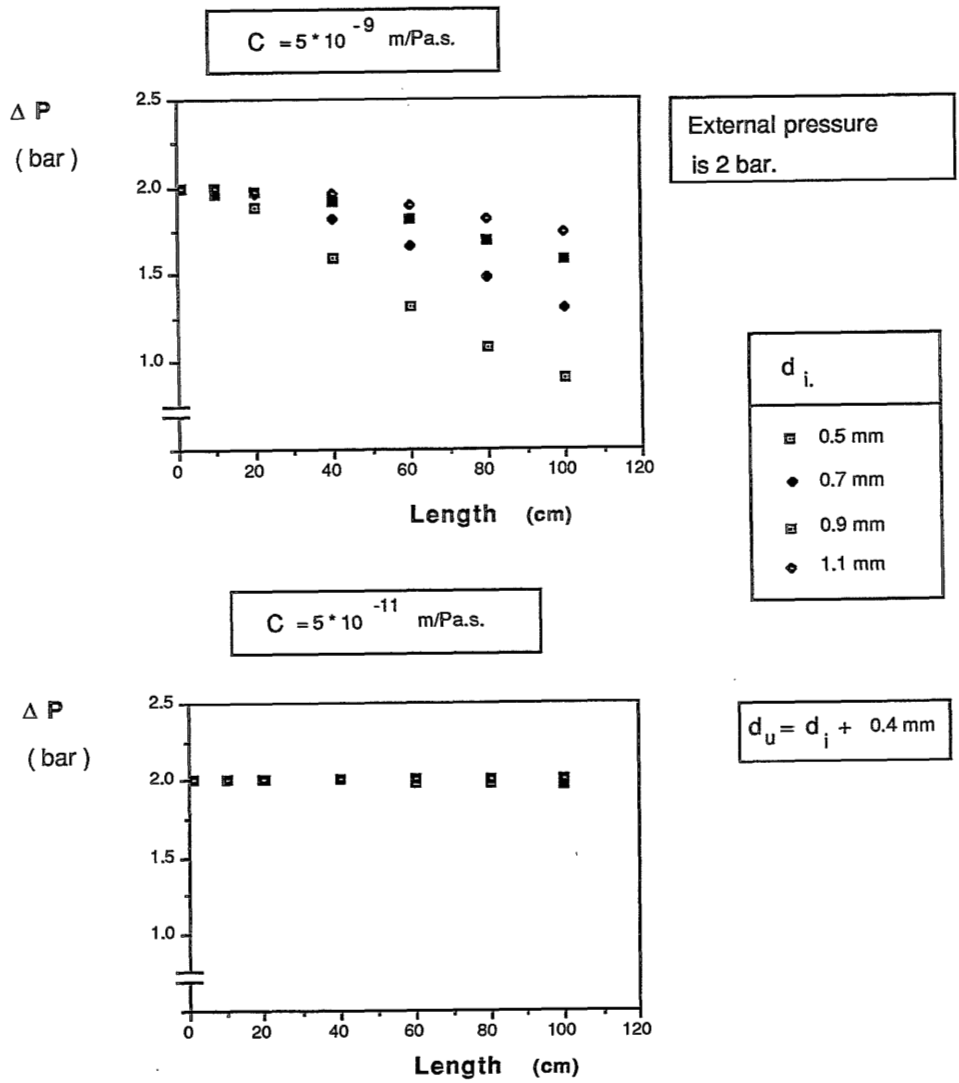

Figure 7: *Calculated transmembrane pressure difference (ΔP) in the backflush mode as a function of the capillary membrane length for different inner diameters (d_i) and permeabilities (C).*

From figures 4 and 5 the conclusion can be drawn, that there is a large influence of the membrane length on the pressure drop in the capillary membranes. In figure 6 and 7 the influence of the length of the capillary membranes on the pressure drop is demonstrated for two different permeabilities and four different inner diameters. In this figures the mean transmembrane pressure difference as a function of the membrane length is given. The arithmetic mean transmembrane

pressure difference is calculated from the pressure drop curves as shown in figure 4 and 5. A transmembrane pressure curve for a certain membrane type is divided in 10 parts (of length) and the arithmetic mean of the transmembrane pressure difference is calculated. At high permeabilities the mean transmembrane pressure difference is much lower than the working pressure of 2 bar, even for membrane lengths of 20 cm this effect is considerable for membranes with a inner diameter of 0.5 mm. At low permeabilities only for small inner diameters and long membranes the transmembrane pressure difference will be reduced. These significantly lower permeabilities can represent the situation when suspensions are filtered and fouling of the membranes causes a flux decline.

8.5 EVALUATION

Given a certain required permeability during the filtration of suspensions one can choose the optimal dimensions (length and diameter) for the capillary membranes. For applications with a low permeability and without backflushing system, a long capillary membrane with a small inner diameter can be used to create a large membrane surface to module volume ratio, although the pressure drop in the annular space of the module can become restrictive if the membranes are too long.
Another effect is the arrangement of the membranes, but in this work the pressure drop in the annular space of the membrane modules will not be discussed.

The most important conclusion is that the choice for the dimensions of the capillary membranes is dependent on the backflush behaviour of the feed solution. The backflush behaviour can be studied in practical situations and will be different for each feed solution. In a situation with a backflush system and membranes with a high water permeability ($> 5*10^{-9}$ m/Pa.s), while the actual permeability reduces with at least a factor of 10, a good choice for the capillary dimensions in this case will be a membrane with a length < 40 cm and an inner diameter > 1mm. From figure 7 it can be concluded that even for high permeabilities the backflush behaviour will then not be influenced by the pressure drop in the capillary membrane.

During the filtration process the flux decreases due to the fouling of the membranes. In this situation the hydraulic permeability is a function of time. Equation (9) is an expression for the permeate flow in the filtration mode taking into account the pressure drop in the capillary membrane. The hydraulic permeability is taken constant, since the filtration medium is clean water. Equation (12) is a similar expression for the permeate flow in the backflush mode and here also the hydraulic permeability is not taken to be time dependent.
When the hydraulic permeabilties are assumed to be time dependent, the following expressions for

the filtration volume and the backflush volume can be derived:

$$V_f = N*(d_u)^{1/2}*\Delta P * \int_{t_1}^{t_2} [C(t)]^{1/2} * \tanh [L* \{K*(d_u/d_i)*C(t)\}^{1/2}] \, dt \qquad (13)$$

$$V_{bf} = N*(d_i)^{1/2}*\Delta P * \int_{t_2}^{t_3} [C(t)]^{1/2} * \tanh [L* \{K*C(t)\}^{1/2}] \, dt \qquad (14)$$

With $N = \dfrac{\pi*(d_i)^2}{(128*h)}$ and $K = \dfrac{128*\eta}{(d_i)^3}$

V_f is the filtration volume collected in the filtration time from t_1 to t_2, the backflush volume V_{bf} is collected during the backflush period from t_2 to t_3.
It is quite possible to describe the fluxes in the filtration and in the backflush mode. One needs to know the hydraulic permeability {C(t)} as a function of time. This function will be different for the filtration mode and the backflush mode and has to be determined experimentally.

8.6 NOTATION

C	hydraulic permeability	m/Pa s
d_i	inner diameter of the capillary membrane	m
d_u	outer diameter of the capillary membrane	m
L	length of the capillary membranes	m
P(u)	external pressure (in filtration mode the working pressure)	N/m^2
P(L)	internal pressure	N/m^2
P(0)	backflush pressure	N/m^2
P(x)	internal pressure as a function of the axial coordinate x	N/m^2
ΔP	transmembrane pressure difference	N/m^2
t	time	s
V_f	volume of permeate during filtration	m^3
V_{bf}	volume of permeate during back flushing	m^3

v	average flow velocity	m/s
v(x)	velocity as a function of the axial coordinate x	m/s
x	axial coordinate	m
Φ_p	volume flow of permeate	m^3/s
η	dynamic viscosity of the feed solution	Pa.s

8.7 ACKNOWLEDGEMENTS

The authors like to thank L. Broens for the stimulating discussions on the subject.

8.8 REFERENCES

1 H.D.W. Roesink and I.G. Ràcz, Modules with capillary membranes: 1- Comparison of the shell-side fed module with the capillary bore fed module, PhD Thesis Chapter 7, University of Twente, Enschede, The Netherlands (1989).

2 H.D.W. Roesink et al., PhD Thesis Chapter 2,3,4 and 5, University of Twente, Enschede, The Netherlands (1989).

3 G.B van den Berg and C.A. Smolders, Flux decline in membrane processes, Filtration and separation, March/April (1988) 115.

CHAPTER 9

SUMMARIES

H.D.W. Roesink

9.1 NEDERLANDS

In dit proefschrift wordt de ontwikkeling van een nieuw type hydrofiele membranen beschreven en bovendien wordt een aanzet gegeven om te komen tot een nieuw ontwerp voor microfiltratie modules met capillair membranen.

Het membraan wordt gemaakt uit een mengsel van twee polymeren, n.l. het hydrofobe, chemisch resistente en thermisch stabiele polymeer polyetherimide (PEI) en het wateroplosbare hydrofiele polymeer polyvinylpyrrolidon (PVP). Als oplosmiddel wordt N-Methyl-2-pyrrolidon (NMP) gebruikt, terwijl water dient als niet-oplosmiddel.
Membranen kunnen gevormd worden door een homogene polymeeroplossing in contact te brengen met een niet-oplosmiddel voor het polymeer. Door uitwisseling van niet-oplosmiddel en oplosmiddel zal de polymeeroplossing ontmengen en er zal zich een poreuze structuur vormen (het uiteindelijke membraan). De omstandigheden waaronder de polymeeroplossing ontmengd bepalen de morfologie van het membraan en dientengevolge het toepassingsgebied. In dit proefschrift is de ontwikkeling van een microfiltratiemembraan beschreven, hetgeen inhoudt, dat het membraan poriën heeft met een diameter tussen 0.05 en 10 µm.
Er zijn twee essentieel verschillende geometriën voor een membraan: buisvormig en vlak. Tijdens het onderzoek beschreven in dit proefschrift is veel aandacht besteed aan het vervaardigen van zgn. capillair membranen. Dit zijn buisvormige membranen met een uitwendige diameter tussen 0.5 en 5 mm, die gemaakt worden door middel van een spinproces (te vergelijken met het vezelspinnen in de textielindustrie). Tijdens dit proces wordt een homogene polymeeroplossing geëxtrudeerd door een opening waarin een holle naald centrisch is gemonteerd. Door de holle naald wordt tijdens het extruderen een vloeistof gepompt (het interne coagulatiemedium), hetgeen zorg draagt voor een daadwerkelijk hol membraan en die bovendien de morfologie van het binnenoppervlak van het capillair membraan bepaald.
Na het verlaten van de spinkop komt de polymeeroplossing eerst in contact met (vochtige of droge) lucht en vervolgens met het externe coagulatiebad, waarin het uiteindelijke membraan wordt gevormd. Men spreekt wel over het droog-nat spinproces.

In hoofdstuk 1 wordt de ontwikkeling beschreven van een relatief oude membraanscheidingstechniek, die start in het begin van deze eeuw, tot een geavanceerde scheidings-technologie; de cross-flow microfiltratie. Er wordt een overzicht gegeven van de verschillende manieren waarop polymere microfiltratiemembranen kunnen worden gemaakt, en door wie ze op de markt worden gebracht. Ook worden de verschillende module typen besproken, evenals de belangrijkste toepassingen en de plaats van microfiltratie op de totale membranen markt.
In hoofdstuk 2 worden ontmengverschijnselen en membraanvorming in het gebruikte vier componenten membraanvormend systeem (PEI/PVP/NMP/water) beschreven. Het membraanvormend systeem is gekarakteriseerd door middel van thermodynamische en kinetische experimenten. Het is gebleken dat PVP een grote invloed heeft op de membraanvormings-eigenschappen. Een belangrijk punt is de aanwezigheid van PVP in de polymere membraanmatrix ondanks de oplosbaarheid van PVP in het coagulatiemedium (water). De aanwezigheid van PVP in de matrix bevordert de vorming van een zeer open poreuze membraanstructuur en bovendien de vorming van open microporeuze toplagen. Deze effecten kunnen zeer goed zichtbaar gemaakt worden door gebruik te maken van cryogene preparatietechnieken in combinatie met electronenmicroscopie. De verklaring berust op het feit dat de poriewanden gedeeltelijk uit een PVP-rijke fase bestaan, die door ontzwelling kunnen breken en zodoende een zeer open poriestructuur opleveren.
Het vervaardigen van microporeuze capillair membranen wordt beschreven in hoofdstuk 3. Uitgaande van een spinoplossing PEI/PVP/NMP is het mogelijk gebleken microfiltratiemembranen te maken met poriediameters tussen 0.05 μm en 1 μm. De poriegrootte en porositeit in het buitenoppervlak wordt geregeld met de temperatuur van het externe coagulatiebad en de verblijftijd in het lucht-traject. De poriegrootte in het binnenoppervlak wordt geregeld door de samenstelling (met name de verhouding oplosmiddel en niet-oplosmiddel) van het interne coagulatiebad te veranderen. De samenstelling van het interne coagulatiebad blijkt ook een grote invloed te hebben op de vorm van het lumen van de capillair membranen.
In hoofdstuk 4 worden de membraanvormende eigenschappen van polyetherimide vergeleken met die van polyethersulfon (PES) en polyimide (PI). Uitgaande van polymeeroplossingen met PVP 360 000 kunnen er poreuze fase-inversie membranen worden gemaakt en kan er telkens een relevante hoeveelheid PVP in de polymere membraanmatrix worden aangetoond.
De hoeveelheid PVP die achterblijft in de polymere membraanmatrix is afhankelijk van de ontmengkinetiek en interactie tussen het gebruikte polymeer en PVP.
PEI en PVP vormen homogene blends, hetgeen aangetoond is door het bepalen van glasovergangstemperaturen. De gemeten glasovergangstemperaturen zijn hoger dan de gewichtsgemiddelde glasovergangstemperatuur, hetgeen op een sterke interactie tussen PEI en PVP wijst.

Indien, uitgaande van een PEI/PVP oplossing, immersie-precipitatiemembranen worden gemaakt, zal afhankelijk van uitgangssamenstelling en molecuulgewicht van het PVP, een bepaalde relevante hoeveelheid PVP in de membraan matrix achter blijven. Het aldus verkregen membraan is geen homogene blend indien hoog moleculair PVP (MW=360 000) wordt gebruikt; met behulp van torsiemetingen kunnen twee verschillende glasovergangstemperaturen worden onderscheiden, die afkomstig zijn van PEI en PVP. Wordt laag moleculair PVP (MW=10 000) gebruikt, dan blijkt het membraan een homogene blend te zijn; ook met torsiemetingen wordt slechts een enkelvoudige glasovergangstemperatuur gevonden.
Door de aanwezigheid van PVP in de membraanmatrix zal een zeer grote zwelling optreden indien de membranen onbehandeld in contact komen met b.v. water, en het gevolg is dan ook dat voor deze membranen geen of nauwelijks een permeabiliteit voor water kan worden gemeten. De permeabiliteit voor aceton (een niet-oplosmiddel voor PVP) daarentegen is erg groot en is ook in overeenstemming met de waargenomen poriegrootte en porositeit van de droge membranen. Resultaten van deze experimenten worden besproken in hoofdstuk 5. De zwelling van het PVP kan op twee essentieel verschillende manieren worden voorkomen, n.l. door het aanwezige PVP te crosslinken of door het PVP te verwijderen. Beide methodes zijn uitgewerkt en leveren membranen met permeabiliteiten in overeenstemming met de poriegroottes en porositeiten. Het crosslinken gebeurt door een eenvoudige warmtebehandeling. Na deze warmtebehandeling zijn de membranen door het aanwezige PVP nog zeer goed bevochtigbaar, terwijl door het crosslinken er geen uitdiffusie van PVP meer zal optreden.
Het PVP kan selectief verwijderd worden met chloorbleekloog (NaOCl), ook na deze behandeling blijven de membranen goed bevochtigbaar.
De invloed van de ontwikkelde nabehandelingsmethoden op de vervuilingseigenschappen is onderzocht door adsorptie-experimenten uit te voeren met een rundereiwit; bovine serum albumine (BSA). Vlakke PEI/PVP membranen worden in contact gebracht met BSA-oplossingen en gekarakteriseerd door voor en na het contact met de BSA-oplossing de waterflux te meten. Uit deze experimenten blijkt dat de aanwezigheid van PVP de adsorptie van BSA en dientengevolge de fluxdaling als gevolg van adsorptie in belangrijke mate kan voorkomen. De permeatie-experimenten zijn in zeer goede overeensteming met adsorptie-experimenten uitgevoerd met radio-actief gelabeld BSA. Uit deze experimenten blijkt o.a. dat de hoeveelheid geadsorbeerd BSA per oppervlakte eenheid erg laag is en vergelijkbaar met in de literatuur gegeven waarden voor de hoeveelheid BSA, die op cellulose-acetaat membranen adsorbeert. Het voordeel van de PEI/PVP membranen is dan echter de veel grotere thermische en chemische resistentie dan de cellulose-acetaat membranen, die nog steeds als voorbeeld gebruikt worden voor niet of nauwelijks vervuilende hydrofiele membranen.

In hoofdstuk 7 en 8 worden tenslotte een aantal meer theoretische studies gepresenteerd, die

kunnen leiden tot een geheel nieuw ontwerp voor modules met capillair membranen. In hoofdstuk 7 worden verschillende mogelijkheden voor aanstromen in modules met capillair membranen vergeleken. De drie verschillende aanstroomvormen zijn:

- stroming door het lumen van de capillair membranen (filtratie van binnen naar buiten)
- stroming langs het uitwendige van de membranen (filtratie van buiten naar binnen); de stroming kan parallel zijn aan de lengte as van de membranen (longitudinale stroming) of loodrecht op de lengte-as (transversale stroming)

Verreweg het meest gunstig is de transversale aanstroming van de membranen. De energie benodigd voor het verkrijgen van een bepaalde hoeveelheid permeaat is dan ongeveer een derde in vergelijking met de veel toegepaste stroming door het lumen.
In hoofdstuk 8 wordt een model gepresenteerd om de drukval in het lumen van de capillair membranen te berekenen tijdens filtreren en tijdens terugspoelen. Dit model is getoetst door het uitvoeren van filtratie-experimenten met schoon water. Met dit model is het mogelijk om de optimale afmetingen (lengte en diameter) van de membranen te bepalen als functie van relevante procesparameters.

9.2 ENGLISH

This thesis describes the development of a new type of hydrophilic microfiltration membranes and in addition some studies are presented, that may result in a completely new design of microfiltration modules containing capillary membranes.

The membranes are prepared from a solution containing two polymers, i.e., the hydrophobic, highly resistant polyetherimide (PEI) and the hydrophilic, water soluble polyvinylpyrrolidone (PVP). N-methyl-2-pyrrolidone (NMP) is used as a solvent, while water is used as a nonsolvent. Membranes can be prepared by means of immersion of a homogeneous polymer solution into a suitable nonsolvent. The polymer solution will demix as a result of a solvent/nonsolvent exchange and a porous structure may be formed: the membrane. The demixing conditions will influence the ultimate membrane morphology and consequently the application.
Two different geometries of membranes can be distinguished: flat or cylindrical. The attention of the present work has been focussed on the development of capillary membranes, i.e., tubular membranes with an outer diameter of 0.5 - 5 mm, that are prepared by means of a so-called dry-wet spinning process. A homogeneous polymer solution is extruded through a tube-in-orifice spinneret. The inner tube is hollow and an internal coagulation fluid (bore liquid) is pumped through this hollow tube to achieve that capillary membranes are formed and to determine the ultimate structure

of the inner membrane surface. After leaving the spinneret the polymer solution first contacts the (humid or dry) air in the air-gap and then the external coagulation bath, in which the ultimate capillary membrane is formed.

Chapter 1 describes the development of the cross-flow microfiltration process from an old membrane separation technique that started in the beginning of this century into a high performance technology. A survey of the different membrane preparation methods for polymeric membranes is given and also a list of microfiltration membrane manufacturers is presented.
The demixing phenomena and membrane formation of the four component system PEI/PVP/NMP/water are described in chapter 2. The membrane forming system is characterized by thermodynamic and kinetic experiments. A very important feature for the development of the present membranes is the fact that despite the solubility of PVP in the coagulation bath (water), an appreciable amount of PVP remains in the polymeric membrane matrix. The presence of PVP in the matrix facilitates the formation of open microporous toplayers and the formation of an open interconnected pore structure. These effects are very clearly demonstrated by means of a cryo-genic preparation technique in combination with scanning electron microscopy. The explanation is based on the fact that the pore walls consist of a PVP enriched phase and collapse upon dehydrating.
The preparation of capillary microfiltration membranes is described in chapter 3. Using a three component polymer solution PEI/PVP/NMP, it is possible to prepare microfiltration membranes with pore sizes in the range of 0.05 - 1 μm using a dry-wet spinning process. The pore size and porosity at the outer surface can be controlled by changing the temperature of the external coagulation bath and the residence time in the airgap. Pore size and porosity at the inner surface is adjusted by changing the solvent concentration in the internal coagulation bath. In addition it is shown that the composition of the internal coagulation bath influences the shape of the bore of the capillary membranes.
In chapter 4 the membrane forming properties of polyetherimide has been compared with those of polyethersulfone (PES) and polyimide (PI). When PVP is added to these polymer solutions and porous phase inversion membranes are prepared, the membrane matrix will contain a appreciable amount of PVP. The amount of PVP present in the membranes is dependent on the interaction between the polymers and the demixing kinetics. The interaction of PVP and the other polymers is demonstrated by measuring the glass transition temperatures of homogeneous polymer films. Single glass transition temperatures are found, which indicates that always homogeneous blends are formed. The measured glass transition temperatures of PEI/PVP blends were higher than the weight average glass transition temperatures indicating a strong interaction between PEI and PVP.
When porous phase inversion membranes are made using PEI/PVP/NMP solutions, a considerable amount of PVP remains in the membrane matrix depending on the molecular weight of the PVP and on the composition of the polymer solution. Using high molecular weight PVP (MW=360 000)

a heterogeneous blend is obtained, since by means of torsion measurements two glass transition temperatures are found that can be ascribed to PEI and PVP. In the case of low molecular weight PVP (MW=10 000) a homogeneous blend is formed (one glass transition temperature).
The presence of PVP will cause a strong swelling when the untreated porous membranes are contacted with water and consequently no water permeability can be measured. The permeability for acetone (a nonsolvent for PVP) is very high and in good agreement with pore sizes and porosity as can be observed using the scanning electron microscope. In chapter 5 two essentially different methods are described to avoid swelling of the PVP, i.e., crosslinking the PVP by means of a simple heat treatment or selective removing of the PVP using sodium hypochlorite (NaOCl). Both methods render wettable membranes and high water permeabilities in agreement with pore sizes and porosity. No leaching out of PVP is found after the membranes are post-treated.
The influence of the post-treatment on the fouling characteristics of the membranes has been investigated and some preliminary results are presented in chapter 6. Bovine serum albumine (BSA) is used as a model foulant. Permation experiments before and after exposure to BSA solutions are in very good agreement with adsorption experiments using radiolabelled BSA. It appears that the measured amount of adsorbed BSA on heat treated PEI/PVP membranes can be compared with the, in literature presented, amount of adsorbed BSA on cellulose acetate membranes. The latter type of membranes still are considered to be the most excellent nonfouling membranes, however the PEI/PVP membranes offer a much better chemical and heat resistance.

In chapter 7 and 8 some theoretical studies are presented that may result in a new design of a microfiltration module containing capillary membranes.
Chapter 7 describes different flow conditions of the feed suspension in the modules:

- flow through the bore of the membranes in so-called capillary bore fed modules (filtration from inside to outside)
- flow at the outside of the membranes in the so-called shell-side fed modules (filtration from outside to inside); the flow direction can either be parallel to the length axis of the membranes (longitudinal flow) or perpendicular to the length axis of the membranes (transverse flow).

The most favourable configuration appears to be the transverse flow. When this transverse flow of the feed is compared with the flow through the bore, one third of the energy is required to obtain the same amount of permeate using the same membrane surface area.
In chapter 8 a model is presented to calculate the pressure drop in the bore of the capillary membrane during filtration and during backflushing. The model is verified with clean water measurements and using this model, it is possible to calculate the optimal dimensions (length and diameter) as a funtion of relevant process parameters.

9.3 DEUTSCH

In der vorliegenden Arbeit wird die Entwicklung eines neuen Types hydrophiler Membranen beschrieben. Ergänzend werden Ansätze dargestellt, die zu einem neuen Design von Mikrofiltrationsmodulen mit Kapillarmembranen führen können.

Die Membranen werden aus einem Gemisch zweier Polymere hergestellt, dem hydrophoben, chemisch und thermisch sehr stabilen Polyetherimid (PEI) und dem hydrophilen, wasserlöslichen Polyvinylpyrrolidon (PVP). Als Lösungsmittel wird N-Methyl-2-Pyrrolidon (NMP) gebraucht, während Wasser als Nichtlösungsmittel dient. Membranen können mittels des Phaseninversionsprozesses durch Ausfällung einer homogenen Polymerlösung in einem geeigneten Nichtlösungsmittel, dem Fällmittel, hergestellt werden. Hierbei werden Lösungsmittel und Fällmittel ausgetauscht, das entstehende Dreikomponentengemisch (P, LM, FM) gelangt in eine Mischungslücke, entmischt hierdurch und bildet so eine poröse Struktur, die Membran. Prozessbedingungen und -verhältnisse während der Entmischung bestimmen die Membranmorphologie und dadurch letztendlich das Anwendungsfeld der Membran.

Grundsätzlich kann man zwischen zwei Membrangeometrien unterscheiden, flach oder zylindrisch. In dieser Arbeit werden hauptsächlich Untersuchungen an der Entwicklung von Kapillarmembranen beschrieben. Diese schlauchförmigen Membranen mit 0.5 bis 5 mm Durchmesser werden mit Hilfe eines Spinnverfahrens hergestellt (ähnlich dem der Textilfaserherstellung). Hierbei wird eine homogene Polymerlösung durch den äusseren Ringspalt einer konzentrischen Doppeldüse extrudiert. Im inneren, ebenfalls hohlen, Kanal der Düse wird eine Flüssigkeit gepumpt (das interne Fällmittel), welche die Bildung der hohlen Kapillarschläuche bewirkt und gleichzeitig die Morphologie der inneren Oberfläche bestimmt. Die so vorgeformte Polymerlösung kommt nach Verlassen der Spinndüse zuerst in Kontakt mit feuchter (oder trockener) Luft und wird hiernach in ein externes Fällbad eingeleitet. Hierin wird die vorgeformte Membranstrukrur endgültig ausgebildet, die Form wird fixiert durch das erstarrende Polymer und man erhält letztendlich die Membran.

Kapitel 1 beschreibt in einem kurzen Abriss die Entwicklung der Kreuzstrom-Mikrofiltrationstechnik von den Anfängen als gewöhnliche Filtertechnik zu Beginn dieses Jahrhunderts bis zum heutigen Einsatz als Hochleistungstrennmethode für vielfälltigste Anwendungen. Die verschiedenen Methoden zur Herstellung von Mikrofiltrationsmembranen, die gebräuchlichsten Modultypen, sowie Hersteller und Anwendungsgebiete dieser Membranen werden in mehreren Übersichtstabellen dargelegt.

Entmischungsphänomene und Membranbildung des Vier-Komponenten-Systems PEI/PVP/NMP/Wasser werden in Kapitel 2 vorgestellt. Die Bildung von Membranen wird durch thermodynamische und kinetische Untersuchungen beschrieben und charakterisiert. Einem wichtiger Faktor der Entwicklung dieser Membranen liegt die Tatsache zugrunde, dass, obwohl PVP im Fällbad Wasser löslich ist, ein beträchtlicher Teil des PVP im Membrangerüst zurückgehalten wird. Diese Anwesenheit von PVP begünstigt einerseits die Ausbildung mikroporöser Oberflächenlagen als auch die Ausbildung einer extrem offenen Porenstruktur in der darunter liegenden Schicht. Diese Effekte konnten sehr gut demonstriert werden mit Hilfe von Elektronenmikroskopie unter Zuhilfenahme spezieller Tieftemperatur-Präparationstechniken. Ein Teil der Erklärung ist in dem Umstand zu finden, dass sich PVP bevorzugt an den Porenwänden anreichert, welche durch Entschwellung kontrahieren und kollabieren was die hochporöse Struktur zur Folge hat.

Die Herstellung von Kapillarmembranen für die Mikrofiltration ist in Kapitel 3 beschrieben. Polymerlösungen mit den drei Komponenten PEI/PVP/NMP werden zu Kapillarschläuchen mit Porengrössen von 0.05 bis 1 µm gesponnen. Porengrösse und Porosität der Aussenoberfläche können durch die Temperatur des externen Fällbades sowie die Verweilzeit im Lufttrajekt variiert und somit kontrolliert eingestellt werden. Porengrösse und Porosität der Innenoberfläche der Kapillaren hingegen können durch Veränderung der Lösungsmittelzusammenstellung des internen Fällbades geregelt werden. Letzteres hat ebenfalls einen grossen Einfluss auf die geometrische Integrität der Innenoberfläche.

Kapitel 4 behandelt die Membranbildungseigenschaften von Polyetherimid im Vergleich zu Polyethersulfon (PES) und Polyimid (PI). Durch Zugabe von PVP an die Polymerlösungen können durch Phaseninversion poröse Membranen hergestellt werden. In allen Fällen konnte PVP im Membrangerüst nachgewiesen werden. Wieviel PVP in der Matrix enthalten ist wird durch Polymer-Polymer-Wechselwirkungen und durch die Kinetik der Entmischung bestimmt. Die Wechselwirkung von PVP mit den anderen Polymeren wurde unter anderem durch Betrachtung der Glassübergangstemperaturen an homogenen Filmen charakterisiert. Die Messungen der PEI/PVP Mischungen ergaben singuläre Glassübergangstemperaturen, welche jedoch über dem jeweiligen Gewichtsmittel lagen, was auf eine starke Wechselwirkung zwischen PEI und PVP schliessen lässt.
Wie bereits oben angetont, verbleibt eine bestimmte Menge PVP im porösen Membrangerüst zurück, welche von Parametern wie dem Molekulargewicht des PVP oder der Zusammenstellung der Polymerlösung abhängt. Wird zum Beispiel hochmolekulares PVP eingesetzt, entstehen hierbei heterogene Polymermischungen, was durch zwei Glassübergangstemperaturen, die des PEI und

des PVP, gekennzeichnet ist. Niedermolekulares PVP hingegen liefert homogene Mischungen mit nur einer Glassübergangstemperatur.

Die Anwesenheit des PVP in der Matrix hat einen weiteren Effekt zur Folge. Bringt man unbehandelte Membranen in Kontakt mit Wasser, so zeigt sich ein starkes Quellen der Membranen. Dies hat zur Folge, dass die Membranen keine oder eine nur sehr kleine Wasserpermeabilität haben. Azeton (ein Nichtlösungsmittel für PVP) hingegen zeigt eine sehr hohe Permeabilität, welche auch gut in Übereinstimmung mit Porengrösse und Porosität zu bringen ist. Ergebnisse dieser Untersuchungen sind in Kapitel 5 beschrieben, worin zwei verschiedene Methoden vorgestellt werden um die Quellung des PVP zu unterdrücken; die Vernetzung des PVP mittels einer einfachen Wärmebehandlung und das Auslaugen des PVP mittles einer Behandlung durch Chlornatronlauge. Durch beide Methoden können gut benetzbare Membranen mit extrem hohen Wasserpermeabilitäten hergestellt werden. In keinem Fall konnte ein Auswaschen des PVP an behandelten Membranen beobachtet werden.

Im Weiteren wurde der Einfluss der Nachbehandlung auf das Adsorptions- und Verschmutzungsverhalten der Membranen untersucht, siehe Kapitel 6. PEI/PVP Flachmembranen wurden mit Bovine Serum Albumin (BSA) Modellösungen beaufschlagt und durch Wasserflussmessungen davor und danach karakterisiert, welche mit Adsorptionsmessungen von radioaktiv markiertem BSA korreliert wurden. Aus den Messungen folgt, dass PVP die Adsorption merklich unterdrückt, was höhere Flüsse zur Folge hat. Die BSA Adsorption an wärmebehandelten PEI/PVP Membranen ist vergleichbar mit der an Celluloseacetat. Letzteres wird vielfach als eines der besten Polymere hinsichtlich geringer Adsorption angesehen. PEI/PVP hat jedoch den Vorteil einer besseren Temperatur- und Chemikalienbeständigkeit.

In zwei weiteren Abschnitten werden mehr theoretische Berechnungen ausgeführt, die zu einem verbesserten Design von Mikrofitrationsmodulen mit Kapillarmembranen führen können. Zum Einen werden verschiedene Anströmbedingungen der Filtrationslösung im Modul betrachtet und miteinander verglichen. Die Berechnungen zeigen, dass von den drei verschiedenen Strömungsformen,

- Anströmung durch das Kapillarlumen (Filtration von innen nach aussen)
- Axiale Anströmung an der Aussenseite der Kapillaren (Filtration von aussen nach innen)
- Radiale Anströmung an der Aussenseite der Kapillaren (Filtration von aussen nach innen)

letztere Anordung die energetisch günstigste zu sein scheint. Verglichen mit der Anströmung von innen her, kann bei gleicher Membranfläche und Filtratmenge ungefähr ein Drittel an Energy gespart werden.
Ein weiterer wichtiger Parameter in der Auslegung von Filtrationsanlagen ist der Druckabfall im

Lumen der Kapillarmembranen. Hierzu wurde ein Model erstellt, welches den Druckabfall während der Filtration oder Rückspülung berechnet. Ergebnisse dieser Modelrechnungen wurden mit experimentell ermittelten Wasserpermeabilitäten verglichen. Mit Hilfe dieses Models ist es ebenfalls möglich, die optimalen geometrischen Abmessungen (Länge und Durchmesser) der Kapillaren als Funktion der wichtigsten Prozessparameter darzustellen.

9.4 ACKNOWLEDGEMENT

The author likes to thank I. Blume for the German translation of the summary.

LEVENSLOOP

Erik Roesink werd geboren op 17 november 1952 te Colmschate.
In 1970 werd het HBS-B diploma gehaald aan de Rijks Hogere Burger School te Deventer en in augustus van datzelfde jaar werd begonnen met de studie Chemische Technologie aan de Technische Hoge School Twente (nu Universiteit Twente). De baccalaureaatsopdracht werd uitgevoerd in de leerstoel organische materiaaltechniek van Prof. Dr. A. Bantjes en betrof de synthese en karakterisering van blokcopolymeren op basis van polypivalolacton en polyethyleenoxide. De afstudeeropdracht werd uitgevoerd onder leiding van van Prof. dr. C.A. Smolders in de onderzoeksgroep membraantechnologie, vakgroep macromoleculaire chemie en materiaalkunde, en had als onderwerp het vervaardigen en karakteriseren van ionogene membranen voor waterontzouting. Het uiteindelijke ingenieurs diploma werd verkregen in januari 1979.
Vanaf augustus 1977 gaf Erik Roesink wiskunde onderwijs op het Twickel College (VWO - Havo scholengemeenschap) te Hengelo en van 1982 tot en met 1984 was hij bovendien taakurenmedewerker van de Stichting Leerplan Ontwikkeling te Enschede.
In 1983 trad hij in het huwelijk met Ria Christiaens en samen hebben ze inmiddels twee kinderen: Derk (21-4-1984) en Margot (31-1-1986).
Van maart 1985 tot april 1989 was hij in dienst als wetenschappelijk medewerker van de Universiteit Twente (vakgroep macromoleculaire chemie en materiaalkunde; onderzoeksgroep membraantechnologie) en verrichtte het onderzoek beschreven in het voorliggende proefschrift.
Vanaf 1 juni 1989 zal hij in dienst treden als manager research en development van de firma X-FLOW BV, te Enschede.

Polymer solution
Lumen